

https://dspace.org/

Platelet-tumour cell interaction in vitro: the effects of anastrozole and anti-platelet therapy

Xulu, Kutlwano Rekgopetswe

2020

https://hdl.handle.net/10539/31806

Downloaded from a DSpace repository. https://dspace.org/

Platelet-tumour cell interaction *in vitro*: the effects of Anastrozole and Anti-platelet therapy



UNIVERSITY OF THE
WITWATERSRAND,
JOHANNESBURG

KUTLWANO REKGOPETSWE XULU

A thesis submitted in fulfilment of the requirements for the Degree of Doctor of Philosophy

FACULTY OF HEALTH SCIENCES

UNIVERSITY OF THE WITWATERSRAND, JOHANNESBURG

2020

Declaration

I, Kutlwano Rekgopetswe Xulu, declare that this thesis entitled “Platelet-tumour cell interaction *in vitro*: the effects of Anastrozole and anti-platelet therapy” is my own unaided work. It is being submitted for the Degree of Doctor of Philosophy at the University of the Witwatersrand, Johannesburg. It has not been submitted before for any degree or examination at any other University.



Kutlwano Rekgopetswe Xulu

_26th ___ day of ___October___ 2020 at ___Johannesburg___

Abstract

Thromboembolic disorders are the second leading cause of mortality in cancer patients. The relationship between cancer and thrombosis is well established with reciprocal interactions between tumour cells and platelets, facilitating thrombosis and tumour progression. Nevertheless, there remains a lack of knowledge regarding therapeutic interventions. Breast cancer is the most commonly diagnosed cancer among women, with hormone-dependant breast cancer, treated with hormone-therapy, the most commonly diagnosed subtype. In cardiovascular disease antiplatelet therapy has been efficacious, thus it could be effective against cancer-related thromboembolic disorders. In this study we investigated the effects of combined Anastrozole (hormone-therapy) with antiplatelet drugs (Aspirin and Clopidogrel cocktail/ Atopaxar), on biological markers associated with thrombosis and tumour progression *in vitro* using breast cancer cell lines exposed to vascular components.

The cytotoxicity of the treatments over 24 hours on hormone-dependant breast cancer cell lines (MCF7 and T47D) were first established by testing various concentration effects on membrane integrity and corresponding cellular morphology. Having determined an optimal concentration, effects on proliferation and migration were assessed. Thereafter, whole blood collected from six healthy female volunteers, was co-incubated with treated breast cancer cells and reciprocal interactions on hypercoagulation and tumour progression assessed. Hypercoagulation was examined by studying thrombin activity and platelet activation was determined using flow cytometry and corresponding morphology. In breast cancer cells, mRNA levels of genes (*TGFβ1, vimentin, E-cadherin, N-cadherin*) which facilitate epithelial-mesenchymal-transition (EMT) and secretion of inflammatory cytokines which mediate growth and angiogenesis, were assessed.

Our findings indicated that combined antiplatelet and Anastrozole treatment induced low but insignificant levels of collective cell migration in both cell lines. Additionally, MCF7 cells had a higher proliferation rate than T47D cells highlighting the heterogeneous nature of the cell lines. Treatment did not prevent breast cancer cells from inducing hypercoagulation as shown by thrombin activity and platelet activation. Gene expression analysis revealed that combined therapy facilitated the maintenance of an epithelial-like phenotype in MCF7 cells and may have induced a partial-EMT in T47D cells. Cytokine secretion revealed elevated levels of growth factors (TGFβ isoforms) and angiogenic factors (PDGF isoforms and VEGF). Thus, collectively these findings show that combined Anastrozole and antiplatelet therapy did not prevent hypercoagulation, and may promote tumour survival by elevating the secretion of inflammatory mediators.

Presentations and publications arising from this work

Local conferences-oral presentations

Cell death in breast cancer cells following treatment with hormone therapy and antiplatelet therapy at different concentrations. Kutlwano Xulu, Raquel Duarte, Tanya Augustine. *46th Annual Conference of the Anatomical Society of Southern Africa (ASSA)*, Johannesburg, 2018.

A dose-dependent study of anastrozole and anti-platelet therapy on breast cancer cell lines. Kutlwano Xulu, Raquel Duarte, Tanya Augustine. *45th Annual conference of the Anatomical Society of Southern Africa (ASSA),* Cape Town, 2017.

International conference-oral presentation

Combined endocrine and anti-platelet therapy fails to reduce platelet activation in breast cancer. Kutlwano Xulu, Raquel Duarte, Tanya Augustine. *19th Congress of the International Federation of Anatomists (IFAA),* London, United Kingdom, 2019.

Published manuscript

Xulu, K., Duarte, R., Augustine, T. (2020). Combined Anastrozole and Antiplatelet Therapy Treatment Differentially Promotes Breast Cancer Survival. *Microscopy and Microanalysis* **26:** 497-508. Doi:10.1017/s1431927620001324.

Acknowledgements

Supervisors

Dr Tanya Augustine: Thank you for your support, guidance and all the many lessons you have taught me. The past few years spent under your supervision and mentorship have been the most formative years of my development as an academic and I look forward to many more. Thank you for being patient with me (I know this took longer than we both anticipated) but throughout the detours I have learnt so many valuable lessons. Thank you for always challenging me beyond my comfort zone, and for bringing out the best in me. Thank you for the countless cups of coffee over the soothing sounds of death metal! I so appreciate you and your excellent work ethic. You are amazing!

Associate Professor Raquel Duarte: Thank you for your constant support and encouragement and for sticking with us until the end. I so appreciate your contribution in making this project a success and for providing valuable resources.

Funding

I wish to thank the following entities for the funding provided for this project:

- NRF Thuthuka grants awarded to Dr T. Augustine (TTK87935, AUGU017)
- Medical Research Council grant awarded to Ass. Prof R. Duarte
- NRF scarce skills grant, awarded to Ms K. Xulu (2015)
- Staff bursary, University of the Witwatersrand, awarded to Ms K. Xulu (2016-2019)
- Faculty Research grant awarded to Ms K. Xulu (2016, 2017, 2018)
- University of the Witwatersrand, Transformation Committee, Enabling grant awarded to Ms K. Xulu (2017)

- NRF-Thuthuka KIC travel grant (KIC190227421392)
- Zeiss for travel grant

Mentor

Emeritus Professor Beverley Kramer: thank you for your support, guidance and encouragement and for investing time in developing me holistically as an academic.

Blood donors

I wish to thank the blood donors for their valuable participation in this study.

Laboratory resources and equipment

I wish to thank the following Schools and Departments within the University of the Witwatersrand for providing resources needed to complete this study:

- The School of Anatomical Sciences for use of laboratory facilities to conduct experiments
- Department of Internal Medicine for the use of laboratory facilities to conduct qPCR and cytokine experiments
- The Microscopy and Microanalysis Unit for training and use of the NOVA 600 Scanning Electron Microscope
- The School of Surgery for use of the Fortessa Flow Cytometer
- The School of Physiology for use of the Labsystems Multiskan Ascent spectrophotometer
- The Day Ward Staff, Charlotte Maxeke Academic Hospital for providing phlebotomy services

- The Department of Molecular Medicine and Haematology for use of the Fortega Glomax Explorer fluorescence spectrophotometer
- The Life Sciences Imaging Facility for use of the LSM confocal microscope

Expertise

I wish to thank the following people for expertise and training towards various equipment and laboratory techniques: Dr Pascaline Fru, Ms Thérèse Dix-Peek, Dr Caroline Dickens, Mrs Hasiena Ali, Mrs Alison Mortimer, Dr Deran Reddy, Mr Jacques Gerber, Ms Monica Gomes, Dr Mark Killick, and Dr Aurelie Deroubaix. Special thank you to Ms Derushka Arnachellen for conducting the experimentation for the scratch-assay and cell proliferation assay and giving consent to use some of the data.

Friends and colleagues

I wish to thank the following people for their support and encouragement: All my colleagues within the School of Anatomical Sciences especially; Prof Maryna Steyn, Ass. Prof Felix Mbajiorgu, Mrs Aleksandra Jovanovic, Mr Thabiso Tshabalala, Dr Ayanda Ngwenya, Mrs Glynis Veale, Dr Brendon Billings, Mr Nicholas Bacci, Dr Wendy Van Der Spuy, Dr Erin Hutchinson, Prof Temitope Esan, Ms Lee-Anne Soobramoney, Ms Mwangala Nalisa, Mrs Emma Miza, and Ms Nomathemba Mnyameni.

Special thank you to the following people

- Ms Kyrtania Pather (affectionately known as “Kat”): for being the best laboratory partner I could have asked for! I’m so glad and grateful to have walked this journey with you, you brought so much fun and laughter even in our moments of “failure” you always saw silver lining, I’ve learnt so much from you. Your friendship means a lot to me.

- Mrs Jaclyn Johnson: thank you for being the best “younger sister” and for taking care of me (i.e. feeding me). I appreciate the constant encouragement and support and for believing in me.

Postgraduate students

I would like to thank the following postgraduate students I have previously supervised and who have contributed to my development and growth: Ms Jeniffer Mokwane, Ms Thanusha Pillay, Ms Bonita Pingo do Nascimento, Ms Refilwe Mathibe, Mr Kiveshen Pillay, Ms Derushka Arnachellen, Ms Nelisiwe Makua and Ms Mahlatse Mahasha.

A special thank you to the following students;

- Ms Refilwe Mathibe for assisting with the recruitment of blood donors.
- Mr Kiveshen Pillay for assisting with certain aspects of laboratory work.
- Ms Derushka Arnachellen for assisting with certain aspects of laboratory work.

Family

- My husband (bab’ Sphamandla Xulu), thank you for your unconditional love and unwavering support. You have been a pillar of strength throughout this journey and always motivated me to achieve what seemed to be insurmountable. I cannot thank you enough.
- My daughter (Faith Nothando Xulu), thank you for bringing so much joy and laughter into our lives, I so appreciated time spent with you, answering your questions about my work and the many cups of tea and biscuits!

- My parents (Philistas and Tshabane Thabethe and Makhosi Zwane) for your prayers, support and encouragement and for always believing in me.
- My siblings (Katlego and Karabo Thabethe and Blessing Xulu) believing in me and giving me the courage to continue.
- The rest of my family members, I cannot mention you all by name but thank you for always supporting and cheering me on.
- Every Nation Rosebank family for the support, encouragement and prayers offered throughout the journey and helping to maintain my sanity.

Finally, but not least, I would like to thank the Lord for giving the strength and courage to pursue this and persevere. All the glory belongs to you.

Dedication

I dedicate this work to my late grandparents whom I wish could have lived to see this day.

In loving memory of;

Thomas Thabethe

1932-1992

Christina Malekane

1951-2008

Jacobeth Thabethe

1938-2012

Mashilo Malekane

1948-2018

List of Abbreviations

Abbreviation	
%	Percent
A	Apoptotic cell
ACTB	Actin beta
ACS	Acute coronary syndrome
ADP	Adenosine diphosphate
AMP	Adenosine monophosphate
ATP	Adenosine triphosphate
ADH	Antidiuretic hormone
ATCC	American Type Culture Collection
Ana	Anastrozole
AnaAspClop	Anastrozole and Aspirin and Clopidogrel
AnaAto	Anastrozole and Atopaxar
C19	Androgens
APT	Antiplatelet therapy
Apo.B	Apoptotic body
ATAC	Arimidex (Anastrozole) and tamoxifen, alone or in combination
AIs	Aromatase inhibitors
AspClop	Aspirin and Clopidogrel
Ato	Atopaxar
ACTIVE-A	Atrial Fibrillation Clopidogrel Trial with Irbesartan for Prevention of Vascular Events
B	Bleb
BMP	Bone morphogenetic protein
Ca^{2+}	Calcium
CD	Cluster of differentiation
CXCR4	Chemokine receptor 4
C27 sterol	Cholesterol
COMMIT	Clopidogrel and Metoprolol Myocardial Infarction Trial
CHARISMA	Clopidogrel for High Atherothrombotic Risk and Ischemic Stabilization, Management and Avoidance
CREDO	Clopidogrel for The Reduction of Events During Observation
CURE	Clopidogrel in Unstable Angina to Prevent Recurrent Events Trial
CAPRIE	Clopidogrel versus Aspirin in Patients at Risk of Ischaemic Events
Cmax	Concentration maximum
cDNA	Complementary deoxyribonucleic acid
CAD	Coronary artery disease
COX	Cyclo-oxygenase
CXCL12	Stromal cell derived factor
cAMP	Cyclic adenosine monophosphate
D	Cell debris
DVT	Deep vein thrombosis
DTS	Dense tubular system
DMSO	Dimethyl sulfoxide

DAPT	Dual Antiplatelet Therapy
DMEM	Dulbecco's Modified Essential Medium
E2	17-β-oestradiol
EDTA	Ethylenediaminetetraacetic acid
EGF	Epidermal growth factor
EGFR	Epidermal growth factor receptor
EMT	Epithelial mesenchymal transition
ERBB2	Receptor tyrosine-protein kinase erbB-2
ELAPSE	Evaluation of Long-Term Clopidogrel Antiplatelet and Systemic Anti-Inflammatory Effects
ECM	Extracellular matrix
FBS	Fetal Bovine Serum FBS
Fi	Filopodia
Fig	Figure
FA	Formaldehyde
g	Centrifugal force
Glut	Glutaraldehyde
FACT	Fulvestrant combined with anastrozole clinical trial
GAPDH	Glyceraldehyde 3-phosphate Dehydrogenase
gMFI	Geometric mean fluorescence intensity
GP	Glycoprotein
HCl	Hydrochloric acid
Hepes	Hydroxyethyl piperazineethanesulfonic
HMDS	Hexamethyldisilazane
Hrs	Hours
IDT	Integrated DNA technologies
IFN	Interferon
IPA	Index of platelet activation
IP3	Inositol triphosphate
INT	Iodonitrotetrazolium
IL	Interleukin
JAK-STAT	Janus kinase signal transducer and activator of transcription
J-LANCELOT	Japanese Lessons from Antagonizing the Cellular Effects of Thrombin
LDH	Lactate dehydrogenase
LANCELOT-CAS	Lessons for Antagonizing the Cellular Effect of Thrombin-Acute Coronary Syndrome
LPS	Lipopolysaccharides
LAMPs	Lysosomal membrane proteins
MHC1	Major histocompatibility complex class 1
MMPs	Matrix metalloproteinases
MCF7	Michigan Cancer foundation
Mins	Minutes
ml	Millilitre
MI	Myocardial infarction
N	Necrotic cell
NK	Natural killer

NR	Neutral red
ng	Nanogram
nm	Nanometer
NSAIDs	Non-steroidal anti-inflammatory drugs
NF-kβ	Nuclear factor-kappa-beta
ER	Oestrogen receptor
OCS	Open canalicular system
PAST	Paleontological statistics software
PBS	Phosphate buffered saline
PIP2	Phosphatidylinositol4, 5-bisphosphate
PDGF	Platelet derived growth factor
PF4	Platelet factor 4
PMPs	Platelet microparticles
Po	Pore
PgR	Progesterone receptor
C21	Progestogens
PI	Propidium iodide
PgH_2	Prostaglandin endoperoxide
PGG_2	Prostaglandin-G_2
PGH_2	Prostaglandin-H_2
PAR1	Protease activated receptor
PS	Phosphatidylserine
Ps	Pseudopodia
PE	Pulmonary embolism
R	Round viable cell
RUTH	Raloxifene Use for The Heart
RT-qPCR	Real time polymerase chain reaction
RA-FLS	Rheumatoid Arthritis
RNA	Ribonucleic acid
RT	Room temperature
RPLO	Ribosomal protein
rpm	Revolutions per minute
Ru	Ruffled membrane
SEM	Scanning electron microscopy
SPS3	Secondary Prevention of Small Subcortical Stroke
SERMs	Selective oestrogen receptor modulators
SWOG	South Western Oncology Group
STIM1	Stromal Interaction Molecule 1
SA-PE	Streptavidin, R-Phycoerythrin
TGFβ	Transforming growth factor-β
TRAP	Thrombin receptor activating peptide
TXA_2	Thromboxane A_2
TF	Tissue factor
TRITON-TIMI38	TRial to assess Improvement in Therapeutic Outcomes by optimizing platelet inhibitioN with prasugrel Thrombolysis In Myocardial Infarction 38

TME	Tumour microenvironment
TNFα	Tumour necrosis factor-α
TCIPA	Tumour-cell induced platelet aggregation
µg	Microgram
µl	Microlitre
µM	Micromolar
V	Volts
VEGF	Vascular endothelial growth factor
VTE	Venous thromboembolism
vWF	Von Willebrand factor
Wnt	Wingless-related integration site
WST	Water soluble tetrazolium

List of Figures

		Page no.
Figure 2.1	Scatterplots showing gating strategy for Annexin V/Propidium iodide staining for cell death	46
Figure 2.2	Schematic diagram illustrating the exposed area at the centre of the well following scraping of the cell monolayer with a pipette tip	48
Figure 2.3	Cell growth analysis for MCF7 and T47D cells.	50
Figure 2.4	Neutral Red (NR) viability assay in MCF7 and T47D cells following treatment	52
Figure 2.5	Representative photomicrographs of neutral red dye staining on MCF7 (A1-7) and T47D (B1-7) cells	53
Figure 2.6	Lactate dehydrogenase (LDH) cytotoxicity assay in MCF7 and T47D cells following treatment	54
Figure 2.7	Cytotoxicity in MCF7 and T47D cells as indicated by flow cytometry	55
Figure 2.8	Representative micrograph showing ultrastructural features in MCF7 and T47D cells	62
Figure 2.9	Representative micrographs showing ultrastructural changes following exposure to Anastrozole and Aspirin-Clopidogrel cocktail	63
Figure 2.10	Representative micrographs showing ultrastructural changes following exposure to Anastrozole and Atopaxar	64
Figure 2.11	The closure rate in breast cancer cells following 24 hrs treatment with Anastrozole and Antiplatele drugs: Ana, AnaAspClop, AspClop, AnaAto and Ato.	68
Figure 2.12	Representative micrographs showing the change in area following a scratch assay to measure the rate of cell migration rate in breast cancer cells (MCF7)	69
Figure 2.13	Representative micrographs showing the change in area following a scratch assay to measure the rate of cell migration rate in breast cancer cells (MCF7) following a 24 hrs treatment	70
Figure 2.14	Representative micrographs showing the change in area following a scratch assay to measure the rate of cell migration rate in breast cancer cells (T47D) following a 24 hrs treatment	71
Figure 2.15	Cell proliferation as measured by the WST-1 assay following a 24 hrs treatment period	72
Figure 2.16	An overview of chapter two and summary of main findings.	81
Figure 3.1	Representative scatter plots and histogram depicting the spread of whole blood	107
Figure 3.2	Scatterplots showing gating strategy used to investigate changes in expression levels of activation markers	108
Figure 3.3	Box and whisker plots showing thrombin activity following whole blood exposure to breast cancer cells (MCF7 and T47D)	116

Figure 3.4	Platelet activation in controls (whole blood only and whole blood exposed to untreated or DMSO-treated MCF7 and T47D cells), as shown by CD62p and CD63 IPA and the corresponding morphological changes.	119
Figure 3.5	Box and whisker plots representing CD62p IPA (A1-D1) and CD63 (A2-D2) IPA in untreated whole blood (WB) and whole blood exposed to untreated and DMSO treated MCF7 and T47D cells between intervals	122
Figure 3.6	Platelet activation in whole blood exposed to MCF7 and T47D cells treated with Anastrozole (Ana) alone and in combination with antiplatelet therapy drugs	127
Figure 3.7	Box and whisker plots representing CD62p IPA in whole blood exposed to MCF7 and T47D cells	128
Figure 3.8	Box and whisker plots representing CD63 IPA in whole blood exposed to MCF7 and T47D cells	129
Figure 3.9	Platelet activation in whole blood exposed to MCF7 and T47D cells treated with Anastrozole (Ana) alone and in combination with antiplatelet therapy drug	133
Figure 3.10	An overview of chapter 3 and summary of key findings.	147
Figure 4.1	Gene expression of EMT markers in controls	166
Figure 4.2	Gene expressions of EMT markers in breast cancer cells (MCF7 and T47D cells) following treatment	171
Figure 4.3	Gene expressions of EMT in breast cancer cells (MCF7 and T47D cells) following treatment	172
Figure 4.4	An overview of chapter 4 and summary of key findings.	198
Figure 5.1	An overview of chapter 5 and summary of key findings.	209
Figure 5.2	A representative electron micrograph displaying a platelet plug	211

List of Tables

		Page no.
Table 2.1	A summary of the effects of antiplatelet therapy drugs; Aspirin, Clopidogrel and Atopaxar on cancer outcome.	35
Table 2.2 A	Treatment groups used to establish optimal drug concentrations	41
Table 2.2 B	The Cmax concentrations used to prepare each drug combination	41
Table 2.3	Scoring criteria used to investigate morphological changes following exposure to combined Anastrozole and antiplatelet therapy for 24 hours.	44
Table 2.4	Semi-quantitative analysis of morphological features noted in MCF7 and T47D cells following 24hour treatment with combined Anastrozole and antiplatelet therapy	61
Table 3.1	Thrombin concentration (ng/ml) detected following whole blood exposure to MCF7 and T47D cells treated with Anastrozole (Ana) alone and in combination with antiplatelet therapy drugs	112
Table 3.2	The relationship between CD62p and CD63 IPA represented by Spearman correlation value (r) and corresponding regression analysis (r^2)	140
Table 4.1	Primer sequences used for quantitative real-time polymerase chain reaction (qPCR)	161
Table 4.2	The assay working range is presented below and delineates the range at which cytokine levels were detected by the assay	165
Table 4.3	Detected cytokine levels (ng/ml) in whole blood following exposure to breast cancer cells treated with Anastrozole (Ana), Anastrozole+Aspirin+Clopidogrel (AnaAspClop) and Aspirin+Clopidogrel cocktail (AspClop).	175
Table 4.4	Detected cytokine levels (ng/ml) in whole blood following exposure to breast cancer cells treated with Anastrozole (Ana), and Atopaxar (Ato)	176
Table 4.5	Detected cytokine levels (ng/ml) in whole blood following exposure to breast cancer cells treated with Anastrozole (Ana), and Aspirin+Clopidogrel (AspClop).	177
Table 4.6	Detected cytokine levels (ng/ml) in whole blood following exposure to breast cancer cells treated with Anastrozole (Ana), and Atopaxar (AnaAto).	178

Contents

Declaration i

Abstract ii

Presentations and publications arising from this work iv

Acknowledgements v

Dedication x

List of Abbreviations xi

List of Figures xv

List of Tables xvii

CHAPTER I: General introduction 1

1.1 The prevalence of breast cancer 1

1.2 The relationship between thrombosis and cancer 3

1.3 Background on platelets and thrombosis 5

1.4 Breast cancer and hypercoagulation in the cancer microenvironment 9

1.5 The role of anti-platelet therapy in thromboembolic disease 12

1.6 The role of hormone therapy in breast cancer and thromboembolic disease 14

1.7 Rationale 16

1.8 Aims and objectives 17

1.8.1 Aims 17

1.8.2 Objectives 17

CHAPTER II: Cytotoxic Effects of Anastrozole & Antiplatelet Therapy 19

2.1 Introduction 19

2.1.1 Properties of breast cancer cell lines and their limitations 19

2.1.2 Drug metabolism *in vitro* 22

2.1.3 Hormone therapy in breast cancer 23

2.1.4 The interactions between antiplatelet drugs and breast cancer cells 25

2.1.5 The effect of combined hormone and antiplatelet therapy on breast cancer cells 32

2.2 Materials and methods 38

2.2.1 Cell culture 38

2.2.2 Cell growth assay 39

2.2.3 Drug treatment.....39
2.2.4 Lactate dehydrogenase assay.....41
2.2.5 Neutral red assay.....42
2.2.6 Scanning electron microscopy.....43
2.2.7 Annexin-V and Propidium Iodide Apoptosis Assay.....45
2.2.8 Statistical analysis for LDH assay, NR assay, SEM and Annexin-V/ PI assay.....46
2.2.9 Scratch assay for migration assessment.....47
2.2.10 WST-1 proliferation assay.....48
2.3 Results.....49
2.3.1 Cell growth analysis.....49
2.3.2 Drug toxicity on breast cancer cells by assessing various parameters.....51
2.3.2 Migration and cell proliferation.....65
2.4 Discussion.....73
2.5 Conclusion.....80
CHAPTER III: Hypercoagulation in response to Anastrozole and antiplatelet-treated breast cancer cells.....82
3.1. Introduction.....82
3.1.1 Platelet structure and physiology.....83
3.1.2 Deciphering the mechanism of platelet activation.....86
3.1.2.1 The role of agonists in facilitating platelet activation.....87
3.1.2.2 Early events of platelet activation.....88
3.1.2.3 The role of CD62p in coagulation and cancer.....91
3.1.2.4 The role of CD63 in coagulation and cancer.....92
3.1.2.5 The coagulation cascade.....93
3.1.2.6 Tumour cell and platelet interactions.....94
3.1.3 The role of hormone and antiplatelet therapy in hypercoagulation.....97
3.1.5 Aims and objectives.....100
3.2 Materials and Methods.....101
3.2.1 Patient recruitment and demographics.....101
3.2.1.1 Ethics.....101
3.2.1.2 Exclusion criteria.....101
3.2.1.3 Blood collection.....101
3.2.2 Whole blood and breast cancer cell exposure.....102

3.2.2.1 Blood cell exposure 102
3.2.2.2 Whole blood storage for thrombin assay 102
3.2.2.3 Whole blood lysis 102
3.2.2.4 Preparation of flow cytometry controls 102
3.2.2.5 Lysed whole blood preparation for morphological studies 103
3.2.3 Thrombin activity assay 103
3.2.3.1 Quantifying thrombin release in whole blood 103
3.2.3.2 Data analysis 103
3.2.4 Detection of platelet activation markers 104
3.2.4.1 Labelling of lysed whole blood with activation markers 104
3.2.4.2 Flow cytometry 105
3.2.4.3 Gating strategy 105
3.2.4.4 Data analysis 109
3.2.5 Platelet morphology 109
3.3 Results 111
3.3.1 Assessment of thrombin activity in whole blood conditioned with breast cancer cells 111
..... 116
3.3.1 Assessment of platelet activation 117
3.3.1.1 Hypercoagulation in control groups 117
3.3.1.2 Anastrozole mediated hypercoagulation 123
3.3.1.3 Anastrozole combined with Aspirin and Clopidogrel cocktail mediated hypercoagulation 124
3.3.1.4 Anastrozole and Atopaxar mediated hypercoagulation 131
3.3.1.5 Platelet activation results summary 135
3.3.1.6 Assessment of $CD62p^+/CD63^+$ events on $CD41a^-$ events 136
3.3.1.7 The relationship (correlation) between CD62p and CD63 137
3.4 Discussion 141
3.5 Conclusion 146
Chapter IV: Reciprocal interactions between vascular components and breast cancer cells in facilitating tumour progression 148
4.1 Introduction 148
4.1.1 Epithelial to Mesenchymal transitions during tumour progression 148
4.1.2 Cytokine mediated communication during tumour progression 153

4.1.3 Aims and objectives 158
4.2 Materials and methods 159
4.2.1 Gene expression using real-time qPCR 159
4.2.4 Cytokine assays 162
4.2.4.1 Sample acquisition and preparation 162
4.2.4.2 Inflammation panel 162
4.2.4.3 TGFβ isoforms detection 163
4.3 Results 166
4.3.1 Gene expression to elucidate epithelial to mesenchymal transition 166
4.3.1.1 Gene expression in controls 167
4.3.1.2 Gene expression in breast cancer cells treated with Anastrozole exposure to whole blood 167
4.3.1.3 Gene expression in breast cancer cells treated with Anastrozole, Aspirin and Clopidogrel and exposed to whole blood 168
4.3.1.4 Gene expression in breast cancer cells treated with Anastrozole and Atopaxar and exposure to whole blood 169
4.3.1.4 Summary of gene expression findings 170
4.3.3 Cytokine analysis 173
4.3.3.1 Overall cytokine secretion 173
4.3.3.2 Cytokine secretion in controls 179
4.3.3.3 Anastrozole-mediated cytokine secretion 180
4.3.3.4 Aspirin and Clopidogrel-mediated cytokine secretion with or without Anastrozole 181
4.3.3.5 Atopaxar-mediated cytokine secretion with or without Anastrozole 183
4.3.3.6 Summary of cytokine secretion findings 185
4.4 Discussion 186
4.5 Conclusion 197
Chapter V: General conclusion 199
5.1 Introduction and rationale 199
5.2 Findings 200
5.2.1 Anastrozole-mediated effects 200
5.2.2 Anastrozole combined with Aspirin and Clopidogrel-cocktail mediated effects 203
5.2.3 Anastrozole and Atopaxar mediated effects 206
5.3 Limitations of the study and future perspectives 209
5.3.1 Limitations 209

5.3.2 Future perspectives 211
5.4 Concluding remarks 213
References 215
APPENDICES 246
APPENDIX A: Chapter II supplementary information 246
A1: Drug preparation 246
A2: Cytotoxicity parameters statistical output (Neutral Red assay, Lactate Dehydrogenase assay, Annexin-V/PI assay) 250
A2.1 Titration for Annexin-V and PI 250
A2.2: Statistica outcome for MCF7 cells 251
A3: Scanning Electron Microscopy statistical output 256
A4.1: Scratch assay supplementary images 259
A4.2: Scratch assay supplementary images 260
A4.3: PAST Friedman output for migration assay within cell lines 261
A4.4: PAST Friedman output within each treatment group at different time points 262
A4.6: PAST output for migration assay at matched treatments between cell lines 266
A5: PAST output for cell proliferation data 268
APPENDIX B: Chapter III supplementary information 269
B1: Ethics document 269
B2: Solutions 270
B3: Thrombin activity output PAST Friedman test and Wilcoxon post hoc 271
B4.1: Compensation control (Part A) 272
B4.1: Compensation control (Part B) 273
B4.2: Titration controls 274
B4.3: FMO controls (Part A) 275
B4.3: FMO controls (Part B) 276
B4.4: Total IPA 277
B4.5: CD62p Intervals (1-2) 278
B4.6: CD62p Intervals (3-4) 280
B4.7: CD63 Intervals (1-2) 282
B4.8: CD63 Intervals (3-4) 284
APPENDIX C: Chapter IV supplementary information 286
C1: RNA concentration and purity 286
C2.1: Gene expression statistics 288

C2.2: Statistics output *TGFβ1* expression 290
C2.3: Statistics output *Vimentin* expression 292
C2.4: Statistics output *N-cadherin* expression 294
C2.5: Statistics output *E-cadherin* expression 296
C3.1: Cytokine standards preparation 298
C3.2: Cytokine statistics output 1 300
C3.3 Cytokine statistics output 2 302
C3.4: Cytokine statistics output 3 304
C3.5: Cytokine statistics 4 306
APPENDIX D: General documents 307
D1.1: Plagiarism declaration 307
D1.2: Turn it in report summary 308
D1.3: Proof of manuscript acceptance 309

CHAPTER I: General introduction

1.1 The prevalence of breast cancer

Breast cancer is the most commonly diagnosed cancer in women worldwide and it causes the most cancer deaths in comparison to other cancers (Kruger and Apffelstaedt, 2009; Youlden *et al.*, 2012). In 2015, 2.4 million new breast cancer diagnoses were noted in women (Adeloye *et al.*, 2018; Azamjah, Soltan-Zadeh and Zayeri, 2019). In Southern Africa, 39 in 100 000 women were diagnosed with breast cancer, according to the International Agency for Cancer Research in 2012 (Ferlay *et al.*, 2015; Jedy-Agba *et al.*, 2016). The burden of breast cancer is estimated to double by 2030 due to various factors such as ageing , population growth and unhealthy lifestyles (Adeloye *et al.*, 2018).

In South Africa, breast cancer incidence has surpassed cervical cancer and is now the most commonly diagnosed cancer in women (Vorobiof, Sitas and Vorobiof, 2001; Kruger and Apffelstaedt, 2009; Singh *et al.*, 2017). Historically cervical cancer was the most commonly diagnosed cancer in women in South Africa but breast cancer has emerged as the leading cancer in South Africa, reflecting the global trend and highlighting the urgency to better understand this disease (Vorobiof *et al.,* 2001; Kruger and Apffelstaedt, 2009; Singh *et al.*, 2017). Breast cancer is still poorly managed in low to middle income countries and results in higher mortality rates compared to high income countries (Brinton *et al.,* 2017). Some of the factors responsible for this includes poor infrastructure and resources, less awareness, poor screening and diagnoses at later stage of disease (Adeloye *et al.*, 2018; Azamjah *et al.*, 2019).

Breast cancer was previously thought to be more prevalent in older, premenopausal and postmenopausal women; however, its prevalence in women younger than 35 years has

increased in recent years (Gabriel and Domchek, 2010; Assi *et al.,* 2013). Studies have shown that breast cancer is diagnosed at a more advanced stage and has a poorer prognosis in younger premenopausal women than older premenopausal women (Gabriel and Domchek, 2010; Assi *et al.,* 2013).

Breast cancer, although more common in women, has also been noted in men whereby it accounts for approximately 0.5-1% of all breast cancer cases (Giordano, 2005; Yalaza *et al.*, 2016). Ductal carcinoma is more common in males than females and it expresses hormone receptors such as oestrogen receptor (ER) and progesterone receptor (PgR) (Giordano, 2005). A similar treatment strategy to that used in female breast cancer cases is used to treat male breast cancer (Giordano, 2005). Breast cancer has a poorer prognosis in men than in women because it is often diagnosed at a more advanced stage (Yalaza *et al.*, 2016).

Breast cancer is a complex disease which displays molecular and morphological heterogeneity (Polyak, 2011; Eliyatkin *et al.*, 2015; Mota *et al.*, 2017). Differences observed within a single tumour are termed intratumoural heterogeneity (Kochel *et al.*, 2017; Mota *et al.*, 2017) and they determine risk for angiogenesis, invasion and metastasis (Polyak, 2011). These differences are driven by evolutionary principles such as cancer stem cell theory and clonal evolution (Martelotto *et al.*, 2014). The differences between tumours are termed intertumoural heterogeneity (Polyak, 2011; Eliyatkin *et al.*, 2015; Mota *et al.*, 2017). Traditionally breast cancer was classified according to its histopathological presentation but this classification has been modified and adapted to reflect the vast differences observed in breast cancer (Polyak, 2011; Eliyatkin *et al.*, 2015; Mota *et al.*, 2017). Molecular classification is now used to provide a thorough description of characteristics and determines treatment plans (Polyak, 2011; Eliyatkin *et al.*, 2015; Mota *et al.*, 2017). Intertumoural heterogeneity is

represented by the different molecular subtypes of breast cancer (Polyak, 2011; Mota *et al.*, 2017).

Breast cancer is broadly classified as luminal phenotype, human epidermal growth factor receptor 2 positive (HER2+) phenotype and basal-like phenotype (Yersal and Barutca, 2014; Tang and Tse, 2016). Each subtype exhibits unique characteristics and disease outcomes (Polyak, 2011; Mota *et al.*, 2017). Luminal phenotype tumours express hormone receptors (ER, PgR) and are commonly treated with hormone therapies (Kemp *et al.*, 2014; Tang and Tse, 2016; Hua *et al.*, 2018). $HER2^{+}$ tumours contain high amount of the oncogene for HER2 (ERBB2) and are thus managed by anti-HER2 therapies (Paik *et al.*, 2004; Allison, 2012; Yersal and Barutca, 2014). Basal-like tumours are associated with poor-prognosis because they lack hormone receptors and HER2 and respond poorly to chemotherapy (Polyak, 2011; Mota *et al.*, 2017). They do not have specific targeted therapy to manage them (Polyak, 2011; Mota *et al.*, 2017). In South Africa more than 60% of breast cancer cases among women are hormone dependant (Joffe *et al.*, 2018).

1.2 The relationship between thrombosis and cancer

Cardiovascular diseases are a leading cause of death in developing countries and they are characterised by arterial and venous thrombosis (Lima and Monteiro, 2013; Vinholt *et al.*, 2016; Matthews *et al.*, 2018). Arterial thrombosis leads to myocardial infarction (MI) and stroke whereas venous thrombosis leads to venous thromboembolism (VTE) and pulmonary embolism (PE) (Holinstat, 2012; Papaxoinis *et al.*, 2018). Phenotypically, arterial thrombosis consists of more platelets and occurs at a site of injury where there is high shear flow (Holinstat, 2012; Koupenova *et al.*, 2017). In contrast, venous thrombosis consists of more fibrin and erythrocytes, in addition to platelets, in low shear flow regions and occurs

independently of vessel injury. It is more commonly associated with cancer (Key *et al.*, 2016; Donnellan and Khorana, 2017; Koupenova s*et al.*, 2017).

Thrombosis is a common complication in cancer patients and it is the second leading cause of death following cancer itself (Phillips *et al.*, 2015; Fuentes, Palomo and Rojas, 2016; Donnellan and Khorana, 2017). Thrombosis is associated with poor prognosis because it reduces short-term and long-term survival in cancer patients (Haddad and Greeno, 2006; Phillips *et al.*, 2015; Papaxoinis *et al.*, 2018). Fibrin or platelet plugs in and around many types of tumours have been observed by histological analyses and this implies local activation of the coagulation process (Prandoni, Falanga and Piccioli, 2005). Thrombosis commonly represents the earliest clinical symptom of cancer and it may further be promoted by the effects of surgery, chemotherapy, radiotherapy, long-term bed rest or trauma (Haddad and Greeno, 2006;Renni *et al.*, 2017; Razak *et al.*, 2018).

Cancer patients are inherently pre-disposed to the development of VTE (Viale, 2005). VTE affects approximately 15- 32% of cancer patients, in contrast approximately 2.5% of non-cancer patients are affected by VTE (Fennerty, 2006; Key *et al.*, 2016). The risk for VTE differs according to the tumour type, for example breast cancer is associated with low risk for VTE whereas pancreatic, colorectal and prostate cancer is associated with higher risk (Fennerty, 2006; Key *et al.*, 2016). In addition, VTE is more aggressive in cancer patients and does not respond well to therapy against it; therefore, it reoccurs (Fennerty, 2006; Key *et al.*, 2016).

The pathophysiology of thrombosis involves abnormalities in blood contents (platelets and aberrant secretion of coagulation factors), the wall of blood vessels and blood turbulence (Choudhury *et al.*, 2007; Blann and Dunmore, 2011; Razak *et al.*, 2018). Cancer patients usually have abnormalities in all three components which then create a prothrombic state

(Choudhury *et al.*, 2007; Blann and Dunmore, 2011). A closer look at the cellular contents of the blood in an attempt to understand the pathophysiology of thrombosis reveals that platelets are the main cell type involved in creating a hypercoagulable state (Goubran *et al.*, 2013; Yun *et al.*, 2016). Platelets in cancer are hyperactive, their capacity for aggregation increases, and they secrete substances that activate the formation of a thrombus (Buergy *et al.*, 2012; Goubran *et al.*, 2013).

1.3 Background on platelets and thrombosis

Platelets are formed from the cytoplasm of megakaryocytes; they are small, anucleate haematopoietic cells (Broos *et al.*, 2011; Machlus and Italiano, 2013). They are known to play a major role of preventing blood loss by forming a plug on the surface of the damaged endothelium, a process known as haemostasis (Broos *et al.*, 2011; Mekaj, 2016). Their membrane is made up of phospholipids and includes glycoproteins and integrins that play an important role in platelet-mediated haemostasis (Broos *et al.*, 2011; Machlus and Italiano, 2013). The different membrane receptors include; glycoprotein Ib-IX-V (GPIb-IX-V), glycoprotein VI (GPVI) and glycoprotein IIb-IIIa (GpIIb- IIIa, also known as integrins αIIbβ3), these receptors are important for complete adhesion and aggregation (Clemetson, 2012; Xu *et al.*, 2016).

Platelets contain various internal granules such as dense, alpha and lysosomal granules (Golebiewska and Poole, 2015; Weber *et al.*, 2016). Dense granules contain platelet agonists that amplify platelet activation such as serotonin, calcium and ADP; whereas alpha granules contain proteins that enhance platelet activation and coagulation such as CD62p (P-selectin), fibrinogen, prothrombin (Golebiewska and Poole, 2015; Vélez and García, 2015; Weber *et al.*,

2016). Lysosomal granules store glycosidases and proteases (Golebiewska and Poole, 2015; Weber *et al.*, 2016).

Platelet activity is usually measured by studying the expression of surface epitopes such as CD63, CD62p, CD40L, GPIIb/ IIIa conformation, phosphatidylserine exposure, platelet-leukocyte conjugates and microparticles (Chirinos *et al.*, 2005; Choudhury *et al.*, 2007; Lu and Malinauskas, 2010; Muhammad *et al.,* 2013). CD41 (αIIb chain, platelet GPIIb) is the main cell surface antigen which is expressed on platelets and megakaryocytes (Slupsky *et al.*, 1997; Mitjavila-garcia *et al.*, 2002). It is associated with many proteins including CD9 and GPIIb/ IIa and a receptor for von Willebrand factor and thrombin, GPIbIIx (CD42b/CD42a) (Slupsky *et al.*, 1997). It forms the integrins GPIIb/IIIa (αIIbβ3) when it is associated with CD61 (β3 integrin, platelet GP IIIa) and subsequently plays a significant role in platelet activity (Mitjavila-garcia *et al.*, 2002). It also acts as a receptor for many adhesion molecules such as fibrinogen (Mitjavila-garcia *et al.*, 2002). In platelets, CD41 is found in an inactive state and only binds fibrinogen upon platelet activation (Mitjavila-garcia *et al.*, 2002).

Selectins are a family of carbohydrate binding proteins that facilitate the recruitment of various cell types from circulation (Barthel *et al.*, 2007; Coupland and Parish, 2014). The interaction between selectins and their ligands results in cells rolling on the endothelium due to hydrodynamic shear flow (Barthel *et al.*, 2007; Coupland and Parish, 2014). CD62p (P-selectin) is expressed on the cell membrane of α-granules and acts as an adhesion receptor to facilitate platelet binding to leukocytes during an inflammation reaction (Inkielewicz-Stepniak *et al.*, 2010; Lu and Malinauskas, 2010; Xu *et al.*, 2016). The membranes of α-granules within platelets express CD62p; however, following platelet activation it translocates

to the surface of platelets; as such a P-selectin specific monoclonal antibody can be used to identify activated platelets (Lu and Malinauskas, 2010; Polanowska-Grabowska *et al.*, 2010).

CD63 belongs to a group of proteins known as tetraspanins, so called because of their arrangement on the plasma membrane, they span the membrane four times (Pols and Klumperman, 2009; Saboor *et al.*, 2013). Tetraspanins play an important role in transmitting signals and facilitating communication between cells and the extracellular environment (Saboor *et al.*, 2013; Remšík *et al.*, 2018). CD63 is a component of platelet lysosomes and plays a role in protecting the plasma membrane from being degraded by lysosomal enzymes (Marquardt *et al.*, 2002; Pols and Klumperman, 2009; Muhammad *et al*., 2013). CD63 is expressed upon platelet activation and is one of the commonly used markers to indicate platelet activation, it was also shown to regulate the spreading of platelets (Van Der Zee *et al.*, 2006; Choudhury *et al.*, 2007; Muhammad *et al.,* 2013). CD62p and CD63 are commonly expressed during platelet activation (Hilberg *et al.*, 2003; Choudhury *et al.*, 2007; Navred *et al.*, 2019).

The coagulatory cascade, platelets and vessel wall components mediate the haemostatic process during vascular injury (Owens and MacKman, 2011; Orellana *et al.*, 2015). Platelet activation is initiated by agonist binding to its receptors on platelet membranes (Broos *et al.*, 2011; Li *et al.*, 2014a). This increases calcium concentration in the cytosol and subsequently activates downstream signalling pathways (Munnix *et al.*, 2009; Ghoshal and Bhattacharyya, 2014; Tomaiuolo, Brass and Stalker, 2017). Platelet activation is a complex process consisting of reversible and irreversible events, and displays heterogeneity (Tomaiuolo *et al.,* 2017). Platelet activation results in shape change, membrane budding, adhesion, aggregation,

release of granular contents and the synthesis of thromboxane, amongst other agonists (Choudhury *et al.*, 2007; Mammadova-Bach *et al.*, 2015; Tomaiuolo, Brass and Stalker, 2017).

Platelet activation and aggregation can be studied *in vitro* through various methods. Platelet aggregometry has traditionally been a commonly used method to study changes in platelets and how they relate to platelet disorders (Sharma and Berger, 2011; Filkova *et al.*, 2019). Platelet aggregometry functions by transmitting a light beam through a platelet suspension, to allow its absorption (Sharma and Berger, 2011; Filkova *et al.*, 2019). Aggregated platelets will allow more light to pass through, creating aggregation curves (Sharma and Berger, 2011; Filkova *et al.*, 2019). In contrast, resting platelets reflect light (Sharma and Berger, 2011; Filkova *et al.*, 2019).

Flow cytometry and electron microscopy are widely used methods to study platelet activation (Choudhury *et al.*, 2007; Pretorius, Engelbrecht and Duim, 2012; Augustine *et al.*, 2016). They are often the preferred methods because they enable the analysis of platelets in their physiological milieu (whole blood) and they are highly sensitive, with the capacity to detect as little as 1% of activated platelets (Choudhury *et al.*, 2007). Flow cytometry is a more modern technique and is commonly used to study changes in the receptor expression, for example the aforementioned glycoproteins, which allows for assessment of early activation (Kamel *et al.,* 2014; Wei *et al.*, 2015; Augustine *et al.*, 2016); its application has also been expanded to measure calcium release and the phosphorylation of signalling molecules (Clemetson, 2012; Lopez *et al.*, 2015; Orellana *et al.*, 2015). Platelet morphology is also a reliable method to study platelet activation and often studied ultrastructurally using a scanning electron microscope for surface changes and a transmission electron microscope for

viewing the internal granules (Pretorius *et al.,* 2012; Neumüller *et al.*, 2013; Wang *et al.*, 2015). These techniques collectively facilitate the accurate study of platelet activation.

1.4 Breast cancer and hypercoagulation in the cancer microenvironment

Hypercoagulation describes a state whereby chances of blot clotting are high, and this condition is often associated with pathological conditions such as cancer which disturbs the equilibrium in blood and thus changes its composition to promote hypercoagulation (Paskauskas *et al.,* 2008; Aschermann, 2013; Mekaj, 2016). Cancer cells promote hypercoagulation by secreting platelet agonists such as thromboxane A_2, ADP and thrombin; additionally, they are able to activate platelets by binding directly to them (Aschermann, 2013). The risk for VTE is 4-7 fold higher in cancer patients (Key *et al.*, 2016). Coagulation cascade consists of various proteins within blood which facilitate coagulation (Projahn and Koenen, 2012; Lima and Monteiro, 2013). It is initiated when FVIIa (activated Factor VII) binds to tissue factor, which via the conversion of pro-thrombin to thrombin facilitates the conversion of fibrinogen to fibrin (Projahn and Koenen, 2012; Lima and Monteiro, 2013). Cancer patients have higher levels of circulating blood coagulation proteins such as tissue factor and thrombin, which by facilitating platelet activation and aggregation aids in promoting tumour survival (Projahn and Koenen, 2012; Aschermann, 2013; Lima and Monteiro, 2013; Menter *et al.*, 2014; Phillips *et al.*, 2015).

The tumour microenvironment (TME) acts as a double-edged sword by facilitating tumour progression and hypercoagulation (Joyce and Pollard, 2009). Upon platelet-tumour cell interaction, inflammatory cytokines are released into the TME to mediate various functions (Pilatova *et al.,* 2012). The relation between breast cancer cells and platelets was shown to

promote cancer and coagulation (Labelle *et al.,* 2011; Lal *et al.,* 2013; Fuentes *et al.,* 2016; Leblanc and Peyruchaud, 2016). Tumour cells are capable of activating platelets by direct contact or by releasing mediators such as adenosine diphosphate (ADP), thrombin, thromboxane A2 or tumour associated proteinases (Falanga and Donati, 2001; Prandoni, Falanga and Piccioli, 2005; Haddad and Greeno, 2006; Aleskandarany *et al.*, 2014).

Cancer patients have elevated platelet counts (Bambace and Holmes, 2011). Platelet activation is elevated in the blood of cancer patients and upon activation, platelets expose certain antigens on their surface (e.g. P-selectin and CD63) releasing granular contents and aggregating (Choudhury *et al.*, 2007; Saboor, 2013; Xu *et al.*, 2016). The plasma of cancer patients has reduced levels of anti-thrombin, protein C and protein S, natural inhibitors of coagulation therefore creating favourable conditions for hypercoagulation to occur (Prandoni, Falanga and Piccioli, 2005; Gomes *et al.*, 2017). Platelet granules contain substances that play a role in tumour progression such as angiogenic factors; vascular endothelial growth factor (VEGF) and platelet derived growth factor (PDGF) (Heijnen and van der Sluijs, 2015). Activated platelets release IL-1β (Ruiz *et al.*, 2004) which is mainly contained in platelet microparticles (PMPs) and plays a role in engaging leukocytes (Boilard *et al.*, 2010).

Cancer cells release molecular mediators known as cytokines which promote and maintain a pro-inflammatory environment which promotes tumour survival (Golebiewska and Poole, 2015; Mekaj, 2016). Cancer cells may also secrete cytokines such as tumour necrosis factor-α (TNFα) and interleukin-1 (IL-1) which are pro-coagulant by activating endothelial cells and leukocytes (Mekaj, 2016; Chen *et al.*, 2018). Furthermore reciprocal interactions between cancer cells and blood components exist whereby platelets adhere to cancer cells shielding

them from immune detection and also release angiogenic cytokines which promote tumour survival (Golebiewska and Poole, 2015; Zhang *et al.*, 2017a; Chen *et al.*, 2018).

Platelets facilitate tumour progression and metastasis by promoting epithelial mesenchymal transition (EMT), matrix degradation, inducing angiogenesis and formation of leaky blood vessels to enable extravasation of tumour cells and tumour dissemination (Miyashita *et al.*, 2015a; Pang *et al.*, 2015; Guillem-Llobat *et al.*, 2016). Angiogenesis is an important process during cancer formation and propagation as it promotes the formation of new blood vessels (Li *et al.*, 2014; Plantureux *et al.*, 2018). Platelets play an important role in angiogenesis and their alpha-granules contain various angiogenic proteins which facilitate this function such VEGF, PDGF and epidermal growth factor (EGF) (Blair and Flaumenhaft, 2009). VEGF is the main angiogenic factor and its secretion is elevated when tumour cells express IL-6, IL-1 and TNFα (Viale, 2005; Li *et al.*, 2014; Plantureux *et al.*, 2018a).

Platelet granules contain high amounts of transforming growth factor-β (TGFβ) which is secreted upon platelet activation (Labelle *et al.,* 2011; Miyashita *et al.*, 2015b). Reciprocal interactions between cancer cells and platelets was shown to mediate an EMT as shown by increased levels of TGFβ1 signalling and downstream signalling genes such as *N-cadherin* and *vimentin* (Xu *et al.,* 2009; Labelle *et al.,* 2011; Miyashita *et al.*, 2015b).

Weibel-palade bodies found in endothelial cells constitutively express CD62p (P-selectin), which is released promptly in response to inflammatory mediators including thrombin (Valentijn *et al.*, 2010; Mccormack *et al.*, 2017; Joffe *et al.*, 2018). Selectins have been shown to play a role in the progression of cancer in a process known as “leukocyte mimicry” during which selectin ligands are expressed on tumour cells in order to facilitate their migration and metastasis (Coupland and Parish, 2014; Tesfamariam, 2016). Platelet activation facilitates

their interaction with endothelial cells, leukocytes and cancer cells by means of adhesion (Munnix *et al.*, 2009; Saboor *et al.*, 2013).

The microenvironment plays an important role in determining response to therapy and disease progression (Polyak, 2011; Martelotto *et al.*, 2014). Cancer treatment is multi-modal in order to effectively target different aspects of tumour and starts from general e.g. radiation, chemotherapy to targeted or specific like hormone therapy (Mota *et al.*, 2017).

1.5 The role of anti-platelet therapy in thromboembolic disease

There are three main pathways that are involved in platelet activation during thrombosis, namely cyclo-oxygenase (COX-1) facilitated by thromboxane A_2 (TXA_2) synthesis, ADP facilitated by the P2Y12 receptors and thrombin facilitated by the protease activated receptor (PAR1) (Tello-Montoliu *et al.*, 2011; Yun *et al.*, 2016). Aspirin (acetylsalicyclic acid) has been used as an anti-inflammatory drug since the 1980s (Rao and Knaus, 2008; Awtry and Loscalzo, 2014; Bruno *et al.*, 2018). It was discovered to have antiplatelet activity about 70 years following its first use (Rao and Knaus, 2008; Awtry and Loscalzo, 2014; Bruno *et al.*, 2018). Aspirin acts by disturbing the biosynthesis of cyclic prostanoids including thromboxane A_2 (TXA_2), prostacyclin and other prostaglandins (Rao and Knaus, 2008; Awtry and Loscalzo, 2014; Bruno *et al.*, 2018). Aspirin blocks the enzymes responsible for catalysing the synthesis of TXA_2 from arachidonic acid, COX-1 (Ferreiro and Angiolillo, 2012; Maity *et al.*, 2015; Bruno *et al.*, 2018). Under physiological conditions, TXA_2 binds to thromboxane and prostaglandin endoperoxide (TP) receptors and causes platelets to change shape (Tello-Montoliu *et al.*, 2011; Ferreiro and Angiolillo, 2012). It also helps in the recruitment and aggregation of platelets (Tello-Montoliu *et al.*, 2011; Ferreiro and Angiolillo, 2012).

Thienopyridines is a family of non-direct, antiplatelet agents that bind irreversibly to platelet ADP P2Y12 receptors and consists of three clinically approved drugs namely; ticlopidine, clopidogrel and prasugel (Passacquale and Ferro, 2011; Eikelboom *et al.*, 2012). Activation of the P2Y12 pathway plays a main role in platelet aggregation (Passacquale and Ferro, 2011; Eikelboom *et al.*, 2012). ADP activates platelets through the P2Y1 and P2Y12 receptors (Jennings, 2009; Wiviott *et al.*, 2011). Clopidogrel is a prodrug that is metabolised in the liver and converted to its active metabolite (Maguire *et al.*, 2007; Yi *et al.*, 2016). It blocks the ADP P2Y12 platelet receptor in an irreversible manner (Maguire *et al.*, 2007; Yi *et al.*, 2016).

The dual administration of antiplatelet therapy with Aspirin and Clopidogrel is often recommended in certain conditions such as coronary syndromes and myocardial infarction (Capodanno *et al.,* 2013; Roop *et al.*, 2013; Roe *et al.*, 2016). Studies have shown that dual treatment with Clopidogrel and Aspirin is beneficial in preventing the reoccurrence of atherothrombosis (Capodanno *et al.,* 2013; Roop *et al.*, 2013; Roe *et al.*, 2016). Dual antiplatelet therapy with aspirin and a P2Y12 receptor inhibitor though effective, does not affect other platelet activation pathways (Capodanno *et al.,* 2013; Roop *et al.*, 2013; Roe *et al.*, 2016). Antiplatelet drugs such as Aspirin and Clopidogrel inhibit platelet activation and are effective agents against cardiovascular disease such as acute coronary syndrome (ACS) and coronary artery disease (CAD) (Capodanno *et al.,* 2013; Roop *et al.*, 2013; Roe *et al.*, 2016).

Thrombin is a potent agonist for platelet activation and an important component of the coagulation cascade (Holinstat *et al.*, 2009; Han *et al.*, 2011; Moschonas *et al.,* 2015). There are currently two orally administered thrombin receptor antagonists (Vorapaxar and Atopaxar), which selectively block the platelet protease-activated receptor-1 (PAR1) receptor

subtypes (Holinstat *et al.*, 2009; Han *et al.*, 2011; Moschonas *et al.,* 2015). Vorapaxar is in phase III whereas Atopaxar is in phase II clinical development (Tello-Montoliu *et al.*, 2011; Moschonas *et al.,* 2015; Flaumenhaft *et al.*, 2018)

1.6 The role of hormone therapy in breast cancer and thromboembolic disease

Oestrogen binding to the oestrogen receptor (ER) activates the receptor and subsequently promotes the growth and survival of normal and cancerous breast epithelial cells (Campagnoli *et al.*, 2013; Haldosén *et al.,* 2014; Dupuis *et al.*, 2019). Upon activation, the ER binds to gene promoters in the nucleus in order to activate genes that play a role in cell division, inhibition of cell death, angiogenesis and protease activity (Campagnoli *et al.*, 2013; Haldosén *et al.,* 2014; Dupuis *et al.*, 2019). Therefore, interruption of oestrogen-dependent processes which play a role in the development and progression of breast cancer is a key target for hormone therapy (Campagnoli *et al.*, 2013; Haldosén *et al.,* 2014; Dupuis *et al.*, 2019).

Aromatase inhibitors (AIs) are the most widely used hormone therapies in the treatment of breast cancer (Puhalla *et al.,* 2012; Lumachi *et al.*, 2013). The efficacy of AIs has been shown in postmenopausal women with advanced breast cancer, hormone-naive women and in women who have experienced failure of tamoxifen alone or in combination with other hormonal agents (Puhalla *et al.,* 2012; Lumachi *et al.*, 2013).

There are three generations of AIs that have been developed thus far (Fabian, 2007; Lumachi *et al.*, 2013). The specificity to the aromatase enzyme has increased with each generation and side effects have reduced (Fabian, 2007; Lumachi *et al.*, 2013). Third generation AIs are

superior to first and second generation AIs because they suppress aromatase activity more (~98%) and they are associated with less side effects (Fabian, 2007; Lumachi *et al.*, 2013).

Third generation AIs are classified into two categories, steroidal AIs (such as Exemestane) and they bind to the aromatase enzyme irreversibly and non-steroidal AIs (such as Anastrozole and Letrozole) which bind to aromatase enzyme in a reversible manner (Smollich *et al.*, 2010; Geisler, 2011; Kemp *et al.*, 2014). All third generation AIs are taken daily orally (Smollich *et al.*, 2010; Geisler, 2011; Kemp *et al.*, 2014). AIs are more effective in postmenopausal women, because in premenopausal women there is a high amount of aromatase substrate in the ovary, and the aromatase promoter in the ovaries is sensitive to gonadotrophins, which are increased following intake of AIs (Smollich *et al.*, 2010; Geisler, 2011; Kemp *et al.*, 2014). Therefore AIs in premenopausal women are administered with an inhibitor of gonadotrophins such as luteinizing hormone-releasing hormone in order to decrease hormone levels (Fabian, 2007; Smollich *et al.*, 2010; Geisler, 2011; Kemp *et al.*, 2014).

A recent study compared the use of AIs (Anastrozole, Letrozole and Exemestane) in post-menopausal women with breast cancer and found that anastrozole was associated with the highest disease-free survival rate at 5 years of 90%, followed by Letrozole (89%) then Exemestane (88%) (De Placido *et al.,* 2018). All these Ais were associated with adverse musculoskeletal effects; furthermore, Anastrozole and Letrozole induced hypercholesterolaemia whereas Exemestane adversely affected the gastrointestinal tract (De Placido *et al.,* 2018). Another study found no significance difference in recurrence rate ratio of these Ais; Anastrozole (0.71), Exemestane (0.67) and Letrozole (0.73) compared to Tamoxifen, thus suggesting there was no difference in efficacy (Dowsett *et al.,* 2015).

Third generation AIs are currently the treatment of choice for first line treatment against metastatic hormone receptor-positive tumours (Lumachi *et al.*, 2013; Cuzick *et al.*, 2014; Kemp *et al.*, 2014). They are widely used in postmenopausal women prior to and post-surgery for ER-positive and/or progesterone receptor (PgR)-positive breast cancer (Lumachi *et al.*, 2013; Cuzick *et al.*, 2014; Kemp *et al.*, 2014). AIs are associated with lower risk for deep vein thrombosis (DVT), compared to other classes of hormonal therapy such as selective oestrogen receptor modulators (SERMs) for example Tamoxifen which increases the risk for DVT and pulmonary embolism (PE) by approximately 2- fold (Lumachi *et al.*, 2013; Cuzick *et al.*, 2014; Kemp *et al.*, 2014). Arimidex (Anastrozole) and Tamoxifen, alone or in combination (ATAC) study showed that Anastrozole alone reduced VTE risk in comparison to Tamoxifen alone (Haddad and Greeno, 2006). Although the risk might be reduced on Anastrozole, it is still greater compared to healthy, untreated women (Haddad and Greeno, 2006).

1.7 Rationale

Breast cancer patients are predisposed to thromboembolic incidences and hormone therapy has been shown to further increase the risk (Haddad and Greeno, 2006; Papaxoinis *et al.*, 2018; Gervaso *et al.*, 2019). The efficacy of antiplatelet therapy in thromboembolic disorders is well known (Jennings, 2009; Tello-Montoliu *et al.*, 2011; Roop *et al.*, 2013) and thus it may reduce the risk and occurrence of thromboembolic incidence when combined with hormone therapy in breast cancer patients. The reciprocal interactions between breast cancer cells and vascular components determine disease outcome (Lee and Levine, 2003; Palumbo, 2008; Fuentes *et al.,* 2016; Waldron *et al.*, 2019), therefore our study approach was focused at understanding both components. Therefore, this study was undertaken to investigate the effects of antiplatelet drugs combined with hormone therapy commonly used to treat luminal breast cancer: Anastrozole in breast cancer cells (MCF-7 and T47D cell lines). This study is

significant because there are currently no *in vitro* studies that have compared the combined effects of Anastrozole with Antiplatelet drugs; Atopaxar (alone) or Aspirin and Clopidogrel cocktail on breast cancer related thrombosis. The outcomes from this study will add new knowledge which may be useful in improving the management of cancer-related thrombosis and ultimately improve quality of life. Furthermore, the findings will inform future studies regarding the possible benefits or adverse effects of the tested antiplatelet therapies on breast cancer progression and inform strategies to maximise the beneficial effects of these antiplatelet therapies alone and when combined with Anastrozole as possible novel therapies for cancer and or thrombosis.

1.8 Aims and objectives

1.8.1 Aims

The aim of this study was to investigate the effects of Anastrozole combined with antiplatelet therapy agents (Aspirin and Clopidogrel cocktail and Atopaxar) on hypercoagulation and tumour progression in breast cancer.

1.8.2 Objectives

Breast cancer cells were pre-treated with combined Anastrozole and Anti-platelet therapy (Aspirin and Clopidogrel cocktail/Atopaxar), following which cultures were exposed to whole blood (except objective 1-3) and the following parameters were assessed:

1. The cytotoxic effects of a range of Cmax concentrations on breast cancer cells by assessing various changes to the membrane integrity which are related to physiological outcome (Neutral red assay/Lactate dehydrogenase assay/Flow cytometry/ ultrastructural changes)
2. To establish optimal dosages of Anastrozole and Antiplatelet therapy drugs

3. To determine the outcome of treatment on migration and proliferation
4. To determine induced hypercoagulation in whole blood following exposure to Anastrozole and Antiplatelet therapy (Aspirin and Clopidogrel cocktail/ Atopaxar) by assessing thrombin secretion and platelet activation
5. To determine alterations in mRNA levels of EMT genes in Anastrozole and Antiplatelet therapy (Aspirin and Clopidogrel cocktail/ Atopaxar) treated breast cancer cells following exposure to whole blood
6. To quantify inflammatory markers in whole blood and assess their role in tumour survival and hypercoagulation

CHAPTER II: Cytotoxic Effects of Anastrozole & Antiplatelet Therapy

2.1 Introduction

2.1.1 Properties of breast cancer cell lines and their limitations

Breast cancer is the most commonly diagnosed cancer among women worldwide (Lumachi *et al.*, 2013; Moodley *et al.*, 2016). Approximately 70% of diagnosed breast cancers are classified as hormone-dependent and express the oestrogen receptor (ER) (Jia *et al.*, 2016; Hilton, Clarke and Graham, 2018). In these tumours, steroid hormones, such as oestrogen, play an important role in mediating progression (Eeckhoute *et al.*, 2006; Jia *et al.*, 2016).

Specifically, the mechanism of action for 17-β-estradiol (E2) involves binding to the ER (alpha and beta) located in the nucleus and in turn activates oestrogen response elements in target genes (Oueslati *et al.*, 2017; Hua *et al.*, 2018). The ER consists of two subtypes namely; ERα and ERβ which have antagonistic actions on tumour growth and progression (Oueslati *et al.*, 2017; Girgert, Emons and Gründker, 2019). ERα acts as a main transcription factor which promotes oncogenesis in hormone receptor positive breast cancer, whereas ERβ has tumour suppressing properties (Haldosén *et al.,* 2014; Hua *et al.*, 2018). ERα was shown to be present in the cytoplasm whereby ligand binding promotes its non-genomic action which does not directly lead to changes in gene expression and has been linked to Tamoxifen resistance and facilitating tumour progression in breast cancer (Welsh *et al.*, 2012; Tian and Schiemann, 2017).

Breast cancer is a heterogeneous disease often presenting with a wide array of phenotypes, molecular characterisation and response to therapy (Polyak, 2011; Luciano G Martelotto *et al.*, 2014). Clinically breast cancers are classified into five main molecular intrinsic subtypes

based on their gene expression pattern; luminal A ($ER\alpha^+/PR^+/HER2^-$/low Ki67), luminal B ($ER\alpha^+/PR^-/HER2^{-\text{ or }+}$/high Ki67), HER2+ ($ER\alpha^-/PR^+/HER2^+$/Ki67), basal-type/triple negative ($ER\alpha^-/PR^-/HER2^-$) and normal-like (high levels of ADH1B) (Nakshatri, Srour and Badve, 2009; Eliyatkin *et al.*, 2015). Additional novel breast cancer subtypes have been identified; claudin-low, molecular apocrine subtype and luminal-like subtype (Tang and Tse, 2016) thus further illustrating the heterogeneity and plasticity of breast cancer. These molecular subtypes determine prognosis and response to treatment (Mosoyan *et al.*, 2013; Eliyatkin *et al.*, 2015; Mota *et al.*, 2017). Expression of the ER is associated with response to hormone therapy (Bae *et al.*, 2015; Awan and Esfahani, 2018).

Studies have shown that the biological and genomic properties, and molecular heterogeneity of breast tumours is reflected in currently available breast cancer cell lines (Holliday and Speirs, 2011; Radde *et al.*, 2015; Dai *et al.*, 2017). Cell lines may thus be a good representation of tumours; however, prolonged *in vitro* culture and passaging provides limitations because cell lines evolve quickly and acquire more genome abnormalities than primary tumours (Neve *et al.*, 2006; Dai *et al.*, 2017). The heterogeneity of breast cancer leads to cancers not responding similarly to treatment (Holliday and Speirs, 2011; Mosoyan *et al.*, 2013) and thus beckons the need for using more than one cell line in breast cancer studies. In this study two cell lines representing the luminal subtype of breast cancer were used (MCF7 and T47D cells). Due to their molecular profile (ERα expression), they were ideal candidates to fulfil the objectives of this study. Even though these cell lines are generally classified similarly, it was anticipated that some differences in their responses would be observed due to their heterogeneity (Neve *et al.*, 2006; Holliday and Speirs, 2011; Yu *et al.*, 2017).

The MCF7 cell line was established in the Michigan Cancer foundation, from a 69 year old female patient with metastatic disease (Soule *et al.*, 1973). Following its establishment, this cell line has been one of the most commonly used cell lines in breast cancer research and has led to numerous breakthroughs in the field of breast cancer research (Aonuma *et al.*, 1999; Barabutis *et al.*, 2007; Klopp *et al.*, 2010; Gest *et al.*, 2013; Lian *et al.*, 2013). MCF7 cells present with ER and low/absent PR (Baguley and Leung, 1995) and most studies classify them as belonging to the luminal A subtype (Comşa, Cîmpean and Raica, 2015; Dai *et al.*, 2017; Yu *et al.*, 2017). T47D cells were derived from a 54 year old female patient with infiltrating ductal carcinoma and are classified as luminal A; however, they contain higher levels of PR than MCF7 cells (Miller *et al.*, 1994; Sweeney *et al.,* 2012). The ER isotypes are present in both cells lines but vary in concentration; in our lab MCF7 cells were shown to contain more *ESR1* and corresponding protein, ERα than T47D cells, whereas T47D cells were shown to contain more *ESR2* and the corresponding protein, ERβ than MCF7 cells (Sastre-Serra *et al.*, 2012; Pather *et al.,* unpublished findings). ERβ levels in MCF7 cells are very low compared to T47D cells (Sastre-Serra *et al.*, 2012). ERβ was shown to have anti-invasiveness properties by promoting cell adhesion through upregulating adhesive protein; E-cadherin (Lymperatou *et al.*, 2013).

The luminal-A subtype occurs in approximately 40% of ER+ breast cancer, whereas the luminal-B subtype occurs in approximately 20% (Lumachi *et al.,* 2013). Luminal-A cell lines express genes that facilitate differentiation and promote a non-invasive phenotype (Neve *et al.,* 2006; Holliday and Speirs, 2011). MCF7 and T47D cells have low migratory and metastatic rates and show features of differentiated mammary epithelium such as E-cadherin, β-catenin and thus would lack mesenchymal markers such as N-cadherin and vimentin (D'Anselmi *et al.*, 2013; Rizwan *et al.*, 2015; Yu *et al.*, 2017). In addition, studies have shown that both these

cell lines (MCF7 and T47D) contain sub-populations of cells that behave differently and often present with stem cell-like characteristics, thus further contributing to the heterogeneity seen in these cell lines (Fillmore and Kuperwasser, 2008; Comşa et al*.,* 2015; Akrap *et al.*, 2016; Chopra *et al.*, 2018).

2.1.2 Drug metabolism *in vitro*

Drug metabolising enzymes activate and deactivate drugs and cytotoxic agents and mediate the response of organs and tissues to treatment (Michael and Doherty, 2005; Li *et al.*, 2017). Cytochrome P450 is a family of heme-protein monooxygenase enzymes which play a role in the pharmacokinetic and pharmacodynamics of drugs as well as the oxidative metabolism of drugs, environmental carcinogens, steroids and endobiotics (Rendic and Guengerich, 2018; Stavropoulou *et al.,* 2018). P450 enzymes are predominantly found in the human liver; however, they are also expressed in extrahepatic tissues (Androutsopoulos *et al.,* 2009; Stavropoulou *et al.,* 2018).

The expression of P450 enzyme in cancer cell lines leads to the production of drug metabolites, thereby influencing the drug outcome by increasing or decreasing its cytotoxic effects (Leung *et al.*, 2013; Li *et al.*, 2017). MCF7 and T47D cell lines have been shown to express P450 enzymes, although the expression is low and not comparable to parent tissues, in addition, P450 enzyme expression was shown to be slightly higher in MCF7 cells than in T47D cells (McDonald *et al.*, 2017).

The CYP2C subfamily of enzymes are responsible for the metabolism of approximately 20% of clinically used drugs (Michael and Doherty, 2005). The expression of enzymes belonging to this subfamily has been shown to be equivalent in normal and malignant breast tissue (Michael and Doherty, 2005). The CYP3A4 sub-family enzymes are among the most important

drug metabolizing enzymes responsible for metabolizing approximately 55% of all drugs (Basheer and Kerem, 2015; Zhou *et al.*, 2019).

2.1.3 Hormone therapy in breast cancer

Hormone therapy is considered to be a targeted endocrine therapy and it is considered to be less harsh on patients compared to other treatments for breast cancer. It is also the preferred treatment choice for older patients who are not suitable for aggressive chemotherapy and women with advanced ER+ breast cancer and non-life threatening disease (Sweeney *et al.,* 2012; Lumachi *et al.*, 2013). The biosynthesis of oestrogen involves various processes and molecules (Lumachi *et al.*, 2013). Cholesterol (C27 sterol) is converted to progestogens (C21) and androgens (C19) through various processes and the aromatase enzyme catalyses these reactions (Bruno and Njar, 2007; Cui, Shen and Li, 2013; Lumachi *et al.*, 2013). Aromatase activity in pre-menopausal women is high in the granulosa cells of the ovaries and in post-menopausal women in adipose tissue (Bruno and Njar, 2007; Cuzick, *et al.*, 2014).

Cytochrome P450 aromatase is encoded by the *CYP19* gene found on chromosome 15q21.2 (Cui, Shen and Li, 2013; Cuzick *et al.*, 2020). Breast cancer patients have been noted to over-express the *CYP19* gene in their adipose tissue (Lumachi *et al.*, 2013; Cuzick *et al.*, 2020), and also have a high expression of inflammatory cytokines that activate cyclooxygenase (COX2) and PgE2 overexpression which in turn increases *CYP19* gene expression (Han *et al.*, 2010; Subbaramaiah *et al.,* 2012).

AIs block the activity of the aromatase enzyme and thereby reduce the circulating levels of oestrogens, notwithstanding their direct effects on tumour cells which also express the aromatase enzyme (McDonald *et al.*, 2017; Awan and Esfahani, 2018; Hua *et al.*, 2018). AIs are ineffective in breast cancer patients with a functionally active ovary because they lead to

an increased secretion of gonadotrophins and subsequently circulating oestrogen (Cuzick, *et al.*, 2014; Awan and Esfahani, 2018). Hence they are not commonly used in premenopausal women although it has been suggested that their use in combination with gonadotrophin realising hormone (GnRH) analogs may benefit some patients (Cuzick, *et al.*, 2014; Awan and Esfahani, 2018).

AIs differ in their chemical structure and mechanism of action and have thus been divided into two types (Ahmad and Shagufta, 2015). Type I are steroidal compounds which inhibit the aromatase enzyme in an irreversible manner whereas type II are nonsteroidal compounds that inhibit the aromatase enzyme in a reversible manner (Geisler, 2011; Ahmad and Shagufta, 2015). Anastrozole and Letrozole are type II third generation AIs and they block the aromatase enzyme in a reversible manner; therefore, their efficacy in reducing oestrogen levels is dependent on their continuous presence (Geisler, 2011; Cuzick *et al.*, 2020). Studies have shown that inhibiting the activity of the aromatase enzyme with third generation AIs as opposed to selective oestrogen receptor modulators (SERMs) improves survival in patients with advanced ER+ breast cancer (Lumachi *et al.*, 2013; Cuzick *et al.*, 2020).

Anastrozole, an AI, has been shown to be more effective as first line therapy in post-menopausal breast cancer patients in comparison to other oestrogen modulators (such as tamoxifen) (Cuzick *et al.*, 2020). AIs are the first class of drugs to directly target a CYP enzyme i.e. aromatase (also known as CYP19) (Bruno and Njar, 2007; Cuzick *et al.*, 2020). CYP19 enzymes catalyse the production of oestrogen and are widely expressed in breast adipose tissue, suggesting they may play a role in carcinogenesis (Jia *et al.*, 2016; Giudice *et al.*, 2019). MCF7 and T47D cells are known to express low levels of aromatase; however, they are generally responsive to AIs (Wong and Chen, 2012).

2.1.4 The interactions between antiplatelet drugs and breast cancer cells

2.1.4.1 Aspirin mediated effects through COX signalling

Non-steroidal anti-inflammatory drugs (NSAIDs) are classified into two categories according to their mechanism of action on the COX enzyme; classical NSAIDs (e.g. Aspirin) and COX-2 inhibitors (e.g. Celecoxib and Rofecoxib) (Rao and Knaus, 2008). The COX enzyme consists of two isoforms: COX-1 is expressed constitutively whereas COX-2 is expressed in response to inflammation or during early tumour development (Mendes *et al.,* 2012). COX-1 has anti-thrombotic effects when exposed to vascular endothelium and in the gastric mucosa it has cyto-protective properties, it also induces platelet aggregation and prevents inappropriate bleeding (Jacobo-Herrera *et al.*, 2014). COX-2 is expressed in many cell lines whereby it plays a role in carcinogenesis, tumour growth, angiogenesis and inhibits apoptosis (Elwood *et al.*, 2009; Langley *et al.*, 2011).

Aspirin and other classical NSAIDs inhibit COX-1 and COX-2 by competing with arachidonic acid for binding irreversibly to the active site of the COX enzyme (Osafo *et al.,* 2016; Cadavid, 2017). The COX enzymes play a role in converting arachidonic acid to prostaglandin endoperoxide (PgH_2) and thromboxanes (Cadavid, 2017). Prostaglandins are compounds with a short life span, they are local mediators of normal cellular reactions and are increased during inflammation and in tumours (Wang and Dubois, 2006). Induction of COX-2 expression in breast tissue triggers PgH_2 production which indirectly stimulates cellular proliferation by stimulating the activity of aromatase enzyme, CYP19, and thus increasing oestrogen synthesis (Hoellen *et al.*, 2011). High levels of PgH_2 in humans have been associated with metastatic potential and reduced patient survival (Jacobs *et al.*, 2007). This process is reversible by inhibiting COX-2 with NSAIDs this reduces the synthesis of PgH_2, thus the use of Aspirin in

hormone dependent breast cancer could suppress aromatase activity, and thus reduce oestrogen production (Jacobs *et al.*, 2007; Jacobo-Herrera *et al.*, 2014).

COX-2 and PgE2 are over-expressed in human mammary tissue and their expression is associated with aromatase-catalysis of oestrogen biosynthesis (Hoellen *et al.*, 2011; Liu, Qu and Yan, 2015; Kochel, Goloubeva and Fulton, 2016). NSAIDs display anti-cancer activity by inhibiting mainly COX-2 enzyme, triggering apoptosis, reducing proliferation and inhibiting carcinogenesis (Cuzick, *et al.*, 2014). Studies suggest that Aspirin could be useful as an alternative treatment or to enhance known therapies for breast cancer (Jacobo-Herrera *et al.,* 2014). It has been suggested that NSAIDs could be used in conjunction with hormonal therapies (Agrawal and Fentiman, 2008) and a study has thus far shown that Aspirin combined with Tamoxifen provided cardio-protective effects and may reduce breast cancer risk (Leite *et al.*, 2018).

2.1.4.2 Clopidogrel mediated effects through purinergic signalling

Clopidogrel is derived from thienopyridine and it binds in an irreversible manner to P2Y12 purinergic receptors in platelets and various cells (Bhatt *et al.*, 2006; Sangkuhla *et al.,* 2008; Capodanno *et al.,* 2013). Clopidogrel-mediated blockage of the P2Y12 receptors prevents ADP-mediated platelet activation and aggregation (Sangkuhla *et al.,* 2008). P2Y12 antagonists are the most widely used antiplatelet therapy agents following Aspirin (Ballerini *et al.*, 2018). ADP is an agonist of platelet activation and elicits its action by binding to P2Y12 receptors and thus inhibits the formation of cyclic adenosine monophosphate (cAMP) (Denslow *et al.*, 2017; Ballerini *et al.*, 2018). Various adenine nucleotides and nucleosides; i.e. adenosine triphosphate (ATP) and ADP, play a role in platelet aggregation and activation (Burnstock, 2017). ATP is catalysed by ecto-nucleoside triphosphate diphospho-hydrolase (CD39) and ecto-5'-nucleotidase (CD73) into ADP then ADP is converted into adenosine monophosphate

(AMP) and ultimately AMP is converted into adenosine (Burnstock, 2017). P2Y1 receptors upon ADP binding induce platelet aggregation through the phospholipase-C and phosphatidlyinositol-signalling pathways (Ballerini *et al.*, 2018).

There are two subtypes of purinergic receptors, P1 and P2. The main ligand for P1 receptors is adenosine, whereas P2 receptors bind ATP and ADP (Burnstock and Di Virgilio, 2013; Mello, Coutinho-Silva and Savio, 2017). P2 receptors are further subdivided into ionotropic P2X and metabotropic P2Y subtypes (Burnstock and Di Virgilio, 2013; Hechler and Gachet, 2015). P2X and P2Y receptors are widely expressed in the body e.g. neurons, smooth muscle, epithelial cells of skin, lungs, gut, kidneys and endothelium (Hechler and Gachet, 2015; Koupenova and Ravid, 2018). P2Y receptors are 7-pass receptors because they contain seven transmembrane domains, have an extracellular N-terminus and an intracellular C-terminus (Tello-Montoliu *et al.*, 2011; Holinstat, 2012).

P2Y12 receptors were shown to play a role in inflammation and immune modulation (Cattaneo *et al.,* 2014; Hechler and Gachet, 2015). Adenosine has been shown to be highly concentrated in solid tumours, where it is postulated to assist cancer cells to evade immunosurveillance by inhibiting the activation of cytotoxic T-cells within the tumour microenvironment (Sek *et al.*, 2018; Arab and Hadjati, 2019). ATP concentration has also been shown to be high in tumours thus suggesting that ATP release and conversion to adenosine occurs frequently within the inflammatory tumour microenvironment, hence the milieu has abundant immune regulatory and growth factors (Sek *et al.*, 2018; Arab and Hadjati, 2019).

Cytochrome P450 enzymes are involved in the metabolism of Clopidogrel, various cytochrome P450 enzymes have been shown to convert Clopidogrel into 2-oxo-clopidogrel in *in vitro* studies and subsequently into its active metabolite (Roden and Stein, 2009; SangKuhl

et al., 2010). CYP2C19 is the major enzyme involved in both oxidation steps in the conversion of Clopidogrel, whereas other enzymes such as CYP34A were only involved in one step (Roden and Stein, 2009; SangKuhl *et al.,* 2010). The active metabolite of Clopidogrel binds to a free cysteine on the P2RY12 receptor via its thiol group (only expressed in its active state). This binding irreversibly blocks the binding of ADP and subsequent activation of the purinergic receptor (Roden and Stein, 2009; SangKuhl *et al.,* 2010).

Clopidogrel is an effective agent against cardiovascular disorders including peripheral artery cerebrovascular and coronary artery diseases (Elmariah *et al.*, 2018). While beneficial, its prolonged use is associated with increased risk for bleeding and it was also shown to increase mortality rate in patients with cardiovascular disease (Mauri *et al.*, 2014). Aspirin and Clopidogrel are often used in combination to treat cardiovascular diseases because their efficacy is better when used as a cocktail than individually (Tello-Montoliu *et al.*, 2011; Eikelboom *et al.*, 2012; Capodanno *et al.,* 2013). In the Clopidogrel versus Aspirin in Patients at Risk of Ischaemic Events (CAPRIE) study combined Aspirin and Clopidogrel reduced the risk of myocardial infarction, stroke and vascular death (Eikelboom *et al.*, 2012). The Clopidogrel for The Reduction of Events During Observation (CREDO) and Clopidogrel and Metoprolol Myocardial Infarction Trial (COMMIT) clinical trials showed that cardiovascular deaths were reduced with the use of Clopidogrel (Eikelboom *et al.*, 2012). The efficacy of Clopidogrel has also been shown in the Clopidogrel in Unstable Angina to Prevent Recurrent Events Trial (CURE) and DAPT clinical trials whereby prolonged use decreased incidence of myocardial infarction (MI) (CAPRIE *et al.*, 2001; Connolly *et al.*, 2009; Mauri *et al.*, 2014). The Atrial Fibrillation Clopidogrel Trial with Irbesartan for Prevention of Vascular Events (ACTIVE-A)

clinical trial showed a reduced incidence of stroke (CAPRIE *et al.*, 2001; Connolly *et al.*, 2009; Mauri *et al.*, 2014)..

Breast cancer cells were shown to have a low baseline expression of P2Y12; however, receptor expression increased after 24 hours and 48 hours in serum deprived environment suggesting a possible protective effect of this receptor against cancer (Ballerini *et al.*, 2018). Studies have shown various outcomes regarding the use of Clopidogrel with or without Aspirin and cancer risk. The Clopidogrel for High Atherothrombotic Risk and Ischemic Stabilization, Management and Avoidance (CHARISMA) clinical trial showed that the combination of Aspirin and Clopidogrel decreased cancer incidence by 54% and cancer-related mortality (Leader *et al.*, 2017). Other clinical trials such as the; Secondary Prevention of Small Subcortical Stroke (SPS3) and Dual Antiplatelet Therapy (DAPT) have shown that prolonged use of Clopidogrel increased cancer-related deaths (Mauri *et al.*, 2014, 2016). The Trial to assess Improvement in Therapeutic Outcomes by optimizing platelet inhibition with Prasugrel Thrombolysis In Myocardial Infarction 38 (TRITON-TIMI 38) clinical trial showed that Prasugrel led to higher risk for breast, colorectal and prostate cancer in patients with acute coronary syndrome than Clopidogrel (Wiviott *et al.,* 2007). However, Clopidogrel combined with Tamoxifen and chemotherapy agents (Cisplatin, Doxorubicin) showed some adverse effects in a mouse model of mammary gland cancer whereby it increased metastasis to the lung (Denslow *et al.*, 2017). Aspirin and Clopidogrel cocktail in a mouse model induced pro-tumourigenic alterations in primary tumours, and increased angiogenesis through vascular mimicry this was associated with high mortality rates *(*Smeda *et al.,* 2018).

2.1.4.3 Atopaxar mediated effects through PAR signalling

Thrombin is the main extracellular serine protease responsible for activating PAR1, PAR3 and PAR4 receptors (Jennings, 2009; Wojtukiewicz *et al.*, 2016). Thrombin is also a potent agonist for platelet activation and essential component of the coagulation cascade (Clemetson, 2012; Leonardi *et al.,* 2012). PAR receptors are activated by low concentration of certain extracellular serine proteases (Kogushi *et al.*, 2011; Estevez *et al.*, 2016). PAR2 is mainly activated by trypsin-like serine proteases such as trypsin, tryptase and other coagulation proteases upstream of thrombin e.g. tissue factor VIIa and Xa (Holinstat *et al.*, 2009; Han *et al.*, 2011). Thrombin has been shown to bind to PAR receptors in cells to mediate various processes including cell proliferation and motility, improvement of vascular permeability and thus plays a role in promoting cancer (Han *et al.*, 2011).

Thrombin activates PAR1 receptors in two stages, firstly by binding to the cleavage site on either side of the PAR1 receptors, then it cleaves the PAR1 receptor between Arg and Ser exposing the N-terminal tethered ligand domain, SFLLRN (Holinstat *et al.*, 2009; Han *et al.*, 2011; Tourdot *et al.*, 2018). The tethered ligand domain interacts with domains in extracellular loop2 which has been suggested to alter conformation of the receptors to allow coupling of G-proteins (Holinstat *et al.*, 2009; Han *et al.*, 2011). Atopaxar was shown to reduce thrombin- and ADP-mediated platelet aggregation and unlike most antiplatelet agents (such as Aspirin and Clopidogrel) it does not adversely increase bleeding time (Goto *et al.*, 2010; O'Donoghue *et al.,* 2011). Furthermore, Atopaxar inhibits thrombin receptor activating peptide (TRAP) (Kogushi *et al.*, 2011). The Lessons for Antagonizing the Cellular Effect of Thrombin-Acute Coronary Syndrome (LANCELOT-CAS) clinical trial showed Atopaxar's efficacy in reducing platelet aggregation and ischemic events (Wiviott, Flather, O'Donoghue,

et al., 2011); however, together with The Japanese Lessons from Antagonizing the Cellular Effects of Thrombin (J-LANCELOT) clinical trial, Atopaxar was also shown to adversely affect liver function and thus phase III studies were not conducted (Goto *et al.*, 2010).

Atopaxar which is metabolised by cytochrome P450 enzyme, CYP3A4, selectively blocks protease-activated receptor-1 (PAR-1) thus preventing platelet activation by thrombin (Capodanno *et al.,* 2013). Cytochrome P450 enzymes and PAR1 are also expressed in breast tumours and cell lines (Yang *et al.,* 2009; Thuy Phuong *et al.,* 2017) with higher PAR-1 expression related to heightened invasiveness and induction of epithelial-mesenchymal transition (Wang *et al.,* 2016).

Tumour cells are capable of producing thrombin because they express transmembrane protein; tissue factor which activates factor X upon exposure to circulating factor VII, this activation cascade leads to thrombin production (Aschermann, 2013; Roop *et al.*, 2013). Thrombin production is a product of the hypercoagulable state present in cancer patients (Bagot *et al.*, 2010; Lipets and Ataullakhanov, 2015).

The role of Atopaxar in tumours has not been well established; however, a recent study showed that Atopaxar is an antagonist to the Janus kinase signal transducer and activator of transcription (JAK-STAT) which promotes cell division and neoplastic transformation in cells and conversely inhibits cell death (Sun *et al.*, 2019). Thus suggesting a potential role for Atopaxar in reducing tumour formation (Sun *et al.*, 2019).

2.1.5 The effect of combined hormone and antiplatelet therapy on breast cancer cells

2.1.5.1 Cancer promoting processes

Cell migration is involved in various biological processes including embryogenesis, inflammation, tissue repair, regeneration and pathological process such as metastasis (Borm *et al.*, 2005; Al-Bahlani *et al.,* 2017). Cell migration involves the extension of membrane protrusions such as pseudopodia and lamellipodia and the release of cell substrate adhesions (Borm *et al.,* 2005; Al-Bahlani et al. 2017). Studies have shown that there are different modes of migration (Friedl and Alexandra *et al.,* 2011; Pandya *et al.,* 2017). Collective migration involves cells moving as a group while maintaining cell junctions, this is the slowest mode of migration but associated with high secretion of pro-migratory factors and matrix proteins, therefore increasing the overall rate of tumour invasion (Chen *et al.,* 2014; Jolly *et al.*, 2017; Pandya, Orgaz and Sanz-Moreno, 2017; Grada *et al.*, 2018). Single cell migration also occurs whereby cells migrate individually and this may be facilitated through polarisation of membrane extensions to form elongated-mesenchymal shape, rounded-amoeboid shape whereby cells display higher contractility and spike-mediated shape (Montt-Guevara *et al.*, 2016; Jolly *et al.*, 2017; Pandya, Orgaz and Sanz-Moreno, 2017). Migration in tumours is often associated with invasion and is facilitated by epithelial to mesenchymal transition (EMT) whereby epithelial cells acquire a less differentiated phenotype which is a precursor for metastasis (Friedl and Alexander, 2011; Lymperatou *et al.*, 2013). Cells undergoing EMT can migrate individually or in groups known as collective cell migration, the latter may occur independent of EMT (Friedl and Alexander, 2011).

2.1.5.2 Cancer inhibiting processes

Apoptosis is a mechanism by which damaged cells are removed from the environment without eliciting a harmful immune response (Cummings *et al.,* 2004; Wlodkowic *et al*., 2011;

Wickman *et al.,* 2013). During this process, cell membrane integrity is maintained in order to prevent the release of intracellular proteins and subsequent inflammation and phosphatidyl serine (PS) is translocated from the cells interior and is expressed on the outer surface and this acts as a signal for cells undergoing apoptosis (Cummings *et al.*, 2004; Wlodkowic *et al.,* 2011; Wickman *et al.,* 2013). Morphological hallmarks associated with apoptotic cells include cell contraction, nuclear condensation, fragmentation, blebbing and formation of apoptotic bodies (Cummings *et al.,* 2004; Wlodkowic *et al.,* 2011; Wickman *et al.,* 2013). Apoptotic bodies are small encapsulated particles that dissociate from blebs, these particles are first released during early apoptosis (Cummings *et al.,* 2004; Wlodkowic *et al.,* 2011; Wickman *et al.,* 2013). Secondary necrosis is a process that occurs *in vitro* following failure to remove apoptotic bodies, whose membrane are permeable to propidium iodide (PI), from the microenvironment (Cummings *et al.,* 2004; Wlodkowic *et al.,* 2011; Wickman *et al.,* 2013). This process involves the loss of cell membrane integrity by apoptotic bodies and this is identified by the failure to exclude PI from crossing the membrane barrier (Cummings *et al.,* 2004; Wlodkowic *et al.,* 2011; Wickman *et al.,* 2013).

In an attempt to elucidate harmful effects of Anastrozole and antiplatelet therapies (Aspirin and Clopidogrel cocktail/ Atopaxar) their effect on these processes were investigated. Endocrine therapies were shown to be generally ineffective on migration (Smollich *et al.*, 2010). Anastrozole was shown to reduce tumour size when combined with another agent ZD4054 but had no effect on migration of MCF7 cells (Smollich *et al.*, 2010). Another study showed that Anastrozole induced low levels of apoptosis and reduced cell proliferation (Chen *et al.*, 2015). This study showed that MCF7 cells have endocrine resistance towards Anastrozole-treatment and thus its effects were enhanced by the addition of testosterone

(Chen *et al.*, 2015). Other studies concur with these findings (Doane *et al.*, 2006; Yu *et al.*, 2011; Campagnoli *et al.*, 2013). 17β-estradiol was shown to promote collective cell migration in MCF7 and T47D cells and little to no effect on single cell migration (Lymperatou *et al.*, 2013).

Several studies have shown that Aspirin has anti-cancer properties (Harris, Beebe-Donk and Alshafie, 2007; Shebl *et al.*, 2012; Qiao *et al.*, 2018). In Hep-2 cells, originally representing an epidermoid tumour of the larynx but has also been shown to contain HeLa cells, Aspirin was shown to reduce cell viability, promote apoptosis and inhibit migration and invasion (Jin *et al.*, 2018). In colorectal cancer cells (T26 cells) Aspirin reduced cell viability, suppressed tumour growth by increasing TGFβ1 and increasing apoptosis (Wang *et al.*, 2018). Aspirin reduced cell viability, inhibited cell proliferation and increased apoptosis in a dose dependant manner in Rheumatoid Arthritis (RA-FLS) cell line by blocking the JAK/STAT3 and nuclear factor-kappa-beta (NF-kβ) signalling pathways (Zhang *et al.*, 2018).

To the author's knowledge there is scant information regarding the direct effects of Clopidogrel on cancer cells. However, the effects of this compound on cellular processes, other than coagulation have been investigated. In periodontitis, Clopidogrel was shown to be involved in the repair process, displaying anti-inflammatory properties and increasing cell proliferation (Coimbra *et al.*, 2015). This capacity to promote cell proliferation was also presented in human mesenchymal stem cells *in vitro* and *in vivo*, whereas Aspirin had no effects on these cells (Ko *et al.*, 2015).

Atopaxar is an antagonist of PAR1, which mediates tumour process such as invasion and metastasis (Liu *et al.*, 2017). Low thrombin concentration promotes cell proliferation in cancer cells (Liu *et al.*, 2017). The role of Atopaxar in cancer is not yet established but due to

the role PAR1 plays in cancer, Atopaxar could potentially be effective in preventing of tumour symptoms (Liu *et al.*, 2017). While the mechanisms of antiplatelet therapies are known in the context of their direct effects on thrombosis, research is required regarding their direct effects on tumour cells and in conjunction with hormone-therapy. This study was designed such that breast cancer cells would be treated directly with hormone and antiplatelet therapy in order to understand the direct effects of therapy on cancer cells and how they modulate thrombosis outcome. As such we had to first establish optimal dosages and possible adverse effects of combined hormone and antiplatelet therapy on breast cancer cells.

Table 2.1 A summary of the effects of antiplatelet therapy drugs; Aspirin, Clopidogrel and Atopaxar on cancer outcome.

Antiplatelet agent	**Effect on cancer**	**Reference**
Aspirin	-Alternative anticancer therapy and enhances known cancer therapies. -Restores normal production of maspin, a tumour suppressor which prevents cellular invasion and metastasis. -Reduces risk for metastasis	Jacobo-Herrera et al., 2014 Girish et al., 2006 Rothwell et al., 2012
Clopidogrel (with or without Aspirin)	-CHARISMA Trial: AspClop reduced cancer incidence and cancer related mortality. - SPS3 trial: Prolonged use of Clopidogrel increased cancer-related deaths. - DAPT trial: Clop with Tamoxifen and chemotherapy drugs (Cisplatin, Doxorubicin) increased metastasis to the lung in a mouse model of breast cancer. -In a mouse model AspClop induced protumourigenic alteration and increased angiogenesis through vascular mimicry and associated with higher mortality rate.	Leader *et al.,* 2014 Mauri *et al.,* 2014 Denslow *et al.,* 2017 Smeda *et al.,* 2018
Atopaxar	Antagonist for JAK-STAT pathway which promotes cell division and neoplastic transformation; therefore, it may inhibit tumour formation	Sun *et al.,* 2019

2.1.6 Aims and objectives

The **aims** of this study were as follows:

1. To investigate the dosage dependant response of luminal-A hormone-dependent MCF-7 and T47D breast cancer cells following treatment with Anastrozole, combined with Aspirin and Clopidogrel cocktail; and Atopaxar at a range of maximum concentrations (Cmax) (1X-, 2X-, 4X-, 8X- and 10X Cmax) in order to establish optimal drug concentrations for subsequent experiments.
2. To investigate whether the optimal drug concentrations for these therapies may promote or inhibit cancer progression as defined by the objectives below

The **objectives** were as follows:

1.1 To measure **cell viability using the neutral red (NR) assay**, a dye that is actively uptaken through the plasma membrane of viable cells into lysosomes.

1.2 To measure **cytotoxicity using the lactate dehydrogenase (LDH) assay** which assesses the leakage of the LDH metabolic enzyme into the extracellular environment upon membrane damage.

1.3 To assess the **mode of cell death** using the flow cytometric Annexin-V/ (propidium iodine) PI assay. This assay allows for the assessment of cells undergoing different stages of cell death including early and late stage apoptosis and necrosis. In addition, it also indicates the number of live cells.

1.4 To **qualitatively assess ultrastructural changes** in tumour cells in response to varying dosages of drug treatment using scanning electron microscopy. Furthermore, to use scoring criteria to semi-quantitatively assess the ultrastructural changes seen.

1.5 To assess **cell migration** by means of a scratch assay to determine the possible effect of treatment on cancer outcomes

1.6 To assess the rate of **cell proliferation** using a WST-1 assay following drug treatment

2.2 Materials and methods

2.2.1 Cell culture

The breast cancer cell lines, MCF7 and T47D (P29-45), where purchased from the American Type Culture Collection (ATCC). MCF7 cells were propagated in Dulbecco's Modified Essential Medium (DMEM) containing phenol red (Lonza, Kempton Park, South Africa, BE12-604F) supplemented with 10 % Fetal Bovine Serum (FBS) (Thermo Fisher Scientific, Fairland, South Africa, 10499044) and 0.1 % Penicillin/streptomycin (Lonza, Kempton park, South Africa, lot no. OMB 206). T47D cells were propagated in Roswell Park Memorial Institute media (RPMI) containing phenol red (Lonza, Kempton Park, South Africa, BE12-115F) supplemented with 10 % FBS (Thermo Fisher Scientific, Fairland, South Africa, 10499044), 0.1 % Penicillin/streptomycin (Lonza, Kempton park, South Africa, lot no. OMB 206) and 0.2U/ ml human insulin (Novo Nordisk, Sanofi-Aventis, Midrand, South Africa).

Both cell lines were propagated in 75 cm^2 tissue culture flasks (Greiner Bio-one, Cape Town, South Africa, 658170) and incubated at 5 % CO_2 in a humid environment and a temperature of 37 °C. When the cells reached approximately 70-90 % confluency, they were passaged, following rinsing in phosphate buffered saline (PBS) pH 7.4, by adding 3 ml of 0.25% trypsin/EDTA (Thermo Fisher Scientific, Fairland, South Africa, 25200072) into each flask and incubated for 5 mins. Thereafter 3ml of complete medium was added to each flask to stop the reaction, and cells were transferred into a 15 ml centrifuge tube (Lasec, Cape Town, South Africa, P1TUB013B-000015). The cells were centrifuged for 5 mins at 400 xg using a Rotafix 32A centrifuge (Hettich, Sigma-Aldrich, Kempton Park, South Africa). Cells were either cryopreserved in freezing media (60% FBC, 30 % complete media and 10 % DMSO) at a temperature of -80 °C in a Forma Scientific freezer (Labx, India) or plated for experimentation.

Following passage, cell viability was assessed using the trypan blue exclusion method (Bio-Rad, Rosebank, South Africa, cat no. 145-0013). A 10 µl cell suspension was added to 10 µl of 0.4 % trypan blue solution (Bio-rad, Rosebank, South Africa, 145-0013) in an Eppendorf tube (Greiner Bio-one, Cape Town, South Africa, 616201). The TC20 automated cell counter (Bio-Rad, Rosebank, South Africa, 145-0101) coupled with the trypan blue exclusion method were used to enumerate cell numbers and determine cell viability for subsequent plating.

The optimal number of MCF7 cells (62500 cells/well) and T47D cells (125000 cells/well) as determined by a preliminary lactate dehydrogenase assay (LDH) experiment (Inqaba Biotech, Pretoria, South Africa, 8078) were seeded in duplicate onto glass coverslips (Lasec, Cape Town, South Africa, cat no. 111500) in 24 well plates (Lasec, Cape Town, South Africa, cat no. 662160) and incubated for 5 mins in order to facilitate attachment. T47D cells were seeded onto glass coverslips coated with 5 mg/ml poly-d-lysine (Sigma-Aldrich, Kempton Park, South Africa, P6407) in order to facilitate attachment. MCF7 cells were incubated for 24hrs and T47D cells were incubated for 48 hrs prior to treatment (based on prior observations which reveal T47D cells take a longer period to adhere than MCF7 cells). Cells were plated in duplicate for each ensuing assay.

2.2.2 Cell growth assay

Cell growth analysis was conducted in order to assess how both (untreated) cell lines proliferated over a period of 24 hrs. Cells were seeded and enumerated using the trypan blue exclusion method as previously described and cell counts were conducted at 6 hour intervals for a period of 24 hrs (i.e. 6 hrs, 12 hrs, 18 hrs and 24 hrs).

2.2.3 Drug treatment

The cells were subsequently incubated with increasing concentrations (1X Cmax, 2X Cmax, 4X Cmax, 8X Cmax and 10X Cmax) of Anastrozole alone (Ana), Anastrozole and Aspirin and

Clopidogrel (AnaAspClop), Anastrozole and Atopaxar (AnaAto), Aspirin and Clopidogrel (AspClop), and Atopaxar (Ato) in appropriate culture media for 24 hrs (Table 2.1). The drug concentrations were derived from the maximum concentration (Cmax) of the drug in plasma following a single dose; Anastrozole 16.16 ng/ml, half-life 50 hrs (Product monograph, 2013) (Sigma-Aldrich, Kempton Park, South Africa, A2736), Aspirin 4.4 µg/ml, half-life 20 mins (Voelker and Hammer, 2012) (Sigma-Aldrich, Kempton Park, South Africa, A2093), Clopidogrel bisulfate 1.86 ng/ml, half-life 6 hrs (Zou *et al.*, 2012) (Sigma-Aldrich, Kempton Park, South Africa, PHR1431) and Atopaxar hydrobromide 0.064 µM, half-life 23 hrs (Kogushi *et al.*, 2011) (Axon Medchem, Groningen, Netherlands, 2030). The diluent controls were prepared by exposing cells to 0.03 % dimethyl sulfoxide (DMSO) (corresponding to final percentage of DMSO in working solutions) for 24 hrs. See Appendix A1 for drug preparation. Following drug treatment, experimental assays including neutral red, lactate dehydrogenase, Annexin-V/ PI, scratch assay and WST-1 proliferation assay were conducted.

Table 2.2A: Treatment groups used to establish optimal drug concentrations.

Culture groups *(MCF7/T47D)*	**Type**	**Concentrations tested** *(where applicable)*
Negative control	Complete medium (DMEM/RPMI)	N/A
Diluent control	DMSO	0.03%
Experiment	Anastrozole (Ana)	1X-, 2X-, 4X-, 8X- and 10X Cmax
	Anastrozole+Aspirin+Clopidogrel (AnaAspClop)	1X-, 2X-, 4X-, 8X- and 10X Cmax at 1:1:1 combination ratio
	Anastrozole+Atopaxar (AnaAto)	1X-, 2X-, 4X-, 8X- and 10X Cmax at 1:1:1 combination ratio
	Aspirin+Clopidogrel (AspClop)	1X-, 2X-, 4X-, 8X- and 10X Cmax at 1:1:1 combination ratio
	Atopaxar (Ato)	1X-, 2X-, 4X-, 8X- and 10X Cmax

Table 2.2B: The Cmax concentrations used to prepare each drug combination.

	1X (mg/ml)	**2X** (mg/ml)	**4X** (mg/ml)	**8X** (mg/ml)	**10X** (mg/ml)
Anastrozole	1.6×10^{-5}	3.2×10^{-5}	6.4×10^{-5}	1.28×10^{-4}	1.6×10^{-4}
Aspirin	4.4×10^{-3}	8.8×10^{-3}	0.018	0.035	0.044
Clopidogrel	1.86×10^{-6}	3.72×10^{-6}	7.44×10^{-6}	1.488×10^{-5}	1.86×10^{-5}
Atopaxar	0.039	0.078	0.156	0.312	0.39

2.2.4 Lactate dehydrogenase assay

Following overnight incubation in 200 µl of relevant treatment, the plate was centrifuged at 400xg for 5 mins and 150 µl of the supernatant was transferred from each well into the corresponding 96 well plate (AEC Amersham, Kyalami, South Africa, 167008). 60 µl of the working reaction mix [containing 2 µl sodium lactate, 2 µl INT, 20 µl substrate mix and 36 µl PBS (pH7.4)] was added to each well and incubated for 20 mins protected from light. Thereafter 20 µl of sodium oxymate solution was added into each well in order to stop the reaction. Experimental controls included media control, and diluent control. Technical controls included background control (media only without cells), serum-free medium control

(serum-free media only, no cells) and a high (positive) control consisting of cells exposed to 1% triton X-100 to induce cell death). The absorbance was measured at a wavelength of 492 nm and 690 nm reference wavelength using a Labsystems Multiskan Ascent spectrophotometer (Amersham Soc Ltd, Kyalami, South Africa). The following formula was used to calculate cytotoxicity (Smith *et al.,* 2011);

$$\textbf{Cytotoxicity}\ (\%) = \frac{(compound - treated\ LDH\ activity) - (media\ control\ LDH\ activity)}{(high\ control\ LDH\ activity) - (media\ control\ LDH\ activity)}\ x\ 100$$

2.2.5 Neutral red assay

Following drug treatment, the medium was removed from all wells and the cells were rinsed with PBS (pH7.4). The cells were incubated with 100 µg/ml of neutral red dye (Gurr BDH Chemical, Poole, England, P34056) in appropriate tissue culture medium for 3 hrs at 37 °C. In order to measure the amount of neutral red dye taken up by cells, the solution was removed and cells were rinsed in PBS. The neutral red dye was eluted in 1% acetic acid in 50 % ethanol for 1 hr at room temperature (RT) on a shaker (1000 rpm). Experimental controls included media control and diluent control. Technical controls included serum-free media. The solution was then transferred into a 96-well plate and the absorbance was measured at a wavelength of 540 nm and 690 nm reference wavelength using a Labsystems multiskan Ascent spectrophotometer (Amersham Soc Ltd, Kyalami, South Africa). The serum free media control was subtracted from all absorbance values then cell viability was calculated. The following formula (Minaeva *et al.,* 2017) was applied;

$$\textbf{Viability}\ (\%) = \frac{corrected\ absorbance}{media\ control}\ x\ 100$$

For visualisation of the neutral red dye within the lysosomes, the cells were incubated with neutral red dye in order to locate its uptake within cells, rinsed in PBS (pH7.4) and coverslips were mounted with Fluoroshield (Sigma-Aldrich, Kempton Park, South Africa, F6182). Images were taken using an Olympus iX51 microscope (Wirsam Scientific, Johannesburg, South Africa) and using the CellSense V11 software.

2.2.6 Scanning electron microscopy

Following drug treatment, media was removed, and cells were rinsed twice in phosphate buffer (pH 7.2) and fixed in 2.5 % Glutaraldehyde (Merck, Darmstadt, Germany, UN2922) and formaldehyde (ACE, Southdale, South Africa, 7181) for 15 mins at room temperature (RT). The fixative was removed, and cells were rinsed thrice in phosphate buffer (pH7.2), then fixed in secondary fixative; 1 % osmium tetroxide (Spi-Chem, West Chester, USA, 2598) for 15 mins at RT. The cells were rinsed in phosphate buffer then dehydrated in a graded alcohol series for 3 mins each; 30 %, 50 %, 70 %, 90 %, 95 % and 100 % (3 changes). The cells were further dried in hexamethyldisilazane (HMDS) (Sigma-Aldrich, Kempton Park, South Africa, H4875), then coated with a single layer of carbon and gold palladium. The cells were imaged using a NOVA 600 Scanning Electron Microscope (FEI Company, Oregon, United States) at 30 KV. Images were obtained at 3000 X magnification, then from that area a high magnification image was obtained at 5000 X and again from the same areas at 1000X and 20000 X. Micrographs were edited for contrast and brightness using PhotoScape software v 3.7 and morphological features in cells were assessed by means of scoring criteria as described in Table2.3.

Table 2.3: Scoring criteria used to investigate morphological changes following exposure to combined Anastrozole and antiplatelet therapy for 24 hours.

Magnification= 3000X			
Cell contacts (Filopodia)	**Cell contacts (Pseudopodia)**	**Cell shape**	**ECM secretions/contents**
1= Present with cell-cell connections	1= Present with cell-cell connections	1= Round	0= Absent
2= Present without cell-cell connections	2= Present without cell-cell connections	2= Flattened/polyhedral	1= Sparse cell secretions (vesicles and microparticles)
3= Absent	3= Absent	3= Elongated/oval	2= Medium cell secretions (vesicles and microparticles)
		4= Mixed shapes	3= Dense cell secretions (vesicles and microparticles)
			4= Sparse cell debris
			5= Medium cell debris
			6= Dense cell debris
			7= Sparse mixture of cell secretions and debris
			8= Medium mixture of cell secretions and debris
			9= Dense mixture of cell secretions and debris
Magnification= 5000X			
Microvilli density	**Microvilli shape/appearance**	**Bleb density**	**Bleb size**
0= Absent	0= Absent	0= Absent	0=Absent
1= Sparse (~0-40% cover)	1= Short and free/ unclumped	1= Sparse (~0-40% cover)	1= Small
2= Medium (~41-69% cover)	2= Long and free/ unclumped	2= Medium (~41-69% cover)	2= Medium
3= Dense (~70-100% cover)	3= Bulbous/ clumped	3= Dense (~70-100% cover)	3= Large
	4= Webbing		4= Mixture of different sizes
	5= Mixture		

2.2.7 Annexin-V and Propidium Iodide Apoptosis Assay

Following drug treatment for 24 hrs as described previously, the treatment was removed and cells were harvested using Accutase for 10 mins (Sigma-Aldrich, Kempton Park, South Africa, 6964) then centrifuged for 5 mins at 400 xg. The supernatant was discarded, and cells were rinsed in PBS (pH7.4) supplemented with 10 % FBS, then centrifuged for 5 mins at 400 xg. The pellet was re-suspended in 1ml of 1X binding buffer supplemented with 10 % FBS. Cells were counted as described previously and a 1ml cell suspension containing $1X10^6$ cells was prepared. From the cell suspension 100 µl (containing approximately $1X10^5$ cells) was transferred into each 5 ml polystyrene tube (BD Falcon, Scientific group, Randburg, South Africa, 352054). The cells were incubated with titrated volumes of the antibodies (Appendix A2.1); 2 µl Annexin-V-FITC and 2 µl propidium iodide (BD Biosciences, Scientific group, Randburg, South Africa, BD556547) for 15 mins at room temperature, in the dark. Cells were fixed in 1 % paraformaldehyde (ACE, Southdale, South Africa, 26276) for 10 mins, then diluted in an equal volume of PBS supplemented with 10 % FBS and centrifuged at 400 xg for 5 mins. The supernatant was discarded and cells were re-suspended in 400 µl of 1X binding buffer supplemented with 2 % FBS and 1mM EDTA. Unstained and single stained controls (Annexin-V/ PI only) were added for compensation. A positive technical control consisted of cells treated for 24 hrs with 1 µM Doxorubicin (Biocom biotech, Centurion, South Africa, AB120629_10) (Synowiec *et al.,* 2015) 12 hrs post seeding. The cells were inspected using an LSR Fortessa flow cytometer and the following voltages were used: FSC 50 v, SSC 200 v, FITC 450 v and PI 401 v. Data was acquired with FACS Diva software. The gating strategy included cells first gated based on forward and side scatter (P1), from which the singlet population was gated based on the area and height of forward scatter (P2). From the P2 population a scatter plot was created and four quadrants separated cells based on their physiological state; live

cells (PS^-PI^-) (Q3-1), early apoptosis (PS^+PI^-) (Q4-1), late apoptosis (PS^-PI^+) (Q2-1) and necrosis (Q1-1) (PS^+PI^+) (Fig 2.1).

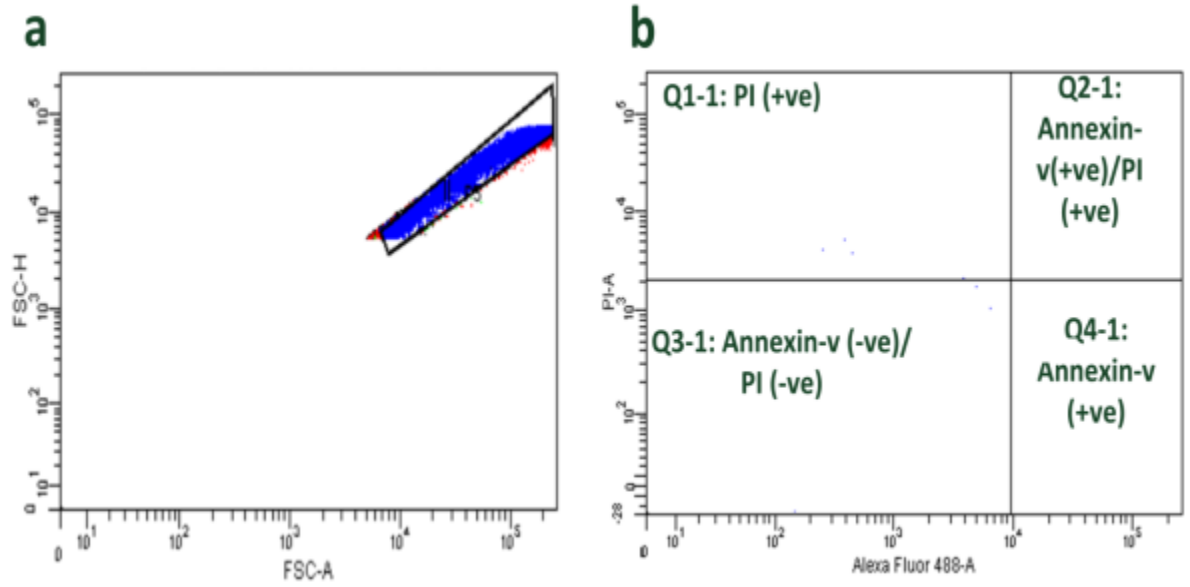


Figure 2.1: **Scatterplots showing gating strategy for Annexin V/Propidium iodide staining for cell death (a)** A singlet population was gated and excluded cell aggregates, all subsequent gates were based on this population. **(b)** A scatter plot representing quadrants were cells were sorted according to their physiological state. **Q1-1:** represents necrotic cells (stain positively with PI) due to damaged membrane integrity are located. **Q2-1:** cells undergoing late stages of apoptosis are found (PS exposure and PI staining). **Q3-1:** represents live/viable cells lacking PS expression and PI staining. **Q4-1:** cells undergoing early stages of apoptosis (PS exposure).

2.2.8 Statistical analysis for LDH assay, NR assay, SEM and Annexin-V/ PI assay

All experiments were conducted three times and numerical data managed in Microsoft Excel 2010. Statistica Version 13 was used to conduct all statistical tests and the significance level was set at $p<0.05$. The Shapiro-Wilk test, used to assess the distribution of the data, showed that the data did not follow a normal distribution ($p<0.05$); therefore, non-parametric tests were used in ensuing analyses. Differences in membrane integrity were investigated by assessing parameters including LDH leakage, NR uptake, PS expression and PI staining. Further, morphological features were scored including cell contacts, microvilli density and shape, bleb density and shape and overall cell shape (Table 2.2). A Friedman test was used to

determine whether there was a significant difference between various concentrations of the same drug /drug combination within each cell line (Appendix A2.2-2.3). A Kruskal-Wallis test and Post *Hoc* test were used to determine whether the changes seen in the various parameters tested were significantly altered within and between cell lines in different treatment groups (Appendix A2.4 and A3). Following the analysis, it was determined for the subsequent migration and proliferation assays that a 1X Cmax concentration of all drugs would be used.

2.2.9 Scratch assay for migration assessment

MCF7 and T47D cell lines were cultured and seeded into 24 well plates as specified in section 2.2.1 chapter II. When the cells were confluent and formed a uniform cell monolayer, a blue pipette tip (100-1000 µl) (Thermofischer Scientific, Fairland, South Africa, cat no 94052410) was used to remove cells at the centre of each well and create an exposed area in which cells can migrate into (Fig 2.2) (Liang *et al.,* 2007; Pinto *et al.*, 2018). Then cells were subsequently incubated in medium containing the drug treatments (Ana, AnaAspClop, AspClop, AnaAto and Ato) at 1X Cmax and incubated for 24 hrs. The wells were imaged at 0 hrs, 6 hrs, 12 hrs, 18 hrs, and 24 hrs using an Olympus iX51 phase contrast microscope (Wirsam Scientific, Johannesburg, South Africa) and the exposed area was measured at each time interval using Image J software V2019. The experiment was conducted three times and the area measurements generated were used to calculate % wound closure (Grada *et al.,* 2016) in Microsoft Excel 2010. PAST13 statistical software, specifically the non-parametric Friedman's test was used to determine whether there were significant reductions in area within each cell line with the different treatments which could be directly related to cell migration. A post *Ho*c analysis (Wilcoxon test) was also used to determine where the differences lie (Appendix A 4.1-4.6).

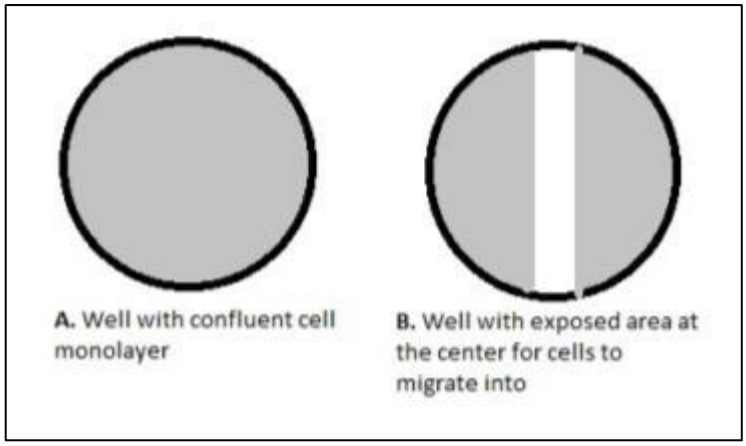


Figure 2.2: Schematic diagram illustrating the exposed area at the centre of the well following scraping of the cell monolayer with a pipette tip.

2.2.10 WST-1 proliferation assay

The Quick Cell Proliferation Assay Kit was used to study cell proliferation and the protocol was followed as per manufacturer's instruction (ab5473, Abcam, Centurion, South Africa). Cells were cultured and seeded as previously mentioned in section 2.2.1. Cells were subsequently treated with Ana, AnaAspClop, AspClop, AnaAto and Ato at 1X Cmax for 24hours then rinsed twice in PBS. To study cell proliferation, 20 µl of WST-1/electrocoupling solution was added into each well and incubated for 4 hrs. The absorbance was measured at a wavelength of 450 nm and reference wavelength of 690 nm in a Labsystems Multiskan Ascent Spectrophotometer (Amersham Soc Ltd, Kyalami, South Africa). The experiment was conducted three times. Data was managed in Microsoft Excel 2010 and statistical analysis was conducted using PAST13 software. The Friedman's test and corresponding post *Hoc* test (Wilcoxon) were conducted in order to investigate whether drugs promoted higher levels of cell proliferation within each cell lines A Kruskal-Wallis test was conducted with corresponding post Hoc test (Dunns) in order to determine differences between cell lines at matched treatments (Appendix A5).

2.3 Results

2.3.1 Cell growth analysis

A cell growth analysis assay conducted over 24 hrs revealed no significant difference in cell densities between untreated MCF7 and T47D cells (Fig 2.3, A and B) at each time point; however, it was noted that there was a slightly higher proportion of MCF7 cells than T47D cells, at 6 hrs, 18 hrs, with exception at 12 hrs, reaching equilibrium at 24 hrs (Fig 2.3, C). This suggests that MCF7 cells adhered and proliferated quicker than T47D cells; therefore, more cells were harvested at each time point. This may be attributed to a shorter doubling time in MCF7 cells of 36 hrs, compared to 43 hrs in T47D cells (Physical Sciences-Oncology Network Bioresource Core Facility, ATCC). At 24 hrs the proportion of MCF7 and T47D cells were seemingly equal (Fig 2.3, A &B) suggesting that T47D cells had recovered from the effects of the stress of the plating process. This suggests that T47D cells are more susceptible to changes occurring within their environment than MCF7, hence they may have induce prolonged stress response as a selective pressure to promote their survival, this phenomenon may support evidence which suggest that T47D cells are more aggressive than MCF7 cells (Aka and Lin, 2012).

Morphologically MCF7 cells formed a uniform spread of flattened cells, T47D cells also showed a uniform spread; however, cells appeared more clustered (Fig 2.3, B). In this instance the T47D cells might have taken longer to overcome the effects of stress induced by harvesting and subsequent seeding and would have remained clustered for a longer period following seeding and this may have contributed to the lower proportion of cells recorded at each time point compared to MCF7 cells.

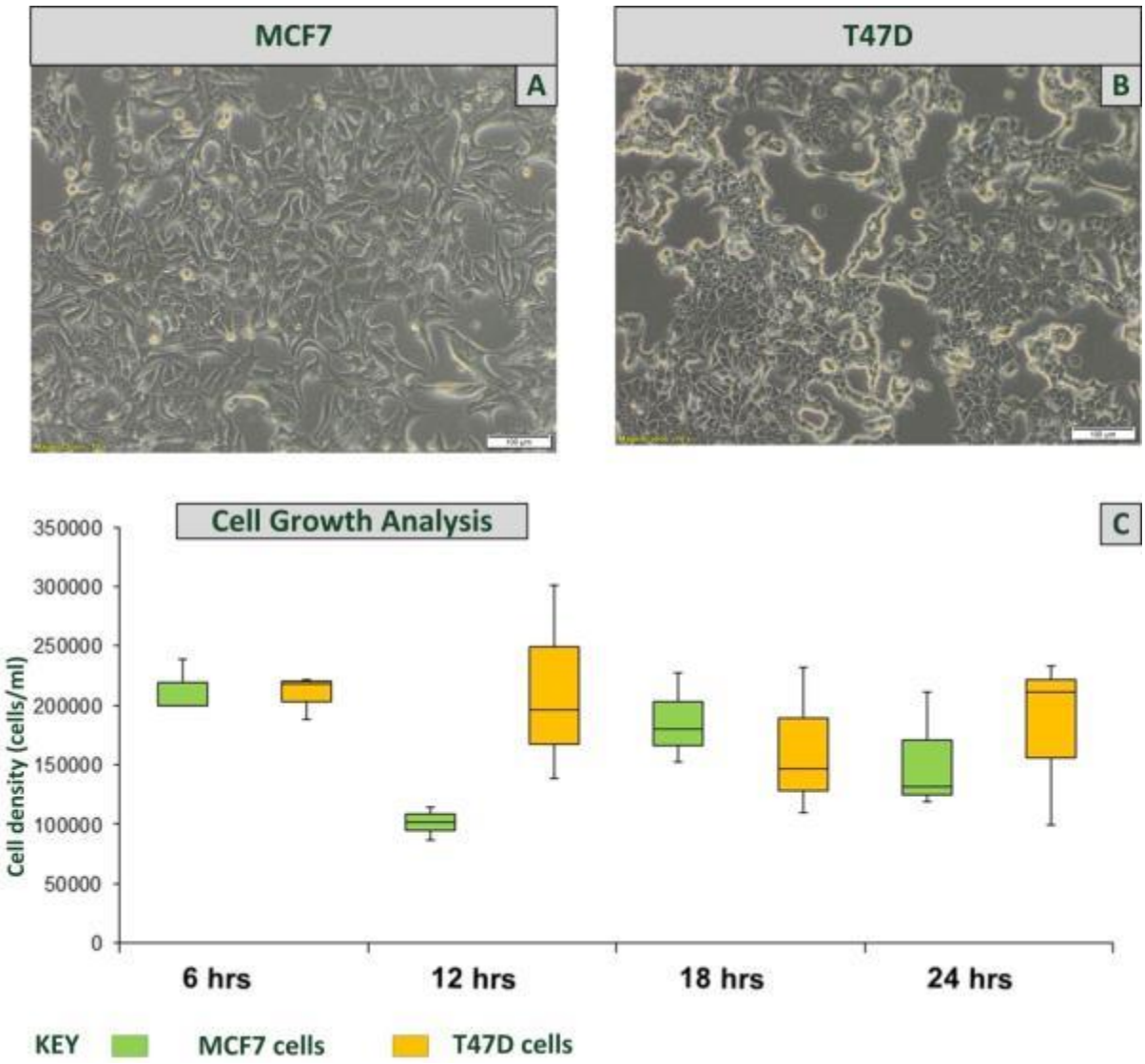


Figure 2.3: Cell growth analysis for MCF7 and T47D cells. Cells were harvested, stained with trypan blue dye and enumerated at 6 hrs intervals over 24 hrs. Representative images of MCF7 cells **(A)** and T47D cell **(B)** in culture (10X magnification). The cell spread is similar between both cell line, MCF7 cells display a more spread polyhedral phenotype whereas T47D cells appear to form tight clusters of varying sizes. **C)** At each time point there was no statistically significant difference in cell density between MCF7 and T47D cells. The trend observed showed that at each time point there was slightly higher proportion of MCF7 cells than T47D cells ($p < 0.05$), except at 12 hrs. This may be attributed to the shorter doubling time in MCF7 cells (36 hrs) compared to that of T47D cells (43 hrs) hence the cell proportion of MCF7 cells at each time point (except 24hours) were slightly higher compared to T47D cells reaching equilibrium at 24 hrs.

2.3.2 Drug toxicity on breast cancer cells by assessing various parameters

In order to achieve the first aim which was to establish drug toxicity, Anastrozole and Antiplatelet drugs (Aspirin and Clopidogrel cocktail and Atopaxar) were tested at a range of concentrations (1X, 2X, 4X, 8X and 10X Cmax); however, no significant differences were observed with increasing concentrations across all the parameters tested (Appendix A2.1-2.3). The parameters used to indicate drug toxicity included assessment of cell viability by neutral red uptake (Fig 2.4, 2.5), and leakage of LDH enzyme (Fig 2.6). Flow cytometry was used to quantify live cells by the lack of expression of PS and no staining with PI and cells undergoing early (PS^+), late apoptosis (PS^+PI^+) and necrosis (PI^+) (Fig 2.7-2.8). These assays were complemented by assessment of cell morphology (qualitatively and semi-quantitatively) (Table 2.3 and Table 2.4).

LDH release across all treatment groups in both cell lines was low (Fig 2.6) and this finding corresponded with a higher proportion of live cells seen using flow cytometry (Fig 2.7). The annexin-V/PI assay showed more specific toxicity outcomes affecting membrane integrity in comparison to both the NR and LDH assays (Fig 2.7). When cells were qualitatively assessed for neutral red staining, both MCF7 and T47D cells showed positive staining in all controls and treatment groups (Fig 2.5). The neutral red dye which accumulates in lysosomes was observed to stainT47D cells more intensely (Fig 2.5, B1-7) in comparison to MCF7 cells (Fig 2.5, A1-7). Lysosomes are involved in cellular stress responses and the higher lysosomal staining intensity with neutral red dye in T47D cells may suggest that these cells induced a heightened stress response than MCF7 cells.

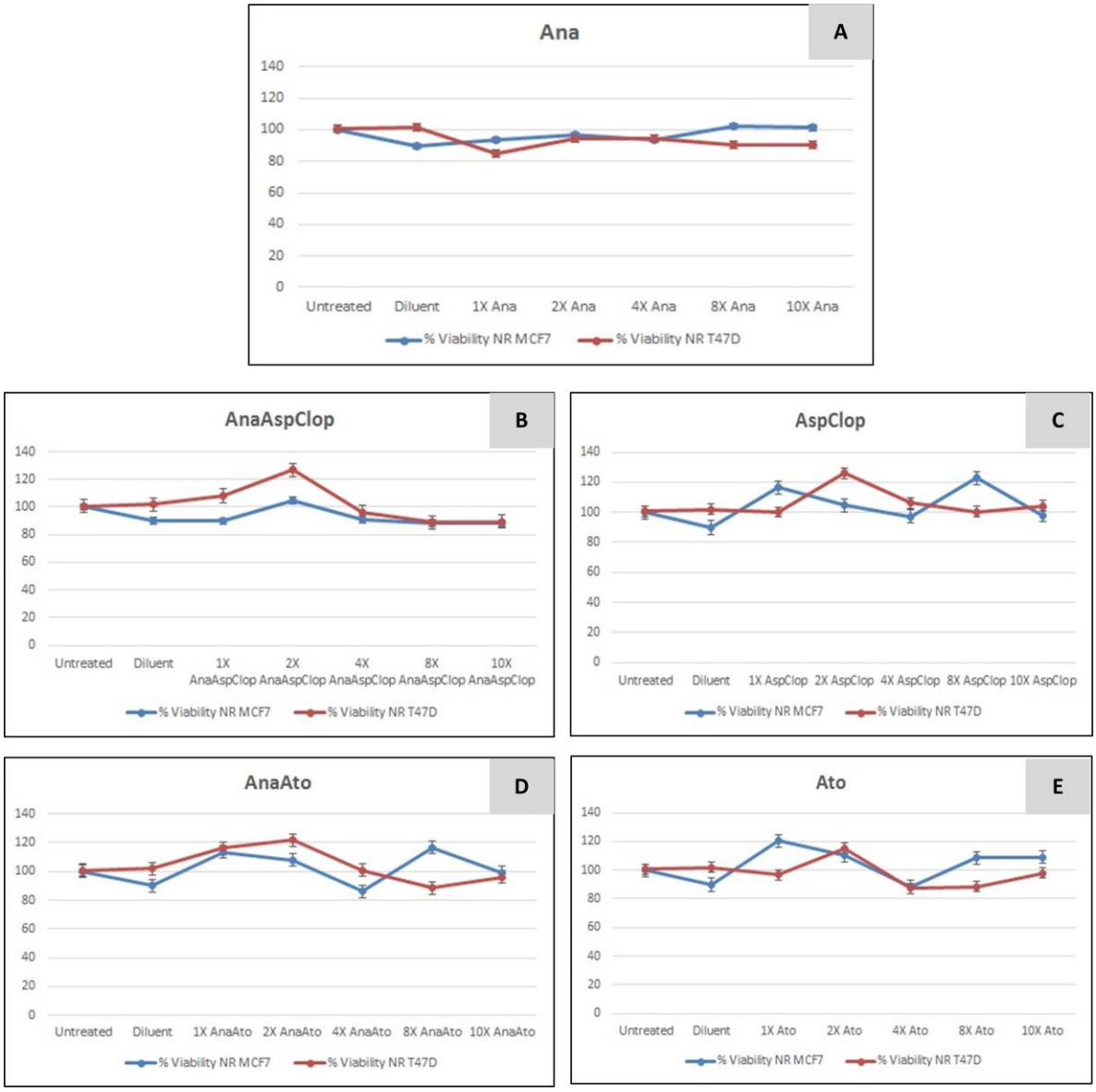


Figure 2.4: Neutral Red (NR) viability assay in MCF7 and T47D cells following treatment; A) Anastrozole (Ana), B) Anastrozole and Aspirin-Clopidogrel cocktail (AnaAspClop), C) Aspirin-Clopidogrel cocktail (AspClop), D) Anastrozole and Atopaxar cocktail (AnaAto) and E) Atopaxar (Ato). Breast cancer cells were treated for 24hours at increasing concentrations of each drug/drug cocktail based on the Cmax concentration (1X Cmax, 2X Cmax, 4X Cmax, 8X Cmax, 10X Cmax), $p>0.05$. Overall cell viability was high across all treatment groups (higher than 80%), suggesting that the drugs did not adversely affect cell viability. There were no significant differences observed between the concentrations for each treatment group. The trend observed shows that Anastrozole treatment slightly reduced cell viability compared to untreated in both cell lines except, at 8X and 10X Cmax for T47D. AnaAspClop-treatment induced higher cell viability in T47D cells at all concentrations except at 4X, 8X and 10X Cmax compared to untreated, in contrast cell viability in MCF7 cells was minimally reduced at all concentrations except at 2X Cmax. AspClop treatment induced higher cell viability at all treatment concentrations in both cell lines. AnaAto treatment induced higher viability at all concentrations in both cell lines compared to untreated cells, except for MCF7 cells at 4X Cmax and T47D cells at 8X Cmax. Ato treatment induced higher cell viability in MCF7 cells at all concentrations except 4X Cmax and in T47D cells, cell viability was reduced at 4X and 8X Cmax.

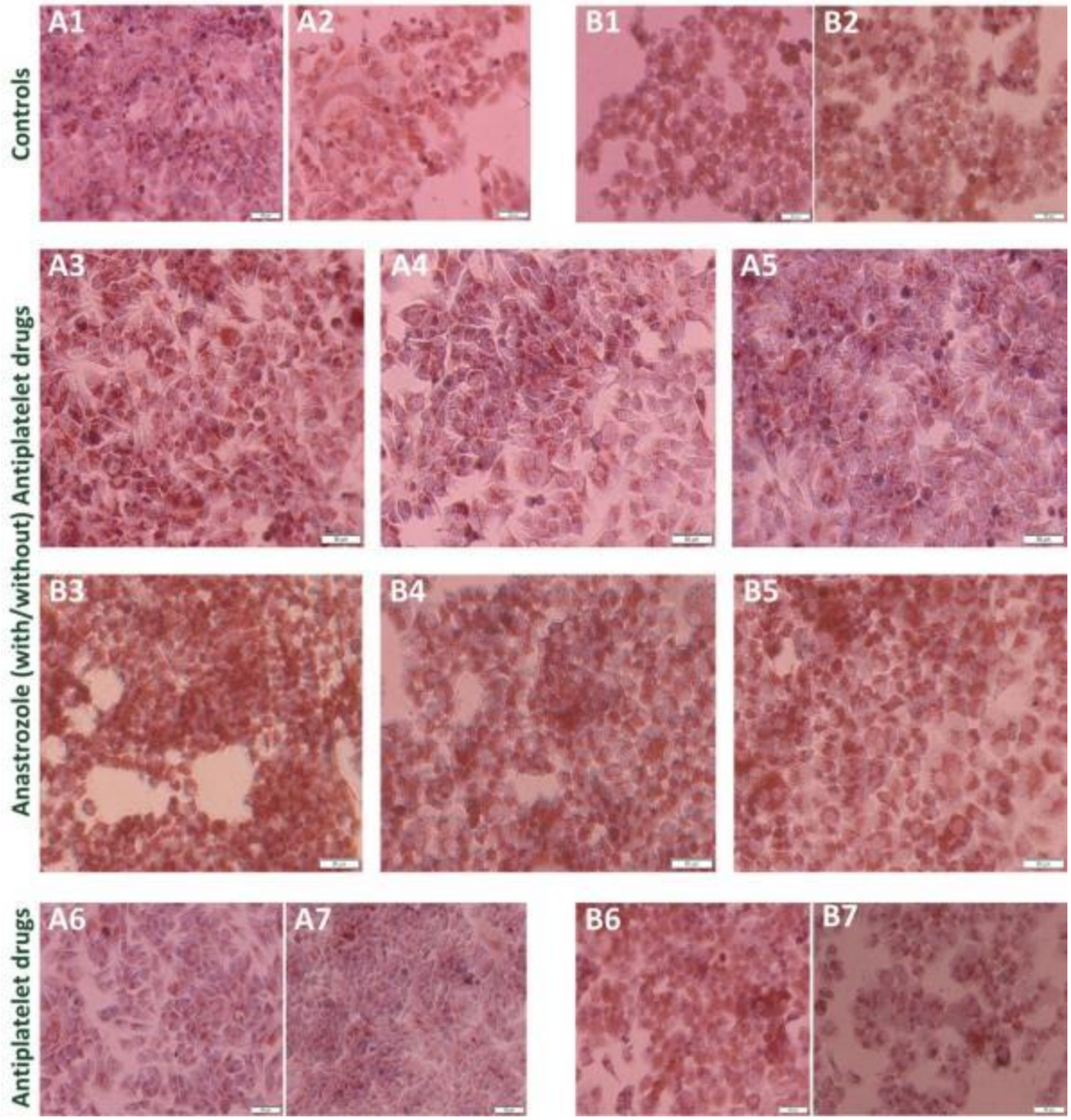


Figure 2.5: Representative photomicrographs of neutral red dye staining on MCF7 (A1-7) and T47D (B1-7) cells. **A1 & B1:** Untreated cells, A2-B2: Diluent control, A3-B3: Anastrozole treated cells, A4-B4: Anastrozole and Aspirin-Clopidogrel cocktail treated cells, A5-B5: Anastrozole and Atopaxar cocktail treated cells, A6-B6: Aspirin and Clopidogrel cocktail treated cells, A7-B7: Atopaxar treated cells. The cells showed uptake of the neutral red dye into lysosomes as evidence by the red cytoplasmic staining. MCF7 cells generally had a lower staining intensity (regardless of the treatment) than T47D cells which stained more intensely with the neutral red dye (dark red cytoplasmic stain) suggesting a higher amount of lysosomes in T47D cells.

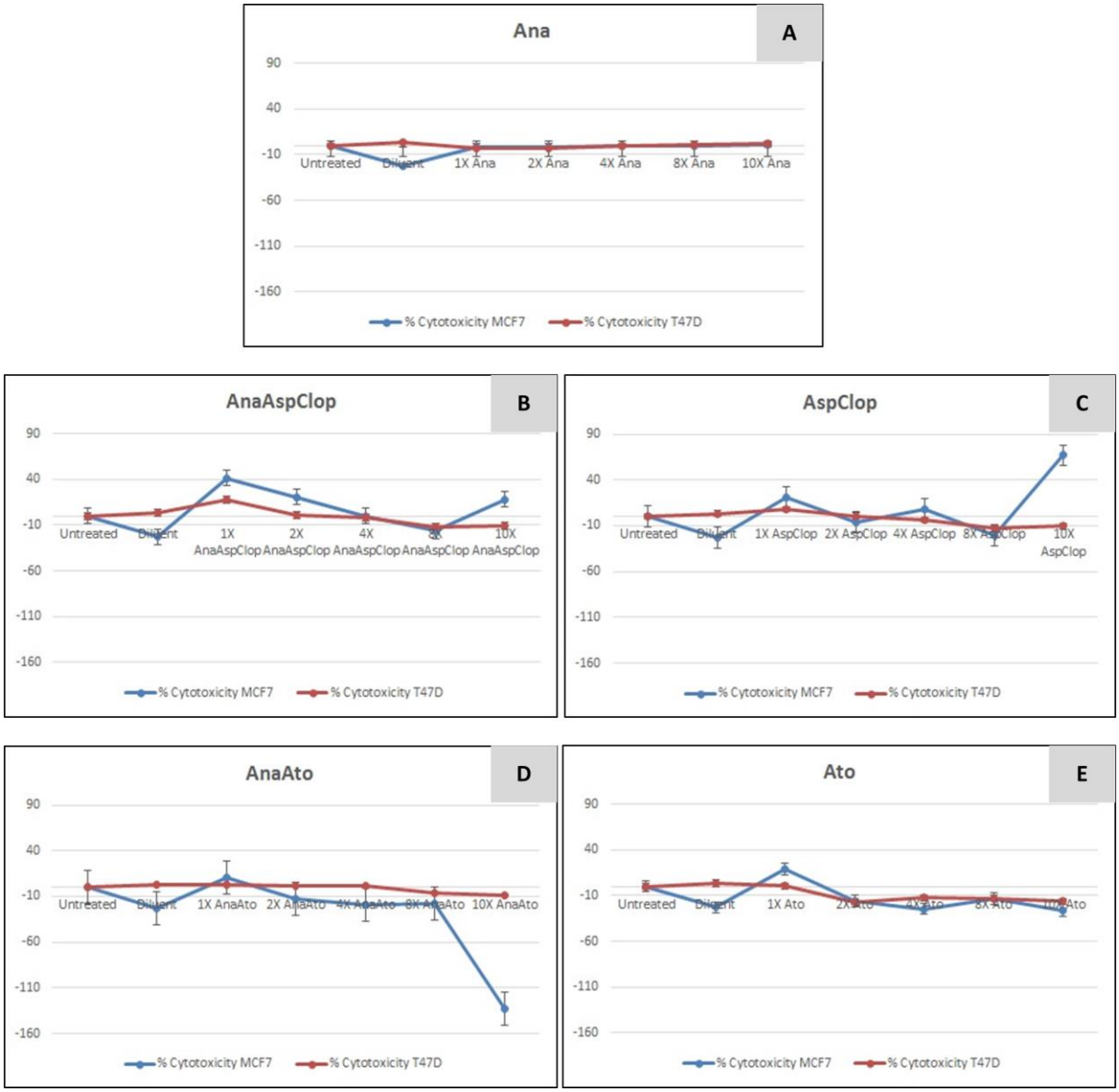


Figure 2.6: Lactate dehydrogenase (LDH) cytotoxicity assay in MCF7 and T47D cells following treatment; A) Anastrozole (Ana), B) Anastrozole and Aspirin-Clopidogrel cocktail (AnaAspClop), C) Aspirin and Clopidogrel cocktail (AspClop), D) Anastrozole and Atopaxar cocktail (AnaAto) and E) Atopaxar (Ato). Breast cancer cells were treated for 24 hrs at increasing concentrations of each drug/drug cocktail based on the Cmax concentration (1X Cmax, 2X Cmax, 4X Cmax, 8X Cmax, 10X Cmax), $p>0.05$. The leakage of lactate dehydrogenase enzyme indicates damage to membrane permeability and therefore cytotoxicity. Overall there was low LDH leakage across the different treatments which suggests that little to no cytotoxicity was induced. The trend observed showed that Ana did not induced cytotoxicity at all concentrations in both cell lines. AnaAspClop induced higher cytotoxicity at 1X Cmax in both cell lines compared to the control and subsequently reduced it in higher concentrations. AspClop treatment induced higher toxicity than untreated controls at 1X, 4X and 10X Cmax in T47D cells, whereas in gradually reduced toxicity in MCF7 cells. AnaAto and Ato did not induce toxicity in both cell lines, with exception for MCF7 cells at 1XCmax whereby low levels of toxicity were induced.

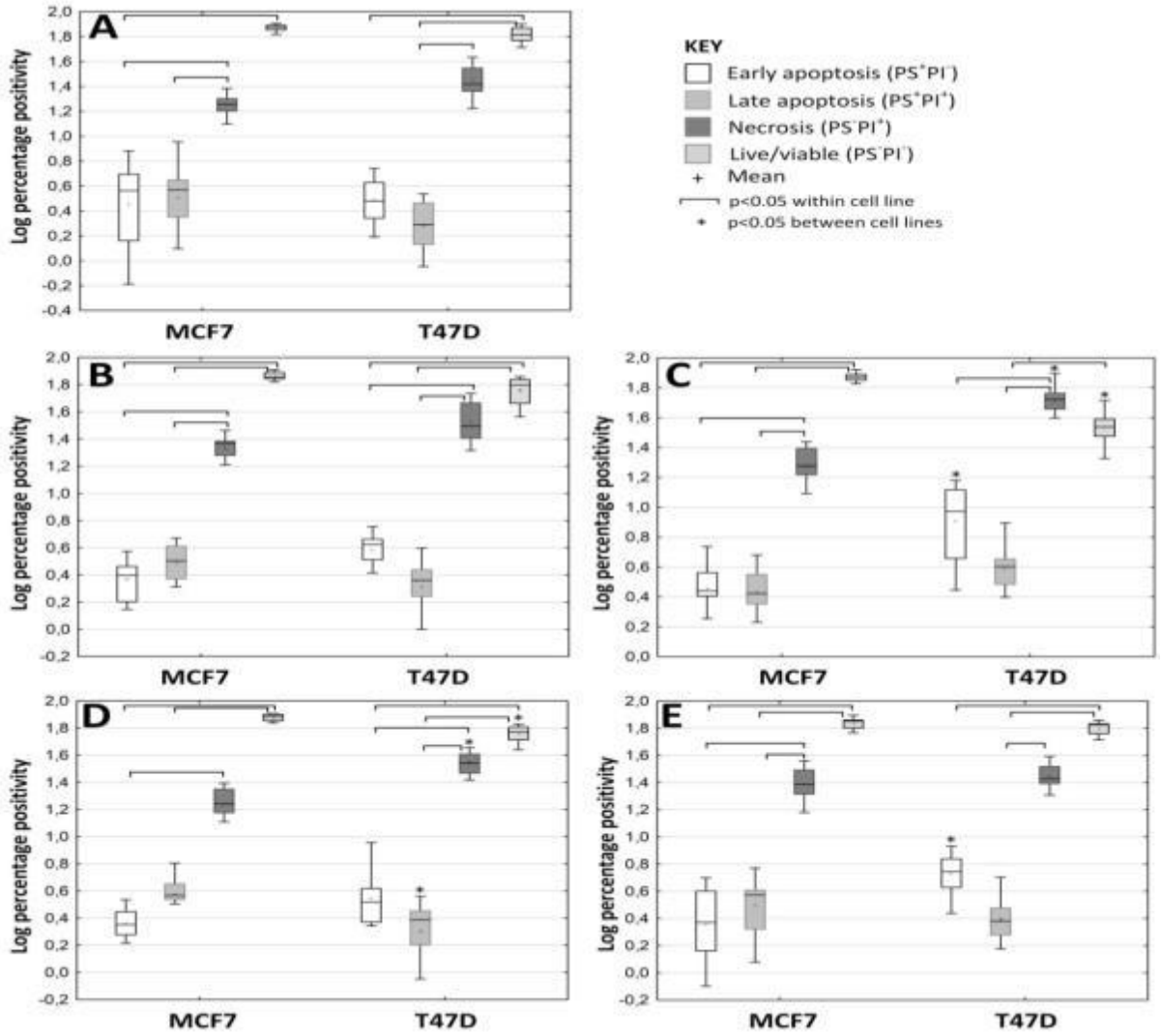


Figure 2.7: Cytotoxicity in MCF7 and T47D cells as indicated by flow cytometry. (A) Anastrozole (Ana): in both cell lines there was a higher proportion of live cells followed by necrosis. Necrosis was higher than late apoptosis in both cell lines, suggesting a higher proportion of cells with damaged membrane integrity and additional early apoptosis in MCF7 cells only. No statistical significant differences were noted between the cell lines (B) Anastrozole, Aspirin and Clopidogrel (AnaAspClop): a similar trend as with Anastrozole treatment is observed (C) Aspirin and Clopidogrel (AspClop): a reduction in the proportion of live and increase in necrotic T47D cells compared to MCF7 cells is observe (D) Anastrozole and Atopaxar (AnaAto): a reduction in the proportion of live cells was observed compared to MCF7 cells, corresponding to an increase in necrosis and decrease in late apoptosis in T47D cells compared to MCF7 cells (E) Atopaxar (Ato): an increase in early apoptosis was observed in T47D cells compared to MCF7 cells. The general trend observed in all treatment groups was that there was a higher proportion of viable cells (PS^-PI^-), followed by necrotic cells (PS^-PI^+) then apoptotic cells (PS^+PI^-). Overall T47D cells were found to be more susceptible to drug treatment over 24hours than MCF7 cells.

Morphologically, ultrastructural analysis revealed that untreated MCF7 and T47D cells appeared fully spread and polyhedral in shape, with a uniform cover of microvilli and few blebs (Fig 2.8: A1, B1). Prominent thick pseudopodia and thin filopodia were seen anchoring and connecting adjacent cells in both cell lines (Fig 2.8: A1, B1). Exposure to the diluent (0.03% DMSO), did not alter cell shape and integrity of pseudopodia in both cell lines. However, MCF7 cells showed a reduction in the density of microvilli with clumping in certain areas, as well as a reduction in filopodia (Fig 2.8: A2). In T47D cells, more blebs were observed (Fig 2.8: B2). With exception of microvilli clumping seen in MCF7 cells, most of the morphological differences were not statistically different compared to the media control (Table 2.3).

Ana-treatment did not significantly alter ultrastructural (Table 2.3) and cytotoxicity parameters (Fig 2.4-2.6) compared to the controls in MCF7 and T47D cells. Further investigation of flow cytometry data revealed that Anastrozole induced higher levels of necrosis (PS^-PI^+) than early (PS^+PI^-) and late (PS^+PI^+) apoptosis; however, cell viability was maintained (PS^-PI^-) (Fig 2.7 A). This was a common finding across all drug groups corresponding to morphological observations whereby cells appeared to be viable regardless of the differences in parameters such as shape change and microvilli density (Fig 2.8: A3, B3). Ana-treatment in both cell lines, did not adversely affect cell shape as most cells retained their spread, flattened morphology with few rounded cells noted; cell contacts were not significantly altered and fewer membrane ruffles, which are regions of actin filament clusters on the cell surface which form when lamellipodia retracts towards the cell body and detached from integrins, were observed in T47D cells than MCF7 cells (Fig 2.8: A3, B3). Both cell lines also showed evidence of reduced microvilli density, albeit not significant (Table 2.4). In both cell lines membrane blebbing was sparse in flattened and round cells ($p>0.05$) (Table 2.4), it

was also noted to be more evident in T47D cells (Fig 2.8: A3, B3). Extracellular contents were not seen due to the uniform layer formed by cells (Fig 2.8: A3, B3).

When cells were treated with Anastrozole combined with Aspirin and Clopidogrel cocktail (AnaAspClop), MCF7 cells showed no significant difference ($p>0.05$) in response across all cytotoxicity parameters (Fig 2.7: B), maintaining a flattened morphology, with a few round cells noted. Cell contacts were maintained by pseudopodia, but filopodia density and integrity was reduced (Fig 2.9: A1.1-1.4). MCF7 cells also presented with ruffled membrane and sparse blebbing (Fig 2.9: A1.1-1.4). In contrast, no significant differences were seen in early apoptosis (PS^+PI^-) between the cell lines but the trend observed suggests that T47D cells showed heightened early apoptosis (PS^+PI^-) (Fig 2.7: B) and cell shape was changed from flattened, as observed in control and Ana-treatment groups (Fig 2.8), to mainly round, forming distinct clusters (Fig 2.9: B1.1-1.4); some flattened cells were noted suggesting active shape change was occurring, overall there was no significant difference in shape change in AnaAspClop-treated cells compared to Ana-treatment (Table 2.4). Clustered T47D cells maintained contacts with pseudopodia; however, there was loss of filopodia integrity, and short microvilli or uniform blebs were noted on the surface of a few round cells (Fig 2.9: B1.1-1.4). More ruffled membranes were noted in T47D cells compared to MCF7 cells (Fig 2.9: B1.1-1.4). The cells displayed a round shape within the clusters, and while a rounded morphology with blebs is typically associated with cell death, the majority of cells with round shape were viable (PS^-PI^-) (Fig 2.9: B). Few round cells had sparse blebs accompanied by a loss in microvilli and those were most likely undergoing apoptosis (Fig 2.9: B1.1-1.4). The round cell clusters seen may be indicative of the migration strategy used by these cells which indicates collective migration (Pandya, Orgaz and Sanz-Moreno, 2017). A few cells with damaged membrane

integrity and leakage of cytoplasmic contents were observed echoing flow cytometry results showing heightened levels of necrosis (PS^+PI^+) (Fig 2.9: A-B 1.1-1.4; Fig 2.7: B). In both cell lines sparse cell debris was noted in the extracellular matrix and this was a common feature in all groups except Anastrozole treatment (Fig 2.9: A-B 1.1-1.4). When cells were treated with the corresponding control Aspirin and Clopidogrel cocktail (AspClop) the proportion of MCF7 cells undergoing early apoptosis (PS^+PI^-) and necrosis (PS^-PI^+) were significantly reduced compared to T47D cells ($p<0.05$) (Fig 6: C). The higher proportion of cells undergoing early apoptosis (PS^+PI^-) and necrosis (PS^-PI^+) in T47D cells was accompanied by a reduction in the number of viable cells (PS^-PI^-). Morphologically, T47D cells formed clusters of round cells suggestive of collective cell invasion (Pandya *et al.* 2016), in association with flattened cells (Fig 2.9: B2.1-2.4). Additionally, the apparent fusion or budding of tumour cells (Fig 2.9: B2.1-2.4) is indicative of a more aggressive profile (Pandya *et al.* 2016). There was a significant loss in the integrity and amount of filopodia, and cell connections with pseudopodia were maintained (Table 2.4). Notably, ruffled edges were more prominent in this treatment group and cell line (T47D). MCF7 cells were mainly flattened with a few round cells noted and microvilli density was reduced (Fig 2.9: A2.1-2.4). Sparse membrane blebbing was seen in some round cells accompanied by a loss of microvilli and only a few cells expressed blebs. Ruffled membranes were seen in a few round cells and distinct large pores were also noted in some cells (Fig 2.9: A2.1-2.4).

When cells were treated with combined Anastrozole and Atopaxar, showed similar findings to that of other treatment groups; higher levels of necrosis (PS^-PI^+) than early apoptosis (PS^+PI^-) were induced in both cell lines although a rise in late apoptosis (PS^+PI^+) ($p>0.05$) was found in MCF7 cells (Fig 2.9: D). Nevertheless, the number of viable cells remained high (PS^-PI^-) (Fig

2.7: D). This was accompanied by morphological assessment which showed that MCF7 cells maintained a flattened shape with fewer membrane ruffles (Fig 2.10: A1.1-1.4). Microvilli density was reduced in comparison to T47D cells; however, this was not significant (Table 2.4). MC7 cells displayed few membrane blebs and necrotic cells (Fig 2.10: A1.1-1.4). In contrast, the majority of T47D cells retained their rounded shape with evidence of filopodia extensions, blebbing and maintenance of cell clusters by pseudopodia (Fig 2.10: B1.1-1.4). Uniform microvilli cover was maintained with clumping in certain regions (Fig 2.10: B1.1-1.4). Membrane ruffles were a common feature and membrane blebs were observed in some viable cells situated mainly at the cell borders (Fig 2.10: B1.1-1.4).

The corresponding antiplatelet control treatment, Atopaxar alone, showed similar outcome as with other treatment groups, induced higher levels of necrosis (PS^-PI^+) than early (PS^+PI^-) or late (PS^+PI^+) apoptosis and a higher proportion of live viable cells (PS^-PI^-) were maintained. A significant increase in early apoptosis (PS^+PI^-) was induced in T47D cells compared to MCF7 cells (Fig 2.7: E). Morphologically MCF7 cells maintained a flattened morphology with a few round cells observed (Fig 2.10: A2.1-2.4). Cell contacts through pseudopodia were maintained and filopodia were present, although reduced in density (Fig 2.10: A2.1-2.4). Sparse microvilli were observed and clumping occurred in some regions. Membrane ruffles were present and a few small blebs were seen (Fig 2.10: A2.1-2.4). T47D cells retained the round cell clusters with denser microvilli cover compared to MCF7 cells, albeit not significant (Fig 2.10: B2.1-2.4; Fig 2.7: E). Cell contacts were maintained, with large blebs regularly seen and located on the periphery of viable cells suggesting an involvement in cell motility (Fig 2.10: B2.1-2.4). Membrane adaptations such as ruffles were also identified (Fig 2.10: B2.1-2.4).

In summary, these findings showed that T47D cells are more susceptible to responding to combined antiplatelet therapy with Anastrozole. Both cell lines presented with variations in membrane integrity, across all parameters observed; however, while cytotoxic effects were noted, cells were able to adapt and maintain overall viability (Fig 2.7). Notably the cells presented with heterogenous features such as: ruffled membrane, pseudopodia and filopodia (although damaged, they were present), microvilli (appearing clumped in some regions); and membrane blebs. These features reflect changes to the cytoskeleton, which play a key role during cell motility, and also reflect metabolic stress. Some membrane pores of varying sizes were also observed in some cells and could indicate damaged cell integrity. Overall changes in morphological features were seen to be more prominent in T47D cells than MCF7 cells following a 24 hrs treatment. Interestingly, the morphological changes observed in cells were independent of the drug concentration. Thus, there was insufficient evidence to suggest that the range of concentrations tested for the different drugs induced significantly different toxicity outcomes. Therefore, the 1X Cmax concentrations were used to treat cells in subsequent experiments. To further establish a toxicity profile for these therapies, a scratch assay to study migration and a WST-1 proliferation assay was conducted. For these studies cells were treated at 1X Cmax concentrations, findings are presented below.

Table 2.4: Semi-quantitative analysis of morphological features noted in MCF7 and T47D cells following 24hour treatment with combined Anastrozole and antiplatelet therapy.

	Shape		**Filopodia**		**Pseudopodia**		**Microvilli density**		**Microvilli shape**		**Bleb density**		**Bleb size**		**Secretions**	
	MCF 7	**T47 D**	**MCF7**	**T47D**	**MCF7**	**T47D**	**MCF7**	**T47D**	**MCF7**	**T47D**	**MCF 7**	**T47D**	**MCF 7**	**T47D**	**MCF 7**	**T47D**
Untreated	F	F	P	PC	PC	PC	Md	Md	Sh/Uc **(ϕ)**	Sh/Uc	Sp	Sp	Mx	Mx	Sp	Sp
Diluent	F	F	P	P	PC	PC	Sp	Sp	Mx **(≠)**	Sh/Uc	Sp	Sp	Mx	Mx	Sp	Sp
Ana	F	F	PC	PC	PC	PC	Sp	Sp	Sh/Uc	Mx	Sp	Sp	Sm	Sm	A	A
AnaAsp Clop	F	F	P	P **(≠)**	PC	P	Sp	Sp	Sh/Uc	Sh/Uc	Sp	Sp	Mx	Mx	Sp	Sp
AspClop	F	R*	P	P **(≠)**	PC	PC	Sp	Sp	Sh/Uc	Sh/C	Sp	Sp	Sm	Sm	Sp	Sp
AnaAto	F	R*	P	P **(≠)**	PC	P	Sp	Sp	Sh/Uc **(ϕ)**	Sh/C	Sp	Sp	Md	Mx	Sp	Sp
Ato	F	R*	P	P **(≠)**	PC	PC	Sp	Sp	Sh/Uc **(ϕ)**	Sh/Uc	A	Sp	A	Sm **(≠)**	Sp	Sp

Statistically significant differences between cell lines indicated by (*); within cell lines differences to controls (untreated and diluent) were indicated by (≠) and (ϕ) respectively. **KEY: A** = absent, **F** = Flat, **Md** = medium, **Mx** = Mixed, **P** = present no cell-cell contacts, **PC** = present with cell contacts; **Sh/Uc** = short/free/unclumped, **Sh/C** = short/clumped, **Sm** = Small, **Sp** = Sparse, **R**= Round.

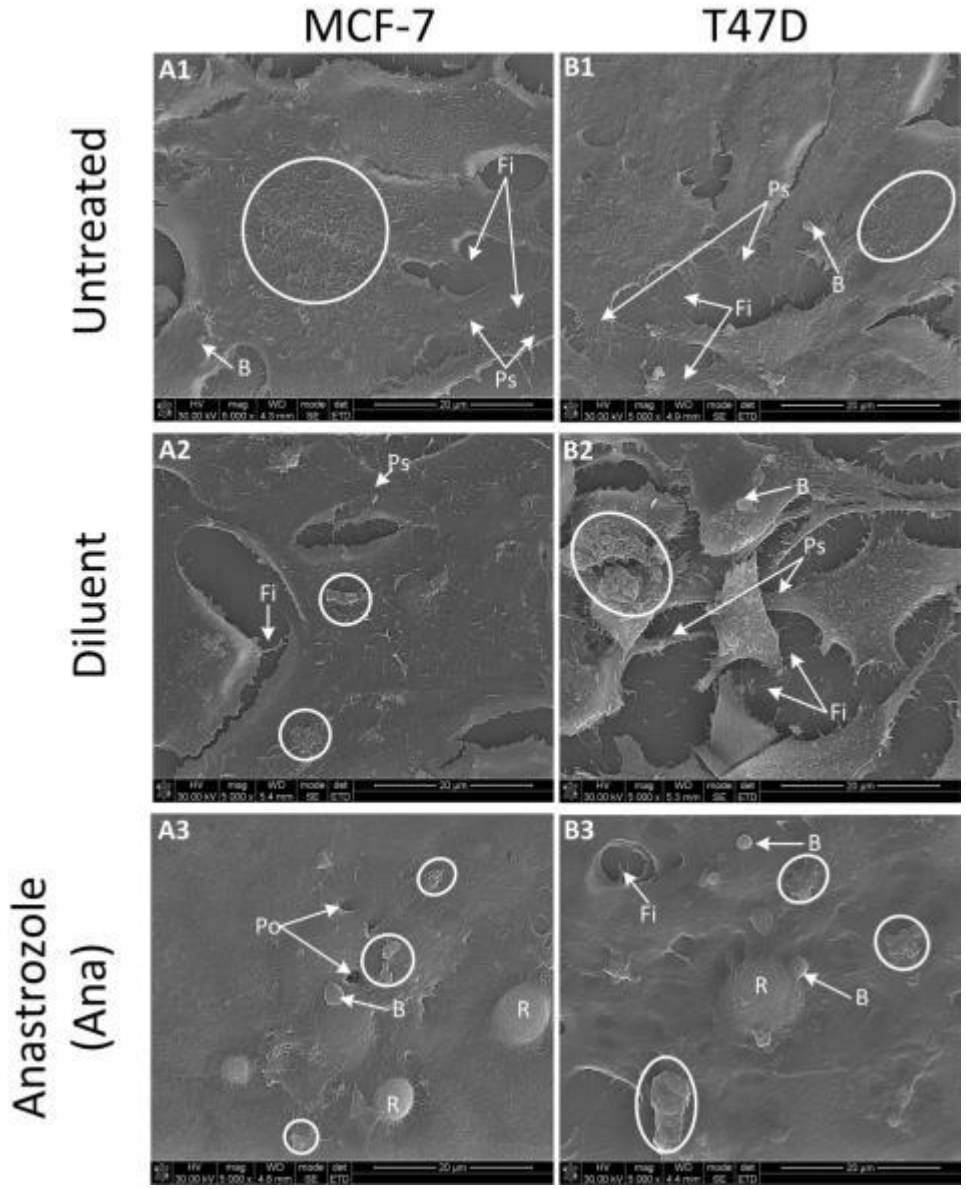


Figure 2.8: Representative micrograph showing ultrastructural features in MCF7 and T47D cells. R: round viable cell, Fi: filopodia, Ps: pseudopodia, B: bleb, D: cell debris, Po: pore, Ru: ruffled membrane. (A1, MCF7 cells) & (B1, T47D cells) cells exposed to medium only (untreated), (A2, MCF7 cells) & (B2, T47D cells) cells exposed to 0.03% DMSO (diluent), and (A3, MCF7 cells) & (B3, T47D cells) treated with Anastrozole for 24hours. The cell shape was flattened/polyhedral, additionally a few round viable cells were noted with Anastrozole treatment, sparse membrane blebbing (B) was noted and dense microvilli cover was present on untreated cells, exposure to diluents and Anastrozole reduced the density of the microvilli cover (albeit not significant). Regions of microvilli clumping (encircled) can be seen. Thin filopodia (Fi) and thicker pseudopodia (Ps) were noted joining adjacent cells. Pores (Po) were also identified with Anastrozole treatment, possibly facilitate exchange of substances.

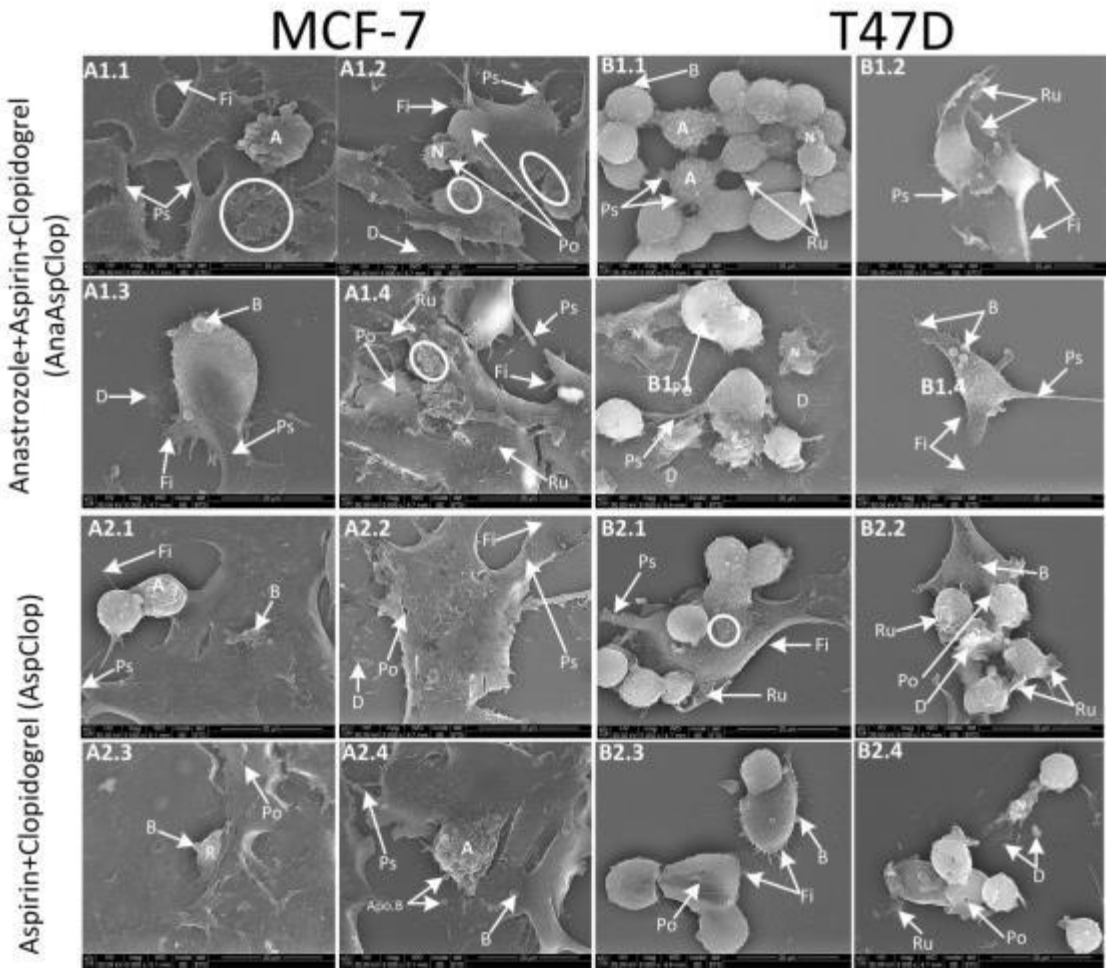


Figure 2.9: Representative micrographs showing ultrastructural changes following exposure to Anastrozole and Aspirin-Clopidogrel cocktail. A: apoptotic cell, N: necrotic cell, R: round viable cell, Fi: filopodia, Ps: pseudopodia, B: bleb, Apo.B: apoptotic body, D: cell debris, Po: pore, Ru: ruffled membrane. (A1.1-1.4, MCF7 cells) & (B1.1-1.4, T47D cells) Anastrozole, Aspirin and Clopidogrel treatment: flattened cell shape was maintained in MCF7 cells whereas T47D were mainly round; elongated cells also noted. Few apoptotic (A) and necrotic (N) cells were observed in both cell lines. Sparse microvilli density and few membrane blebs (B) towards the cell periphery on viable cells were noted. (A2.1-2.4, MCF7cells) & (B2.1-2.4, T47D cells) Aspirin-Clopidogrel cocktail treatment: MCF7 cells maintained a flattened shape with a few round apoptotic (A) and viable (R) cells. Apoptotic cells had uniform bleb cover and apoptotic bodies were seen budding off from the cell surface (Apo.B). T47D cells formed round clusters with ruffled membrane borders. In both cell lines pseudopods and filopodia were prominent, although their density was reduced compared to untreated cells. Membrane pores were evident. Microvilli were sparsely distributed on the cell membrane and clumped in certain areas (encircled), overall appearing to be denser in T47D cells compared to MCF7 cells. Few membrane blebs were observed in viable cells in both cell lines. Sparse cell debris (D) was observed in the extracellular space in both treatments and for both cell lines.

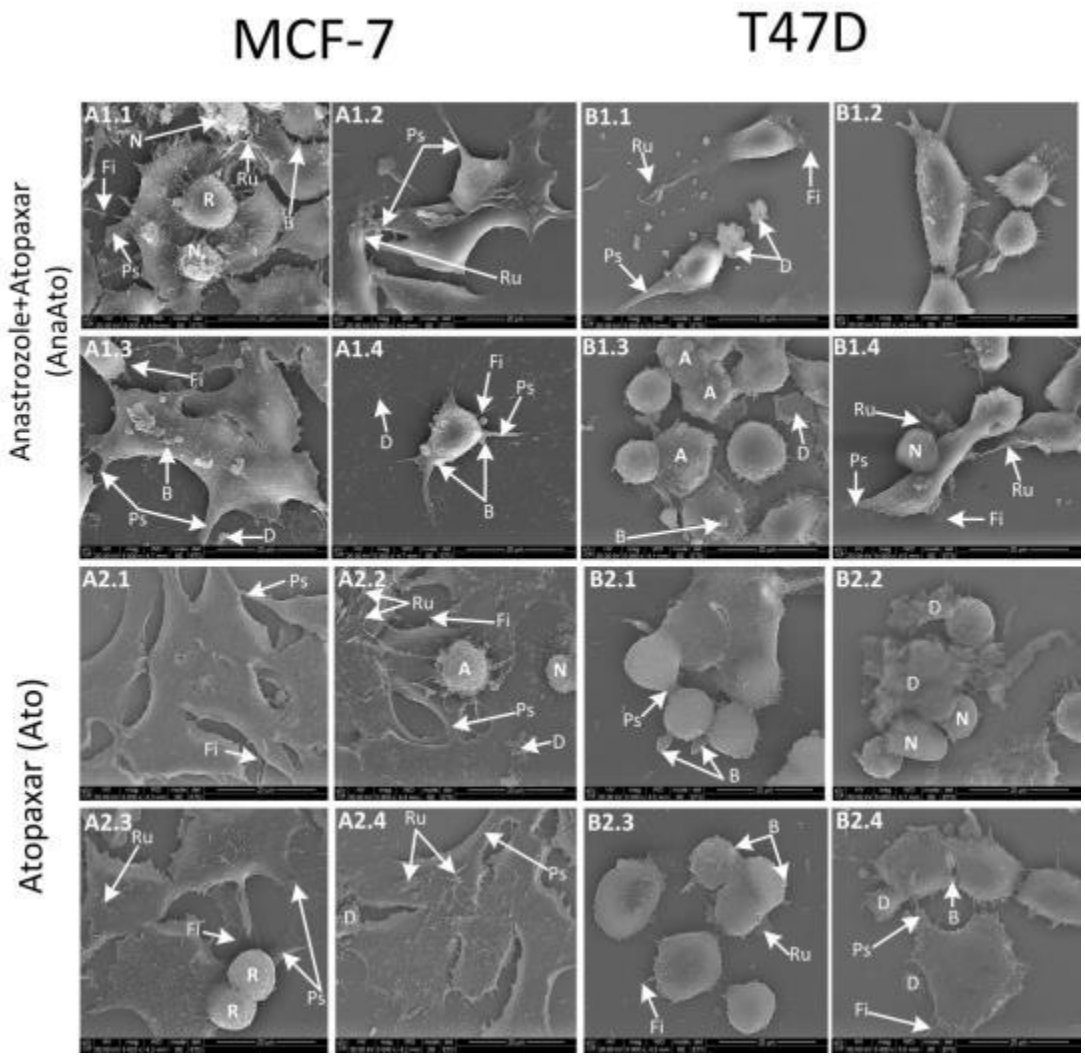


Figure 2.10: Representative micrographs showing ultrastructural changes following exposure to Anastrozole and Atopaxar. A: apoptotic cell, N: necrotic cell, R: round viable cell, Fi: filopodia, Ps: pseudopodia, B: bleb, D: cell debris, Po: pore, Ru: ruffled membrane. (**A1.1-1.4,** MCF7cells) & (**B1.1-1.4,** T47Dcells) Anastrozole and Atopaxartreatment: MCF7 cells maintained a flattened shape whereas T47D cells were mostly rounded. Prominent pseudopods and filopodia were noted in both cell lines, although reduced density compared to the untreated cells. Sparse membrane blebbing was noted in viable cells towards the cell periphery and few apoptotic (A) and necrotic (N) cells were observed. T47D cells presented with more ruffled membranes than MCF7 cells. (**A2.1-2.4,** MCF7 cells) & (**B2.1-2.4,** T47Dcells) Atopaxar treatment: MCF7 cells maintained the flattened morphology with sparse microvilli and ruffled borders. Prominent pseudopods and filopodia were noted. Few round viable (R), apoptotic (A) and necrotic (N) cells were observed. In T47D cells the round cell clusters as seen in previous treatments were maintained, less prominent pseudopods and filopodia compared to MCF7 cells. A few ruffled membranes and blebs were observed in viable cells and necrotic cells were observed with leaked cell contents (D) into the extracellular space due to damaged membrane integrity.

2.3.2 Migration and cell proliferation

Migration was investigated by means of a scratch assay whereby an area was exposed at the centre of a cell monolayer, then cells were treated with 1X Cmax concentrations of Anastrozole and antiplatelet therapies (Aspirin and Clopidogrel cocktail or Atopaxar) and during the treatment period, cell migration was monitored at 6 hr intervals for 24 hrs. The change in area over 24 hrs was compared to the area measurement at 0 hrs in order to establish whether there was a gradual closure of the exposed area by calculating the % closure rate (Fig 2.11). The wound closure assessed over 24 hrs was directly proportional to the rate of migration. Both cell lines (MCF7 and T47D) generally demonstrated a low migratory rate as the exposed area was not closed or was populated by relatively few cells at 24 hrs. This was observed in all treatments (Fig 2.12,2.13, 2.14).

When MCF7 cells were exposed to medium only, there was minimal migration compared to treated cells (Fig 2.11) and very few cells were observed within the exposed area, this was observed in both cell lines (Fig 2.12: A-B). This indicates that baseline migration rate in these cell lines is generally low. When cells were exposed to the diluent (Fig 2.12: A-B), cell migration rate remained relatively low, expect in Ana-treated and Ato-treated MCF7 cells (Fig 2.11), and relatively more cells were observed in the exposed area compared to those seen when cells were exposed to medium only (Fig 2.12: A-B).

Ana-treatment in MCF7 cells induced significantly higher migration compared to AnaAspClop-treated MCF7 cells (Fig 2.11). In contrast, Ana-treatment inhibited migration in T47D cells (Fig 2.11). When Ana was combined with AspClop (AnaAspClop), it significantly reduced migration in MCF7 cells; however, when AspClop was used alone it significantly increased migration in MCF7 cells. Thus suggesting that combined treatment may reduce migration rate compared to each treatment modality alone. In AnaAspClop-treated MCF7 cells the exposed area had

more cells occupying it at each time point thus suggesting that migration was occurring at an equal rate at each time point (Fig 2.13: B). In AnaAspClop-treated T47D cells migration rate was higher than in MCF7 cells, and few cells were seen occupying the exposed area (Appendix A6.1). This finding suggests that AnaAspClop-treatment induced higher migration in T47D cells than MCF7 cells. When cells were treated with AspClop control, few MCF7 cells were observed migrating into the exposed area, fewer than when cells were treated with AnaAspClop (Fig 2.13: C). In contrast, there were more T47D cells found in the scratched area at each time point, compared to when cells where treated with AnaAspClop.

When MCF7 cells were treated with Ana combined with Ato (AnaAto) cell migration was significantly higher compared to Ato-treatment control, but cell migration was significantly reduced compared to Ana treatment alone (Fig 2.11). Thus suggesting that the promigratory effects on Anastrozole in MCF7 cells were reduced by Atopaxar. No migration was seen in AnaAto and Ato treated T47D cells. With AnaAto treatment in both cell lines, fewer cells were seen migrating into the exposed area (Fig 2.14: D). Atopaxar treatment control inhibited migration in both cell lines (Fig 2.11), this observation corresponded with few cells seen occupying the exposed area (Fig 2.14: C).

In summary both cell lines showed a low migratory rate. MCF7 cells generally displayed higher migration than T47D cells, cell treatments increased migration rate in MCF7 cells; however, reduced migration in T47D cells compared to untreated cells, suggesting that MCF7 cells were more susceptible to the effects of the drugs. In contrast T47D cells displayed some resistance to drug treatment, except with combined Ana and AspClop treatment, which increased migration rate.

When cell proliferation was assessed using WST-1 cell proliferation assay it further showed that cell proliferation in MCF7 cells was significantly higher than T47D cells at all matched treatments (Fig 2.15). Ana-treatment in MCF7 cells was comparable to medium control (Untreated cells) but higher than in AnaAsClop-treated MCF7 cells (albeit not significant) (Fig 2.15). AnaAspClop-treated MCF7 cells induced lower cell proliferation compared to Ana-treatment and AspClop-treatment alone (albeit not significant) (Fig 2.15). AspClop-treatment control in MCF7 cells induced the highest cell proliferation compared to Ana and AnaAspClop (albeit not significant) (Fig 2.15). When MCF7 cells were treated with AnaAto, cell proliferation was low compared to Ana-treatment and Ato-treatment (albeit not significant) and Ato-treatment in MCF7 cells induced the highest cell proliferation (significant when compared to medium control only (Fig 2.15) (albeit not significant). In T47D cells, cell proliferation was comparable between all treatment groups and no significant differences were observed (Fig 2.15); however, the diluent control induced significantly higher cell proliferation than AspClop-treated and Ato-treated T47D cells (Fig 2.15). In summary these findings suggest that MCF7 cells had a higher proliferation rate than T47D cells and thus could be more susceptible to the effects of therapy and the higher cell proliferation rate could be a stress response, and antiplatelet therapy alone (AspClop or Ato) induced higher proliferation than when combined with Anastrozole (AnaAspClop or AnaAto). T47D cells in contrast did not alter their proliferation rate in response to treatment and may indicate a higher resistance to stress stimuli.

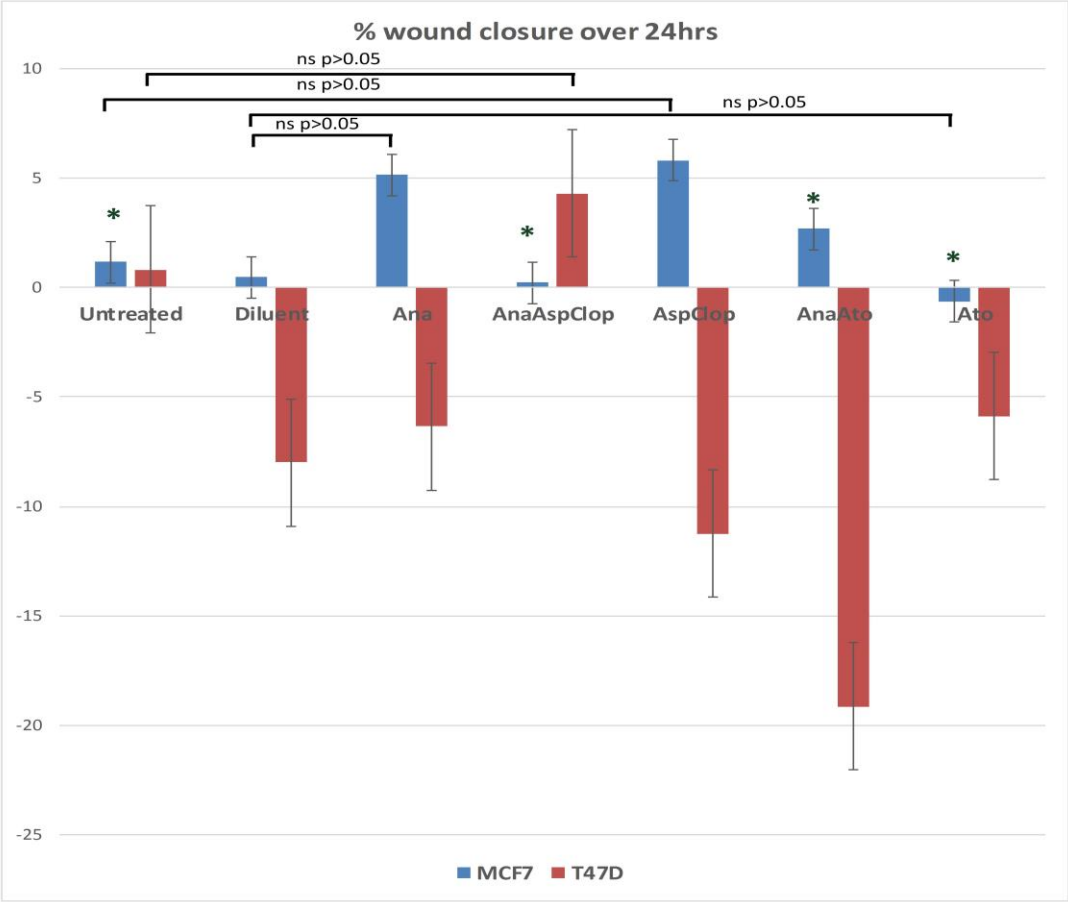


Figure 2.11: The closure rate in breast cancer cells following 24 hrs treatment with Anastrozole and Antiplatele drugs: Ana, AnaAspClop, AspClop, AnaAto and Ato. The closure rate is directly proportional to the rate of migration and MCF7 cells displayed faster migration rate than T47D cells. Ana treatment induced higher migration than when combined with AspClop cocktail or ato in MCF7. AspClop-treatment in MCF7 cells induced highest migration rate whereas Ato treatment did not iduce migration. T47D cells showed a reduction in migration with all treatments in relation to the untreated control, expect for AnaAspClop treatmnet which induced the highest migration rate in this cell line.* indicates $p<0.05$ between cell lines at matched treatment.

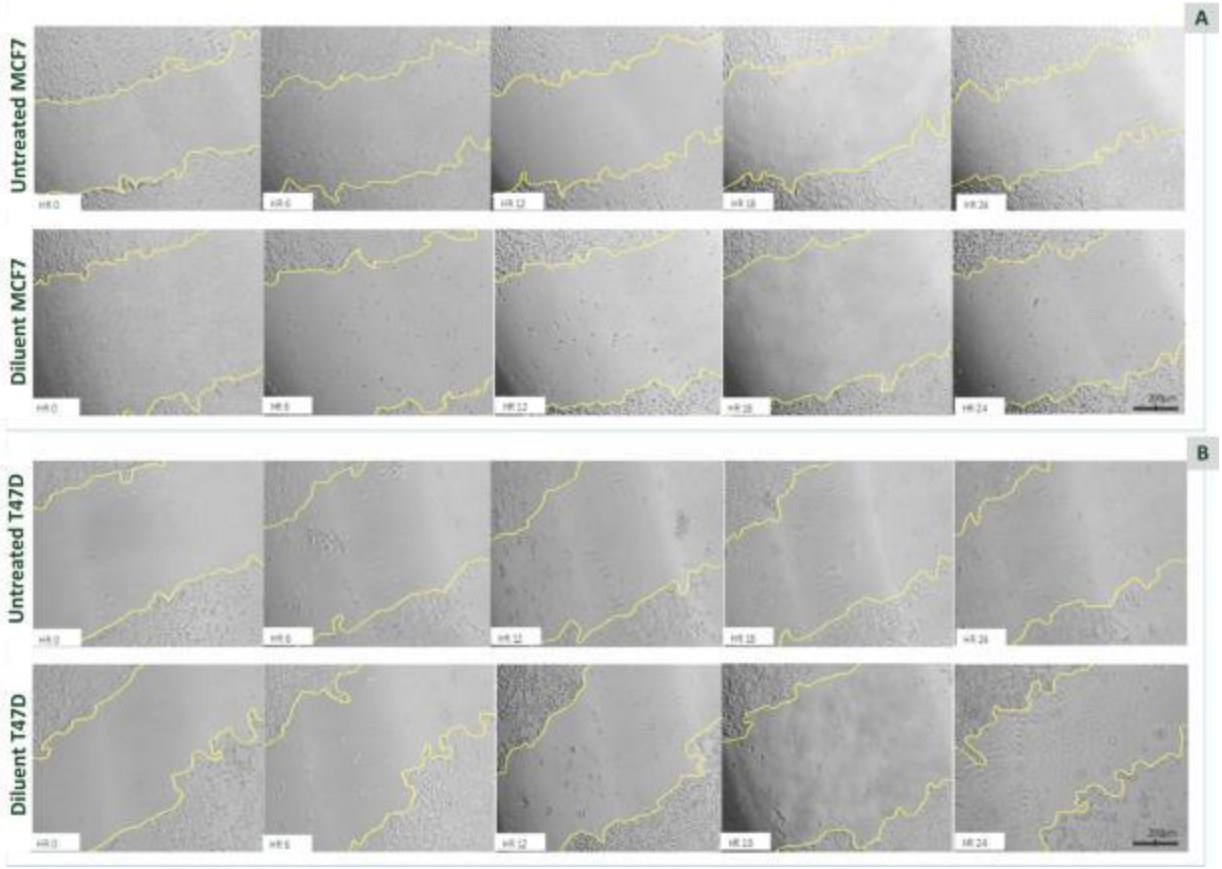


Figure 2.12: Representative micrographs showing the change in area following a scratch assay to measure the rate of cell migration rate in breast cancer cells (MCF7). A) Untreated control (Medium only) and B) Diluent control (0.03% DMSO). Images were obtained at 0hrs, 6 hrs, 12 hrs, 18 hrs and 24 hrs in order to measure the progression of cell migration over a 24 hrs period. Micrographs were imaged at with the 10X objective.

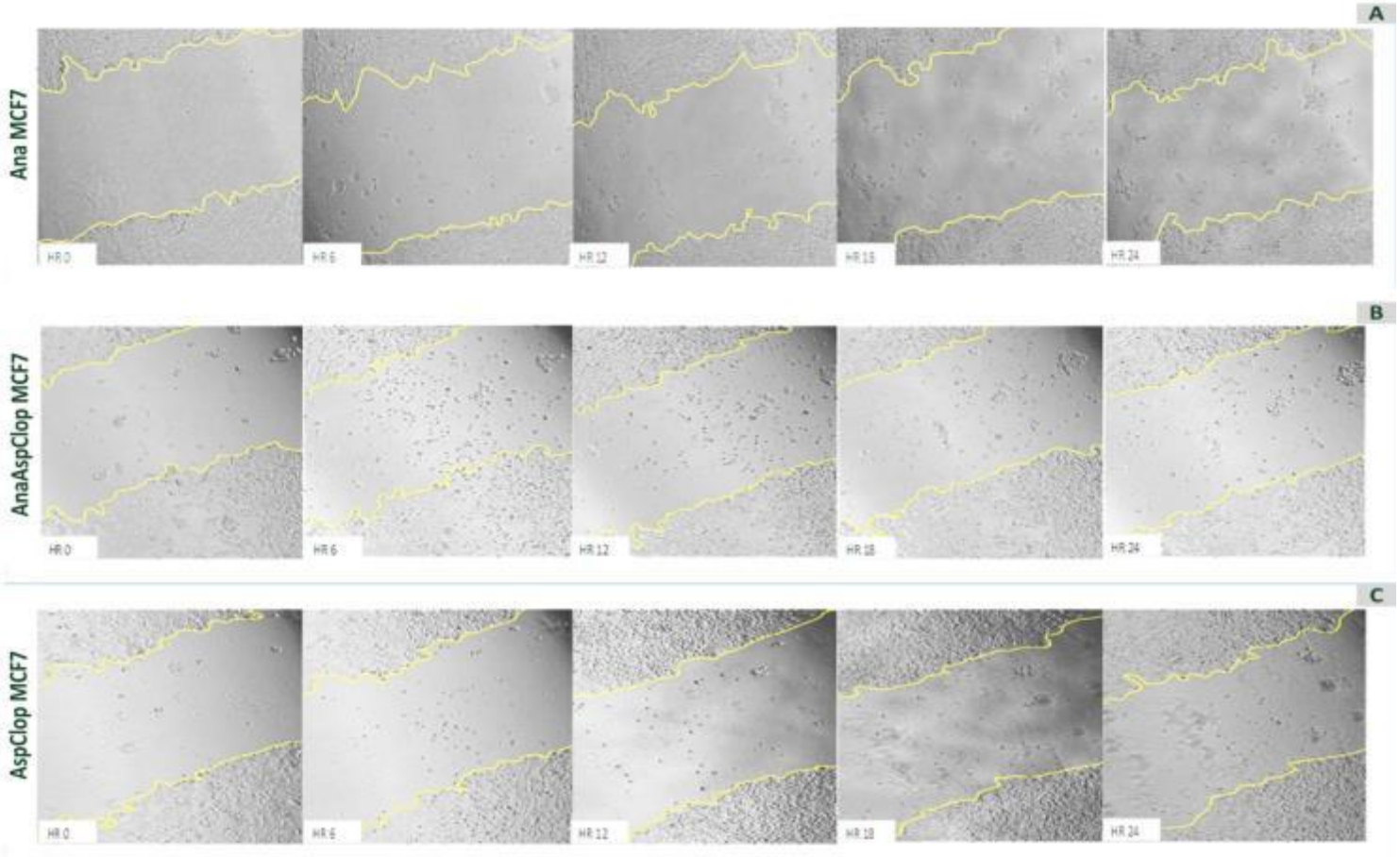


Figure 2.13: Representative micrographs showing the change in area following a scratch assay to measure the rate of cell migration rate in breast cancer cells (MCF7) following a 24 hour treatment; A) Anastrozole (Ana), B) Anastrozole+Aspirin+Clopidogrel (AnaAspClop) and C) Aspirin+Clopidogrel (AspClop). Images were obtained at 0 hrs, 6 hrs, 12 hrs, 18 hrs and 24 hrs in order to measure the progression of cell migration over a 24 hrs period. T47D cells showed a similar trend; however, fewer cells were observed in the exposed area at the centre (Appendix A4.1). Micrographs were imaged with the 10X objective.

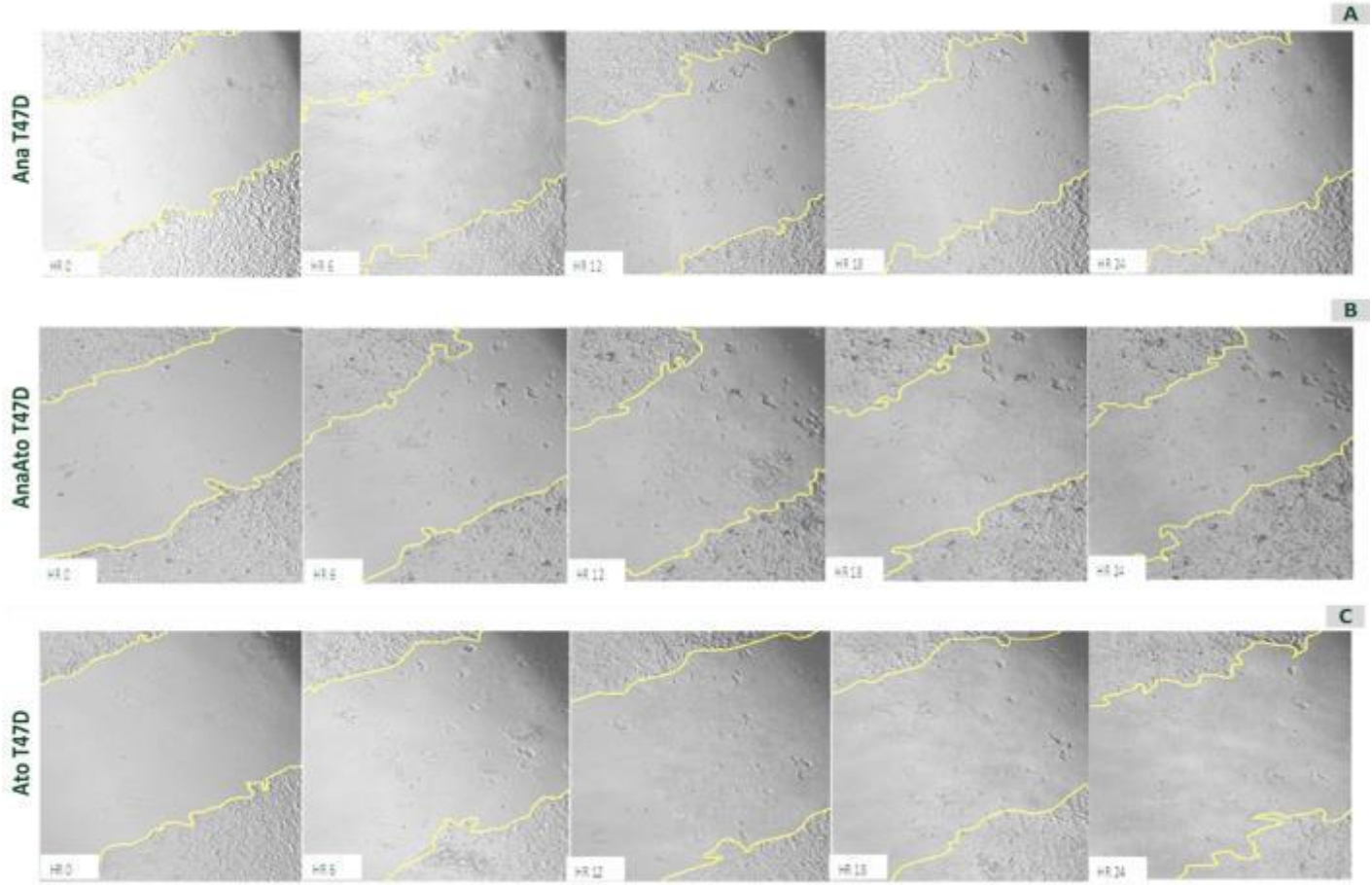


Figure 2.14: Representative micrographs showing the change in area following a scratch assay to measure the rate of cell migration rate in breast cancer cells (T47D) following a 24 hour treatment; A) Anastrozole (Ana), B) Anastrozole+Atopaxar (AnaAto) and C) Atopaxar (Ato). Images were obtained at 0 hrs, 6 hrs, 12 hrs, 18 hrs and 24 hrs in order to measure the progression of cell migration over a 24 hrs period. MCF7 cells showed a similar trend (Appendix A4.2). Micrographs were imaged with the 10X objective.

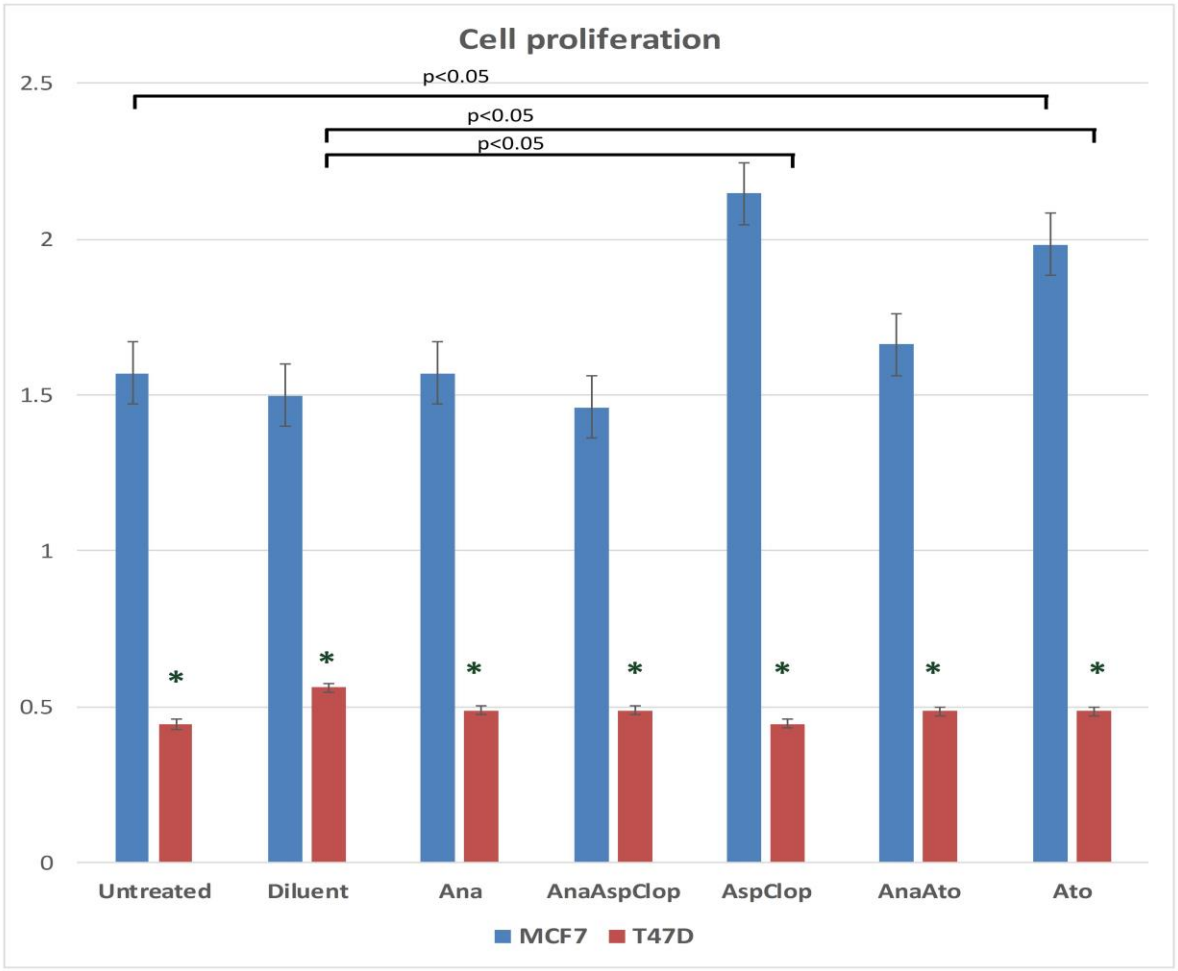


Figure 2.15: Cell proliferation as measured by the WST-1 assay following a 24 hrs treatment period. Anastrozole, Aspirin and Clopidogrel treatment, Anastrozole and Atopaxar treatment. MCF7 cells generally showed significantly higher levels of cell proliferation than T47D cell and antiplatelet therapy treatment alone induced higher proliferation than when combined with Ana. T47D cells displayed lower proliferation and no differences were observed with the various treatments. * indicates $p<0.05$ between cell lines at matched treatment, the interval bar indicates $p<0.05$ within cell line at different treatments.

2.4 Discussion

This study aimed to investigate the direct effects of combined hormone (Anastrozole) and antiplatelet therapy (Aspirin-Clopidogrel cocktail and Atopaxar) on breast cancer cells (MCF7 and T47D cells). This knowledge is important in light of the established relationship between thromboembolic disorders and tumour incidence (Phillips *et al.*, 2015; Donnellan and Khorana, 2017; Razak *et al.*, 2018). The addition of antiplatelet therapy to known cancer therapy may provide a novel treatment strategy against cancer induced-thromboembolic disorders; however, this relationship has not been thoroughly tested. Hence these findings will provide possible benefits or adverse effects of Anastrozole, a commonly used hormone therapy combined with Aspirin and Clopidogrel (commonly used for cardiovascular diseases) and uncover novel effects of Atopaxar on breast cancer cells.

In an effort to uncover the cytotoxic effects of Anastrozole, Aspirin, Clopidogrel and Atopaxar on breast cancer cell lines (MCF7 and T47D) various techniques were employed. This was done because cancer cells are dynamic and it was anticipated that they would find mechanisms to defend themselves prior to succumbing to toxic stimuli, this would then confound the true effects of the drug if only one technique were used. Therefore, a holistic approach to the cells response which included assessing cell viability through the active uptake of neutral red dye into lysosomes (Repetto *et al.,* 2008; Minaeva *et al.,* 2017), and cell death indicated by membrane leakage of lactate dehydrogenase enzyme was tested. Additionally, these assays were complemented by more specific methods to indicate cytotoxicity using flow cytometry. The detection of a specific marker, phosphatidylserine (PS) was used to identify cells undergoing apoptosis (late and early) and the staining of nucleic acids by propidium iodide (PI) was used to indicate cells undergoing necrosis suggesting damage to membrane integrity. This method coupled with ultrastructural assessment of cells

proved to be a more accurate method to study drug toxicity. Furthermore, upon establishing the desired concentration cell migration and proliferation as aspects of tumour progression was investigated.

Cell stress response in breast cancer cells

Cells were able to adapt to changes within their environment, such as hypoxia, lack of nutrients, and therapy (Leung *et al.*, 2013; Lee *et al.*, 2018). The stress responses often determine a cells response to various stimuli and survival (Horváth *et al.*, 2008; Leblanc and Peyruchaud, 2016). The cell growth assay was conducted on cells in media in order to determine their normal growth pattern over 24 hrs without any intervention; this was monitored at regular intervals. The findings showed that at each interval the was a higher proportion of MCF7 cells than T47D cells; however, the levels were relatively equal at 24 hours thus suggesting that T47D cells induced a prolonged stress response from seeding and harvesting, which may have led to slower adhesion to substratum at each time point, hence lesser cells harvested. This prolonged adherence time may be an adaptation to acclimatise to environmental conditions and suggests a more resistant tumour profile in T47D cells (which may also be more aggressive) than MCF7 cells.

Anastrozole-mediated effects

When cells were treated with Anastrozole, no significant change was observed with membrane integrity as indicated by LDH leakage suggesting no cytotoxic effects. The NR assay showed that cell viability was not adversely reduced. Flow cytometric analysis showed that there was a greater proportion of live viable cells than cells undergoing death mechanism; however, there were more necrotic cells than cells undergoing apoptosis in both cell lines. This is in contrast with another study which showed that Anastrozole may reduce cell viability, although the concentration used was higher than that use in this study (Smollich *et al.*, 2010)

and cell ultrastructure in both cell lines was not adversely affected with Anastrozole treatment and cells maintained a uniform monolayer thus suggesting minimal toxicity effects. MCF7 cells were shown to have less migratory rate than T47D cells; however, Anastrozole induced higher proliferation in MCF7 cells than T47D cells probably mediated by a higher expression of ERα receptor subtype in MCF7 cells (Mota *et al.*, 2017). The reported adverse effects of Anastrozole on cancer (Smollich *et al.*, 2010) were not evident in this study and may suggest that cells have a certain level of resistance to cytotoxic effects of Anastrozole or are able to overcome them *in vitro* as part of a selection pressure to promote their survival.

Anastrozole and Aspirin and Clopidogrel cocktail mediated effects

When cells were treated with Anastrozole combined with Aspirin and Clopidogrel no adverse effects on membrane integrity was observed and cell viability indicated by neutral red uptake. Flow cytometric analysis showed that cell viability was generally maintained; however, a small proportion of T47D cells succumbed to early apoptosis. These findings suggest that this treatment (AnaAspClop) induced minimal or no cytotoxic effects on cells. Antiplatelet drugs alone have shown anticancer properties with some conflicting findings studies (Gierach *et al.*, 2008; Holmes *et al.*, 2010; Algra and Rothwell, 2012; Zhong *et al.*, 2015). In this study, minimal anticancer properties were observed, instead, cell viability was maintained, although low levels were induced this is contrary to studies which have shown that Anastrozole, Aspirin may reduce viability and promote apoptosis (Smollich *et al.,* 2010; Liu *et al.,* 2017; Zhang *et al.*, 2018) but supports studies which show that Clopidogrel may promote tumour progression (Coimbra *et al.*, 2015; Smeda *et al.,* 2018). In contrast, distinct changes in ultrastructure were induced in T47D cells whereby cell shape was altered to form round distinct cell clusters with prominent cell ruffles. Cell migration was found to be higher in MCF7 cells than in T47D cells. The cell morphology seen in both cell lines suggests that AnaAspClop induced collective cell

migration in both cell lines although the cell shape was different; MCF7 cells formed flattened clusters whereas T47D cells formed round cell cluster. This suggests differences in cytoskeletal remodelling (Fackler and Grosse, 2008; Friedl and Alexander, 2011) between the two cell lines. This might also be reflected by the different proliferation rates between the cell lines, with higher proliferation in MCF7 cells suggesting a higher turn-over of cytoskeletal elements (Fackler and Grosse, 2008; Friedl and Alexander, 2011) and may influence the migration rate.

T47D cells might be migrating at a slower rate, the slower migration mode seen in T47D cells might not be directly proportional to the rate of invasion as suggested of cells undergoing collective migration (Friedl and Alexandra *et al.,* 2011; Pandya *et al.,* 2017). This might in fact render these cells more conducive for invasion to occur, a limitation in this study is that we did not measure extracellular matrix parameters such as matrix metalloproteinases (MMPs); therefore, we cannot elucidate further regarding the invasion capacity of these cell types. T47D cells have also been shown to express higher levels of ERβ than MCF7 cells (Sastre-Serra *et al.*, 2012; Pather *et al.,* unpublished findings) and this protein has been shown to assist in the formation of strong adhesions between the cells by preventing loss of E-cadherin (Lymperatou *et al.*, 2013), hence, this cell line displayed more prominent cell clusters following treatment.

The control Aspclop cocktail alone, did not change membrane integrity and viability indicated by LDH and NR assay respectively, compared to AnaAspClop-treatment. Flow cytometric analysis showed that this treatment maintained cell viability in both cell lines, and induced less apoptosis and necrosis in MCF7 cells than T47D cells. Ultrastructural features were similar to AnaAspClop-treatment; however, it induced sparse blebbing in MCF7 and reduced

filopodia integrity in T47D cells. In both cell lines, more membrane ruffles were observed, especially in T47D cells. This was corresponding to a higher migratory rate in T47D cells than MCF7 cells. The prominent membrane ruffles seen especially in T47D cells could indicate higher risk of migration. Membrane ruffles formed when lamellipodia detach from the substrate and retract towards the cell body, forming folds at the cell periphery (Borm *et al.,* 2005; Al-Bahlani *et al.,* 2017). They are composed of densely packed arrays of actin filaments with associated proteins, it has previously been shown that increased membrane ruffle frequency signalled inefficient cell migration because it indicates low lamellipodia attachment; however, other studies have found that membrane ruffles are associated with cell migration (Borm *et al.*, 2005; Al-Bahlani *et al.,* 2017).

In this study, membrane ruffles observed at the edge of the cells following treatment with all treatment groups across the different dosages suggesting that cells were involved in migration, although the outcome from the scratch assay indicated that generally low levels of migration were induced in both cell lines. This feature was more prominent in T47D cells, than in MCF7 cells suggesting a more efficient motility in T47D cells despite a generally lower migration rate seen in this cell line, these findings are in line with the collective migration strategy that T47D cells induce (Jolly *et al.*, 2015, 2017; Pandya, Orgaz and Sanz-Moreno, 2017; Grada *et al.*, 2018; Seddiki *et al.*, 2018). Both cell lines have a low metastatic rate (D'Anselmi *et al.*, 2013; Rizwan *et al.*, 2015; Yu *et al.*, 2017); although T47D cells express more proteins involved in cell growth, carcinogenesis and anti-apoptosis regulation (Aka and Lin, 2012), therefore suggesting that they are more prone to survival than MCF7 cells. This could explain the shape change and higher membrane ruffles seen in T47D cells.

Anastrozole and Atopaxar mediated effects

Anastrozole combined with Atopaxar did not adversely affect membrane integrity and cell viability as indicated by the LDH and NR assay. The flow cytometric data showed that cell viability was maintained and with few necrotic cells and apoptotic cells observed. Overall these findings show that little toxicity was induced. Anastrozole was shown to reduce cell viability and promote apoptosis (Chen *et al.*, 2015) and thus showed mild cytotoxic effects when combined with Atopaxar. The effects of Atopaxar on breast cancer are unknown; however, it was shown to inhibit the JAK-STAT pathway which signals for cell survival processes, thus its inhibition by Atopaxar suggests an anti-cancer role (Sun *et al.*, 2019). Ultrastructural analysis showed that AnaAto-treated cells maintained features associated with collective cell migration and MCF7 cells induced higher migration rate than T47D cells. T47D cells had lesser migration but showed more microvilli, blebs and membrane ruffles than MCF7 cells. Thus, these findings suggest no inhibitory effects on breast cancer of Atopaxar combined with Anastrozole on cancer. Furthermore, cell proliferation was not adversely affected in MCF7 cells, but was lower in T47D cells, thus suggesting that AnaAto treatment may adversely affect T47D cells. The Atopaxar control did not adversely affect membrane integrity and viability. While it also maintained higher proportion of viable cells, early apoptosis in T47D cells was increased compared to MCF7 cells. The cell ultrastructure maintained features associated with collective cell migration and cell migration in MCF7 cells remained higher than in T47D, showing that T47D cells were more susceptible to Atopaxar treatment than MCF7 cells. Atopaxar is an antagonist for PAR receptors (Kogushi *et al.*, 2011; Moschonas *et al.,* 2015); therefore it is likely that PAR receptor expression may have mediated differential response between the cell lines. Although no difference in PAR receptors expression was shown previously between these cell lines (Kamath *et al.,* 2001; Olivier *et al.*,

2013) the differential response to Atopaxar with or without Anastrozole suggest higher PAR-expression in T47D cells which may have led to more inhibition of cells since PAR receptors when bound to thrombin induce the release of growth factors which mediate cell proliferation and migration, hence its inhibition adversely affects these processes (Han *et al.*, 2011; Heuberger and Schuepbach, 2019).

Summary

Overall these finding suggests that MCF7 and T47D cells were not easily susceptible to cytotoxic effects of increasing dosages of Anastrozole, Aspirin and Clopidogrel cocktail and Atopaxar in different combinations and concentrations over a 24 hour period. These cell lines, while having the capacity to metabolise the drugs and possibly succumb to high concentrations which may be toxic, were somehow able to avoid severe toxicity even at very high concentrations of Cmax. Instead, the cells may have manipulated the *in vitro* environment in order to promote their survival as cancer cells typically do in *in vivo* conditions. Studies have shown that cancer cells thrive more in a pro-inflammatory environment because it is often accompanied by the secretion of growth factors and cytokines that promote their survival and this may have been the case in this study although to a lesser degree (Agnoli *et al.,* 2017; Tobias *et al.,* 2017). The mode of death commonly associated with inflammation is necrosis (Cummings *et al.,* 2004; Wlodkowic *et al.,* 2011; Wickman *et al.,* 2013) and the proportion of cells undergoing necrosis was found to be higher than those undergoing apoptosis in both cell lines across all treatment groups even though overall there was a higher proportion of live viable cells. Ultrastructurally, only a few cells were detected which displayed necrotic features; such as damaged cell membrane and leakage of internal contents into the extracellular space. It might have been that those few cells which were necrotic or undergoing secondary apoptosis were removed during the

morphological preparation because they would essentially be disintegrated and lost during the multiple washes; however, while they are in the environment they would have provided the inflammatory signal needed to influence viable cells within their environment. In contrast during flow cytometric assessment cells or apoptotic bodies expressing necrotic markers would still be interrogated.

Overall low levels of migration were detected in both cell lines, in keeping with the known low migratory rate in these cells (D'Anselmi *et al.*, 2013; Rizwan *et al.*, 2015; Yu *et al.*, 2017). In both cell lines (MCF7 and T47D cells) AnaAspClop-treatment reduced cell migration, whereas other treatments modulated relatively higher levels of migration. Despite this, T47D cells may be more invasive due to the mode of migration employed (collective migration and associated motility features such as membrane ruffles). Meanwhile MCF7 cells displayed higher propensity for proliferation even in the midst of cell treatment.

2.5 Conclusion

In conclusion, antiplatelet therapy (Aspirin-Clopidogrel cocktail /Atopaxar) with or without Anastrozole treatment induced minimal cytotoxic effects and may promote survival in both cell lines. While no significant difference was observed between the drugs in terms of their toxicity outcomes; AnaAspClop-treatment reduced migration in both cell lines whereas AnaAto- treatment and Ato-treatment mediated increased migration in MCF7 cells and decreased it in T47D cells. In contrast; Ana-treatment and AspClop-treatment reduced cell migration in MCF7 cells but increased it in T47D cells. In Addition, combined Anastrozole and antiplatelet therapy (AspClop/Ato) reduced cell proliferation compared to antiplatelet treatment alone (AspClop/Ato) in MCF7 cells. Furthermore, higher levels of cell proliferation were induced in this cell line compared to T47D cells at all treatments. T47D cells displayed

lower cell proliferation with all treatments. These findings also highlight the heterogeneity between the cell lines, which led to differential and sometimes opposing effects.

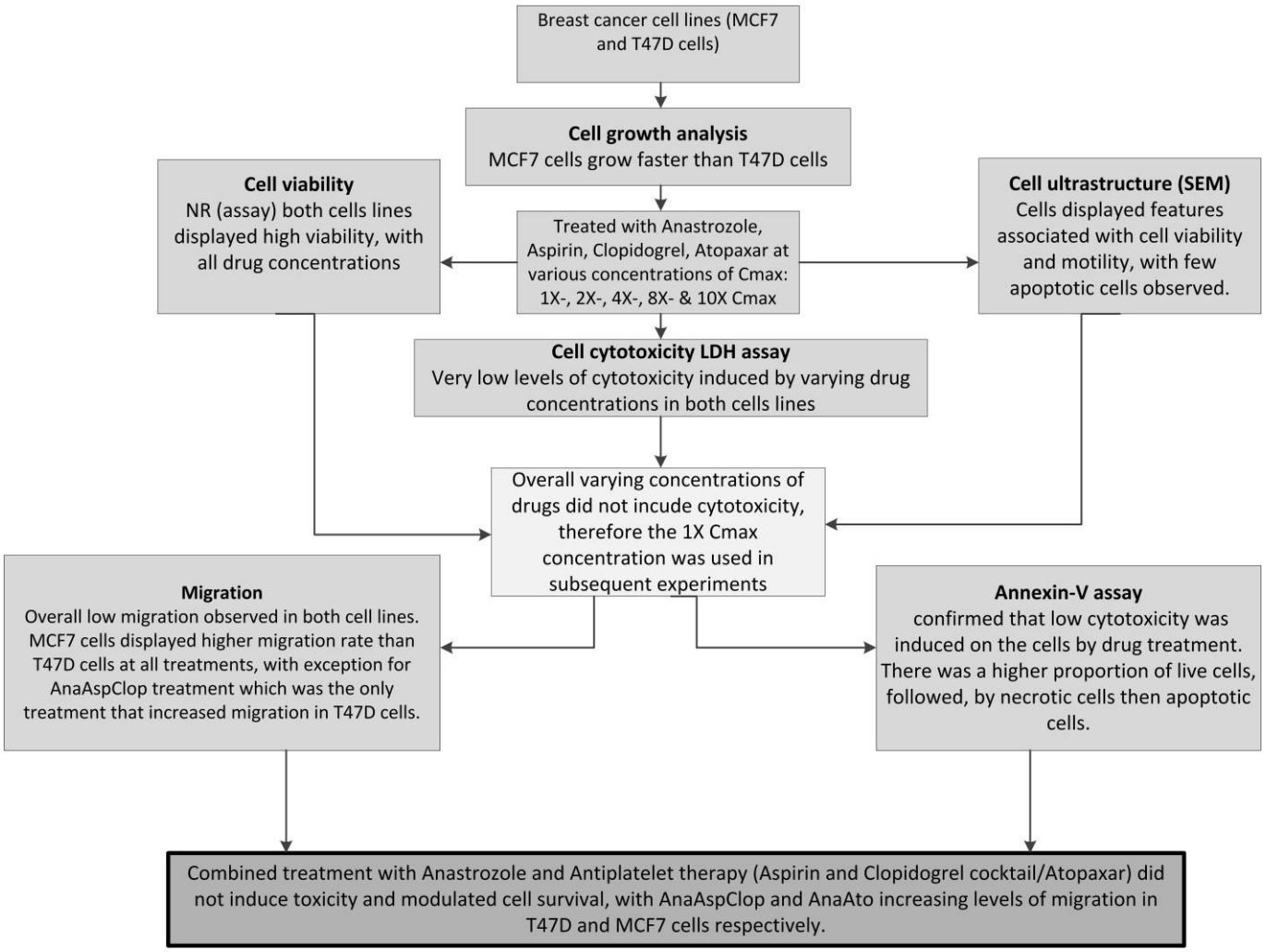


Figure 2.16: An overview of chapter two and summary of main findings.

CHAPTER III: Hypercoagulation in response to Anastrozole and antiplatelet-treated breast cancer cells

3.1. Introduction

An association between thromboembolic disorders and breast cancer has long been established (Elyamany *et al.,* 2014; Wang *et al.,* 2018; Gervaso *et al.*, 2019). The reciprocal interactions between cancer cells and vascular components promote a hypercoagulable state, whereby there is an increased secretion of substances that lead to blood clothing (Lipets and Ataullakhanov, 2015). Blood components that are mainly responsible for facilitating this process are platelets, and they release soluble molecules and inflammatory factors which mediate hypercoagulation (Buergy *et al.*, 2012; Goubran *et al.*, 2013; Menter *et al.*, 2014). Breast cancer cells are known to interact with platelets and manipulate their functions in order to promote their own survival (Bambace and Holmes, 2011; Egan *et al.*, 2011). The use of hormone therapy has thus far not shown any favourable outcome in reducing thromboembolic disorders associated with breast cancer, with studies showing that these treatments increase risk for thrombosis (Deitcher and Gomes, 2004; Haddad and Greeno, 2006; Walker *et al.*, 2016; Pather *et al.*, 2019).

Antiplatelet therapy is commonly used in the treatment and prevention of cardiovascular disorders and it could act as a potential treatment strategy in combination with hormone therapy; however, its efficacy in reducing hypercoagulation when combined with hormone therapy has not been elucidated. The main aim of this chapter was to discuss in detail some of the mechanisms involved in hypercoagulation and present findings of the effects of Anastrozole and antiplatelet therapy treatment in breast cancer on hypercoagulation by investigating early stages of platelet activation (pre-cursor to coagulation) and thrombin formation (which mediates the coagulation pathway).

3.1.1 Platelet structure and physiology

Platelets are small anucleate fragments with a diameter of approximately 3.1 μm and they originate from megakaryocytes in bone marrow (Bearer and Prakash, 2002; Thon and Italiano, 2012). The mature megakaryocyte extends long cytoplasmic protrusions known as pro-platelets into blood vessels from which platelets bud (Thon and Italiano, 2012; Voutsadakis, 2014). This process of platelet formation is known as thrombopoiesis and it is initiated by thrombopoietin and various cytokines including stromal cell derived factor (CXCL12), chemokine receptor 4 (CXCR4), integrins and platelet factor 4 (PF4) (Voutsadakis, 2014; Johnson *et al.,* 2016). Inflammation drives this process via the secretion of inflammatory cytokines, hence cancer, regarded as a pro-inflammatory condition, is associated with elevated levels of platelet formation (i.e. thrombocytosis) (Buergy *et al.*, 2012; Heijnen and van der Sluijs, 2015; Haemmerle *et al.*, 2018a). The lifespan of platelets is typically 1-10 days; however, it can range between 1-120 days thus explaining the heterogeneity seen in size and additionally, the variable response to agonists (Bearer and Prakash, 2002; Thon and Italiano, 2012; Johnson *et al.,* 2016).

Platelets have an elaborate plasma membrane that forms invaginating channels called the open canalicular system (OCS) and a closed-channel network called the dense tubular system (DTS) (Gruba *et al.*, 2015; Heijnen and van der Sluijs, 2015). The OCS provides a channel for entry of external substances into platelets and for the release of platelet granule substances (Gruba *et al.*, 2015; Heijnen and van der Sluijs, 2015). It also provides a reservoir of internal plasma membrane which will protrude outwards to form extensions such as pseudopodia and filopodia during adhesion and also acts as a storage site for certain glycoproteins such as GPIb/IX (Ghoshal and Bhattacharyya, 2014; Repsold *et al.,* 2015). The DTS is an internal

network of closed-channels formed by remnants of the endoplasmic reticulum and they provide a storage site for Ca^{2+} (Gruba *et al.*, 2015; Heijnen and van der Sluijs, 2015).

When circulating in blood, resting platelets display a discoid shape, which is maintained by the complex cytoskeleton composed of different components including a spectrin membrane skeleton, actin cytoskeleton and marginal microtubule coil (Pretorius *et al.,* 2012). Spectrin is the main component of the membrane skeleton which maintains integrity and actin is an important part of the cytoskeleton (Zhao *et al.,* 2011; Zelen *et al.,* 2012). Microtubules are positioned peripherally, and various organelles are found in the cytosol including alpha granules, dense granules, lysosomes, peroxisomes and mitochondria (Zhao *et al.,* 2011; Zelen *et al.,* 2012). The phospholipid bilayer of platelet plasma membrane is composed of different phospholipids whose location between the inner and outer leaflet is controlled by flipases (Zhao *et al.,* 2011; Zelen *et al.,* 2012).

Each platelet contains approximately 50-80 alpha-granules, with a diameter of 200-500 nm (Sehgal and Storrie, 2007; Thon and Italiano, 2012). Alpha-granules contain a variety of proteins including; chemokines, cytokines and growth factors which facilitate platelet various functions such as PF4, interleukin-8 (IL-8), platelet derived growth factor (PDGF), tumour growth factor beta (TGF-β), and vascular endothelial growth factor (VEGF) (Heijnen and van der Sluijs, 2015; Cedervall *et al.,* 2018; Pokrovskaya *et al.*, 2018). The distribution of proteins within alpha granules was shown to be heterogeneous although the true cause of this is unknown, but has been suggested to be either due to differential packaging within individual granules during derivation from the trans-Golgi network in megakaryocytes (Sehgal and Storrie, 2007; Thon and Italiano, 2012).

Dense granules are 250 nm in diameter and each platelet contains approximately 3-9 dense granules (King *et al.,* 2009; Fitch-Tewfik and Flaumenhaft, 2013; Ambrosio *et al.,* 2017). They are alleged to be derived from endosomal precursors and contain lysosomal membrane proteins (LAMPs) such as LAMP 2/3 (CD63) (Fitch-Tewfik and Flaumenhaft, 2013; Ambrosio *et al.,* 2017). Lysosomes are the least numerous platelet granule and are approximately 175-250 nm in diameter and exhibit more heterogeneity than other platelet granules (Rendu and Brohard-Bohn, 2001; Fitch-Tewfik and Flaumenhaft, 2013). Lysosomes secrete substances that facilitate receptor cleavage, fibrinolysis, and extracellular matrix degradation and remodelling of the vasculature (King and Reed, 2000).

Upon activation by platelet agonists, platelets change their shape, and this involves a series of morphological and biochemical events (Bearer *et al.,* 2002; Thon and Italiano, 2012). Shape alterations involve changes to the actin cytoskeleton and begins with platelets changing from discoid to round, then dynamic surface protrusions called pseudopodia are formed (Augustine *et al.*, 2016; Repsold *et al.,* 2016; Pather *et al.*, 2019). Upon adhesion to the surface, lamellipodia arise from the lateral membrane between pseudopodia (Augustine *et al.*, 2016; Repsold *et al.,* 2016; Pather *et al.*, 2019). This shape change allows for platelets to function in their main physiological role which is to facilitate blood clotting through a process known as haemostasis.

This additionally requires the production and release of various coagulation factors, pro-angiogenic factors and adhesion molecules such as fibrinogen, von Willebrand factor (vWF), P-selectin (CD62p), fibronectin, and platelet derived growth factor (PDGF) which are stored in their granules (Sehgal and Storrie, 2007; Thon and Italiano, 2012). Some of these proteins are produced primarily in megakaryocytes (e.g. P-selectin/CD62p), while others are synthesized

in other cell types and endocytosed into platelet granules (e.g. fibrinogen) (Sehgal and Storrie, 2007; Thon and Italiano, 2012). Platelets also have the capacity to produce proteins and this process is facilitated by cytosolic mRNA which originates from megakaryocytes (Mayeda and Krainer, 1999; Denis *et al.,* 2005; Dahiya *et al.,* 2015; Zhang *et al.,* 2017).

Platelets are the most numerous blood component, suggesting a wide variety of functions (Dineen *et al.*, 2009; Menter *et al.*, 2014b). In pathological conditions such as cancer, platelets can be modulated by or interact with other cells such as leukocytes, erythrocytes and cancer cells to facilitate metastasis (Kumar *et al.,* 2017; Zhang *et al.,* 2017). The role of platelets is not only restricted within the vasculature, but platelets can secrete growth factors and angiogenic factors extra vascular directly onto tumour cells and this is facilitated by the leaky blood vessels in tumours and thus promotes tumour progression (Li *et al.*, 2014; Costa *et al.*, 2019).

3.1.2 Deciphering the mechanism of platelet activation

During vascular injury there is a delicate interplay between various factors that facilitate haemostasis such as adhesion molecules, platelet surface receptors and components of the coagulation cascade (Stalker *et al.,* 2012; Tomaiuolo *et al.,* 2017). Platelets initiate haemostasis by adhering to the site of injury through their adhesive receptors (GPIb-IC-V, CD62p) binding to vWF exposed by damaged blood vessels (Stalker *et al.,* 2012; Tomaiuolo *et al.,* 2017). This results in the formation of a vWF-GPIb complex (Stalker *et al.,* 2012; Tomaiuolo *et al.,* 2017). This receptor complex is stabilised for maximum platelet attachment through the adhesion of members of the integrin family $\alpha_2\beta_1/\alpha_{IIb}\beta3$ (binding mainly to collagen and vWF respectively) (Stalker *et al.,* 2012; Tomaiuolo *et al.,* 2017).

3.1.2.1 The role of agonists in facilitating platelet activation

In resting platelets Ca^{2+} levels in the cytosol are kept low by restricting Ca^{2+} entry and increasing Ca^{2+} exit through the plasma membrane or by sequestering Ca^{2+} within the dense tubular system (Varga-Szabo *et al.,* 2011; Dolan and Diamond, 2014). During platelet activation, the increase in cytosolic Ca^{2+} concentration is facilitated by inositol triphosphate-3 (IP_3)-mediated Ca^{2+} release from the dense tubular system (Varga-Szabo *et al.,* 2011; Dolan and Diamond, 2014). Thereafter, Ca^{2+} entry across the plasma membrane resumes when the dense tubular system Ca^{2+} stores are depleted and it is mediated by direct contact between the dense tubular system membrane protein (STIM1) and plasma membrane protein orai-1 (Varga-Szabo, Braun and Nieswandt, 2011).

Platelet agonists including thrombin, thromboxane (TXA_2) and adenosine diphosphate (ADP) bind to their receptors which are coupled to Gq units of the heterotrimeric G-protein which activates phospholipase-C and thus promotes hydrolysis of phosphoinositide (Stalker *et al.,* 2012). This leads to increasing cytosolic Ca^{2+} levels within platelets, which result in the activation of integrins partly through the CalDAG-GEF/Rap1/RIM pathway (Lee *et al.*, 2009; Sanford *et al.,* 2010). Thrombin is the most potent platelet agonist (Jennings, 2009; Baaten *et al.*, 2017; Denslow *et al.*, 2017) because its efficiency is associated with activation of phospholipase-C and thus this agonist causes higher and more effective hydrolysis of phosphoinositide (Haase *et al.,* 1996). Thrombin activity is restricted to the procoagulant membrane of platelets (where factors Va and Xa are localised) therefore restricting thrombin distribution and facilitating its role in the formation of a stable core of fully activated platelets (Tomaiuolo *et al.,* 2017). Furthermore thrombin receptors; PAR1 and PAR4 are associated with Gq signalling pathways on the cytosolic side and thus lead to increased Ca^{2+} levels (Han *et al.*, 2011; Tourdot *et al.*, 2018).

There are various sources of ADP within the vascular system including damaged erythrocytes, and dense granules contained within platelets (Kalwa *et al.*, 2014). ADP binds to P2Y1 and P2Y12 receptors on platelets which associates with Gq signalling pathways to increased Ca^{2+} concentrations, this leads to platelet activation, $\alpha_{IIb}\beta3$ activation and subsequently, degranulation (Ghoshal and Bhattacharyya, 2014; Kalwa *et al.*, 2014; Zarà *et al.*, 2018). The P2Y12 signalling pathway regulates platelet activation by recruiting and retaining platelets in the outer layers of a forming plug, thus regulating thrombus stability (Tomaiuolo *et al.,* 2017; Zarà *et al.*, 2018).

Thromboxane A_2 (TXA_2) is generated through the COX-1 pathway in platelets and plays a role in reinforcing platelet activation (Wang and Dubois, 2006; Langley *et al.*, 2011; Zarà *et al.*, 2018). COX-1 catalyses the formation of prostaglandin-G_2 (PGG_2) and prostaglandin-H_2 (PGH_2) from arachidonate, TXA_2 results when thromboxane synthase metabolises PGH_2 (Stalker *et al.*, 2012; Guillem-Llobat *et al.*, 2016). TXA_2 is a potent activator of platelets; however, it has a short half-life (Egan, Crowley, Smyth, Toole, *et al.*, 2011; Guillem-Llobat *et al.*, 2016). TXA_2 binds to the thromboxane receptor α and β on the surface of platelets which are associated with Gq signalling pathway, thus increasing Ca^{2+} concentration, activating $\alpha_{IIb}\beta3$ and causing degranulation (Langley, 2013; Tomaiuolo, Brass and Stalker, 2017). TXA_2 contributes to platelet recruitment and ultimately facilitates platelet retention to the outer shell of a developing thrombus during advanced stages of platelet activation when thrombus formation becomes prominent (Guillem-Llobat *et al.*, 2016; Tomaiuolo *et al.,* 2017).

3.1.2.2 Early events of platelet activation

Platelet activation is a graded series of reversible and non-reversible events (Tomaiuolo *et al.,* 2017). Most platelet agonists such as; collagen, thrombin, TXA_2 and ADP bind to G-protein coupled receptors expressed in platelet membranes, upon binding cytosolic Ca^{2+} levels

increase activate signalling pathways that lead to varied cellular responses collectively known as platelet activation (Yun *et al.*, 2016; Serhan, Gartung and Panigrahy, 2018). Reversible events occur at early stages of activation and include shape change (from discoid to irregular), and platelet aggregation formed by the activation of $\alpha_{IIb}\beta3$ integrin and the formation of thromboxane A_2 (Tomaiuolo *et al.,* 2017; Filkova *et al.*, 2019). At later stages of activation, irreversible events occur including degranulation of alpha and dense granules, phosphatidlyserine (PS) exposure, membrane blebbing and the formation of microparticles (Holinstat *et al.*, 2009; Tomaiuolo *et al.,* 2017).

Some of the critical events that occur during early platelet activation include the cleavage of phosphatidylinositol 4, 5-bisphosphate (PIP2) to inositol trisphosphate (IP3) and diacylglycerol by phospholipase-C (Marat and Haucke, 2016). The subsequent activation of monomeric G-proteins in the Rho and Ras family leads to the re-organization of the actin cytoskeleton to form extensions such as pseudopodia, filopodia and lamellipodia (Marat and Haucke, 2016), which can be viewed ultrastructurally. Suppression of cyclic adenosine monophosphate (cAMP) synthesis is required in order to allow platelet activation to proceed (Stalker *et al.,* 2012; Marat and Haucke, 2016). Formation of phosphoinositide 3- kinase (PI3-kinase) through the activation of PI3-kinase isoforms found in platelets is required and PI3-kinase will in turn facilitate platelet activation (Laurent *et al.*, 2014; Marat and Haucke, 2016).

Multiple signalling pathways facilitate platelet activation during the initiation phase including those that activate collagen receptor GPVI, ATP and ADP receptors, GPIl-IX-V complex, and thromboxane A_2 release (Holinstat *et al.*, 2009; Tomaiuolo *et al.,* 2017). During the extension phase, platelet aggregates form through platelet-platelet cohesion which is facilitated by the binding of fibrinogen to $\alpha_{IIb}\beta3$ integrin (i.e. GPIIbIIIa/CD41a), clot stabilization is an important

final step in platelet-plug formation during haemostasis (Holinstat *et al.*, 2009; Broos *et al.*, 2011). Thrombin facilitates this process by converting fibrinogen to fibrin which will in turn form a network which stabilises the platelet plug (Brzoska *et al.*, 2013; Versteeg *et al.*, 2013; Zarà *et al.*, 2018).

During platelet activation, smaller (40-100 nm) exosomes are released from intracellular multi-vesicular bodies and larger platelet micro particles (PMPs) (0.1-1 μm) pinch directly from the plasma membrane (Zhang *et al.*, 2017). These vesicles which contain various molecules are released to mediate cell-cell communication (Piccin *et al.,* 2007; Boilard *et al.*, 2010).

Recent studies based on *in vivo* experiments have provided evidence to suggest a more complex mechanism to haemostasis unlike the classic simplistic one (Stalker *et al.,* 2012; Tomaiuolo, Brass and Stalker, 2017). This new model hypothesizes that regional architecture within a thrombus exists whereby platelets display differing levels of activation, and fibrin fibers are located at specific regions (Stalker *et al.,* 2012; Tomaiuolo *et al.,* 2017). This haemostatic plug consists of highly activated, closely opposed, degranulated platelets at the centre of the haemostatic plug surrounded by an outer shell of loosely associated platelets displaying lesser activation state (Stalker *et al.,* 2012; Tomaiuolo, Brass and Stalker, 2017). This platelet heterogeneity is influenced by the interplay of platelet agonists and the microenvironment which affects the amount of agonist available (Baaten *et al.*, 2018; Koupenova and Ravid, 2018). Due to this, antiplatelet drugs will have different effects on the development of thrombi because individual platelets might have reduced or increased susceptibility to a specific agonist (Baaten *et al.*, 2018; Koupenova and Ravid, 2018). The heterogeneity seen in platelets might reflect the presence of different platelet

subpopulations with unique properties (Baaten *et al.*, 2017; Koupenova and Ravid, 2018); however, further evidence is required to define this relationship more clearly.

3.1.2.3 The role of CD62p in coagulation and cancer

During platelet activation, platelets acquire morphological changes that would facilitate their adhesion to the vessel wall for their role in haemostasis (Passacquale and Ferro, 2011). A number of factors can activate platelets independent of vessel injury, including platelet agonists, pro-inflammatory cytokines, infective agents and shear stress (Haddad and Greeno, 2006; Menter *et al.*, 2014; Sabrkhany *et al.*, 2017). CD62p is a transmembrane protein found in platelet alpha granules, which translocates to the platelet membrane upon activation through exocytosis of alpha granules (Neumüller *et al.*, 2013; Kamel *et al.*, 2014; Navred *et al.*, 2019). CD62p is released at the initiation of platelet activation and is known as an early marker of platelet activation (Pather *et al.*, 2019). When platelets are activated, they release CD62p on their surface and also secrete soluble form into plasma (Hilberg *et al.,* 2003). It binds to its receptor (P-selectin ligand receptor) which may be found in leukocytes and endothelial cells and thus contributes to thrombosis (Yip *et al.*, 2013; Navred *et al.*, 2019). CD62p is commonly used as a biomarker to indicate platelet activation (Choudhury *et al.*, 2007; Kamel *et al.,* 2014). CD62p was also used to quantify platelet activation through a parameter known as index of platelet activation which measures the number of activated platelets by using platelet activation marker: CD62p (Leytin *et al.*, 2000; Augustine *et al.*, 2016).

The membrane of platelets acts as a bioactive surface and facilitates the various functions of platelets and enables them to interact with other cell types (Neumüller *et al.*, 2013; Zhang *et al.,* 2017). Tumour cells can activate platelets directly by cell-cell receptors on the plasma membrane of platelets such as CD62p, integrins, and glycoproteins (Bambace and Holmes,

2011; Heldin *et al.,* 2018). In malignancies, CD62p binds to cancer cells and this promotes tumorigenesis (Ghen and Geng, 2006; Heldin, Lennartsson and Westermark, 2018). In addition, levels of soluble CD62p are high in cancer patients and thus used as a prognostic marker for thrombosis and metastasis (Ay and Pabinger, 2012; Qi *et al.,* 2015).

3.1.2.4 The role of CD63 in coagulation and cancer

The tetraspanin superfamily consists of proteins which play a role in organizing cell communication on the surface of the plasma membrane (Maecker *et al.,* 1997; Termini *et al.,* 2017). Their interactions with various signalling molecules and participation in activation, adhesion and cell differentiation mediates this role (Seipold *et al.,* 2016). In addition, they have been identified as tumour-associated proteins (Seipold *et al.,* 2016; Termini *et al.,* 2017). CD63 is localized subcellularly in platelets, found in dense granules (Florin *et al.,* 2018). It is highly concentrated in exosomes and may assist in the tethering of exosomes to its target cells (Charrin *et al.,* 2014). CD63 is also expressed on leukocytes and other mammalian tissues (Bradford *et al.,* 1997; Seipold *et al.,* 2016). It has diverse functions due to their associations with various proteins including integrins, co-receptor molecules and other tetraspanins (Charrin *et al.,* 2014; Florin *et al.,* 2018). CD63 is a component of weibel-palade bodies in endothelial cells, and upon activation it co-localises with P-selectin and von Willebrand factor in these granules (Valentijn *et al.,* 2011; McCormack *et al.,* 2017; Kaufman *et al.,* 2019). Due to their association with integrins, tetraspanins can mediate changes in cell morphology, cell-cell and cell-matrix adhesion and motility following activation (Termini *et al.,* 2017; Florin *et al.,* 2018). CD63 is also a commonly used marker to indicate platelet activation and it was used together with CD62 to indicate platelet activation (Saboor, 2013; Navred *et al.*, 2019). Platelet activation is a dynamic process which displays great heterogeneity, thus the use of

multiple activation markers better represents platelet activation (Baaten *et al.*, 2017; Swieringa *et al.*, 2018).

3.1.2.5 The coagulation cascade

During late stages of platelet activation stable platelet contacts are formed and adjacent platelets have direct contact and thus begin to form aggregates; this process is facilitated by the coagulation cascade (Owens and MacKman, 2011; Berndt *et al.,* 2014). The coagulation system is a regulated cascade that results in the formation of clots, facilitated by the interplay between extrinsic and intrinsic pathways (Versteeg *et al.*, 2013; Göbel *et al.*, 2018). Both pathways intercept when they activate tissue factor (TF), which is a transmembrane glycoprotein that physically associates with factor VIIa to form the TF-VIIa complex which leads to the activation of factor X (Göbel *et al.*, 2018; Zarà *et al.*, 2018). Factor X cleaves prothrombin (factor II) into thrombin (factor IIa) and thrombin will subsequently activate platelets via PAR receptors, and catalyse the cleavage of fibrinogen to fibrin monomers which will stabilise the formed clot (Tripodi, 2016; He *et al.*, 2019).

Thrombin plays a central role in mediating haemostasis and thrombosis through its interaction with proteins involved in the coagulation pathway (Clemetson, 2012; Swieringa *et al.*, 2018). It also assists various processes including angiogenesis, inflammation and cell proliferation, thus its involvement in pathological processes such as cancer, chronic inflammatory diseases and atherosclerosis (Palumbo, 2008; Elyamany, Alzahrani and Bukhary, 2014; ten Cate and Hemker, 2016).

PAR1 receptors were initially identified in platelets but have since been shown to be expressed in various cell types including cancer cells (Kamath, Meydani and Foss, 2001; Liu *et al.*, 2017; Covic and Kuliopulos, 2018). Various agonists have been identified to irreversibly

activate PAR-1, including, thrombin, tissue factor, matrix metalloproteinase (MMPs) (Holinstat *et al.*, 2009; Liu *et al.*, 2017). The expression of PAR-1 is highly regulated in normal cells by sorting signals which mediate its trafficking and expression to the plasma membrane and subsequent internalization and degradation in lysosomes (Wojtukiewicz *et al.*, 2016, 2017). In contrast, PAR1 is constitutively activated in cancer cells and its expression levels correlate with the degree of invasiveness in primary breast tissue and cell lines (Kamath *et al.,* 2001; Li *et al.*, 2017; Covic and Kuliopulos, 2018).

Breast cancer cell lines including MCF7 and T47D cells classified as low migratory and non-invasive, both express PAR1 (D'Anselmi *et al.*, 2013; Rizwan *et al.*, 2015; Covic and Kuliopulos, 2018). Tumour invasiveness is closely associated with the production of MMPs which among other functions, degrade the ECM and activate signalling pathways that can co-ordinate the cyclic cytoskeleton motions that mediate attachment and traction through integrin-ECM contacts (Han *et al.*, 2011; Guan, 2015; Pang *et al.*, 2015). Additionally, studies have shown that MMP-1 derived from the tumour microenvironment can promote progression, invasion and metastasis by binding to PAR-1 (Foley *et al.*, 2012; Juncker-jensen *et al.*, 2014). Thus, the expression of PAR-1 receptors in platelets and breast cancer cells not only facilitates their role in the coagulation cascade but also facilitates tumour progression by interacting with extracellular matrix (ECM) degrading molecules such as MMP1. Therefore, PAR inhibitors could act as novel agents against tumour progression.

3.1.2.6 Tumour cell and platelet interactions

The interaction between cancer cells and platelets promote hypercoagulation and is responsible for the increased risk of thrombosis in cancer patients which is 4-7 folds higher than in non-cancer patients (Meikle *et al.*, 2017; Zhang *et al.*, 2017; Papaxoinis *et al.*, 2018).

High platelets counts are commonly found in cancer patients and associated with poor prognosis for metastasis (Voutsadakis, 2014; Chadha *et al.*, 2015; Smeda *et al.,* 2018).

The release of ADP and thrombin from tumour cells facilitates platelet activation (Bambace and Holmes, 2011) as well as direct contact between tumour cells and platelets through CD62p (Erpenbeck and Schön, 2010; Menter *et al.*, 2014; Li, 2016). When tumour cells activate platelets, this promotes their growth, invasion and metastasis (Goubran *et al.*, 2013). Tumour cells also prime platelets to behave in a particular way by transferring their RNA through microvesicles which are then endocytosed by platelets (Nilsson *et al.*, 2011).

Platelets also adhere to tumour cells, surrounding them and thus shielding them from detection and removal by immune cells such as natural killer (NK) cells, mainly by secreting TGF-β which downregulates receptors found on NK-cells and inhibits key functions of NK-cells such as interferon gamma production, cytotoxicity and granule secretion (Palumbo, 2008; Kopp, Placke and Salih, 2009; Chatterjee *et al.,* 2013; Meikle *et al.*, 2017). Another mechanism used by platelets to protect tumour cells from immune detection is by transferring major histocompatibility complex class 1 (MHC1) antigens to tumour cells, thus preventing their removal by T-cells (which target cells that lack MHC1 antigens on their surface) (Placke *et al.*, 2012; Seliger, 2014).

During exposure and adherence to tumour cells, platelets also secrete substances that promote epithelial-mesenchymal transition (EMT), degrade the ECM, increase vascular permeability, and promote formation of a pre-metastatic niche such as TGFβ and PDGF (Labelle *et al.,* 2011; Miyashita *et al.*, 2015b; Pang *et al.*, 2015; Guillem-Llobat *et al.*, 2016; Leblanc and Peyruchaud, 2016; Hua *et al.*, 2018). Platelets also regulate intra-tumour vasculature (Wojtukiewicz *et al.*, 2017). Platelet-mediated tumour dissemination is a well-

established concept (Wojtukiewicz *et al.*, 2017), whereby platelets also enhance the extravasation of tumour cells (Denslow *et al.*, 2017).

Platelets also increase the expression of tissue factor (TF) on tumour cells, therefore activating the coagulation cascade and maintaining an activated state, thus ensuring a steady supply of growth factors needed for tumour progression such as serotonin, ATP, MMPs and histamines (Deryugina and Quigley, 2006; Date *et al.*, 2013; Orellana *et al.*, 2015; Li, 2016). Through secreting TF directly and via tumour-derived micro-particles, cancer cells activate the coagulation cascade which facilitates thrombosis (Owens and MacKman, 2011; Van Den Berg *et al.*, 2012; Menter *et al.*, 2014; Phillips *et al.*, 2015).Due to the reciprocal effects of platelets and tumour cells, which often promote tumour survival (Denslow *et al.*, 2017) it is anticipated that antiplatelet therapy would also have a positive impact in reducing tumour survival.

Glycoproteins are expressed in platelets and cancer cells and thus facilitate interactions between these two cell types (Mammadova-Bach *et al.*, 2015; Estevez *et al.*, 2016). Integrin $\alpha_{IIb}\beta3$ interacts with tumour cells to facilitate their interaction with the endothelium and metastasis (Mammadova-Bach *et al.*, 2015; Estevez *et al.*, 2016). GPIbα is highly expressed in platelets and forms part of the GPIb-V-IX complex, it has been shown to be expressed in MCF7 cells whereby it facilitates platelet aggregation which proceeds platelet activation (Zhang *et al.*, 2017a). Thrombin also stimulates PARs in order to activate platelets (Denslow *et al.*, 2017; Zhang *et al.*, 2017) subsequently platelets express adhesion molecules such as CD62p and integrin $\alpha_{IIb}\beta3$ (Pang *et al.*, 2015).

Cancer cells have been shown to release extracellular microparticles and exosomes which contain various substances such as CD63, PDGF, VEGF, and thrombin which may promote tumour-cell induced platelet aggregation (TCIPA) (van der Pol *et al.,* 2012; Woei and

Tesselaar, 2016). These microparticles have been shown to bind to platelets through CD62p and are eventually sequestered by platelets in order to further promote tumour progression via the reciprocal interactions between these cell types (Thomas *et al.,* 2009). Through the sequestration of microparticles, platelets acquire ribonucleic acid (RNA) from tumour cells which alters their genotype and thus enables them to produce pro-tumourigenic substances (Rak, 2010; Nilsson *et al.,* 2011). Cancer cells not only change the protein expression patterns on platelet membranes, they also increase the release of platelet secretory granules and platelet microparticles (Zhang *et al.,* 2017).

3.1.3 The role of hormone and antiplatelet therapy in hypercoagulation

Aromatase inhibitors such as Anastrozole decrease the production of oestradiol and thus are effective against cell proliferation in ER^+ breast cancer (Lumachi *et al.*, 2013; Cuzick *et al.*, 2014; Matthews *et al.*, 2018). Oestradiol also facilitates protection against cardiovascular disease by regulating the metabolism of serum lipid, increasing vasodilation and preventing atherosclerosis (Matthews *et al.*, 2018). Thus, inhibition of oestradiol production by AIs is associated with increased cardiovascular disease as seen by the persistence of VTE in patients taking AIs (Cuzick *et al*., 2014; Kemp *et al.,* 2014). Pre-treatment of breast cancer cells (MCF7 and T47D) with Anastrozole did not prevent tumour cell-induced platelet activation, thus highlighting the potential role of antiplatelet therapy in this interaction (Pather *et al.,* 2019). Despite the beneficial effects of Anastrozole in reducing cancer recurrence in post-menopausal women, it is associated with among other adverse effects; cardiovascular disorders (Cuzick *et al.,* 2014; *Kemp et al.,* 2014).

Aspirin is an effective antiplatelet agent and has been shown *in vitro* to prevent TXA_2 generation (Rao and Knaus, 2008; Stalker *et al.,* 2012; Lucotti *et al.*, 2019). It has also been shown to inhibit platelet activation by arachidonate and disturbs platelet activation by

thrombin and ADP in conjunction with target antiplatelet therapies against PARs and ADP receptors (Stalker *et al.,* 2012; Panova-Noeva *et al.,* 2013). Aspirin is an antagonist of mainly dense granule release, its efficacy in inhibiting alpha granule exocytosis was shown to be minimal as alpha granule exocytosis was not inhibited by the inhibition of COX-1 (Passacquale and Ferro, 2011). Clopidogrel inhibits ADP mediated platelet activation and aggregation but also inhibits alpha granule exocytosis and therefore reduce the expression of P-selectins (Passacquale and Ferro, 2011). Dual anti-platelet therapy consisting of Aspirin and Clopidogrel is often used for thromboembolic disorders; however, the risk of recurrent cardiovascular events, mainly in the form of ischemic events, remains high (Tello-Montoliu *et al.*, 2011; Capodanno, Ferreiro and Angiolillo, 2013). Studies have shown that recurrence of thromboembolic disorders is mediated by thrombin through PAR-1 receptors, hence suggesting a role for PAR1 antagonists or inhibitors in reducing this risk (Kogushi *et al.*, 2011; Moschonas, Goudevenos and Tselepis, 2015; Heuberger and Schuepbach, 2019). Thrombin has multiple functions mediated through PAR receptors, its primary role in the coagulation cascade is to cleave fibrinogen into fibrin (Liu *et al.*, 2017; Göbel *et al.*, 2018).

Atopaxar is one of two PAR1 antagonists that has been tested *in vitro* and *in vivo* with regard to cardiovascular diseases whereby it was shown to reduce platelet aggregation and risk for bleeding (Kogushi *et al.*,2011; Wiviott *et al.*, 2011; Wang *et al.*, 2016). Atopaxar is most effective against thrombin-induced platelet aggregation (Kogushi *et al.*,2011; Wiviott *et al.*, 2011; Wang *et al.*, 2016). The activation of PAR1 by thrombin also leads to a positive feedback system in the production of thrombin and thus further increases its levels (Holinstat *et al.*, 2009; Han *et al.*, 2011; Kogushi *et al.*, 2011b). The activation of platelet activation through PAR1 receptors was mainly observed in patients with thromboembolic disorders and was

least involved during haemostasis (Holinstat *et al.*, 2009; Han *et al.*, 2011; Kogushi *et al.*, 2011). Therefore, PAR1 antagonists are more desirable neoadjuvant antiplatelet therapy (APT) because they would affect the physiological pathways that mediate haemostasis (Holinstat *et al.,* 2009; Han *et al.,* 2011; Olivier *et al.,* 2013). Atopaxar was shown to inhibit thrombin receptor-activating peptides (TRAP) and platelet aggregation mediated by thrombin without adversely increasing bleeding time unlike most APT agents (Kogushi *et al.,* 2011; Tello-Montoliu *et al.,* 2011).

The effect of Anastrozole combined with antiplatelet agents (Aspirin and Clopidogrel cocktail and Atopaxar) on coagulation is not known despite the established association between thromboembolic disorders and cancer, thus these outcomes are important in providing possible outcomes of these treatment interventions.

3.1.5 Aims and objectives

The aim of this study was to investigate the reciprocal interactions between hormone therapy and antiplatelet therapy-exposed breast cancer cells (MCF7 and T47D) on platelet activation and coagulation.

The **objectives** are stated as follows:

1. To investigate **induced hypercoagulability** by assessing levels of secreted thrombin in plasma of whole blood exposed to hormone and antiplatelet therapy exposed breast cancer cells
2. To investigate changes in the **index of platelet activation** (using CD62p and CD63 platelet activation markers) with combined hormone and antiplatelet therapy
3. To investigate **morphological changes** in platelets following exposure to hormone and antiplatelet therapy-treated breast cancer cells

3.2 Materials and Methods

3.2.1 Patient recruitment and demographics

3.2.1.1 Ethics

Ethical clearance to conduct this study was obtained from the Human Research Ethics Committee of the University of the Witwatersrand, clearance number: M150263 (Appendix B1). Six (6) seemingly healthy female participants between the ages of 19-30 years were recruited from the Faculty of Health Sciences, University of the Witwatersrand. The background and purpose of the study was explained to the prospective participants, and they were given an information sheet and required to sign a consent form stating their willingness to participate in the study.

3.2.1.2 Exclusion criteria

Participants with the following criteria were excluded from the study: pregnancy (Ciobanu *et al.,* 2016), smoking (Pamukcu *et al.,* 2011), use of oral contraceptives or injection, immunodeficiency (Pituch-Noworolska *et al.,* 2015) autoimmune disease (Liu *et al.,* 2019) and consumption of anti-platelet and anti-coagulation medication (e.g. Aspirin and Warfarin) (Ornelus *et al.,* 2017) in the previous 72 hours because these conditions are known to have adverse effects on platelets and would therefore compromise our findings.

3.2.1.3 Blood collection

Peripheral blood was only collected from participants between day 1-10 of their menstrual cycle i.e. during the follicular phase whereby oestrogen and progesterone levels are at the lowest and platelets have less affinity for fibrinogen (Dupuis *et al.,* 2019). Peripheral blood was collected by venepuncture into 3.2% sodium citrate vacutainers (4.5ml) (Biocom Africa, Centurion, South Africa, AUGP17002) using a 20 gauge needle by a phlebotomist at Charlotte Maxeke Academic Hospital Johannesburg. The first 2 ml of blood was collected into a separate

vacutainer tube and then discarded in order to avoid inclusion of mechanically activated platelets (from the needle prick). Thereafter, three vials (13.5 ml) of blood were collected.

3.2.2 Whole blood and breast cancer cell exposure

3.2.2.1 Blood cell exposure

In order to facilitate interaction between breast cancer cells and platelets, 300 µl of whole blood was exposed to breast cancer cells (MCF7 and T47D) seeded in 24 wells (as previously stated (Chapter II: 2.2.1) following the treatment of breast cancer cells with Cmax concentrations of hormone therapy (Anastrozole) and/or antiplatelet therapy (Aspirin, Clopidogrel, and Atopaxar) for 24 hrs (Chapter II: Table 2.2A, 2.2B all treatment groups). Whole blood was exposed to breast cancer cells seeded onto 24 well plates, for 5 mins at room temperature (20 °C to 25 °C), then transferred into appropriate 15 ml polypropylene tubes.

3.2.2.2 Whole blood storage for thrombin assay

For assessment of thrombin activity (Chapter III; section 3.2.2.1) 200 µl of whole blood was transferred to 1.5 ml Eppendorf tubes, snap frozen in liquid nitrogen, and stored at -80 °C.

3.2.2.3 Whole blood lysis

Blood erythrocyte lysis was conducted in polypropylene tubes (Lasec, Midrand, South Africa, P1TUB013B-000015) by adding 3 ml of ammonium chloride lysis buffer (1:10) for 10 minutes. Samples were centrifuged for 5 mins at 200 xg using a Rotina 420r Hetting centrifuge (Sigma Aldrich, Modderfontein, South Africa). The supernatant was discarded, and the pellet resuspended in 150 µl Tyrode's buffer.

3.2.2.4 Preparation of flow cytometry controls

The positive control and technical control samples were prepared by adding 0.1U/ml of human thrombin to lysed whole blood suspended in 150 µl Tyrode's buffer for 5 mins at room temperature in order to induce platelet activation.

3.2.2.5 Lysed whole blood preparation for morphological studies

For morphological assessment, 20 µl of lysed whole blood samples was pipetted onto glass coverslips (Lasec, Midrand, South Africa, 1809-207152005) and further processed for morphological analysis as specified in Chapter III; Section 3.2.2.5.

3.2.3 Thrombin activity assay

3.2.3.1 Quantifying thrombin release in whole blood

In order to conduct the assay, samples were first thawed at room temperature. Thrombin activity was measured using the fluorometric thrombin activity assay kit (Abcam, Centurion, South Africa ab197006) and the manufacturer's protocol was followed. Briefly, samples for the standard wells were prepared by diluting a volume of known standard with the assay buffer in order to create six standards with the following concentration per well; 0 ng, 5 ng, 10 ng, 15 ng, 20 ng and 25 ng. Reaction wells were prepared by mixing 5 µl of whole blood (unlysed) samples with 45 µl of thrombin assay buffer (1:10 dilution) into appropriate wells. A master mix containing 5 µl of thrombin substrate and 45 µl of thrombin assay buffer was prepared and added into each well. Fluorescence was measured in a Fortega Glomax Explorer fluorescence spectrophotometer, in kinetic mode at excitation wavelength of 350 nm and emission wavelength of 450 nm. Readings were obtained at regular intervals for a duration of 60 minutes at 37 °C.

3.2.3.2 Data analysis

Data was managed in Microsoft Excel 2010 and data was analysed as specified in the kit manuals. The mean absorbance value of the blank was subtracted from all values to create the corrected absorbance for each sample. Then the corrected absorbance values were plotted against the known thrombin concentrations in order to create a standard curve. The

standard curve was used to calculate thrombin concentration in each sample using the following formulae (Thrombin activity assay kit, Abcam, Centurion, South Africa ab197006);

$$Time\ point\ value\ = (\frac{corrected\ absorbance - (y - intercept)}{slope})$$

Then the change in time point value between the final and initial time point was calculated.

Thrombin activity was calculated as follows;

$$Thrombin\ activity = \left[\frac{\text{Amount of thrombin per well (ng)}}{\text{Sample vloume added per well (ml)}}\right] * Sample\ dilution\ factor$$

A Shapiro-Wilk test revealed the data was non-parametric. PAST13 statistical software was used to determine whether there were significant differences in thrombin activity over time in whole blood exposed to breast cancer cells (MCF7 and T47D) which had been treated with endocrine therapy (Anastrozole) and/or antiplatelet therapy using a Friedman's test and corresponding post hoc analysis (Appendix B3).

3.2.4 Detection of platelet activation markers

3.2.4.1 Labelling of lysed whole blood with activation markers

To detect platelet activation using flow cytometry; 180 µl of lysed whole blood volume was incubated with optimal volumes of monoclonal antibodies (determined through titration, Appendix B4.2) specific for the platelet activation markers of interest: 10 µl of APC conjugated mouse anti-human CD41a (BD Biosciences, Woodmead, South Africa, 559777), 10 µl of FITC-conjugated mouse anti-human CD62p (BD Biosciences, Woodmead, South Africa, 555523) and 2.5 µl PE-CY7-conjugated mouse anti-human CD63 (BD Biosciences, Woodmead, South Africa, 561982) for 15 mins at room temperature. Thereafter lysed whole blood was fixed in 0.5% paraformaldehyde for 10 mins, centrifuged with a Hettich centrifuge at 200 g for 5 mins. The supernatant was discarded and the pellet was resuspended in 500 µl Tyrode's buffer and

kept at 4°C overnight. Samples were analysed the following day on the LSR Fortessa flow cytometer equipped with four lasers (blue, red, violet and UV).

3.2.4.2 Flow cytometry

Cytometer setting and tracking beads diluted in sheath fluid were run prior to each experiment in order to check the status of the detectors and ensure that the instrument was functioning optimally prior to experiments being conducted. FACSDiva software was used to capture results and compensation controls (single stained technical controls; CD41a-APC only/CD62p-FITC only/CD63-PECY7 only) were used to correct for spectral overlap between the different fluorochromes and determine optimal voltages for each fluorochrome (Appendix B4.1). Fluorescence minus one (FMO) controls were also included in order to confirm the sensitivity of each channel and ensure specificity for each marker at the relevant channel (Appendix B4.3). The following voltages were used to obtain data; forward side scatter (approximate measure of cell size) (FSC) 300 v, side scatter (approximate measure of internal complexity/granularity) (SSC) 275 v, APC 460 v, FITC 469 v, PECY7 674 v. A total of $1x10^5$ events were measured for each sample. The threshold was set at 500.

3.2.4.3 Gating strategy

In principle, the gating strategy defines parameters for which different populations of interest are selected and represented on the flow graphs using specific criteria. Gating plays an important role in ensuring that data analysis is conducted on the correct population of interest. Firstly, putative platelets were gated by drawing a gate (P1) around a population which was defined by the low forward and side scatter properties of platelets (please note that debris was included in this gate due to size) (Fig 3.1: A). Then a singlet population designated P2 was gated, based on P1, in order to minimise data loss due to cell clumping (Fig 3.1: B). A platelet population was then gated using a histogram showing cells from P2

expressing CD41a only (P3) (Fig 3.1: C). Subsequently from the P3 population a scatter plot was created to represent platelets which were expressing both activation markers $CD62p^+$ and $CD63^+$ (designated Q3, Figure 3.2: C). The independent expression of either CD62p or CD63 was represented in scatter plots based on the singlet population (P2). These scatter plots showed platelets ($CD41a^+$) which were expressing either CD62p (designated Q3, figure 3.2: A) or CD63 (designated Q3, figure 3.2: B). The graded expression levels of CD62p and/or CD63 were represented within intervals (I1-6) in the Q3 quadrants as defined in figure 3.2: A-C. Intervals were determined based on the spread of each population within the quadrant (Augustine *et al.,* 2016).

Furthermore, other cell types besides platelets ($CD41a^-$) which were expressing $CD62p^+$ (Fig 3.2: A) and $CD63^+$ (Fig 3.2: B) were identified in quadrants Q4. In the Q1 quadrant, platelets ($CD41a^+$) which were not expressing activation markers CD62p (Fig 3.2: A) and CD63 (Fig 3.2: B)) were found. In the Q2 quadrant, other cell types or debris were found which were neither platelets (CD41a), nor expressed CD62p (Fig 3.2: A) or CD63 (Fig 3.2: B). Platelets ($CD41a^+$) expressing $CD62p^+$ only were depicted in Q3 (Fig 3.2: C), those expressing $CD63^+$ only where depicted in Q1 (Fig 3.2: C) and those which lacked both CD62p and CD63 were expressed in Q2 (Fig 3.2: C).

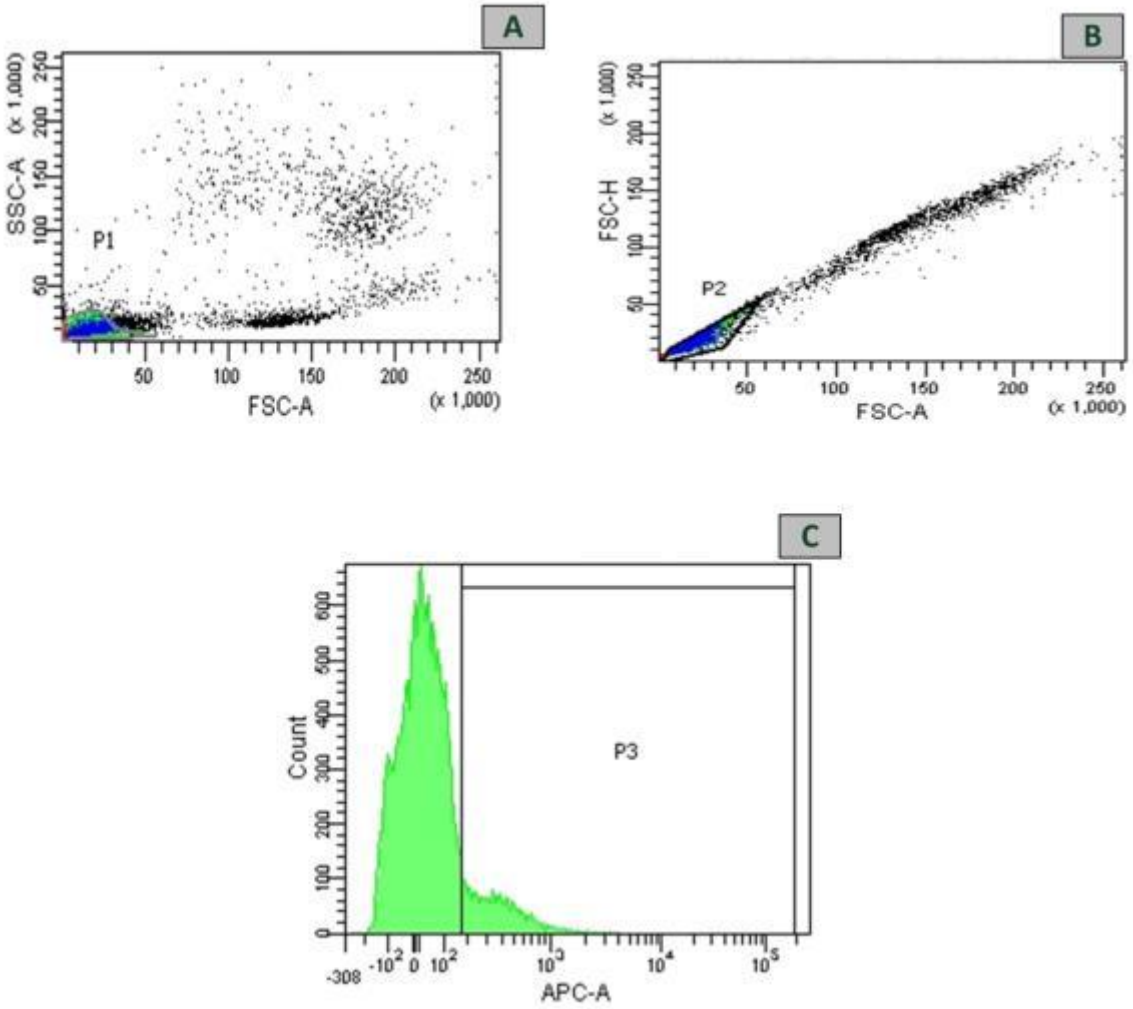


Figure 3.1: Representative scatter plots and histogram depicting the spread of whole blood. **A)** This scatter plot shows the gating of platelets based on forward and side scatter properties. Due to their small size and less internal complexity, platelets aggregate at the bottom left corner in the scatter plot (P1). **B)** This scatter plot shows how the singlet population was gated (P2) using forward scatter area and height. Thus, aggregated cells were excluded from the analysis in order to accurately analyse data. **C)** The histogram shows platelet population gated (P3) based on the expression of $CD41a^{+}$ events.

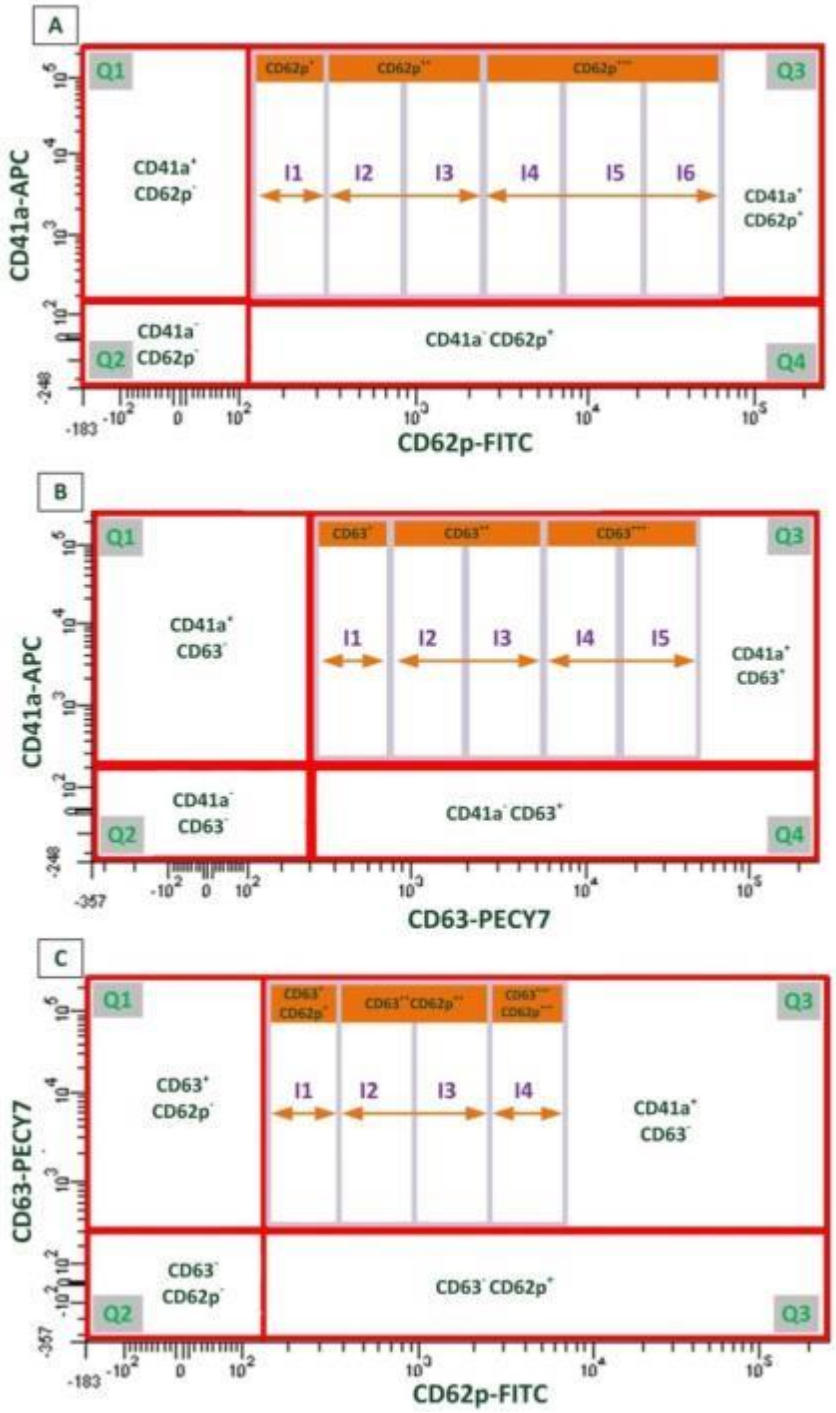


Figure 3.2: Scatterplots showing gating strategy used to investigate changes in expression levels of activation markers: CD62p and CD63 in platelets. **A)** Represents quadrants and intervals used to show the expression of CD62p only in CD41a$^+$platelets, **B)** Represents quadrants and intervals used to show the expression of CD63 only in CD41a$^+$platelets and **C)** Represents gates and intervals used to define CD41a$^+$ platelets expressing CD62p and CD63 (based on pure CD41a$^+$platelets).

3.2.4.4 Data analysis

Data acquired using FACSDiva software was exported to Microsoft Excel 2010 for data management. The index of platelet activation (IPA) was calculated using the following formulae (modified equations from Leytin *et al.,* 2000);

IPA CD62p = gMFI (CD62p)*n ($CD41^+CD62^+$) (Augustine *et al.,* 2016) and

IPA (CD63) = gMFI (CD63)*n ($CD41^+CD63^+$).

IPA was calculated for each quadrant (Q3) and interval (I1-6) (Fig 3.2 A-C) (Leytin *et al.*, 2000; Augustine *et al.*, 2016). The IPA allows for derivation of a parameter that describes geometric mean fluorescence intensity (gMFI) of $CD62p^+$ or $CD63^+$ expression in direct relation to the number of platelets ($CD41a^+$) expressing the marker. Thus, IPA gives a measurable quantity of the number of platelets which were activated. Statistical analyses were performed using PAST3 software. The non-parametric Friedman test and corresponding *post hoc* test (Wilcoxon) were conducted in order to determine whether the index of platelet activation (IPA) was significantly altered following platelet exposure to Anastrozole and/or antiplatelet therapy-treated breast cancer cells. Significance was set at $p<0.05$ (Appendix B4.4-4.8).

3.2.5 Platelet morphology

The glass coverslips containing 20 µl of lysed whole blood (refer to section 3.2.2.5) were transferred into 24 well plates, then incubated at 37°C for 5 mins in order to allow for adhesion of platelets to the glass coverslip (van der Spuy & Pretorius, 2013). Coverslips were then washed in 0.1M PBS and agitated on a micro-plate shaker at 1000 rpm for 20 mins to remove trapped proteins and debris. Samples were fixed in a 1:1 ratio of 2.5% formaldehyde/glutaraldehyde (FA/Glut) for 15 mins at room temperature, then rinsed thrice in 1M phosphate buffer at pH 7.2. Subsequently, samples were mounted in a drop of

fluoroshield (Sigma Aldrich, Modderfontein, South Africa, F6182) and left to dry overnight. Platelet morphology was qualitatively assessed at high magnification (63X objective) under phase contrast using the LSM confocal microscope.

Technical note: The samples were initially fixed for scanning electron microscopy (SEM) (hence preserved in 2.5% formaldehyde and glutaraldehyde (FA/Glut). However, due to mechanical breakdown of the NOVA scanning electron microscope, samples were alternatively viewed using a confocal microscope using the 63X objective. The higher magnification of the 63X objective allowed for viewing the general morphological changes; however, some of the finer details on the platelets and extracellular matrix contents (such as presence of fibrin fibres), which are traditionally viewed using an SEM, could not be detected.

3.3 Results

3.3.1 Assessment of thrombin activity in whole blood conditioned with breast cancer cells

Thrombin (factor IIa) is converted from prothrombin (factor II) and it is a potent factor in the coagulation cascade and in addition to facilitating platelet activation, it catalyses the conversion of fibrinogen to fibrin which occurs during clot formation (Palumbo, 2008; Göbel *et al.*, 2018). In this study the activity of thrombin in whole blood following exposure to breast cancer cell lines MCF7 and T47D was measured over time in order to predict hypercoagulability in whole blood following its exposure to hormone therapy- and/or antiplatelet therapy-treated breast cancer cells. The activity of thrombin was indicated by the release of the AMC-fluorophore which was conjugated to a thrombin substrate, the fluorophore was released from the thrombin substrate following exposure to thrombin, which cleaved the substrate and released the fluorophore, hence; its fluorescence is directly proportional to the activity of thrombin (Product sheet, Thrombin Activity Assay Kit, ab197006).

Thrombin activity was measured regularly for a period of ~60 mins, and the changes in AMC fluorescence which indicate thrombin activity were studied. The concentration of thrombin (ng/ml) generated over 60 mins in each sample was then calculated (Table 3.1). Overall the thrombin generated in whole blood exposed to treated MCF7 and T47D cells (Ana, AnaAspClop, AspClop, Ato) was slightly higher, but not significantly so, compared to the amount of thrombin generated in controls (whole blood, untreated cells, diluent) (Table 3.1). Whole blood exposed to thrombin only was used as a positive control for measuring levels of thrombin activity in the absence of cells. Whole blood exposed to MCF7 cells (treated and

untreated) resulted in higher levels of thrombin than the positive control. In contrast, whole blood exposed to T47D cells (treated and untreated) resulted in lower levels of thrombin than the positive control.

Table 3.1 Thrombin concentration (ng/ml) detected following whole blood exposure to MCF7 and T47D cells treated with Anastrozole (Ana) alone and in combination with antiplatelet therapy drugs and antiplatelet drugs alone; Aspirin and Clopidogrel cocktail (AnaAspClop and AspClop) and Atopaxar (AnaAto and Ato). Controls include untreated whole blood and the positive control, whole (WB) exposed to thrombin.

	Thrombin concentration (ng/ml)	**Thrombin concentration (ng/ml)**
Whole blood	19.0263	
WB Thrombin	19.5665	
Whole blood conditioned with cells	***MCF7 cells***	***T47D cells***
Untreated cells	20.9691	17.0831
Diluent control	20.9692	17.0831
Ana	20.9690	17.0832
AnaAspClop	20.9689	17.0832
AnaAto	20.9691	17.0831
AspClop	20.9691	17.0832
Ato	20.9692	17.0832

Baseline thrombin activity was indicated by untreated whole blood (Fig 3.3: A). MCF7 cells (untreated and treated with DMSO) induced significantly higher thrombin activity compared to baseline, as expected in whole blood (Fig 3.3: A). In contrast; T47D cells (at matched treatments) induced significantly lower thrombin activity than baseline. Thus suggesting that whole blood conditioned with MCF7 cells (untreated and DMSO-treated) had higher detectable thrombin levels than whole blood conditioned with T47D cells at matched treatments.

When cells were treated with Anastrozole then exposed to whole blood, thrombin activity in whole blood exposed to MCF7 cells was significantly higher compared to baseline, untreated cells and DMSO-treated cells (Fig 3.3: B). Furthermore, thrombin activity was significantly higher in whole blood exposed to Ana-treated MCF7 cells than Ana-treated T47D cells (Fig 3.3: B). Thrombin activity detected in Anastrozole-treated T47D cells, was significantly lower than baseline, but significantly higher than in whole blood exposed to untreated T47D cells (Fig 3.3: B). This suggests that Anastrozole-treatment on MCF7 cells, led to higher levels of thrombin in whole blood (compared to untreated or DMSO-treated cells) hence may increase coagulation. In T47D cells, Anastrozole treatment increased thrombin levels in whole blood compared to when cells were untreated and may suggest that this treatment may increase coagulation induced by T47D cells.

The addition of Aspirin and Clopidogrel cocktail to Anastrozole (AnaAspClop) led to significantly higher thrombin activity in whole blood exposed to AnaAspClop-treated MCF7 cells compared to baseline, untreated MCF7 cells, and MCF7 cells treated with DMSO and Anastrozole (Fig 3.3: B). Furthermore, this was significantly higher than in T47D cells at matched treatment (Fig 3.3: B). Whole blood exposed to AnaAspClop-treated T47D cells had significantly higher thrombin activity compared to baseline, DMSO-treated cells, and Ana-treated cells (Fig 3.3: B). This suggests that AnaAspClop treatment in both cell lines, increased the amount of thrombin detected in whole blood even further and thus may lead to higher levels of coagulation than Anastrozole alone, these effects were more pronounced in whole blood conditioned with MCF7 cells than T47D cells.

When cells were treated with Aspirin and Clopidogrel cocktail alone, thrombin activity in MCF7 cells was significantly higher compared to baseline, but significantly lower compared to

MCF7 cells exposed to medium only, DMSO, Ana, and AnaAspClop (Fig 3.3: B). In contrast, T47D cells treated with AspClop displayed significantly higher thrombin activity than most treatments (i.e. baseline, T47D cells exposed to medium only, DMSO, Ana and AnaAspClop) (Fig 3.3: B) suggesting that this treatment may lead to higher risk of coagulation. As with other treatments, AspClop induced significantly higher levels of thrombin in MCF7 than T47D cells.

When Atopaxar was combined with Anastrozole, thrombin activity in whole blood exposed to AnaAto-treated MCF7 cells was slightly but significantly increased compared to baseline, MCF7 cells treated with DMSO and Ana (Fig 3.3: C). In whole blood exposed to AnaAto-treated T47D cells, thrombin activity was significantly reduced compared to baseline and Ana and it was significantly increased compared to untreated T47D cells (Fig 3.3: C). Whole blood conditioned with MCF7 cells had significantly higher detectable thrombin levels than T47D cells (Fig 3.3: C). Furthermore AnaAto-treatment reduced thrombin levels below baseline in T47D cells suggesting that it may reduce risk of coagulation induced by this phenotype.

Whole blood exposed to Atopaxar-treated MCF7 cells resulted in significantly higher thrombin activity than baseline, slightly lower than DMSO-treated MCF7 cells and significantly lower than Ana-treated MCF7 cells (Fig 3.3: C). Whole blood exposed to Ato-treated T47D cells had no distinct differences compared to other groups; however, had significantly lower thrombin than that exposed to MCF7 cells (Fig 3.3: B). These findings thus suggest that Atopaxar treatment moderately reduced coagulation but was unable to completely prevent it by both cell lines, even though it is a PAR-antagonist.

In summary, all the drug treatments resulted in high thrombin detection in whole blood which may lead to platelet activation and ultimately increased risk of coagulation. It is noteworthy that MCF7 cells (treated and untreated) resulted in higher thrombin levels in whole blood

compared to T47D cells at matched treatments, and thus suggests that the MCF7 cell line may promote higher levels of coagulation than T47D cells; however, the low levels of thrombin detected in whole blood exposed to T47D cells may indicate that more thrombin was bound to PAR receptors in T47D cells and resulting in less thrombin detected in whole blood. This may allude to pro-tumourigenic effects in T47D cells which are facilitated by PAR signalling.

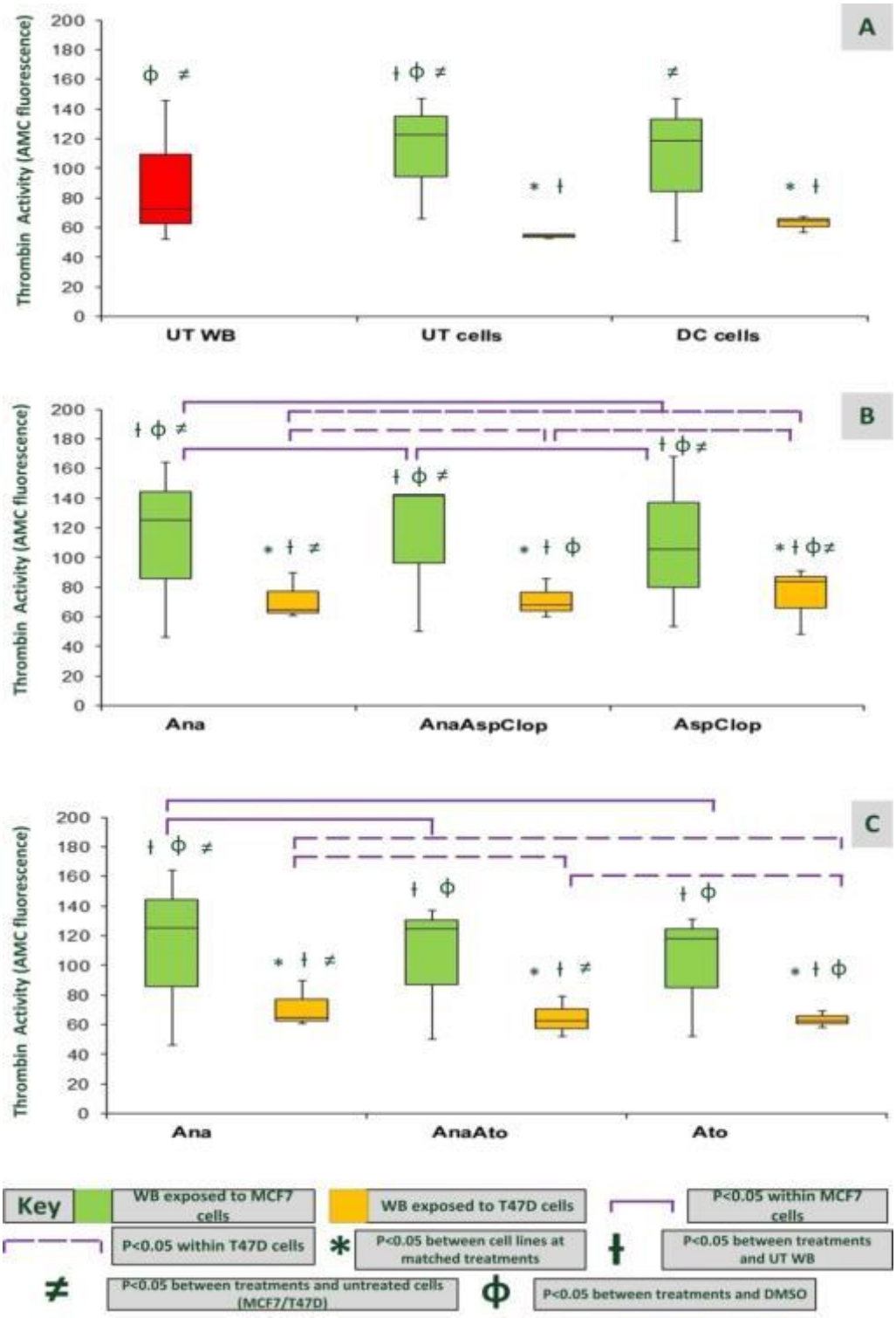


Figure 3.3: Box and whisker plots showing thrombin activity following whole blood exposure to breast cancer cells (MCF7 and T47D). A) Thrombin activity in controls:untreated whole blood (WB), untreated cells (UT) and DMSO- treated cells (DC). B) Thrombin activity in cells treated with anastrozole (Ana) and antiplatelet therapy cocktail: aspirin and clopidogrel (AnaAspClop or AspClop). C) Thrombin activity in cells treated with anastrozole (Ana) and antiplatelet therapy drug: Atopaxar (AnaAto or Ato). Overall, thrombin activity was significantly higher in MCF7 cells than T47D cells.

3.3.1 Assessment of platelet activation

Platelet activation was measured by calculating the index of platelet activation (IPA) which considers the number of platelets ($CD41a^{+}$) and the geometric mean intensity (gMFI) of platelet activation markers CD62p or CD63. Total IPA (Q3) was assessed for CD62p and CD63 (Figs 3.4, 3.6, 3.9: B1-2). The scatterplots (Figs 3.4, 3.6, 3.9: A1-3) showed that most events were concentrated within the first two intervals (I1-2) within Q3, with a slight right shift observed within Q3 for both markers suggesting a graded response. Few platelets expressed much higher levels of CD62p and CD63 in later intervals (I3-4) (Figs 3.4, 3.6, 3.9: A1-3). It is noteworthy that in all treatment groups, no events were observed in Interval 5; therefore, further analysis was not conducted for that interval (Figs 3.4, 3.6, 3.9: A1-3). Whole blood exposed to thrombin was used as a technical positive control and platelet activation was induced (Appendix B4.2). Statistical analysis using the Friedman's test with post-hoc analysis revealed that there were no significant differences in total IPA (Figs 3.4, 3.6, 3.9: B1-2) between the various treatments and cell lines ($p>0.05$); however, significant differences were observed within intervals (Fig 3.5, 3.7, 3.8).

The assessment of IPA within intervals yielded more definitive results regarding the differences induced in platelet activation between the treatment groups. Most platelets were concentrated between intervals 1 and 2 for both CD62p and CD63, with some found in interval 3 and fewer events in interval 4 (Figs 3.4, 3.6, 3.9: A1-3). This suggests that a majority of platelets generally had low to moderate expression of CD62p and CD63 and a lesser proportion were highly expressing these activation markers, thus alluding to a heterogeneous response of platelets to activation (Figs 3.5: A &B 1-4).

3.3.1.1 Hypercoagulation in control groups

IPA Total

Assessment of total IPA for CD62p between all controls (untreated whole blood and whole blood exposed to untreated or DMSO treated cells) showed that there were generally minimal induced levels of platelet activation, with untreated T47D cells inducing a more heterogeneous response in comparison to other controls (Fig 3.4: B1). A similar trend was observed when total IPA for CD63 was assessed; however, the total IPA for CD63 was consistently higher than that for CD62p (Fig 3.4: B2). Corresponding changes in platelet morphology were assessed qualitatively and related to the changes seen in platelet activation markers (CD62p IPA and CD63 IPA). The morphological features shown in platelets were representative of the change that occurred in platelet morphology irrespective of any quadrant or interval as delineated by flow cytometry.

In untreated whole blood, the majority of platelets were at early stages of activation as shown by the appearance of some discoid platelets with the extension of primary pseudopodia from the cell body, corresponding to the low levels of activation markers (Fig 3.4: C1). Some platelets expressed more pronounced pseudopodia formation and minimal membrane (hyalomere) spreading, indicative of a range of activation, albeit primarily early stage (Fig 3.4: C1).

When whole blood was exposed to untreated breast cancer cells (Figs 3.4: C2-3); platelets displayed more pronounced pseudopodia and thinner filopodia, with hyalomere presence displayed in some platelets. Similar morphological features were observed following whole blood exposure to DMSO-treated breast cancer cells (Figs 3.4: C4-5); however, some platelets were fully spread and displayed more distinct hyalomere formation. In all control groups minimal microparticle secretion into the extracellular space was observed (Figs 3.4: C1-5).

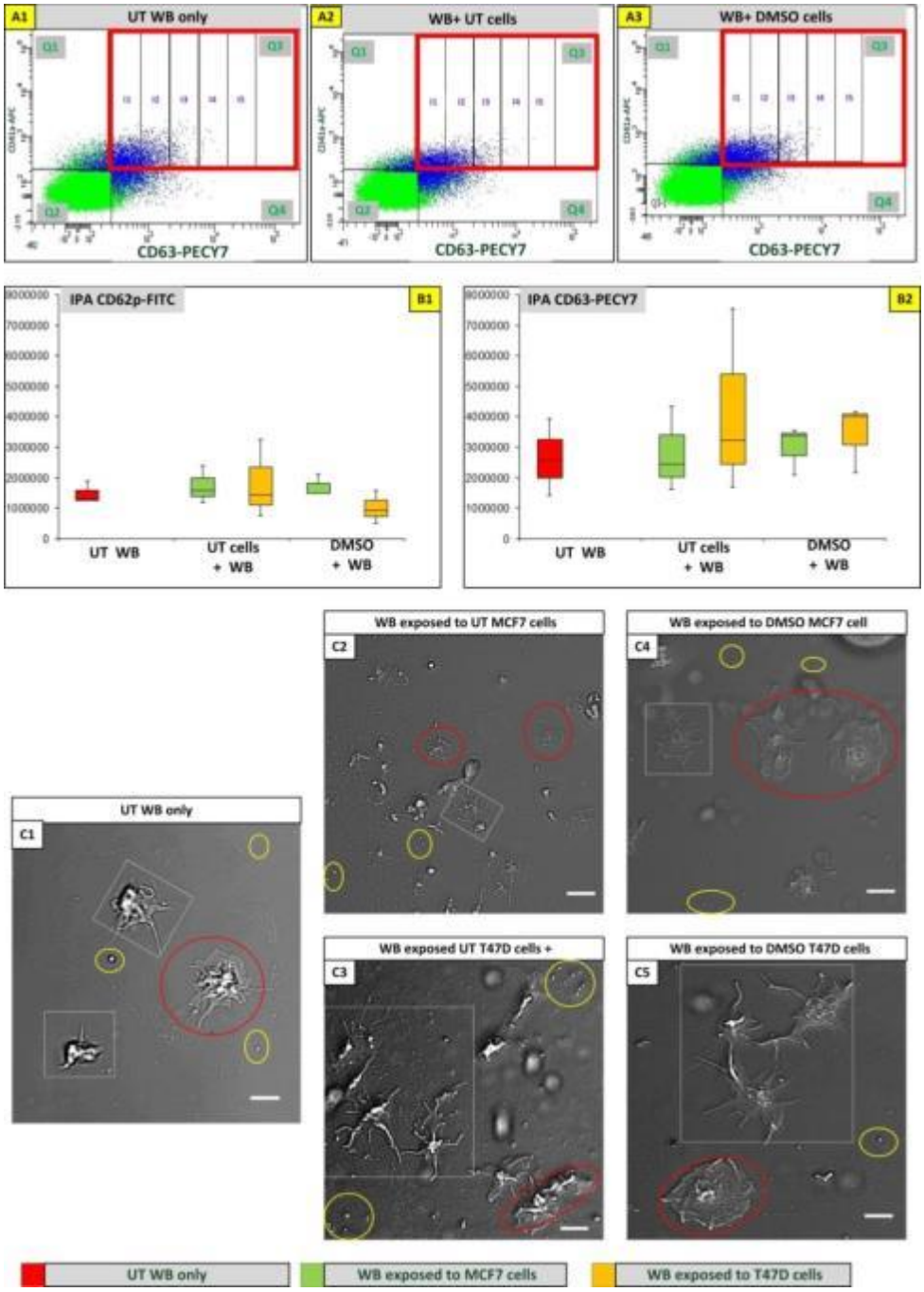


Figure 3.4 Platelet activation in controls (whole blood only (WB) and whole blood exposed to untreated (UT) or DMSO-treated (DC) MCF7 and T47D cells), as shown by CD62p and CD63 IPA and the corresponding morphological changes. A 1-3: shows the representative spread of CD63 activation marker within Q3 and associated intervals. A right shift was observed in the data spread. A similar spread was identified for CD62p. B1-2: shows box and whisker plots for CD62p IPA (B1) and CD63 IPA (B2). C 1-5: shows morphological changes in platelets which reveal different levels of activation. Platelets encircled in red display morphology associated with late stages of activation such as membrane spreading (hyalomere) and platelets within the white square display morphology associated with early stages of activation such as pseudopodia formation. The yellow circles contain small particles within the extracellular space (microparticles). Scale bar =1µm.

IPA within Intervals

In interval 1, CD62p IPA in media (untreated cells) and diluent (DMSO) control (significant in MCF7 cells) were higher than untreated whole blood (Fig 3.5: A1). CD63 IPA was generally higher in media (significant in MCF7 cells) and diluent controls compared to untreated whole blood (Fig 3.5: A2). Furthermore, CD63 IPA in untreated MCF7 cells was significantly higher than in DMSO-treated MCF7 cells (Fig 3.5: A2).

In interval 2, CD62p IPA for untreated whole blood was higher than that induced in interval 1 (Fig 3.5: A1). Untreated MCF7 cells induced significantly higher CD62p IPA compared to untreated whole blood (Fig 3.5: B1). No significant differences were seen in CD63 IPA in all treatment groups (Fig 3.5: B2).

In interval 3, CD62p IPA in media (untreated cells) and diluent (DMSO) control in T47D cells was significantly lower compared to untreated whole blood (Fig 3.5: C1). Whole blood exposed to untreated MCF7 cells induced significantly higher levels of CD62p IPA in comparison to that exposed to DMSO-treated MCF7 cells (Fig 3.5: C1). The levels of CD63 IPA were generally similar between the control groups (Fig 3.5: C2). DMSO-treated T47D cells induced significantly higher CD63 IPA than untreated T47D cells (Fig 3.5: C2).

In interval 4, all control groups induced very low levels of CD62p IPA; untreated whole blood induced the lowest CD62p IPA (significantly lower than untreated-MCF7 cells) and untreated-MCF7 cells induced a significantly higher CD62p IPA than DMSO-treated MCF7 cells (Fig 3.5: D1). DMSO-treated T47D cells induced significantly higher CD62p IPA than MCF7 cells at matched treatment (Fig 3.5: D1). No significant differences were observed in CD63 IPA across all controls (Fig 3.5: D2).

In summary, CD62p IPA was higher across all controls in interval 1 and 2 and from interval 3 CD62p IPA levels were reduced across all treatments reaching its lowest level in interval 4. In contrast the levels of CD63 IPA were lowest at interval 1 and 2 and high at interval 3 and 4. Whole blood represented baseline levels of platelet activation and thus had the lowest levels of CD62p except at interval 3, similarly CD63 IPA was lowest at interval 1 and 2. This finding corresponds to the morphology seen in whole blood which showed platelets displaying discoid morphology with few pseudopodia and membrane spreading. Whole blood exposed to untreated MCF7 cells generally induced higher levels of CD62p and CD63 IPA at all intervals compared to whole blood exposed to DMSO-treated MCF7 cells (with exception to CD63 IPA at intervals 3 and 4). This may reflect the effects of DMSO, despite being at a low concentration, on MCF7 cells, thus reducing their capacity to activate platelets. In contrast, whole blood exposed to DMSO-treated T47D cells induced higher CD62p and CD63 IPA in all intervals (with exception for CD62p in interval 1). Thus suggesting that DMSO did not modulate the response of T47D cells, and despite exposure, this cell line was able to induce platelet activation. Despite this, untreated and DMSO treated-MCF7 cells induced higher levels of CD62p and CD63 IPA and this corresponds with morphological changes induced which reveal that platelets were at more advanced stages of activation following exposure to MCF7 cells than T47D cells (Figs 3.4: C2-5).

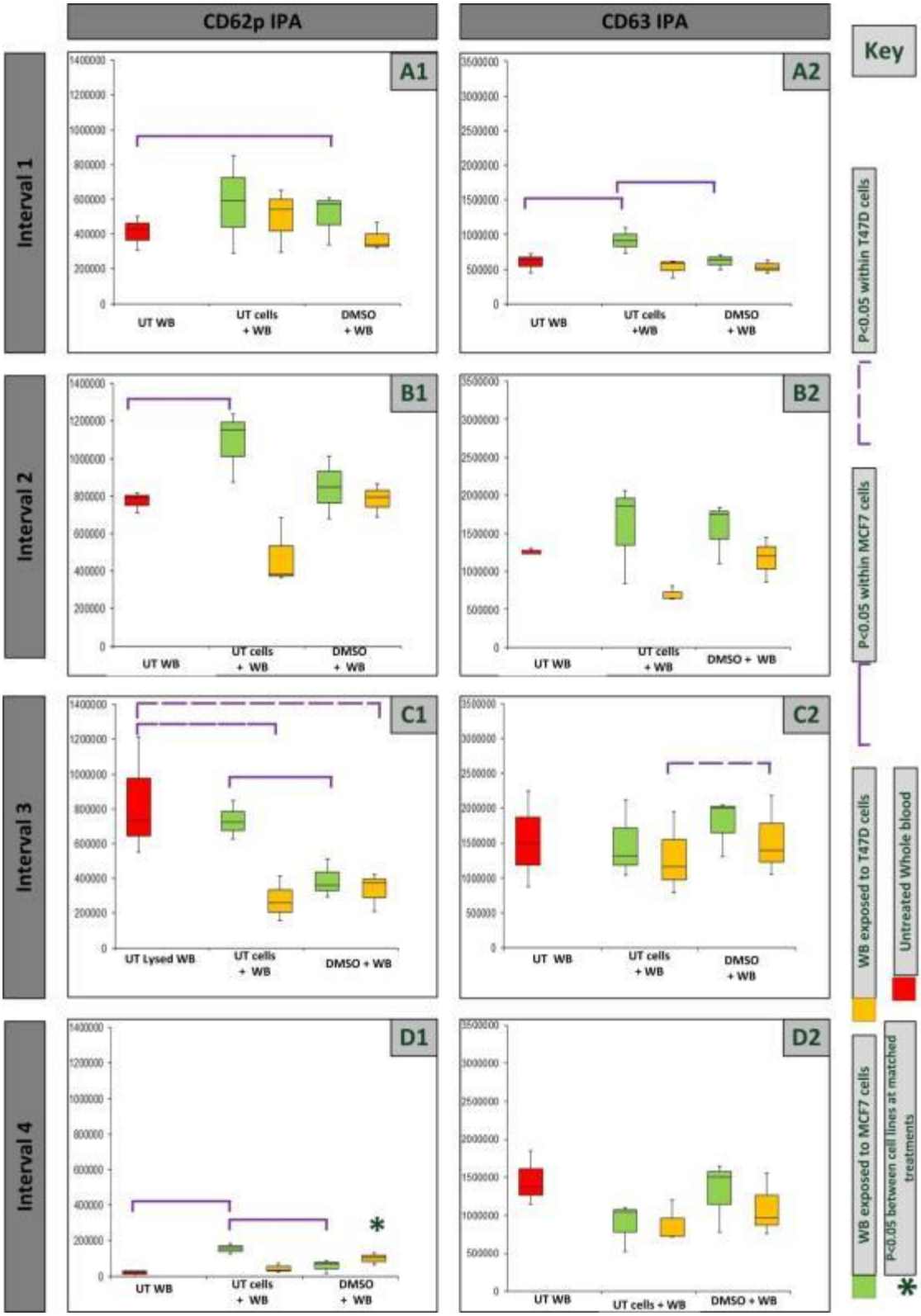


Figure 3.5 Box and whisker plots representing CD62p IPA (A1-D1) and CD63 (A2-D2) IPA in untreated whole blood (WB) and whole blood exposed to untreated and DMSO treated MCF7 and T47D cells between intervals: A1&2) Interval 1, B1&2) Interval 2, C1&2) Interval 3 and D1&2) Interval 4. Overall CD63 IPA was higher than CD62p at all quadrants, and CD62p IPA levels gradually dropped from interval 1, whereas that of CD63 were maintained throughout each interval.

3.3.1.2 Anastrozole mediated hypercoagulation

IPA Total

Whole blood exposed to breast cancer cells treated with Anastrozole displayed a uniform CD62p IPA response in MCF7 cells and no significant difference was observed in its levels between the cell lines (Fig 3.6: B1). In contrast, no significant differences were seen in CD63 IPA between cell lines; however, the trend observed showed that CD63 IPA was higher in whole blood exposed to MCF7 cells than T47D cells (Figs 3.6: B1-2). Statistical analysis indicated that Anastrozole treatment did not significantly alter the capacity of either cell line to affect platelet activation markers compared to the controls ($p>0.05$). The corresponding morphological assessment revealed that most platelets exposed to Anastrozole-treated MCF7 and T47D cells displayed extensive pseudopodia development with minimal membrane spreading (hyalomere formation) (Figs 3.6: C1-2). In both cell lines, microparticles secretion was observed in the extracellular space, although slightly more in T47D cells than in MCF7 cells (Figs 3.6: C1-2). Thus this finding indicates a more active platelet phenotype in whole blood exposed to MCF7 cells.

IPA within Intervals

In interval 1, whole blood exposed to Ana-treated MCF7 cells induced a significantly higher CD62p IPA than AspClop-treated MCF7 cells (Fig 3.7: A1). In T47D cells CD62p IPA was significantly higher compared to untreated WB (Figs 3.7: A1). CD63 IPA was the lowest in this interval (Fig 3.8: A1-2). Ana-treated MCF7 cells significantly increased CD63 IPA compared to untreated MCF7 cells (Fig 3.8: A1).

In interval 2, CD62p IPA generally increased in relation to interval 1 (Fig 3.7: A1). Ana-treated MCF7 cells significantly increased CD62p IPA in relation to untreated MCF7 cells (Fig 3.6: A1

& 3.7: B1). In interval 2, induced CD63 IPA was higher than in interval 1 for both cell lines (Figs 3.8: A &B 1-2).

No distinct differences in CD62p IPA were seen in Interval 3 (Fig 3.7:D1). In contrast, the highest levels of CD63 IPA were observed in this interval (Fig 3.8: C1-2). Moreover, there was a significant increase in CD63 IPA following whole blood exposure to Ana-treated MCF7 cells when compared to T47D cells at similar treatment (Fig 3.8: C1). In addition, the induced CD63 IPA in whole blood exposed to Ana-treated MCF7 cells was significantly higher than in untreated whole blood (Fig 3.5: C1). CD63 IPA induced in Ana-treated T47D cells was significantly higher than in untreated T47D cells (Fig 3.5: C2 & Fig 3.8: C2) but significantly lower compared to AnaAto-treated T47D cells (Fig 3.8: C2).

In Interval 4, CD62p IPA was low in both cell lines compared to other intervals (1-3) (Fig 3.7: D1). CD62p IPA in whole blood exposed to Ana-treated MCF7 cells was significantly higher compared to untreated whole blood and whole blood exposed to DMSO-treated cells, but significantly lower than that induced by untreated MCF7 cells and T47D cells (at matched treatment) (Fig 3.7: D1). Ana-treated T47D cells significantly increased CD62p IPA in relation to untreated WB (Fig 3.7: D1). CD63 IPA was reduced compared to interval 3 (albeit not significant) in whole blood exposed to Ana-treated cells (MCF7 and T47D) (Fig 3.8: D1) but in Ana-treated T47D cells, CD63 IPA was significantly higher than in untreated T47D cells (Fig 3.5: D1 & Fig 3.8: D1).

3.3.1.3 Anastrozole combined with Aspirin and Clopidogrel cocktail mediated hypercoagulation

IPA Total

Statistical analysis indicated that treatment with combined Anastrozole, Aspirin and Clopidogrel (AnaAspClop) treatment did not significantly alter the capacity of either cell line

to affect platelet activation markers compared to controls, Anastrozole treatment alone (Ana), and Aspirin and Clopidogrel (AspClop) treatment alone ($p>0.05$). CD62p IPA was generally lower in comparison to CD63 IPA, consistent with other observations of this marker (Figs 3.4, 3.6: B1-2).

Corresponding platelet morphology revealed that AnaAspClop treatment of MCF7 and T47D cells induced full hyalomere spreading and microparticles were present in the extracellular space (Figs 3.6: C3-4). The features observed are commonly associated with advanced stages of platelet activation and this corresponds to the loss of CD62p observed, CD63 expression remained high and was not affected by the stage of activation induced (Figs 3.6: B1-2). The presence of microparticles might also further contribute to the high levels of CD63 detected (Figs 3.6: C3-4). It is worth noting that few platelets displaying early morphological changes associated with platelet activation were noted, this reveals a heterogeneous response of platelets.

The matched treatment control (AspClop) of breast cancer cells did not significantly change CD62p IPA levels in both cell lines but induced slightly higher levels of CD63 IPA MCF7 than T47D cells (Fig 3.6: B1-2). This treatment induced similar morphological features in platelets which were associated with different stages of activation (Figs 3.6: C5-6). Some platelets displayed distinct pseudopodia and little membrane spreading reflecting early stages of activation while others showed fully spread membrane hyalomere, reflecting the variability observed in platelet activation markers (Figs 3.6: C5-6).

In summary, hormone therapy (with Anastrozole) and antiplatelet therapy (with Aspirin and Clopidogrel) individually or combined did not prevent platelet activation. Anastrozole treatment alone induced similar levels of CD62p IPA in both cell lines and higher CD63 IPA in

MCF7 cells than T47D cells. Similar morphological changes were observed in both cell lines following treatment in Anastrozole which correspond to platelets mainly at early stages of activation. When Anastrozole was added to Aspirin and Clopidogrel cocktail (AnaAspClop), no differences were observed in CD62p IPA in both cell lines; however, it increased CD63 IPA induced by MCF7 cells compared to T47D cells. The corresponding morphological changes were similar in both cell lines and revealed more distinct membrane spreading which reflects a greater loss in CD62p related to advanced stages of platelet activation. The antiplatelet therapy cocktail (AspClop) control induced similar levels of CD62p IPA in both cells and reduced CD63 IPA in both cell lines (compared to Ana- and AnaAspClop-treatment). The corresponding morphology revealed mixed platelet phenotypes between early and late stages of activation.

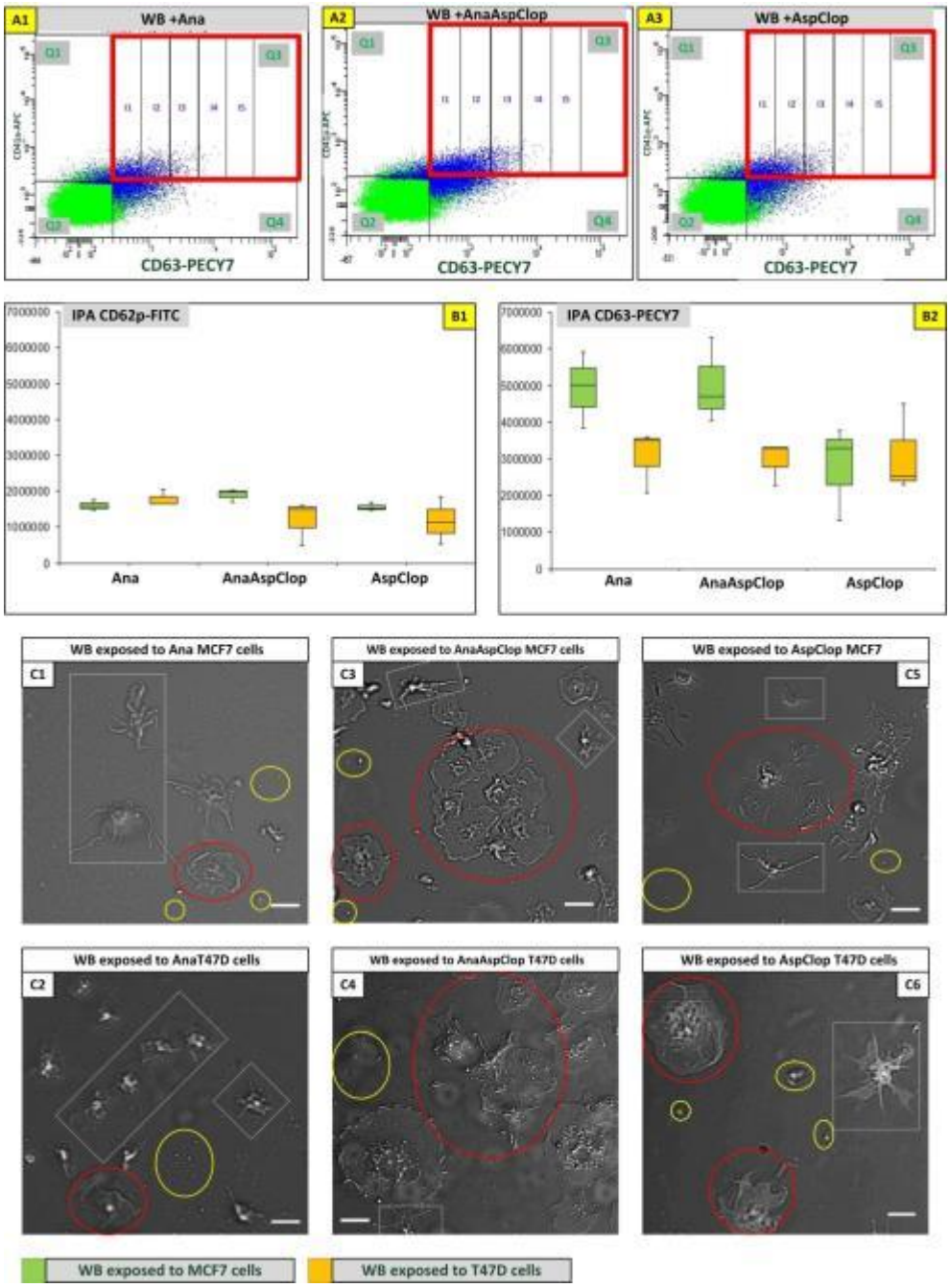


Figure 3.6 Platelet activation in whole blood exposed to MCF7 and T47D cells treated with Anastrozole (Ana) alone and in combination with antiplatelet therapy drugs; aspirin and clopidogrel (AnaAspClop) and aspirin and clopidogrel alone (AspClop) as shown by CD62p and CD63 IPA and the corresponding morphological changes. A 1-3: shows the representative spread of CD63 activation marker within Q3 and associated intervals. A right shift was observed in the data spread. A similar spread was identified for CD62p. B1-2: shows box and whisker plots for CD62p IPA (B1) and CD63 IPA (B2). C 1-6: shows morphological changes in which reveal different levels of activation. Platelets encircled in red display morphology associated with late stages of activation such as membrane spreading (hyalomere) and platelets within the white square display morphology associated with early stages of activation such as pseudopodia formation. The yellow circles contain small particles within the extracellular space (microparticles). Scale bar =1µm.

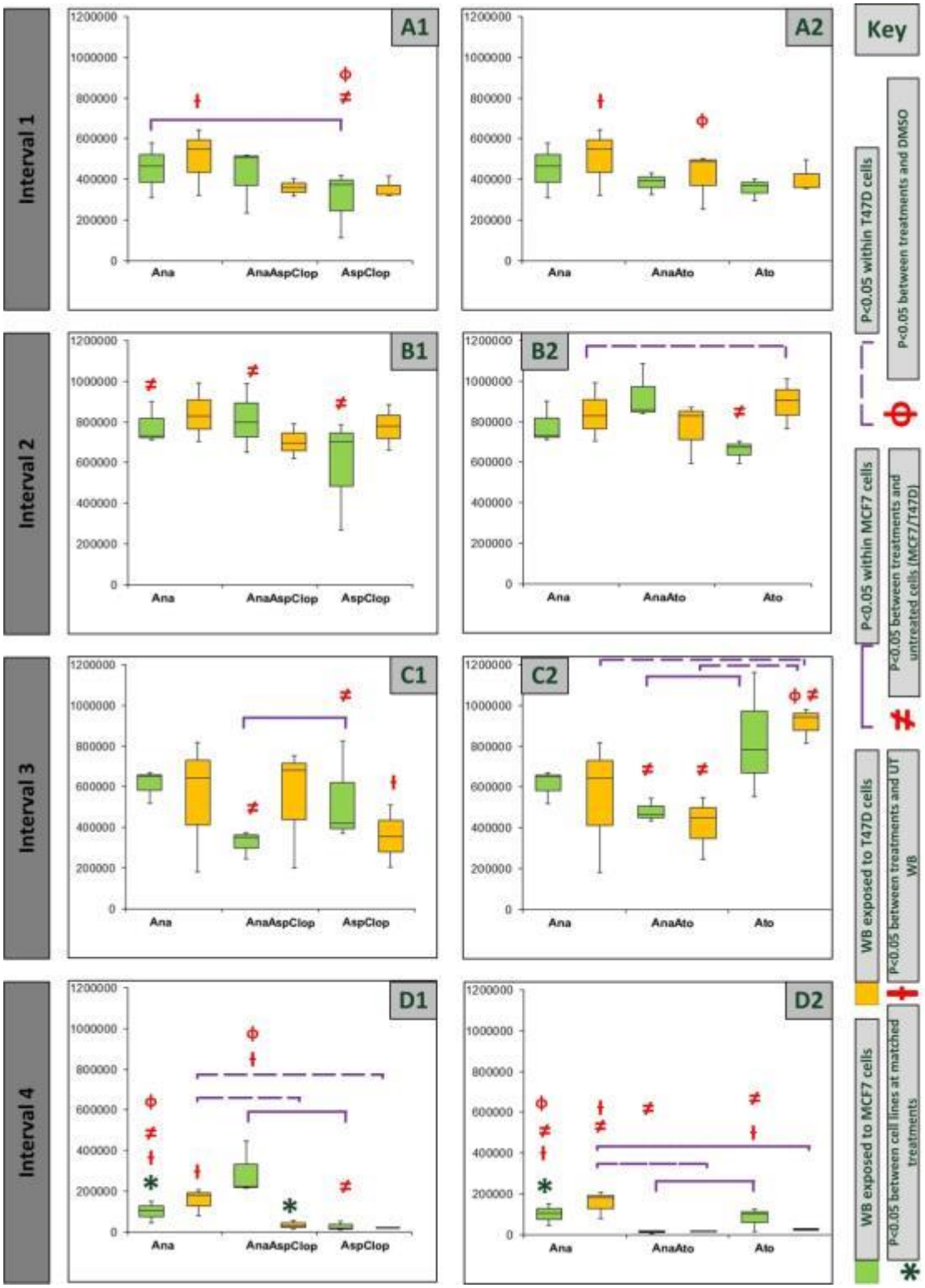


Figure 3.7 Box and whisker plots representing CD62p IPA in whole blood exposed to MCF7 and T47D cells treated with Anastrozole (Ana), with (AnaAspClop) and without Aspirin and Clopidogrel (AspClop) (A1-D1) and Anastrozole with Atopaxar (AnaAto) and without Atopaxar (Ato) between intervals (A2-D2). A1&2) Interval 1, B1&2) Interval 2, C1&2) Interval 3 and D1&2) Interval 4.

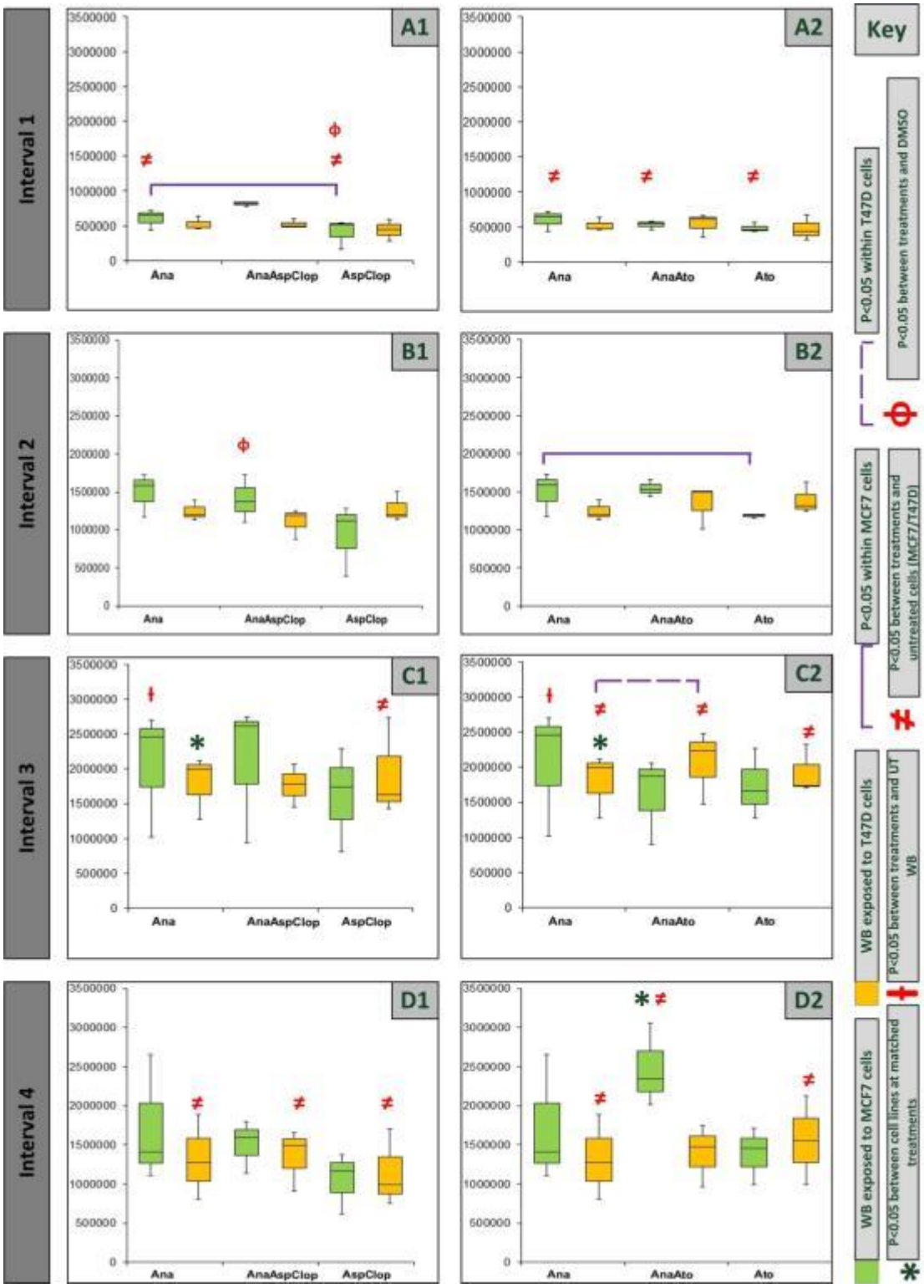


Figure 3.8 Box and whisker plots representing CD63 IPA in whole blood exposed to MCF7 and T47D cells treated with Anastrozole (Ana), with (AnaAspClop) and without Aspirin and Clopidogrel (AspClop) (A1-D1) and Anastrozole with Atopaxar (AnaAto) and without Atopaxar (Ato) between intervals (A2-D2). A1&2) Interval 1, B1&2) Interval 2, C1&2) Interval 3 and D1&2) Interval 4.

IPA within Intervals

In interval 1, CD62p IPA was generally low in whole blood exposed to AnaAspClop-treated and AspClop-treated cells (MCF7 and T47D) (Figs 3.7: A1-2). AspClop-treated MCF7 cells induced significantly higher CD62p IPA than in untreated- and DMSO-treated MCF7 cells (Fig 3.5: A1 & Fig 3.7: A1), but significantly lower than in Ana-treated MCF7 cells (Fig 3.7: A1). CD63 IPA was the lowest in this interval (Fig 3.8: A1-2). AspClop treatment in MCF7 cells induced significantly low CD63 IPA in comparison to that induced by untreated-, DMSO-treated and Ana-treated MCF7 cells (Fig 3.5: A1 & Fig 3.8 A1).

In interval 2, CD62p IPA was higher in whole blood exposed to AnaAspClop-treated and AspClop-treated cells (MCF7 and T47D) compared to interval 1 (Fig 3.5: B1 & Fig 3.7: B1). AnaAspClop-treated and AspClop-treated MCF7 cells significantly reduced CD62p IPA in comparison to untreated MCF7 cells (Fig 3.5: B1 & Fig 3.7: B1), whereas no differences were seen in T47D cells (Fig 3.7: B1). The level of CD63 IPA was generally higher across all treatment groups compared to that observed in interval 1 (Figs 3.8: A1 & B1). AnaAspClop-treated MCF7 cells induced significantly lower CD63 IPA compared to DMSO-treated MCF7 cells (Fig 3.5: B1 & Fig 3.8: B1).

In interval 3, CD62p IPA reduced across all treatment groups in comparison to that observed in interval 2 (Fig 3.7: B1-C1). AnaAspClop-treated MCF7 cells induced significantly lower CD62p IPA in comparison to untreated-MCF7 cells (Fig 3.5: C1 & Fig 3.7: C1) and AspClop-treated MCF7 cells (Fig 3.7: C1). AspClop-treated T47D cells induced significantly lower CD62p IPA than untreated whole blood (Fig 3.5:C1 & Fig 3.7: C1). CD63 IPA was the highest in this interval across all treatments (Fig 3.8: A-D 1) and AspClop-treated T47D cells induced a significantly higher CD63 IPA than in untreated T47D cells (Fig 3.5: C1 and Fig 3.8: C1).

In interval 4, AnaAspClop-treated MCF7 cells induced significantly higher CD62p IPA than AspClop-treated MCF7 cells, untreated whole blood, DMSO-treated MCF7 cells and T47D cells (at matched treatment) (Figs 3.5: D1 & Fig 3.7: D1). Furthermore, induced CD62p IPA in AspClop-treated MCF7 cells was significantly lower compared to untreated MCF7 cells (Fig 3.5: D1 & Fig 3.7: D1). Induced CD62p IPA was significantly reduced in AnaAspClop-treated and AspClop-treated T47D cells in comparison to Ana-treated T47D cells (Fig 3.7: D1). CD63 IPA was generally reduced in this interval across all treatments compared to interval 3 (Fig 3.8: C1 & D1). In whole blood exposed to AnaAspClop-treated and AspClop-treated T47D cells, CD63 IPA was significantly higher than that induced by untreated T47D cells.

3.3.1.4 Anastrozole and Atopaxar mediated hypercoagulation

IPA Total

The assessment of total CD62p IPA and CD63 IPA following whole blood exposure to MCF7 and T47D cells treated with AnaAto and Ato revealed that platelet activation was induced in all treatment groups although no significant differences were noted (Figs 3.9: B1-2). CD62p IPA was approximately equivalent in both cell lines; however, CD63 IPA was higher in MCF7 cells than T47D cells (albeit not significant) (Fig 3.9: B1-2). The morphological changes seen reveal that platelets exposed to AnaAto-treated MCF7 and T47D cells showed mixed features of early (pseudopodia extension, and discoid irregular shape) and late stages (hyalomere formation and microparticles in ECM) of platelet activation (Figs 3.9: C3-4). Particularly, ECM microparticles in whole blood exposed to MCF7 cells was much higher than in T47D cells, and could have contributed to the higher CD63 IPA seen in MCF7 cells because microparticles are a source of CD63 (Fig 3.9: B2).

Whole blood exposed to Ato-treated cells induced similar CD62p IPA in both cell lines, although more uniform induced by MCF7 than that observed in the T47D cell group at the

same treatment (Fig 3.9: B1). CD63 IPA was slightly higher in MCF7 cells than T47D cells (albeit not significant) (Figs 3.9: B2). The corresponding morphological features in platelets exposed to Ato-treated cells (MCF7 and T47D) revealed features which represent platelets in different stages of activation; prominent pseudopodia extensions were observed in some platelets (typical of early stages of activation) and some membrane spreading to form hyalomere were observed (late stages of activation) (Fig 3.9: C5-6). In addition, more microparticles were observed in the extracellular space in whole blood exposed to Ato-treated MCF7 cells (Fig 3.9: C5).

In summary hormone therapy (with Anastrozole) and antiplatelet therapy (with Atopaxar) individually or combined did not prevent platelet activation. When Anastrozole was added to Atopaxar (AnaAto), CD62p and CD63 IPA were increased in both cell lines (slightly higher in MCF7 than T47D cells). The corresponding morphological changes revealed more microparticles in the ECM of MCF7 cells which correspond to higher levels of CD63 IPA and blood exposed to T47D cells mainly revealed features corresponding to early platelet activation. Atopaxar alone in both cell lines reduced levels of CD62p and CD63 IPA (compared to Ana- and AnaAto-treatment). The corresponding morphology revealed mixed platelet phenotypes between early and late stages of activation.

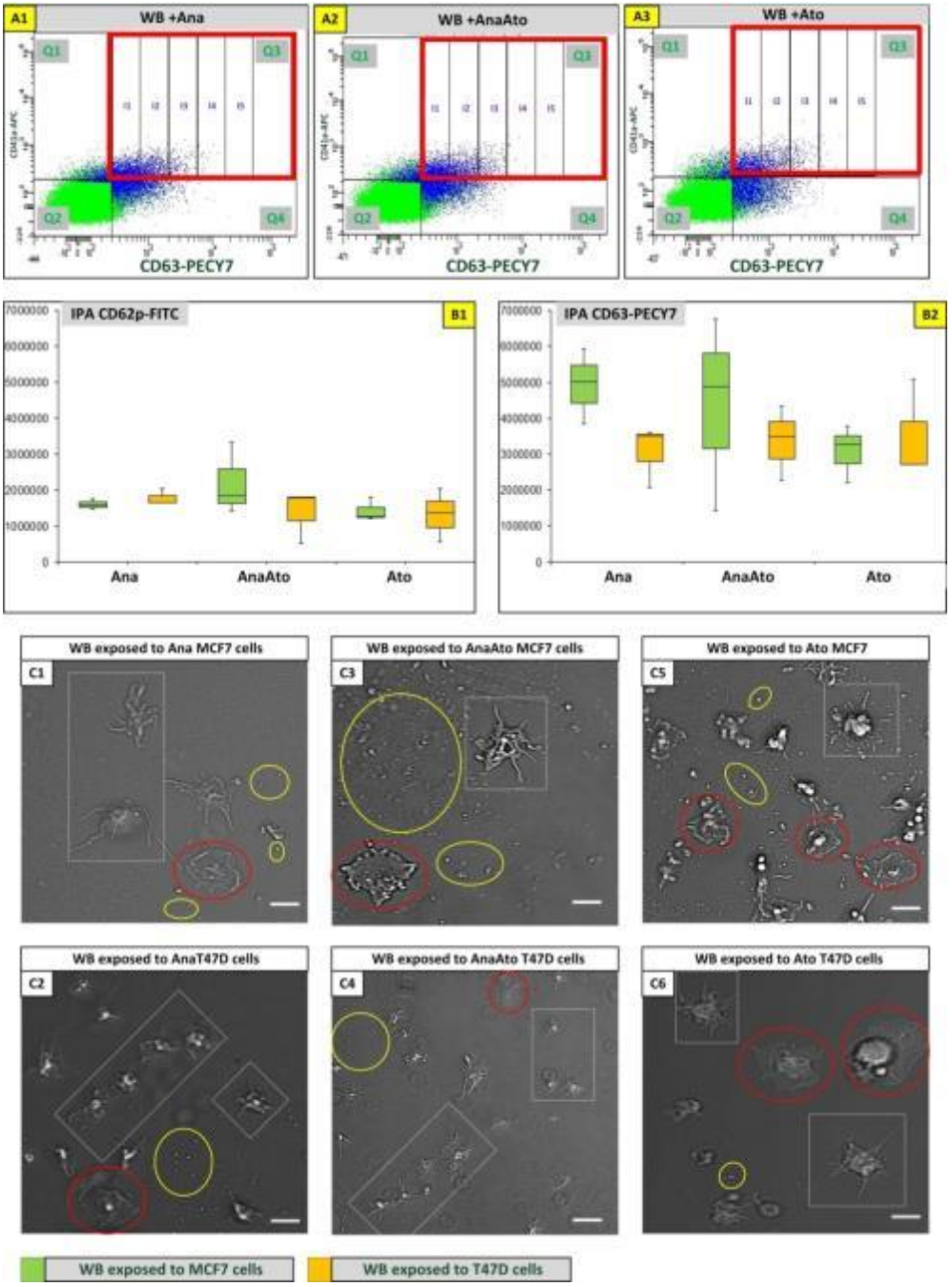


Figure 3.9 Platelet activation in whole blood exposed to MCF7 and T47D cells treated with anastrozole (Ana) alone and in combination with antiplatelet therapy drug; atopaxar (AnaAto) and atopaxar alone (Ato) as shown by CD62p and CD63 IPA and the corresponding morphological changes. A 1-3: shows the representative spread of CD63 activation marker within Q3 and associated intervals. A right shift was observed in the data spread. A similar spread was identified for CD62p. B1-2: shows box and whisker plots for CD62p IPA (B1) and CD63 IPA (B2). C 1-6: shows morphological changes in platelets and in all treatments evidence of platelet activation. Platelets encircled in red display morphology associated with late stages of activation such as membrane spreading (hyalomere) and platelets within the white square display morphology associated with early stages of activation such as pseudopodia formation. The yellow circles contain small particles within the extracellular space (microparticles). Scale bar =1µm.

IPA within Interval

In interval 1, CD62 IPA was generally low in whole blood exposed to AnaAto-treated and Ato-treated cells (MCF7 and T47D) (Fig 3.7:A2). Ana-treated T47D cells significantly increased CD62p IPA in relation to untreated whole blood and AnaAto-treated T47D cells significantly CD62p IPA in relation to DMSO-treated T47D cells (Fig 3.5: A2 & Fig 3.7: A2). CD63 IPA was generally the lowest in this interval (Fig 3.8 A2). In AnaAto-treated and Ato-treated MCF7 cells it was significantly lower than in untreated MCF7 cells (Fig 3.8: A2).

In interval 2, CD62p IPA was significantly lower in whole blood exposed to Ana-treated T47D cells than that exposed to Ato-treated T47D cells (Fig 3.7: B2). This finding suggests that Atopaxar was ineffective in preventing or reducing platelet activation or that CD62p expression in blood exposed to Ana-treated T47D cells was lost at this interval. No significant differences were observed in CD63 IPA in most treatments except Ato-treated MCF7 cells significantly reduced CD63 IPA compared to Ana-treated MCF7 cells (Figs 3.8: A2 & B2).

In interval 3, CD62p IPA was significantly higher in AnaAto-treated MCF7 cells when compared to untreated MCF7 cells, but significantly reduced when compared to Ato-treated MCF7 cells, a similar trend was observed in T47D cells (Fig 3.5: C2 & Fig 3.7: C2). Furthermore, Atopaxar-treated T47D cells induced significantly higher CD62p IPA compared to untreated- and DMSO-treated T47D cells (Fig 3.5: C2 & Fig 3.7: C2). CD63 IPA was generally higher in this interval compared to other intervals (Fig 3.8: A2-D2). Whole blood exposed to T47D cells treated with AnaAto and Atopaxar induced significantly higher CD63 IPA compared to untreated T47D cells and AnaAto treatment in T47D cells further induced significantly higher CD63 IPA than Anastrozole alone (Fig 3.5: C2 & Fig 3.8: C2).

In interval 4, whole blood exposed to AnaAto-treated MCF7 cells induced significantly lower CD62p IPA in comparison to untreated- and Ato-treated MCF7 cells (Fig 3.5: D2 & Fig 3.7: D2). Furthermore Ato-treated MCF7 cells induced a significantly lower CD62p IPA than that induced in untreated whole blood but significantly higher than in untreated MCF7 cells (Fig 3.5: D2 & Fig 3.7: D2). CD62p IPA in AnaAto- and Ato-treated T47D cells was generally very low and in AnaAto-treated T47D cells, it was significantly lower than in untreated T47D cells (Fig 3.5: D2 & Fig 3.7: D2). Whole blood exposed to AnaAto-treated MCF7 cells induced significantly higher CD63 IPA compared to untreated MCF7 cells (Fig 3.5: D2 & Fig 3.8: D2), and T47D cells at matched treatment (Fig 3.8: D2). Ato-treated T47D cells induced significantly higher CD63 IPA than untreated T47D cells (Fig 3.5: D2 & Fig 3.8: D2).

3.3.1.5 Platelet activation results summary

Total IPA did not reveal distinct differences in platelet activation induced by treatment and we found that when platelet activation was assessed within interval, more distinct differences were observed. In summary, CD62p IPA levels were low at interval 1, reaching its peak in interval 2 and gradually dropped interval 3 and 4. CD63 IPA was low across all treatment groups in interval 1 and 2 and increased in interval 3 and 4. In interval 3 and 4, no distinct differences in CD63 IPA were observed between the treatment groups and cell lines. This suggests that platelets at these intervals were at higher stages of activation, whereby CD63 levels are higher, possibly due to its role in mediating finals events of platelet activation such as fibrinolysis (Ghoshal and Bhattacharyya, 2014). This may also be attributed to the various source of CD63, including microparticles which were observed in the ECM.

Ana-treatment induced higher CD62P IPA in T47D cells than MCF7 cells across all intervals; however, CD63 IPA was higher in MCF7 cells than T47D cells across all intervals and MCF7

cells displayed more activated platelet phenotype, thus suggesting that Anastrozole modulated higher platelet activation in MCF7 cells than T47D cells.

AnaAspClop-treatment generally induced higher levels of CD62p IPA than AspClop in both cell lines across all intervals (with exception of AspClop treatment in T47D cells at interval 2), thus suggesting that combined Anastrozole and AspClop may promote a more hypercoagulable state. In addition, this treatment induced higher CD63 IPA in MCF7 cells than T47D cells, thus modulated higher platelet activation in MCF7 cells than T47D cell.

AnaAto-treatment showed no differences in CD62p IPA and CD63 IPA in both cell lines in interval 1, a similar finding for Ato-treatment was found. In interval 2; CD62p IPA was higher in AnaAto-treated MCF7 cells than T47D cells, whereas no difference in CD63 IPA was observed between both cell lines. The Ato control at Interval 2, revealed CD62p IPA and CD63 IPA were higher in Ato-treated T47D cells than MCF7 cells. At interval 3 and 4, CD62p IPA was lower in both cell lines compared to the Ato control. In contrast, CD63 IPA was higher in T47D cells than MCF7 cells at Interval 3, whereas at Interval 4 it was higher in MCF7 cells than T47D cells. These findings suggest that AnaAto-treatment modulated higher platelet activation in MCF7 cells whereas Ato treatment modulated higher platelet activation in T47D cell. Thus further highlighting the differential response to treatment with AnaAto and Ato.

3.3.1.6 Assessment of $CD62p^{+}/CD63^{+}$ events on $CD41a^{-}$ events

In scatterplots showing the gating strategy, in quadrant 4 (Q4), blood components that were $CD41^{-}$ were identified as expressing either CD62p or CD63 (Figs 3.4: A1-3). These blood components are likely microparticles or exosomes, evidence of which was represented in the micrographs (Figs 3.4, 3.6, 3.9: A1-3). The source of microparticles or exosomes is blood components and possibly breast cancer cells (transmitted to blood during blood and cell co-

incubation). These vesicles are known to contain some of the substances contained in platelet granules, including CD62p and CD63. In addition studies have shown that exosomes have a high expression of CD63 in their membranes and due to their small size (in comparison to other vesicles such as platelet microparticles) tend to be more numerous and thus may have contributed to the increased levels of CD63 seen in quadrant 4 (Figs 3.4: A1-3) (Tao, Guo and Zhang, 2017; Hikita *et al.*, 2018; Kaur *et al.*, 2018).

3.3.1.7 The relationship (correlation) between CD62p and CD63

In an attempt to understand the mechanism of platelet activation a Spearman correlation was used to determine whether there was a linear relationship between CD62p and CD63. A regression analysis was also conducted which was indicated by r^2 value in order to determine to what extent the linear relation was influenced by the changes observed in each marker. A Spearman correlation showed that overall (Q3), there was a moderate relationship between CD62p IPA and CD63 IPA (r=0.5726) and this was significant. The regression analysis value was low (r^2 =0.3278), indicating a weak overall relationship between CD62p and CD63 IPA.

At intervals 1 and 2, there was a strong correlation (r=0.8-1) seen between CD62p and CD63 IPA in all controls (except blood exposed to DMSO treated MCF7 cells), but this correlation was only significant for whole blood exposed to untreated T47D cells (Table 3.2). Other treatment groups generally presented with a low to moderate correlation between CD62p and CD63 IPA (Table 3.2). The regression analysis (r^2) value showed that CD62p and CD63 IPA from untreated whole blood and whole blood exposed to untreated MCF7 cells were moderately influenced by each other (r=0.51-0.79). Whereas for whole blood exposed to untreated T47D cells, there was a strong correlation between CD62p and CD63.

At interval 3 (I3), a strong positive correlation (r>0.51-0.79) between CD62 and CD63 IPA was observed in all controls; however, this was significant in untreated whole blood and whole blood exposed to T47D cells (untreated and DMSO treated) (Table 3.2). The regression analysis (r^2) values obtained showed that in these groups more than 85% of the variation in CD62p and CD63 IPA was co-dependant. In whole blood exposed to both cell lines (MCF7 and T47D) a strong, positive correlation was observed, it was significant in T47D cells. The regression analysis showed that more than 80% of the variance in CD62p and CD63 IPA was co-dependent (Table 3.2). A strong positive correlation was seen in whole blood exposed to MCF7 and T47D cells treated with AnaAspcClop (significant for the MCF7 group) and AspClop (significant for T47D group) (Table 3.2). Regression analysis (r^2) showed that the levels of CD62p and CD63 moderately depended on each other (r^2 % > 50%).

In interval 4 (I4) a strong positive correlation between CD62p and CD63 IPA was observed in all treatment groups and this was significant (except for whole blood exposed to untreated-MCF7 cells, Anastrozole-treated and AnaAspClop-treated T47D cells) (Table 3.2). The regression analysis showed strong co-dependancy (r^2 % > 50%) between CD62p and CD63 IPA at all treated groups (Table 3.2).

In summary, at early intervals (1 and 2) whereby the amount of CD62p and CD63 IPA was low to moderate, the expression of these markers was independent of each other and the regression analysis showed that the markers had less of an influence on each other. At late intervals (3 and 4), whereby CD63 IPA was found to be higher than CD62 IPA (Figs 3.5, 3.6, 3.9), there was a higher correlation between CD62p and CD63 IPA and the relationship was dependant as shown by high regression values. This suggests that when platelets were highly activated, the levels of activation markers such as CD62p and CD63 are directly dependant on

each other as opposed to when moderate amounts of activation markers are present. In general there was a positive correlation between CD62p and CD63 IPA suggesting that when one increases so does the other; however, in interval 1 and 2 (where most platelets were found) this linear correlation was independent of each individual marker (Table 3.2) and may have been influenced by other underlying factors such as the rate of platelet activation or intensity of activating stimuli. In later intervals 3 and 4 (relatively where fewer but highly activated platelets where found) there was a strong positive correlation between CD62p and CD63 and the linear relationship observed was dependant on each other. The apparent loss of CD62p as indicated by generally lower CD62p IPA may have been related to the role of this marker in adhesion, and thus its levels were lower than that of CD63.

Table 3.2: The relationship between CD62p and CD63 IPA represented by Spearman correlation value (r) and corresponding regression analysis (r^2). r-values between 0-1 represent the strength of the linear relationship; 0-0.5=weak, 0.51-0.79=moderate, 0.8-1=strong. $p<0.05$ significance for Spearman correlation. A strong correlation and regression was found between CD62p and CD63 at late intervals.

Treatment group	Interval 1				Interval 2				Interval 3				Interval 4			
	Spearman correlation value (r)	p-value	r^2	Percentage of varience r^2 (%)	Spearman correlation value (r)	p-value	r^2	Percentage of varience r^2 (%)	Spearman correlation value (r)	p-value	r^2	Percentage of varience r^2 (%)	Spearman correlation value (r)	p-value	r^2	Percentage of varience r^2 (%)
UT WB	0.80	0.0559	0.64	64	0.94	0.0046	0.89	89.12	0.96	0.0018	0.93	93.06	0.98	0.0006	0.96	96
UT MCF7+WB	0.78	0.0654	0.61	61	0.54	0.2716	0.29	28.87	0.79	0.0599	0.63	62.88	0.76	0.0784	0.58	58
UT T47D+WB	0.92	0.0095	0.85	85	0.85	0.0328	0.72	71.94	0.95	0.0035	0.91	90.54	1.00	0.0000	0.99	99
DMSO MCF7+WB	0.48	0.3394	0.23	23	0.61	0.1953	0.38	37.63	0.77	0.0724	0.60	59.51	0.95	0.0041	0.90	90
DMSO T47D+WB	0.71	0.1177	0.50	50	0.72	0.1095	0.51	51.27	0.93	0.0066	0.87	87.01	0.97	0.0016	0.94	94
Ana MCF7+ WB	0.77	0.0744	0.59	59	0.51	0.2961	0.27	26.50	0.92	0.0097	0.84	84.38	0.81	0.0493	0.66	66
Ana T47D+ WB	0.48	0.3319	0.23	23	0.50	0.3138	0.25	24.89	0.91	0.0108	0.84	83.55	0.71	0.1152	0.50	50
AnaAspClop MCF7+WB	-0.04	0.9341	0.00	0	0.34	0.5064	0.12	11.73	0.83	0.0432	0.68	68.09	0.85	0.0340	0.71	71
AnaAspClop T47D+WB	0.58	0.2291	0.33	33	-0.25	0.6277	0.06	6.43	0.67	0.1458	0.45	44.82	0.77	0.0718	0.60	60
AspClop MCF7+WB	0.75	0.0882	0.56	56	0.70	0.1244	0.48	48.48	0.71	0.1128	0.51	50.63	0.99	0.0001	0.98	98
AspClop T47D+WB	0.41	0.4225	0.17	17	0.56	0.2438	0.32	31.80	0.85	0.0302	0.73	73.02	0.88	0.0193	0.78	78
AnaAto MCF7+WB	0.70	0.1238	0.49	49	0.54	0.2651	0.30	29.53	0.91	0.0106	0.84	83.64	0.98	0.0004	0.97	97
AnaAto T47D+WB	0.31	0.5455	0.10	10	0.38	0.4588	0.14	14.36	0.65	0.1608	0.42	42.48	0.90	0.0142	0.81	81
Ato MCF7+WB	0.10	0.8478	0.01	1	0.12	0.8178	0.01	1.49	0.25	0.6254	0.06	6.48	0.93	0.0075	0.86	86
Ato T47D+WB	0.53	0.2763	0.28	28	0.39	0.4454	0.15	15.17	0.81	0.0511	0.65	65.48	0.85	0.0337	0.72	72

3.4 Discussion

Hypercoagulation results from factors that create suitable conditions for blood clotting to occur and thus facilitates thromboembolic disorders (Lipets and Ataullakhanov, 2015). These factors include thrombin generation, platelet activation and secretion of procoagulant substances (such as tissue factor, ADP) (Sehgal and Storrie, 2007; Zhang *et al.*, 2017a). The relationship between breast cancer and thrombosis is well established; and a mutual beneficial relationship exists between cancer cells and blood components whereby there is secretion of factors that promote cancer survival and concomitantly, hypercoagulation (Meikle *et al.*, 2017; Zhang *et al.*, 2017; Papaxoinis *et al.*, 2018). Furthermore, cancer therapy including commonly used hormone-therapy agents in post-menopausal women (Anastrozole) are known to further increase the risk of thrombosis (Cuzick, Sestak, *et al.*, 2014; Kemp *et al.*, 2014; Plantureux *et al.*, 2018). Antiplatelet therapy is an effective treatment for thromboembolic disorders and is commonly used clinically for thromboembolic disorders associated with the cardiovascular system (Olivier *et al.*, 2013; Moschonas, Goudevenos and Tselepis, 2015); however, it is not used clinically as standard therapy to target cancer-associated thromboembolic disorders. This study thus hopes to shed some light on its potential efficacy against cancer-associated hypercoagulation.

Platelet activation initiates the process of thrombosis which ultimately leads to thrombus formation which is characterised by platelet aggregation and this process involves coagulation factors such as thrombin which catalyse the formation of fibrin from fibrinogen for clot stabilisation (Tripodi, 2016; He *et al.*, 2019). In the current study, hypercoagulation was first illustrated in whole blood exposed to untreated cells (MCF7 and T47D) whereby thrombin generation was increased compared to untreated blood and the index of platelet activation for CD62p and CD63 was high in relation to whole blood only. This supports previous studies

which show that breast cancer increases the risk of thrombosis (Meikle *et al.*, 2017; Zhang *et al.*, 2017; Papaxoinis *et al.*, 2018).

Anastrozole treatment heightened the innate capacity of MCF7 cells to induce hypercoagulation by increasing thrombin concentration in whole blood; complementing another study in our laboratory which showed similar findings; however, at higher concentrations of Anastrozole (Pather *et al.*, 2019). In T47D cells, Anastrozole treatment reduced detectable thrombin levels in whole blood and this may be related to the reciprocal interaction between cells and blood components. Thrombin binds to PAR receptors which are expressed on platelets and breast cancer cells (Yang *et al.*, 2009; Sun *et al.*, 2019), and thus the reduced thrombin detection in T47D cells could indicate the preferential binding of thrombin to PAR receptors on T47D cells. The PAR1 receptors have been shown to facilitate a number of processes which promote cancer survival, invasion, migration and metastasis (Even-ram *et al.*, 2001; Kamath, Meydani and Foss, 2001; Yang *et al.*, 2009), and as such could indicate that T47D cells have a higher propensity for survival in comparison to MCF7 cells. Additionally, this may further suggest that T47D cells may be more responsive than MCF7 cells, since these cell lines express generally equal and low levels of PAR1 receptors (Kamath, Meydani and Foss, 2001).

The Anastrozole treatment in both cell lines also heightened hypercoagulation by activating platelets, a precursor for thrombosis, as illustrated by differential expression of platelet activation markers CD62p and CD63 with corresponding platelet morphology which indicated mixed morphology but mainly early stages of activation. Platelets are multifunctional cells and thus display heterogeneity in their responses (Kempton *et al.*, 2005; Baaten *et al.*, 2018; Swieringa *et al.*, 2018). It has been hypothesized that platelets also display heterogeneity

within a growing thrombus which is illustrated by highly aggregated platelets in the inner core and loosely attached platelets in the outer shell (Munnix *et al.*, 2009; Swieringa *et al.*, 2018). Thus, platelets associated with the inner core would display less detectable selectins such as CD62p due to their involvement in adhesion, whereas platelets in the outer shell would express high levels of CD62p and CD63 in order to facilitate further activation, recruitment and aggregation of platelets (Swieringa *et al.*, 2018).

Oestrogen has been shown to protect against cardiovascular disease and thus Anastrozole use increases the risk of thrombosis by reducing oestrogen levels through inhibiting aromatase enzyme (Cuzick *et al.*, 2014; Wang *et al.*, 2016; Matthews *et al.*, 2018). Our study supports this finding in that following Anastrozole treatment in breast cancer cells there was no reduction in platelet activation.

Thereafter the ability of antiplatelet therapies to reduce hypercoagulatory effects of Anastrozole was investigated. Aspirin and clopidogrel cocktail is commonly used to treat cardiovascular diseases (Moschonas, Goudevenos and Tselepis, 2015; Smeda *et al.*, 2018). This antiplatelet cocktail is more effective because it targets two platelet activation pathways; Aspirin reduces the production of platelet agonist, thromboxane A2 by inhibiting COX enzymes (Leonardi *et al.,* 2012; Lian *et al.*, 2013) whereas Clopidogrel inhibits P2Y12 receptors which bind platelet agonist, ADP (Passacquale and Ferro, 2011; Stalker *et al.,* 2012) and thus the inclusion of this cocktail to Anastrozole was anticipated to have more pronounced inhibitory effects on hypercoagulation.

However, the addition of AspClop cocktail to Anastrozole increased hypercoagulation in both cell lines by increasing the amount of thrombin availability in whole blood; however, thrombin levels were higher in whole blood exposed to MCF7 cells than T47D cells. In contrast, Aspirin

and Clopidogrel cocktail alone, minimally reduced thrombin levels induced by MCF7 cells but increased that induced by T47D cells.

An assessment of platelet activation revealed differential expression of platelet activation markers with higher levels of CD63 than CD62p in both cell lines thus illustrating the prolonged expression of CD63. The levels of detectable CD62p reduced when platelets adhered to each other but this was not an indication of less activation but rather the release of this marker during the activation process to more advanced stage (Augustine *et al.*, 2016), whereas CD63 remained detectable at advanced stages of platelet activation due to its role in mediating platelet recruitment and fibrinolysis (Baaten *et al.*, 2018; Haemmerle *et al.*, 2018b). The corresponding morphological features showed platelets at early and late stages of activation (Thon and Italiano, 2012; Stalker *et al.,* 2012; Tomaiuolo, Brass and Stalker, 2017) reflecting the heterogeneity of platelet activation and more microparticles were observed with this treatment and thus may have further increased levels of CD63 detected (Maia *et al.,* 2018).

This finding suggests that the antiplatelet cocktail; Aspirin and Clopidogrel minimised the amount of platelet activation induced by modulating breast cancer cells such that they become less susceptible to inducing activation in whole blood. This effect was seemingly higher in T47D cells than MCF7 cells. It is interesting to note that the addition of Anastrozole to the Aspirin and Clopidogrel cocktail increased CD62p and CD63 IPA in comparison to Aspirin and Clopidogrel cocktail alone, although these APT-drugs target different platelet activation pathways, the inability of Aspirin and Clopidogrel cocktail to reduce platelet activation when combined with Anastrozole suggests that Anastrozole may play a role in modulating the activity of Aspirin and Clopidogrel. This is likely facilitated through drug metabolism pathways;

Anastrozole inhibits the aromatase enzyme also known as CYP2C19 (Bruno and Njar, 2007; Jia *et al.*, 2016; Cuzick *et al.*, 2020). This enzyme is also involved in the conversion of Clopidogrel to its active metabolite (Roden and Stein, 2009; Sangkuhla *et al.,* 2010), therefore the inhibition of CYP219 by Anastrozole also inhibits the activity of Clopidogrel and thus platelet activation continues unabated.

Atopaxar targets a different platelet activating pathway, by blocking PAR1 receptors and thus preventing thrombin binding (Capodanno, Ferreiro and Angiolillo, 2013). Thrombin is the most potent platelet agonist and when unbound in blood remains a risk factor for blood clotting (Jennings, 2009; Denslow *et al.*, 2017; Baaten *et al.*, 2018). The risk of hypercoagulation was higher when Atopaxar was added to Anastrozole; there were higher thrombin levels in whole blood exposed to AnaAto-treated MCF7 cells than T47D cells at matched treatment. In contrast, when cells were treated with Atopaxar only, thrombin levels slightly reduced thus suggesting that Atopaxar was unable to overcome hypercoagulatory effects of Anastrozole in the drug cocktail; however, when used alone it may; although not entirely, reduce hypercoagulation. This supports its role in cardiovascular disease (Tello-Montoliu *et al.*, 2011; Costopoulos *et al.,* 2013).

Assessment of platelet activation revealed that Anastrozole-mediated platelet activation was not prevented by the addition of Atopaxar, despite blocking thrombin receptor-activating peptides (TRAP) and thrombin-mediated platelet aggregation (Kogushi *et al.*, 2011a), CD62p and CD63 remained high. Platelets displayed features of early activation and more abundant microparticles, especially in the MCF7 cell group. Even though Atopaxar is a direct inhibitor of PAR1 receptors (Tello-Montoliu *et al.*, 2011; Olivier *et al.*, 2013; Pan, Boucher and Kaunelis, 2016), it did not entirely prevent platelet activation, despite some reduction in levels of CD62p

and CD63, platelet activation continued with morphology corresponding to early and late stages of activation. Thus, while platelet aggregation may be limited, platelets were activated such that growth factors and angiogenic factors may be released and thus could impact tumour progression (Bambace and Holmes, 2011; Yu *et al.*, 2014; Elaskalani *et al.*, 2017).

3.5 Conclusion

In conclusion, preconditioned breast cancer cell lines to hormone therapy (Anastrozole) and antiplatelet therapy (Aspirin and Clopidogrel cocktail and Atopaxar) did not prevent hypercoagulation as shown by thrombin levels in whole blood and activated platelets. The higher thrombin levels in MCF7 cells suggest increased risk of hypercoagulation, whereas the lower thrombin levels in T47D cells suggest that this cell line binds more thrombin directly through its PAR receptors in order to promote tumour survival. Platelet activation revealed that CD63 IPA was generally higher than CD62p IPA and this could facilitate consistent signalling as it is postulated that CD63 facilitates cell communication, although it is unknown for which specific pathways. Due to its stable expression, it is likely to be involved in a wide range of signalling pathways such as those involved in migration, cellular communication, fibrinolysis. Lower levels of CD62P IPA when coupled with consideration of the morphological changes confirm the presence of platelet activation and also reflect its diversity/heterogeneous nature.

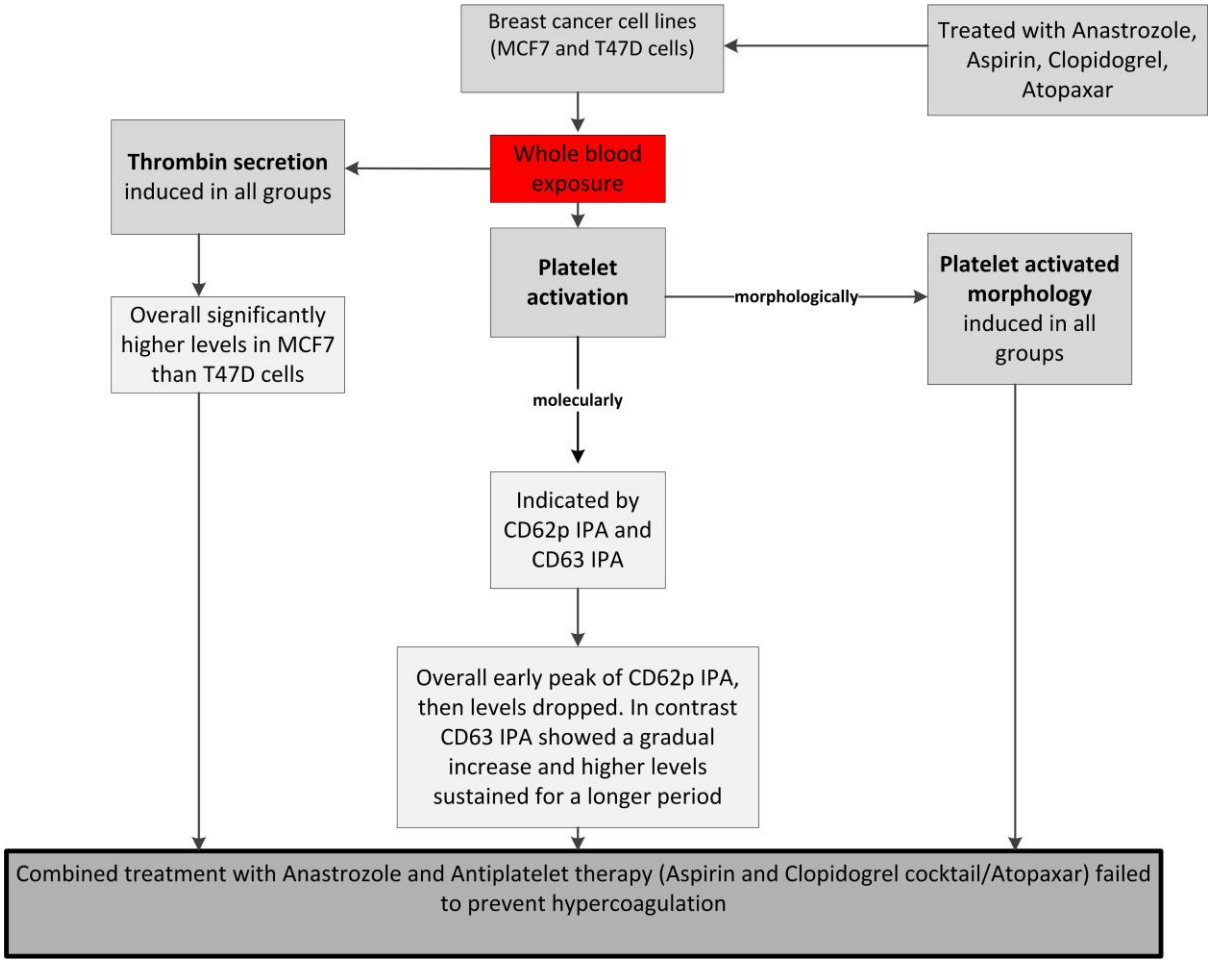


Figure 3.10: An overview of chapter 3 and summary of key findings.

Chapter IV: Reciprocal interactions between vascular components and breast cancer cells in facilitating tumour progression

4.1 Introduction

4.1.1 Epithelial to Mesenchymal transitions during tumour progression

The tumour microenvironment (TME) provides a physiological milieu for facilitating various processes related to tumour such as initiation, progression, metastasis, recurrence and drug resistance because it contains blood vessels, lymphatic vessels, extracellular matrix components, immune cells, and cell-derived exosomes (Gallego-Muñoz *et al.*, 2018;Waldron *et al.*, 2019). Various factors including cytokines and growth factors are also secreted into the TME in order to facilitate epithelial to mesenchymal transition (EMT), and angiogenesis (Guo and Deng, 2018). EMT is an versatile process that mediates physiological and pathological events through controlling cell migration and differentiation (Zarzynska, 2014; Li *et al.*, 2017). Type I EMTs facilitate trans-differentiation during development under normal physiological conditions (Nieto, 2011), they are also associated with dissemination of wound healing and tissue fibrosis (Moustakas and Heldin, 2016).

Cancer is facilitated by type II EMTs which facilitate invasion and metastatic dissemination (Kalluri, 2010). All EMTs are controlled by developmental pathways such as Notch, hedgehog, Wnt, nuclear receptor and transforming growth factor β (TGFβ) (Moustakas and Heldin, 2007; Xu and Lamouille, 2009; Wang *et al.*, 2016). TGFβ pathway is the main mediator of cancer-associated EMT and is activated by cytokine secretion (Xu and Lamouille, 2009; Wang *et al.*, 2016; Moustakas and Heldin, 2016).

TGFβ is well known for its dichotomous role in cancer initiation whereby it acts as a tumour suppressor at early stages of tumour and inhibits proliferation in epithelial cells (Zhang, 2017).

This role changes during advanced stages of cancer whereby it promotes EMT and facilitates tumour growth and progression. The Smad transcription factors are the main effectors responsible for facilitating downstream signalling following TGFβ receptor activation (Kubiczkova *et al.*, 2012; Lee and Schiemann, 2014; Zhang, 2017). TGFβ and its isoforms are secreted into the ECM, and following activation binds onto TGFβ type I or II receptors which subsequently phosphorylate Smad 2 and Smad 3, which in turn bind to and forms a complex with Smad 4. All Smad pathways intercept at Smad 4 and form a complex that associates with the nucleus and activates transcription in the nucleus; this subsequently activates downstream signalling pathways such as AKT and ERK (Xu and Lamouille, 2009; Kubiczkova *et al.*, 2012; Poniatowski *et al.*, 2015).

TGFβ receptors also signal through non-Smad dependant/non-canonical method which includes mitogen-activated protein kinase (MAPK) pathways, c-Jun amino terminal kinase (JNK), P38 MAPK, IkB kinase (IKK), PI3K and AKT and Rho family GTPases (Parvani, Taylor and Schiemann, 2010, 2011). The non-Smad signalling inducers function independently or may associate with Smads to transduce signals (Moustakas and Heldin 2005). TGFβ non-canonical signalling is said to be responsible for the oncogenic signalling of TGFβ during tumour initiation (Parvani, Taylor and Schiemann, 2010, 2011). TGFβ promotes EMT in Smad-dependant and independent pathways (Lee and Schiemann, 2014; Zhang, 2017).

EMT is characterised by complete or partial loss of epithelial differentiation which involves changes in the cellular adherence junctions whereby E-cadherin is lost, notwithstanding that EMT can occur without loss of E-cadherin and levels of N-cadherin increase (Yadav and Shankar, 2019). The loss of adherent proteins during EMT is also coupled with changes in the cytoskeleton which reflect actin polymerisation, and destabilisation of the adherens junction

facilitates cells movement (Thiery *et al.,* 2009; Lee and Schiemann*,* 2014). EMT facilitates migration and invasion (Thiery *et al.*, 2009; Yadav and Shankar, 2019). Cross-talk between TGFβ signalling pathway engages other signalling pathways inducing the secretion of PDGF, EGF and other cytokines (Nieto, 2011).

Partial loss of EMT markers has been shown (Yadav and Shankar, 2019) and this may facilitate different modes of migration such as collective streaming whereby cells migrate collectively, thus no loss of E-cadherin would occur despite presence of cell migration (Jolly *et al.*, 2016). Hybrid epithelial-mesenchymal phenotype characterises stemness and is a marker of poor prognosis (Strauss *et al.*, 2011; Grosse-Wilde *et al.*, 2015). A conversion from EMT to mesenchymal to epithelial transition (MET) is associated with reduced invasion as tumours settle at distant site and begin to differentiate (Moen *et al.*, 2009). MET was shown to occur following metastasis and colonisation of a secondary site (Moen *et al.*, 2009; Aleskandarany *et al.*, 2014; Jolly *et al.*, 2016). This indicates cellular adaptation to a new site and promotes proliferation (Aleskandarany *et al.*, 2014; Jolly *et al.*, 2016). Suppression of TGFβ signalling promotes formation of MET which re-programmes cells (Moen *et al.*, 2009; Aleskandarany *et al.*, 2014; Jolly *et al.*, 2016).

During complete-EMT, transformed epithelial cells acquire features of mesenchymal cells and thus become more migratory, invasive, resistant to apoptosis and secrete more ECM components (Thiery *et al.*, 2009; Raghu Kalluri, 2010; Wendt *et al.,* 2011). These changes are associated with a poor prognosis (Araki *et al.*, 2011; Aleskandarany *et al.*, 2014; Mrozik *et al.*, 2018). Changes associated with EMT include the loss of epithelial markers such as E-cadherin and an upregulation of mesenchymal markers such as vimentin and N-cadherin (Zeisberg and Neilson, 2009). Cancer cells can also undergo a partial-EMT which exhibits features of both

epithelial and mesenchymal phenotypes and is more aggressive and chemoresistant than each phenotype individually (Jolly *et al.*, 2015, 2017).

E- and N-cadherin belong to a group of Ca^{2+} -dependant proteins known as cadherins (Loh *et al.*, 2019). Collectively cadherins act as adhesion proteins and also mediate important developmental processes such as morphogenesis and differentiation (Stemmler, 2008; Vestweber, 2015). Cadherins typically consists of a single span transmembrane domain and five extracellular cadherin repeat domains (Colás-Algora and Millán, 2019). The extracellular domain is responsible for communication and cell signalling and the cytosolic domain, which interacts with the cytoskeleton through its association with catenins, thus facilitates phenotypic changes associated with cell migration and differentiation (Aleskandarany *et al.*, 2014; Seddiki *et al.*, 2018).

E-cadherin is a marker for an epithelial phenotype and regulates homeostasis through various signalling pathways (Aleskandarany *et al.*, 2014; Rosso *et al.*, 2017). During EMT, E-cadherin is lost and this is linked with the expression of transcription factors which facilitate EMT (Onder *et al.*, 2008; Viloria-Petit and Wang, 2010). There is conflicting evidence regarding the necessity of E-cadherin for EMT to occur, most studies suggest that loss of E-cadherin is a defining feature of EMT; however, other studies have shown evidence of EMT occurring without loss of E-cadherin (Hollestelle *et al.*, 2013; Chen *et al.*, 2014; Nilsson *et al.*, 2014). Furthermore, the loss of E-cadherin during EMT has been linked to poor prognosis and more aggressiveness (Nilsson *et al.*, 2014; Hu *et al.*, 2016). The switch between E-cadherin and N-cadherin is often used as an indicator for EMT (Halbleib and Nelson, 2006; Loh *et al.*, 2019).

N-cadherin is mainly abundant in neuronal tissue whereby it not only forms strong adhesions between cells but regulates proliferation and differentiation (Paik *et al.*, 2004; Blaschuk,

2015); however, it is also aberrantly expressed in cancer cells undergoing EMT and is associated with poor prognosis (Hulit *et al.*, 2007; Wang *et al.*, 2016; Cao *et al.,* 2019). N-cadherin has been shown to indicate metastasis and tumour invasion by promoting collective migration (Klymenko *et al.,* 2017; Waldron *et al.*, 2019), binding to FGFR (Hulit *et al.*, 2007) and associating with the wingless-related integration site (Wnt) signalling pathway (Zhang *et al.*, 2013; Aleskandarany *et al.*, 2014; Su *et al.*, 2016). Breast cancer patients were found to have higher levels of soluble N-cadherin, which was also able to bind to fibroblast growth factor receptor, thereby promoting angiogenesis (Derycke *et al.*, 2006; Hulit *et al.*, 2007; Waldron *et al.*, 2019).

Another important EMT-associated protein is vimentin, a small (57kDa) protein which forms type II intermediate filaments, and is typically found in mesenchymal cells whereby it maintains cell and tissue integrity (Liu *et al.*, 2015). Vimentin has been shown to replace cytokeratin, a marker of epithelial phenotype, in malignant breast cancer and its expression is thus associated with invasive potential (Thompson and Newgreen, 2005; Liu *et al.*, 2015). MCF7 and T47D cell lines represent invasive ductal carcinoma cells (Tasdemir *et al.*, 2018); while vimentin expression was shown to be higher in invasive ductal carcinoma subtype, these cell lines tend to have much lower levels due to their low metastatic profile (Liu *et al.*, 2015). Vimentin expression assists invasion and leads to poor prognosis (Satelli and Li, 2011; Lehtinen *et al.*, 2013). The increased expression of vimentin and N-cadherin, and a loss of epithelial markers such as E-cadherin, represent a more mesenchymal phenotype and may be a mechanism to facilitate metastasis in cancer (Blaschuk, 2015; Liu *et al.*, 2015). During metastasis cells detach from the primary tumour, intravasate into blood vessels and travel through the blood stream. These circulating tumour cells interact with platelets to evade

immune detection and for protection against high velocity forces (Fuentes *et al.,* 2016; Chen *et al.*, 2018). Platelets also assist tumour cells in extravasation from the bloodstream at secondary sites which they then colonise (Guan, 2015). Thus tumour cells undergo various phenotypic changes, facilitated by cell-cell communication in order to mediate the various steps of tumour progression (Huang *et al.*, 2017).

4.1.2 Cytokine mediated communication during tumour progression

Cell communication is an important factor during malignancy and this is facilitated by cytokines and other chemical factors, adhesion molecules and MMPs (Rudolph and Freeman, 2009). These cytokines are broadly categorised as pro- or anti-inflammatory (New and Aikawa, 2011). TNFα, IL-1β, IL-6 and IL-8 are among pro-inflammatory cytokines whereas IL-2, IL-4, IL-10, IL-13, and TGFβ are anti-inflammatory (Marik and Flemmer, 2012). Under normal physiological conditions a fine balance is maintained between pro- and anti-inflammatory cytokines, this balance is disturbed during disease states (Du and Tan, 2014). The tumour microenvironment plays an important role in facilitating EMTs and tumour cells will secrete various proinflammatory cytokines and growth factors which will further promote this process (Guo and Deng, 2018). A positive feedback mechanism is involved in the production of cytokines and following the right stimuli, will promote biochemical cascades including thrombosis (Frangogiannis, 2008). Thus within the tumour microenvironment, cytokine secretion not only signals cancer survival but also the development of thromboemboli to facilitate platelet-associated tumour progression (Fuentes *et al.,* 2016; Chen *et al.*, 2018).

The history of cytokine discovery begins with Larco and Todaro who were the first to identify a compound named the sarcoma growth factor in 1978 (Larco and Todaro, 1978). This compound was later identified to consist of two compounds TGFβ and TGFα (Poniatowski *et*

al., 2015). Transforming growth factor beta (TGFβ) is classified as belonging to a group of cytokines forming a "growth factor network" due to the fundamental role they play (Poniatowski *et al.*, 2015). The TGFβ superfamily consists of various regulatory polypeptides such as the TGFβ isoforms (1, -2, -3), bone morphogenetic protein (BMP), inhibins, and activins (Poniatowski *et al.*, 2015). The different isoforms of TGFβ are encoded by specific genes; however, they show structural and functional homogeneity, but heterogeneity in their affinity for the TGFβ receptor (Hachim *et al.*, 2018). These isoforms show TGFβ plays an important role in the normal physiology and pathology of the mammary gland (Panis *et al.*, 2013; Poniatowski *et al.*, 2015). During disease states, such as cancer, functional heterogeneity in the TGFβ isoforms is evident (Hachim *et al.,* 2018).

In early stage tumours, TGFβ1 prevents tumour progression by activating the Smad signalling pathway(Pang *et al.*, 2016); however, TGFβ promotes tumour progression in later stages of cancer, and it is associated with poor prognosis in ER^+ breast tumours (Panis *et al.*, 2013; Poniatowski *et al.*, 2015). TGFβ1 mainly facilitates processes such as cell motility, tumour invasion, and EMT-mediated metastasis (Padua and Massagué, 2009; Araki *et al.*, 2011). *In vitro,* TGFβ1 was shown to induce invasion in breast cancer cells (Padua and Massagué, 2009; Araki *et al.*, 2011). TGFβ2 is mainly involved during tumourigenesis whereby it promotes cell proliferation and suppresses immune surveillance (Hachim *et al.*, 2018). TGFβ3 mainly facilitates EMT, and together with TGFβ1 is predominantly associated with progression of hormone-dependent breast tumours (ER^+, PR^+) (Hachim *et al.,* 2018). TGFβ2 is primarily associated with hormone-independent breast (ER) tumours) and basal tumours show a higher expression of TGFβ1 and TGFβ2 mRNA whereas TGFβ3 expression is higher in luminal-A tumours (Hachim *et al.,* 2018).

Various other cytokines play important functions within the tumour microenvironment. IL-6 and VEGF promote metastasis in breast cancer (Nagasaki *et al.*, 2014). TGFα binds the epidermal growth factor receptors to promote regeneration of tissue, and bone homeostasis (Xian, 2007; Bhuminder Singh, 2014). Its increased levels are associated with tumour initiation of the breast, stomach and bone (Coffey *et al.*, 2007). TNFα has diverse roles which are determined by other inflammatory mediators (Pircher *et al.*, 2012). It has been shown to promote cell death, proliferation, differentiation and migration (Pircher *et al.*, 2012). The associated pro-inflammatory condition promotes thrombosis (Pircher *et al.*, 2012). PDGF (consist of various isoforms) promotes cell growth and motility in various cell types (Andrae *et al.,* 2008). PDGF isoforms mediate their functions by binding to their receptors PDGFRα and PDGFRβ (Heldin, 2013). Breast cancer cells show high expression of PDGF and its receptors which facilitate tumour progression and invasion (Heldin, 2013). PDGF alongside VEGF and TGFβ also promote angiogenesis (Strande and Phillips, 2009; Liu *et al.*, 2018). PDGF-BB was shown to promote migration and angiogenesis (Pinto *et al.*, 2014).

Angiogenesis is a process describing new blood vessel formation occurring under normal physiological conditions (Li *et al.*, 2014; Plantureux *et al.*, 2018). Angiogenesis also occurs in disease states and it is associated with EMT during cancer progression (Huang *et al.*, 2017; Guo and Deng, 2018). Cells secrete proangiogenic factors such as PDGF, VEGF in order to promote and enhance this process (Tesfamariam, 2016; Huang *et al.*, 2017; Plantureux *et al.*, 2018; Schlesinger, 2018). Blood vessels form an important part of the TME by supplying oxygen and nutrients and thus enhance tumour growth and invasion (Liu *et al.*, 2018). PDGF promotes proliferation in MCF7 cells in a pathway not dependant on oestrogen (Farooqi and Siddik, 2015). Instead it binds to its receptors located on breast cancer cells (Pinto *et al.*,

2014). PDGF can direct mesenchymal cells to a secondary site by acting as a potent chemo-attractant and mitogen (Heldin *et al.,* 2018). In addition to providing access to the haematological system for metastasis; tumour cells are able to engage with intratumoural platelets as well as with platelets within and outside of the vasculature and to induce platelet activation and aggregation for signalling for tumour survival (Li *et al.*, 2014; Costa *et al.*, 2019).

In illustrating the important role that the interaction between platelets and cancer plays in mediating cancer progression and thrombosis, some studies have assessed the impact of antiplatelet therapy. Aspirin, a NSAID, was shown to be associated with reduced risk of breast cancer (Maity *et al.*, 2015). Furthermore, metastasis was inhibited in an animal model treated with low-dose aspirin by disrupting cancer and platelet interaction (Guillem-Llobat *et al.*, 2016). Low-dose aspirin also prevented the occurrence of EMT *in vitro* and when combined with a P2Y12 antagonist, it also reduced platelet-induced metastasis in lung cancer, these effects were mediated through its prevention of platelet aggregation (Guillem-Llobat *et al.*, 2016). Aspirin combined with Clopidogrel was also shown to reduce cancer risk in various cancers (Leader *et al.*, 2017).

Tumour growth rate and metastasis was reduced in mice with pancreatic cancer, following daily use of Clopidogrel (Mezouar *et al.*, 2015); however, Clopidogrel has also been associated with promoting cancer progression despite some pre-clinical studies which show antiplatelet therapy reduces cancer progression (Denslow *et al.*, 2017; Ballerini *et al.*, 2018; Smeda *et al.*, 2018). Dual APT in mice with breast cancer with Aspirin and Clopidogrel was shown to prevent thrombosis but promoted vascular mimicry in the primary tumour (Smeda *et al.,* 2018). Vascular mimicry is a process occurring independently of angiogenesis and involves the formation of vascular networks by aggressive tumour cells displaying stem cell properties and

it is commonly associated with metastasis (Fouad and Aanei, 2017; Fernandez-Cortes, Delgado-Bellido and Oliver, 2019). While the direct role of PAR receptors in mediating EMT has not been shown, it is proposed that PAR antagonists may be promising agents against PAR-induced EMTs and while little is known about the direct effects of Atopaxar on cancer, varopaxar (a PAR-1 inhibitor) has shown beneficial effects against PAR-1 mediated EMT and metastasis (Moschonas, Goudevenos and Tselepis, 2015). Thus, these studies show that while some effects of these drugs are known regarding their effect on tumours, there is still a gap in our knowledge specifically regarding the direct effect of Anastrozole combined with Aspirin and Clopidogrel cocktail and/ Atopaxar.

Due to the established association between hypercoagulation and tumour progression (Xu *et al.*, 2019), it is important to investigate whether antiplatelet therapy used in a tumour setting combined with hormone therapy for breast cancer would affect cancer outcome, specifically in light of the interaction with vascular components. In this chapter we outline some of the changes occurring in cells that may explain disease status such as cancer progression by specifically looking at whether co-incubation of treated breast cancer cells with vascular components promotes epithelial to mesenchymal transition (EMT) and also investigate some of the secreted factors that might promote cancer progression within the cancer microenvironment.

4.1.3 Aims and objectives

The aim of this chapter was to investigate whether the reciprocal interactions between Anastrozole and antiplatelet therapy (Aspirin and Clopidogrel/ Atopaxar)-treated breast cancer cells (MCF7 and T47D) and blood components, promote tumour progression through epithelial to mesenchymal transitions and alterations of the inflammatory profile.

The **objectives** of this study were:

1. To investigate **gene expression** of *E-cadherin*, *N-cadherin*, *Vimentin* and *TGFβ1* in breast cancer cell lines treated with hormone and antiplatelet therapy and exposed to whole blood
2. To investigate the levels of **cytokines secreted** in whole blood exposed to hormone and antiplatelet therapy-treated breast cancer cells and relate them to tumour processes which promote survival

4.2 Materials and methods

4.2.1 Gene expression using real-time qPCR

Cell treatment, lysis and storage

Cells were treated with 1X Cmax concentrations of Anastrozole (Ana), Anastrozole and Aspirin and Clopidogrel cocktail (AnaAspClop), Aspirin and Clopidogrel cocktail alone (AspClop), Anastrozole and Atopaxar (AnaAto) and Atopaxar alone (Ato) for 24 hours as previously stated (Chapter II, section 2.2.3). Then exposed to whole blood for 5 mins as stated previously (Chapter III, section 3.2.2.1); cells were subsequently rinsed in PBS (pH 7.4) thrice. RNA extraction was conducted using the Qiagen RNeasy kit (Qiagen, cat no. 74104) and manufactures guidelines were followed. Following blood exposure to cells, whole blood was snap-frozen in liquid-nitrogen and stored in the -80°C fridge for ~7-8 months prior to cytokine analysis being conducted. Corresponding cells were rinsed thrice in PBS and lysed with 350µl of buffer RLT (containing beta-mercaptoethanol) using a 22 gauge needle. Three wells were pooled for each treatment groups (starting cell number >150000). The lysed cell homogenate was stored at -80°C until further RNA extraction (~6-7 months).

RNA extraction

The lysed cell homogenate (350 µl) was thawed and 350 µl of 70 % ethanol added to the lysate and mixed by pipetting. 700 µl of the lysate was transferred into an RNeasy spin column, and centrifuged at 10000 rpm for 30 sec. The flow-through was discarded and the collection tube reused for the following steps:

On column DNase digestion: 350µl of RW1 buffer was added to the RNeasy spin column and centrifuged at 10000 rpm for 15 sec. Then 80 µl of DNase I incubation mixture (containing 10 µl DNase I stock solution and 70 µl buffer RDD) was added to the RNeasy spin column, and

left at RT (20-25 °C) for 15 mins. 350 µl of RW1 buffer was added to the RNeasy spin column, centrifuged at 10000 rpm for 15 sec and the flow-through was discarded.

Wash steps and elution: 500 µl of RPE buffer was added to the RNeasy spin column, centrifuged at 10000 rpm for 15 sec, and flow-through discarded. The step was repeated, but centrifugation time increased to 2 mins. The RNeasy spin column was placed in a new collection tube and, centrifuged at full speed for 1 min. RNA was eluted into 30 µl RNase-free water in a new collection tube by centrifugation of the spin column at 10000 rpm for 1 min. This step was repeated using the same eluate, in order to increase yield of RNA eluted. The RNA was immediately stored at -80 °C. RNA concentration and purity was measured using the NanoDrop 2000. RNA concentration was differentially affected in both cells lines by different treatments, and AspClop treatment reduced RNA concentration the most; however, RNA purity was found to be above 2 for all treatment groups (Appendix C1). RNA integrity was not conducted for the purpose of this study; however, it will be conducted prior to publication of this data as per MIQE guidelines (Taylor *et al.*, 2019).

cDNA preparation

Complementary deoxyribonucleic acid (cDNA) was prepared using the High Capacity Reverse Transcription kit (4368814, Applied Biosystems) according to the manufacturer's guidelines. The mastermix containing 10X RT buffer, 25X dNTP mix, 10X RT random primers, multiscribe RT and nuclease-free water was mixed with RNA to a ratio of 1:1. The tubes were centrifuged for 30 sec 1000 xg, then placed in a thermal cycler model at specific temperatures (Appendix C1.3) to make cDNA.

qPCR preparation

Primers were designed on the Eurofins website (www.eurofinsgenomics.com) then validated using the oligoanalyzer tool on the IDT website (www.idtdna.com). A primer blast was conducted on Pubmed (www.ncbi.nlm.nih.gov) for further validation and authentication of the primers (Table 4.1).

Table 4.1 Primer sequences used for quantitative real-time polymerase chain reaction (qPCR).

Gene	Primer sequence (5'-3')	Accession number
ACTB (Reference gene)	**F:** GGC CGA GGA CTT TGA TTG CAC **R:** TTA GGA TGG CAA GGG ACT TCC TGT	NM_001101.3
RPLO (Reference gene)	**F:** TGC AGC TGA TCA AGA CTG GAG ACA **R:** TCC AGG AAG CGA GAA TGC AGA GTT	BC001834.2
GAPDH (Reference gene)	**F:** TGC ACC ACC AAC TGC TTA GC **R:** GGC ATG GAC TGT GGT CAT GAG	NM_002046.5
TGFβ-1	**F:** 5'-CTCGCCAGAGTGGTTATCTT-3' **R:** 5'-AGTGTGTTATCCCTGCTGTC-3'	NM_000660.7
Vimentin	**F:** 5'-CCT CTT CCA AAC TTT TCC TCC-3' **R:** 5'-CGT TGA TAA CCT GTC CAT CTC-3'	NM_003380.5
CDH1	**F:** 5'-TTC CTC CCA ATA CAT CTC CC-3' **R:** 5'-TTG ATT TTG TAG TCA CCC ACC-3'	NM_004360.5
CDH2	**F:** 5'-CAT CAT TGC CAT CCT GCT C-3' **R:** 5'-TCT TCT TCT CCT CCA CCT TC-3'	XM_017025514.2

The PCR reaction was prepared in duplicate for six volunteers to a final volume of 10 µl (SPL096150, ThermoFischerScientific) and each well within a piko plate (ThermoFisher, Fairland, South Africa, cat no.SPL096150) contained: RNase-free water, 10 µM forward primer, 10 µM reverse primer, 2 ng cDNA and 2X SYBR green (A25742, applied Biosystems). The qPCR reaction was conducted for 40 cycles in the (PikoReal Real-Time PCR System, Thermo Fisher), thermocycler conditions in Appendix C1.4.

Data analysis

The fold change in gene expression was calculated as outlined in (Hellemans *et al.*, 2007). The fold change represents the expression ratio of the gene of interest in relation to the untreated

control. First an average of the biological repeats was obtained, then the following formulae were applied to obtain fold change in gene expression:

1. **Geometric mean of the reference genes**:= $\sqrt{\ }(Ave\ Ref\ gene\ 1) * (Ave\ Ref\ gene\ 2) * (Ave\ Ref\ gene\ 3)$
2. $\mathbf{\Delta Cq} =$ Cq(Gene of interest) - Avg Cq (Geometric mean of reference genes)
3. **ΔCq Expression** = $(-\Delta Cq)^2$
4. **ΔΔCq =**ΔCq(Gene of interest)-ΔCq(Control)
5. **Fold Change** = $(-\Delta\Delta Cq)^2$

Thereafter the mean of the fold change was calculated and missing data or outliers were imputed, provided missing values were not 50% or more of the whole data set (Goni, García and Foissac, 2009). The data were subsequently analysed in PAST 13 statistical software using the Friedman test and corresponding Post hoc (Wilcoxon) in order to determine whether mRNA levels for *E-cadherin*, *N-cadherin, vimentin and TGFβ1* were altered by in breast cancer cells in response to treatment with Anastrozole combined with antiplatelet therapy (Aspirin and Clopidogrel/ Atopaxar) and subsequent exposure to whole blood. See Appendix C2.1-2.5.

4.2.4 Cytokine assays

4.2.4.1 Sample acquisition and preparation

The whole blood collected from seemingly healthy female volunteers (Chapter III, section 3.2.1.2 and 3.2.1.3) was exposed to the treated cells for 5 mins as stated previously (Chapter III, section 3.2.2.1). Whole blood, along with conditioned media from controls which had been stored at -80°C was thawed at RT prior to being used to determine cytokine expression levels.

4.2.4.2 Inflammation panel

Panel: Two separate plates containing different combination panels of cytokines were used: IL1β, TNF-α, PDGF-AB (R&D Systems, Inc., Minneapolis, MN, cat no. LXSAHM-03, Lot:

L127797) and IFN-β1, IL6, PDGF-BB, VEGF-A, IL4, IL10, TGF-α (R&D Systems, Inc., Minneapolis, MN, cat co. LXSAHM-07, Lot: L126911).

Solution preparation: The following solutions were prepared prior to conducting the assay and were stored protected from light. The microparticle cocktail was prepared by sonicating the vial for 30 sec then adding 5 ml of RD2-1 buffer to the vial containing 500 µl of microparticles. The biotin antibody cocktail was prepared by firstly spinning the vial containing this antibody for 30 sec, then adding 5 ml RD2-1 buffer to 500 µl biotin antibody. The streptavidin-PE (SA-PE) cocktail was prepared by spinning the vial for 30 sec, then 35 ml wash buffer was added to 220 µl SA-PE. Standards were prepared as stated in Appendix C3.1.

Assay: 50 µl of each blood sample or standard and 50 µl of the microparticle cocktail were added to each well in a 96 well plate, sealed in foil and incubated at RT on a shaker (800±50 rpm) for 2 hrs. The plate was placed on a magnetic device and the contents discarded. Wells were rinsed (3 times) by adding 100 µl wash buffer. 50 µl of biotin antibody cocktail was added to each well, the plate was sealed with foil and incubated at RT on a shaker (800±50 rpm) for 1 hr. The plate was again placed on a magnetic device, the contents discarded, and wells rinsed (3 times) by adding 100 µl wash buffer. Then 50 µl of streptavidin-PE was added to each well, the plate was sealed with foil and incubated at RT on a shaker (800±50 rpm) for 30 mins. The plate was placed on a magnetic device, the contents discarded, and wells rinsed (3 times) by adding 100 µl wash buffer. The microparticles in each well were then re-suspended in 100 µl of wash buffer and incubated at RT for 5 mins on a shaker (800 ± 50 rpm). Cytokine levels were measured using a Bio-Plex 200 analyzer.

4.2.4.3 TGFβ isoforms detection

Panel: The plate contained the following: TGFβ -1, -2, -3 (Bio-Plex Pro ™ TGF-β Panel 3-Plex, Bio-Rad Laboratories, Inc., Hercules, CA, cat no. 171W40001M).

Solution preparation: The following solutions were prepared prior to conducting the assay, and stored protected from light. The wash buffer was diluted by adding 540 ml distilled water to 60ml wash solution concentrate (10X). The coupled beads were prepared by sonicating the vial in which they were contained for 30 sec then adding 5472 µl of assay buffer to 288 µl of coupled beads. Detection antibodies were prepared by vortexing the vial in which they were contained for 15 sec then adding 2850 µl detection antibody diluent to 150 µl detection antibody. The streptavidin-PE was prepared by vortexing the vial for 5 sec and adding 5940 µl assay buffer to 60 µl streptavidin-PE.

Assay: Blood samples/culture media or standards were first activated by adding 5 µl of 1 N HCl to 25 µl of the sample and incubating at RT for 10 mins. Then 5 µl of 1.2 N NaOH/0.5 M Hepes was added to neutralise the reaction and the sample diluted by adding 365 µl of Bio-Plex sample diluent. To conduct the assay, 50 µl of coupled beads was added to each well. The plate was placed on a magnetic device, the contents discarded and wells rinsed (2 times) by adding 100 µl wash buffer. 50 µl of the activated sample was added to each well, the plate was sealed in foil and incubated at RT for 2 hrs on a shaker (850±50 rpm). The plate was placed on a magnetic device, the contents were discarded and the wells were rinsed (2 times) by adding 100 µl wash buffer. 25 µl of detection antibodies were added to each well, the plate sealed with foil and incubated for 1 hr at RT on a shaker (850±50 rpm). Again, the plate was placed on a magnetic device, the contents discarded and the wells rinsed (3 times) by adding 100 µl wash buffer. 50 µl streptavidin-PE was added to each well, the plate sealed with foil and incubated at RT for 30 mins in a shaker (850±50 rpm). The plate was again placed on a magnetic device, followed by discarding of contents and rinsing of wells (3 times) by adding 100 µl wash buffer. The beads attached to the surface of the plate were resuspended in 125

µl of assay buffer, sealed and incubated for 5 min at RT on a shaker (850±50 rpm). Cytokine levels were measured in the Bio-Plex 200 analyzer.

Data analysis: Data were managed in Microsoft Excel 2010, the mean for each group was calculated, where values were missing data was imputed but only if the total number of values present were greater than or equal to 50% of the total values for the groups. The blank control did not detect any cytokine levels; therefore, raw data was used in subsequent analysis without removing the blank control values. Values which fell below the lower limit of quantification as shown in Table 4.2 could not be quantified. Statistical analysis was conducted using PAST13 statistical software. Friedman's test and corresponding post hoc (Wilcoxon) test were used to determine whether there were differences in cytokine levels in whole blood exposed to treated (Ana, AnaAspClop, AspClop, AnaAto, Ato) breast cancer cells (MCF7 and T47D cells). See Appendix C3.2-3.5.

Table 4.2 The assay working range is presented below and delineates the range at which cytokine levels were detected by the assay. Values obtained from product specification sheets; Human Magnetic Luminex Assays, cat. no LXSAHM-03, Lot no. L127797, cat no. LXSAHM-07, lot no. L126911 and Bio-Plex Pro TGFβ 3-Plex cat no. 10024984 and lot no. 64130734.

	Assay working range	
Cytokines tested	**Lower limit of quantification (LLOQ) (pg/ml)**	**Upper limit of quantification (ULOQ) (pg/ml)**
IFN-β	1.3	2800
IL-1β	1.8	3950
IL-10	0.4	900
IL-6	0.3	730
TNFα	0.9	2050
TGFα	0.7	1640
TGFβ3	1.1	17128
IL-4	1.5	3380
VEGF-A	0.8	1970
TGFβ2	1.2	18925
PDGF-AB	2.5	5380
TGFβ1	1.6	26688
PDGF-BB	1.4	3140

4.3 Results

4.3.1 Gene expression to elucidate epithelial to mesenchymal transition

Genes encoding for proteins involved in EMT were investigated in order to elucidate the effects of treatment with hormone and antiplatelet therapy, and exposure to whole blood on breast cancer cells. Baseline expression levels of each gene were indicated in cells exposed to culture media only and used as a reference point to establish fold change in gene expression (Fig 4.1).

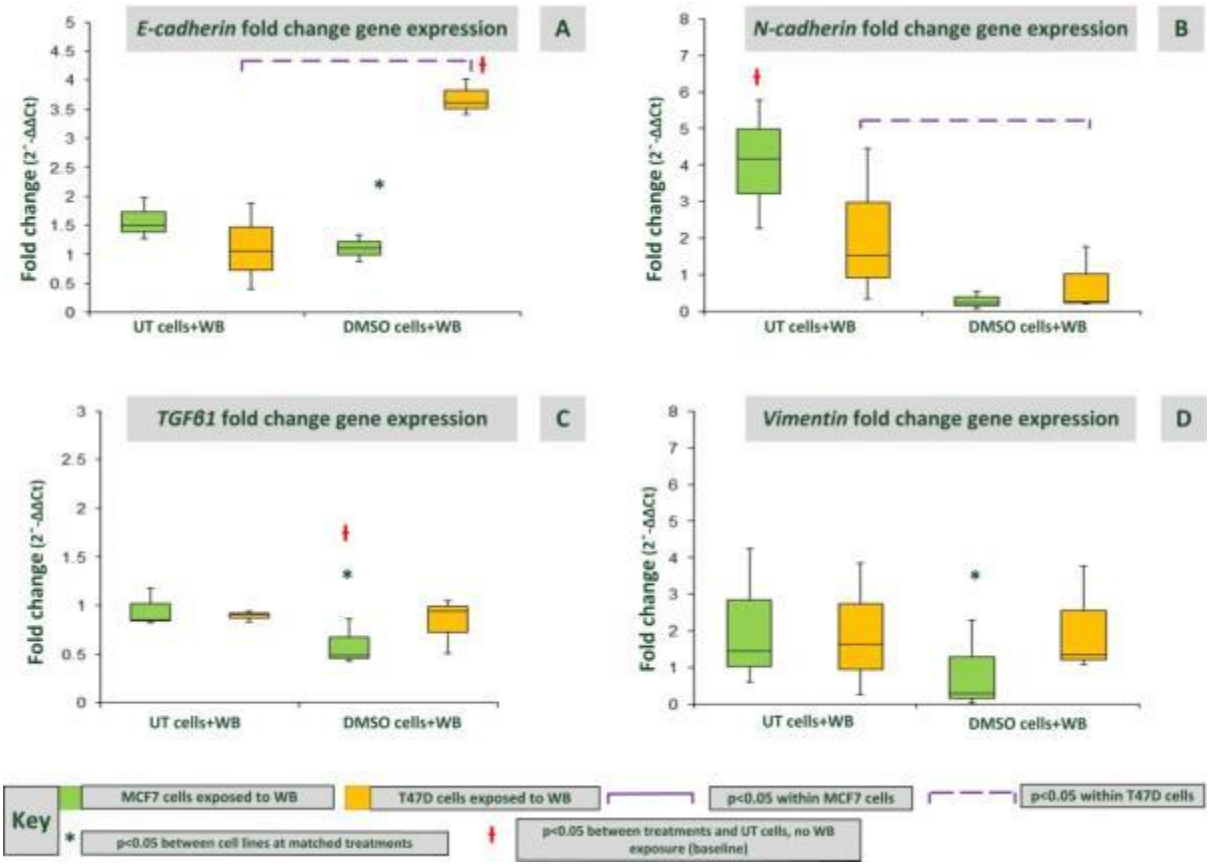


Figure 4.1 Gene expression of EMT markers in controls A) *E-cadherin*, B) *N-cadherin*, C) *TGFβ-1*, and D) *Vimentin* in MCF7 and T47D cells in culture media (UT) and diluent (DMSO) exposed to whole blood (WB). Gene expression from cells exposed to culture media only was used as a baseline to establish fold change. Following blood exposure, *E-cadherin* was unchanged in MCF7 cells but upregulated in DMSO-treated T47D cells compared to baseline. *N-cadherin* was upregulated in both untreated MCF7 and T47D cells following exposure to whole blood. Following blood exposure, *TGFβ1* and *vimentin* were downregulated in DMSO-treated MCF7 cells but remained unchanged in both untreated MCF7 and T47D cells compared to baseline.

4.3.1.1 Gene expression in controls

Following exposure to blood, untreated and diluent-treated cells showed variability in gene expression. *E-cadherin* expression was upregulated in untreated and DMSO-treated MCF7 cells exposed to WB, albeit not significant (Fig 4.1: A); however, expression was significantly upregulated in T47D cells treated with DMSO, than untreated T47D cells, and MCF7 cells at matched treatments (Fig 4.1: A). Thus, showing that whole blood did not significantly alter the epithelial phenotype in untreated cells; however, consideration to DMSO must be given as the diluent control. Conversely, *N-cadherin* was significantly upregulated in untreated MCF7 cells exposed to whole blood. In both cell lines exposed to WB, *N-cadherin* was higher in untreated-cells than in DMSO-treated cells; this was significant in T47D cells ($p<0.05$) (Fig 4.1: B). This indicates that even though epithelial features were maintained there was a gradual increase in mesenchymal phenotype and DMSO did not induce more pronounced effects than media only. Corresponding assessment of the mesenchymal marker, vimentin, revealed no significant changes, despite being raised compared to baseline, in the untreated group of both cell lines exposed to blood (Fig 4.1: D); however, *vimentin* expression was significantly downregulated in DMSO-treated and whole blood-conditioned MCF7 cells than T47D cells at matched treatments (Fig 4.1: D). *TGFβ1* expression in untreated cell lines (MCF7 and T47D) exposed to whole blood, was comparable ($p>0.05$) (Fig 4.1: C). *TGFβ1* was downregulated in MCF7 cells following treatment with DMSO ($p<0.05$) and it was significantly lower than in T47D cells at matched treatment (Fig 4.1: C).

4.3.1.2 Gene expression in breast cancer cells treated with Anastrozole exposure to whole blood

When cells were treated with Anastrozole and subsequently exposed to whole blood, the following changes in gene expression for EMT markers were observed MCF7 cells did not alter *TGFβ1* expression compared to media control (Fig 4.1: C; Fig 4.2: C). In Ana-treated T47D cells

TGFβ1 levels were slightly increased compared to medium control (Fig 4.1: C; Fig 4.2: C). When mesenchymal markers were assessed; *N-cadherin* expression levels were down regulated in both cell lines compared to media control (Fig 4.1: B; Fig 4.2: B) and *vimentin* expression levels were unaffected in both cell lines (Fig 4.1: D; Fig 4.2: D). Epithelial marker; *E-cadherin* was downregulated in MCF7 cells and upregulated in T47D cells (Fig 4.1: A; Fig 4.2: A). These findings suggest that Ana-treatment may have reduced epithelial features in MCF7 cells but promoted partial-EMT or MET in T47D cells.

4.3.1.3 Gene expression in breast cancer cells treated with Anastrozole, Aspirin and Clopidogrel and exposed to whole blood

When cells were treated with Anastrozole and Aspirin-Clopidogrel cocktail and subsequently exposed to whole blood, the following changes in gene expression for EMT markers were observed. *TGFβ1* expression was downregulated in AnaAspClop-treated cells (MCF7 and T47D) compared to Ana-treatment (Fig 4.2: C) and this was significant when compared to matched untreated cells (Fig 4.1: C & 4.2: C). When mesenchymal markers were assessed; *N-cadherin* expression levels were upregulated in both cell lines compared to Ana-treatment and this was significant in T47D cells when compared to AspClop (Fig 4.2: B), whereas *vimentin* expression was downregulated in both cell lines (Fig 4.2:D). Epithelial marker, *E-cadherin* expression was upregulated in MCF7 cells but downregulated in T47D cells (Fig 4.2: A). This finding suggests that AnaAspClop-treatment in MCF7 cells maintained epithelial differentiation, whereas in T47D cells it reduced the epithelial phenotype.

When compared to the AnaAspClop-treatment the AspClop control upregulated *TGFβ1* expression levels in both cell lines (Fig 4.2: C). *N-cadherin* expression levels were downregulated in both cell lines (Fig 4.2: B), whereas no change was seen in *vimentin* expression levels in MCF7 cells but it was downregulated in T47D cells (Fig 4.2: D). AspClop

treatment in T47D cells induced significantly lower levels of *vimentin* expression than the diluent control (Fig 4.1 & 4.2: D) and this shows that the diluent had an impact on gene expression in this cell line. Epithelial marker; *E-cadherin* expression levels was upregulated in MCF7 cells but unchanged in T47D cells (Fig 4.2: A). Thus suggesting that AspClop-treatment may increase epithelial-like characteristics in MCF7 cells and maintain the epithelial phenotype in T47D cells.

4.3.1.4 Gene expression in breast cancer cells treated with Anastrozole and Atopaxar and exposure to whole blood

When cells were treated with Anastrozole and Atopaxar and subsequently exposed to whole blood, the following changes in gene expression for EMT markers were observed. T*GFβ1* expression in AnaAto-treated cells (MCF7 and T47D) was downregulated compared to Ana-treatment (Fig 4.3: C); furthermore, it was shown to be significantly downregulated in T47D cells compared to the diluents (Fig 4.1: C; Fig 4.3: C).When mesenchymal markers were assessed; *N-cadherin* expression levels were unchanged in both cell lines compared to Ana-treatment (Fig 4.3: B), whereas *vimentin* expression levels were upregulated in MCF7 cells, but significantly downregulated in T47D cells (Fig 4.3: D). Epithelial marker; *E-cadherin* expression was upregulated in MCF7 cells but downregulated in T47D cells (significant compared to media and diluent control, and Ana-treated cell) (Fig 4.3: A). These findings suggest AnaAto-treatment maintained epithelial-like phenotype in MCF7 cells but reduced epithelial and mesenchymal features in T47D cells.

When compared to AnaAto-treatment, Ato-treatment control upregulated *TGFβ1* expression in both cell lines; however, it was significantly lower in MCF7 cells compared to diluent control (Fig 4.1: C; Fig 4.3: C). Mesenchymal markers; *N-cadherin* expression was upregulated in MCF7 cells but unchanged in T47D cells (Fig 4.3: B) whereas *vimentin* expression was downregulated

in MCF7 cells (significant when compared to diluents) but upregulated in T47D cells (albeit significantly lower compared to Ana-treatment) (Fig 4.1: D; Fig 4.3: D). *E-cadherin* expression was unchanged in Ato-treated MCF7 cells compared to Ato-treated MCF7 cells but upregulated in T47D cells at matched treatments (Fig 4.3: A); however, *E-cadherin* expression levels were significantly higher in MCF7 cells compared to diluent-treated cells, and T47D cells at matched treatment (Fig 4.1: A & Fig 4.3: A). Furthermore Ato-treated T47D cells significantly downregulated *E-cadherin* expression compared to the diluent control (Fig 4.1: A; Fig 4.3: A). These findings suggest that Ato-treatment may promote partial-EMT in both cell lines independent of E-cadherin loss.

4.3.1.4 Summary of gene expression findings

Anastrozole treatment maintained epithelial the epithelial-like phenotype in MCF7 cells and promoted partial-EMT in T47D cells. These effects were unchanged in MCF7 cells following the addition of AspClop cocktail (AnaAspClop). However, this treatment combination attenuated the epithelial phenotype in T47D cells. The antiplatelet therapy alone (AspClop), increased epithelial-like differentiation in MCF7 cells but maintained an epithelial phenotype in T47D cells. The effects of Anastrozole combined with Atopaxar (AnaAto) maintained an epithelial phenotype in MCF7 cells but reduced both epithelial and mesenchymal markers in T47D cells. When used alone Atopaxar (Ato), may promote partial-EMT while maintaining the differentiated epithelial phenotype.

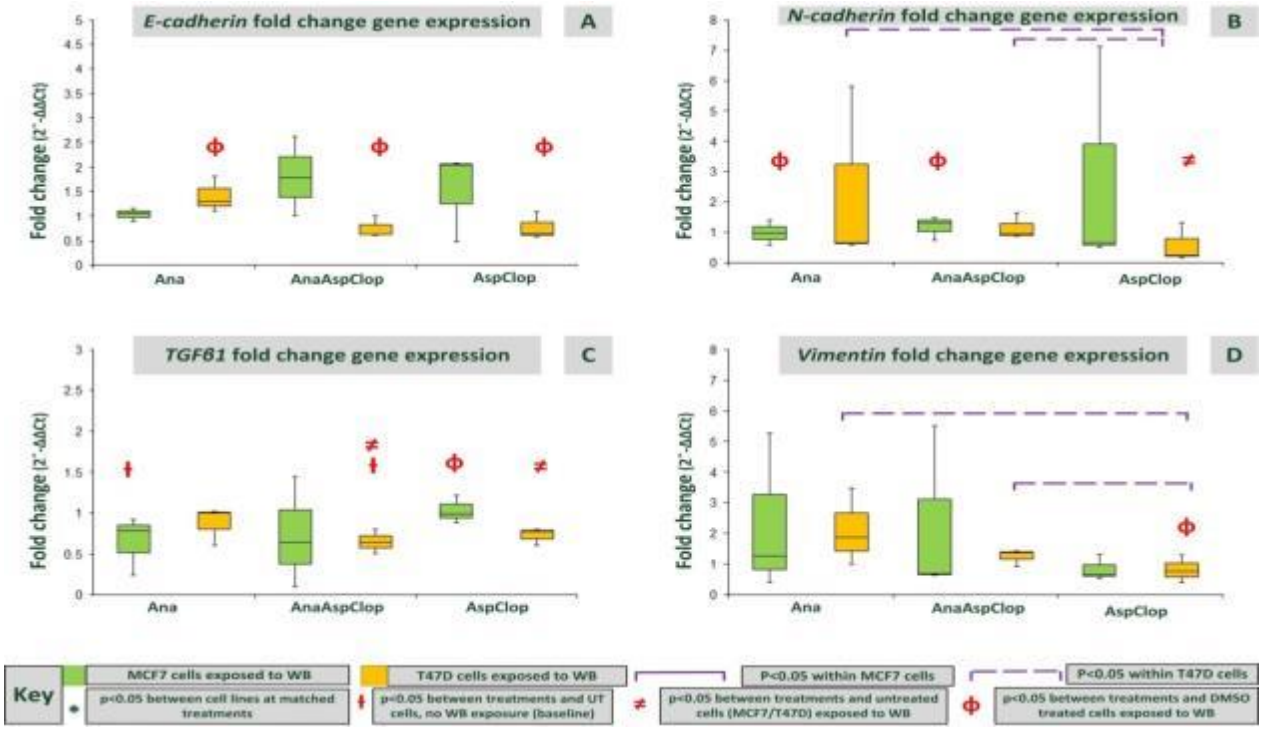


Figure 4.2 Gene expression of EMT markers in breast cancer cells (MCF7 and T47D cells) following treatment with Anastrozole (Ana), Anastrozole+Aspirin+Clopidogrel (AnaAspClop) and Aspirin+Clopidogrel (AspClop) and exposure to whole blood A) *E-cadherin*, **B)** *N-cadherin*, **C)** *TGFβ1,* and **D)** *Vimentin*. Gene expression from cells exposed to culture media only was used as a baseline to establish fold change. Following blood exposure, Ana-treatment maintained epithelial phenotype in MCF7 cells as shown by maintenance of *E-cadherin*, and low levels of *TGFβ1, N-cadherin* and *vimentin.* In T47D cells, a partial-EMT was induced as indicated by higher levels of *E-cadherin, vimentin* and *TGFβ1.* AnaAspClop treatment maintained the epithelial phenotype in MCF7 cells but reduced it in T47D cells; however, AspClop-treatment seemed to increase epithelial differentiation in MCF7 cells (by increasing *TGFβ1* and *E-cadherin* levels) and it maintained an epithelia phenotype in T47D cell.

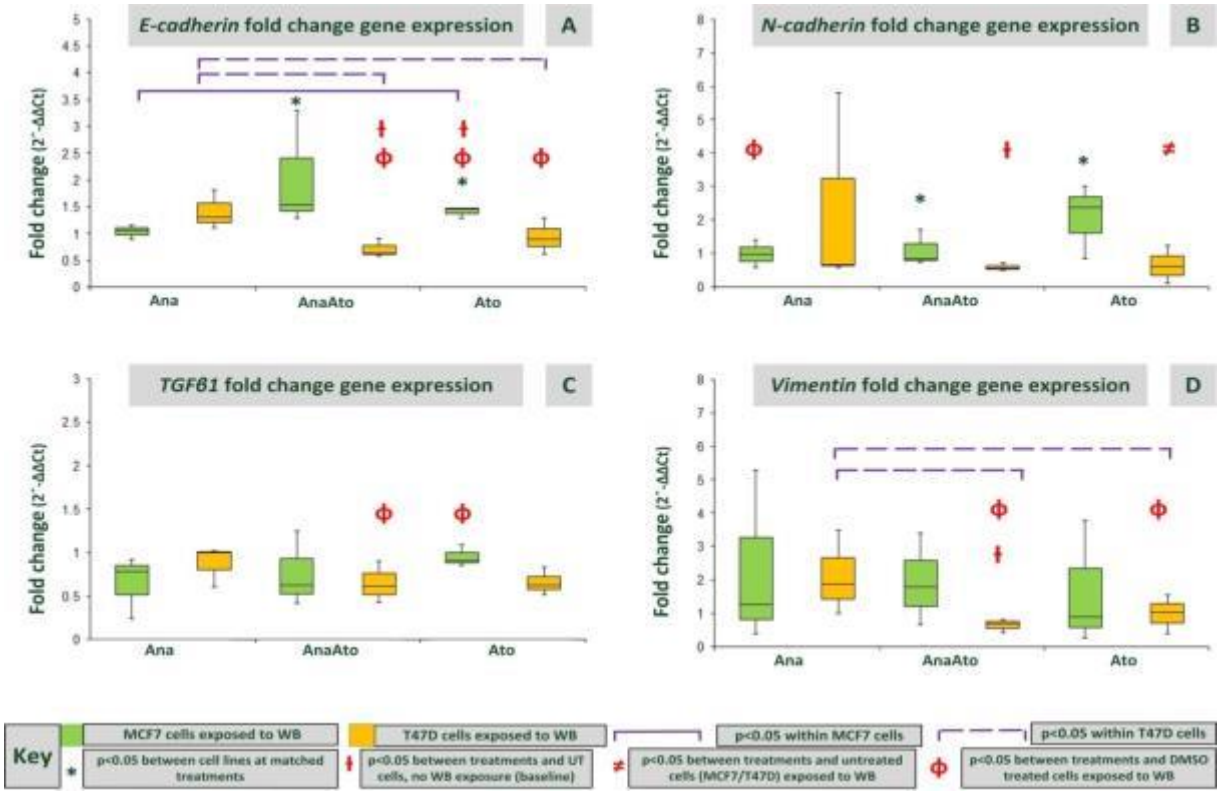


Figure 4.3 Gene expression of EMT markers in breast cancer cells (MCF7 and T47D cells) following treatment with Anastrozole (Ana), Anastrozole+Atopaxar (AnaAto) and Atopaxar (Ato) and exposure to whole blood A) *E-cadherin*, **B)** N-*cadherin*, **C)** *TGFβ1,* and **D)** *Vimentin.* Gene expression from cells exposed to culture media only was used as a baseline to establish fold change. Following blood exposure*,* AnaAto-treatment maintained epithelial-likephenotype in MCF7 cells as shown by significantly higher *E-cadherin* expression (compared to T47D cells); whereas epithelial and mesenchymal markers were downregulated in T47D cell. In contrast, Ato-treatment may induce partial-EMT by elevating *TGFβ1,* and *N-cadherin* in MCF7 cells while maintaining epithelial-like features. In T47D cells, it increased *TGFβ1* expression but maintained its phenotype*.*

4.3.3 Cytokine analysis

4.3.3.1 Overall cytokine secretion

Cytokine secretion in whole blood pre-conditioned with breast cancer cells was investigated in order to determine reciprocal interactions between breast cancer cells exposed to hormone and antiplatelet therapy and vascular components and how they may affect tumour progression. It is noteworthy that some cytokines could not be detected because they were below the limit of detection (Table 4.2); these include IL-10, IFN-β1, and IL-1β, they were thus omitted from the analyses (Appendix C, 3.2-3.5). Treatment of breast cancer cells with either Anastrozole with or without antiplatelet therapies (AspClop cocktail or Ato) or antiplatelet therapy alone showed no significant changes to the levels of cytokines tested (IL-6, TNFα, TGFα, TGFβ3, IL-4, VEGF-A, TGFβ2, PDGF-AB, TGFβ1 and PDGF-BB). The concentration of each cytokine was quantified and overall (across all treatment and in both cell lines) there were relatively low to moderate levels of (in ascending order); IL-6, TNFα, TGFα, TGFβ3, IL-4 (Table 4.3-4.4) and relatively moderate to high levels of (in ascending order); VEGF-A, TGFβ2, PDGF-AB, TGFβ1 and PDGF-BB (Table 4.5 & 4.6). It is noteworthy that while some of the cytokines tested generally displayed relatively low levels, upon thorough assessment, it was evident that some fluctuations in their levels was induced by various treatments thus suggesting that treatment was effective in modulating their levels, despite the lack of significance which may be a factor of the small sample size.

Treatment with Anastrozole alone or combine with antiplatelet therapy produced no significant change in the cytokines secreted within each cell line and no differences between cell lines were observed at each treatment. However, an overall assessment of cytokine secretion between cell lines showed that the level of TGFα and PDGF-AB were significantly

higher in T47D cells than MCF7 cells. The overall trend observed in cytokine secretion will be discussed below, in all cases $p>0.05$.

Table 4.3 Detected cytokine levels (ng/ml) in whole blood following exposure to breast cancer cells treated with Anastrozole (Ana), Anastrozole+Aspirin+Clopidogrel (AnaAspClop) and Aspirin+Clopidogrel cocktail (AspClop). The table shows levels of cytokines detected in ascending order. Cytokine secretion in both cell lines followed a similar pattern and while the concentration of these cytokines was generally lower, the drug treatment showed some effect in modulating cytokine secretion. AnaAspClop generally reduced Ana -mediated increase of IL-6, TNFα, TGFβ3 and IL-4 in MCF7 cells and a similar effect was induced for IL-6 and TGFβ3 in T47D cells. Furthermore, T47D cells, increased IL-4, TNFα, and TGFα. AspClop treatment in MCF7 cells increased the levels of TNFα, TGFβ3 and IL-4 but reduced IL-6 and TGFα. In T47D cells AspClop treatment reduced the levels of TNFα, TGFα and IL-4 but increased the level of IL-6 and TGFβ3. This highlights that Anastrozole modulates the effects of AspClop.

Treatment group	IL-6 (ng/ml)		TNFα (ng/ml)		TGFα (ng/ml)		TGFβ3 (ng/ml)		IL-4 (ng/ml)	
WB	0.58 ± 0.50		1.76 ± 0.70		1.70 ± 0.89		12.79 ± 7.01		31.97 ± 4.96	
	MCF7	**T47D**	**MCF7**	**T47D**	**MCF7**	**T47D**	**MCF7**	**T47D**	**MCF7**	**T47D**
Media	0.38 ± 0.19	0.65 ± 0.32	1.42 ± 0.81	1.76 ± 0.70	2.09 ± 0.22	2.81 ± 0.67	14.34 ± 12.31	14.01 ± 1.11	23.63 ± 7.75	22.17 ± 14.85
Diluent	0.56 ± 0.39	0.56 ± 0.39	2.74 ± 1.39	1.76 ± 0.70	2.63 ± 0.59	2.72 ± 0.62	21.13 ± 12.71	17.60 ± 6.72	35.15 ± 2.58	28.34 ± 7.80
Ana	0.65 ± 0.40	0.60 ± 0.20	1.76 ± 0.70	1.76 ± 1.00	2.15 ± 0.90	2.57 ± 1.74	16.65 ± 10.10	19.39 ± 10.16	34.74 ± 11.48	30.44 ± 12.74
AnaAspClop	0.52 ± 0.19	0.49 ± 0.30	1.16 ± 0.55	2.98 ± 1.79	2.25 ± 1.03	2.85 ± 1.53	6.67 ± 6.61	17.35 ± 10.74	25.44 ± 7.02	36.38 ± 9.25
AspClop	0.38 ± 0.33	0.52 ± 0.23	2.01 ± 0.82	1.75 ± 1.40	2.03 ± 1.20	1.76 ± 0.80	11.16 ± 4.08	29.94 ± 21.93	37.87 ± 6.90	27.21 ± 10.25

Table 4.4 Detected cytokine levels (ng/ml) in whole blood following exposure to breast cancer cells treated with Anastrozole (Ana), and Atopaxar (Ato). The table shows levels of cytokines detected in ascending order. Cytokine secretion in both cell lines followed a similar pattern and while the concentration of these cytokines was generally lower, the drug treatment showed some effect in modulating cytokine secretion. Ato reduced Ana -mediated increase of IL-6, and TNFα, in MCF7 cells but reduced the rest of the cytokines. In T47D cells, Ato-treatment reduced Ana-mediated increase of IL-6, TGFβ3, and IL-4 but increased (TNFα and TGFα). AnaAto treatment in MCF7 cells increased the levels of TGFα TGFβ3 and IL-4 but reduced IL-6 and TNFα. In T47D cells AnaAto treatment reduced the levels of IL-6, TGFβ3 and IL-4, but increased the level of TNFα, and TGFα. This highlights that Anastrozole modulates the effects of AspClop.

Treatment group	IL-6 (ng/ml)		TNFα (ng/ml)		TGFα (ng/ml)		TGFβ3 (ng/ml)		IL-4 (ng/ml)	
WB	0.58 ± 0.50		1.76 ± 0.70		1.70 ± 0.89		12.79 ± 7.01		31.97 ± 4.96	
	MCF7	**T47D**	**MCF7**	**T47D**	**MCF7**	**T47D**	**MCF7**	**T47D**	**MCF7**	**T47D**
Media	0.38 ± 0.19	0.65 ± 0.32	1.42 ± 0.81	1.76 ± 0.70	2.09 ± 0.22	2.81 ± 0.67	14.34 ± 12.31	14.01 ± 1.11	23.63 ± 7.75	22.17 ± 14.85
Diluent	0.56 ± 0.39	0.56 ± 0.39	2.74 ± 1.39	1.76 ± 0.70	2.63 ± 0.59	2.72 ± 0.62	21.13 ± 12.71	17.60 ± 6.72	35.15 ± 2.58	28.34 ± 7.80
Ana	0.65 ± 0.40	0.60 ± 0.20	1.76 ± 0.70	1.76 ± 1.00	2.15 ± 0.90	2.57 ± 1.74	16.65 ± 10.10	19.39 ± 10.16	34.74 ± 11.48	30.44 ± 12.74
AnaAto	0.59 ± 0.43	0.54 ± 0.30	1.56 ± 0.45	2.15 ± 1.33	2.42 ± 1.27	2.87 ± 0.89	24.83 ± 11.51	15.23 ± 6.08	35.50 ± 15.13	22.95± 11.02
Ato	0.62 ± 0.32	0.59 ± 0.57	1.16 ± 0.89	1.75 ± 1.21	2.25 ± 1.18	2.14 ± 1.13	20.78 ± 12.56	17.38 ± 9.80	25.53 ± 5.58	24.79 ± 5.82

Table 4.5 Detected cytokine levels (ng/ml) in whole blood following exposure to breast cancer cells treated with Anastrozole (Ana), and Aspirin+Clopidogrel (AspClop). The table shows levels of cytokines detected in ascending order. Cytokine secretion in both cell lines followed a similar pattern and while the concentration of these cytokines was generally lower, the drug treatment showed some effect in modulating cytokine secretion. AnaAspClop treatment in MCF7 cells reduced Ana-mediated increase in VEGF-A and PDGF-BB and reduced TGFβ1-2 and PDGF-AB, in T47D cells it reduced Ana-mediated increase of PDGF-AB and TGFβ1 and increased VEGF-A, TGFβ1 and PDGF-BB. AspClop reduced TGFβ1 in MCF7 cells but increased VEGF-A, TGFβ2, PDGF-AB and PDGF-BB. In T47D cells it increased VEGF-A, PDGF-AB and PDGF-BB and increased TGFβ1-2.

Treatment group	VEGF-A (ng/ml)		TGFβ2 (ng/ml)		PDGF-AB (ng/ml)		TGFβ1 (ng/ml)		PDGF-BB (ng/ml)	
WB	52.41 ± 22.46		665.99 ± 80.82		1071.98 ± 144.38		5094.62 ± 1176.35		8843.15 ± 2082.49	
	MCF7	T47D	MCF7	T47D	MCF7	T47D	MCF7	T47D	MCF7	T47D
Media	46.44 ± 16.91	50.86 ± 23.22	709.71 ± 96.22	647.40 ± 86.41	1178.89 ± 121.40	1201.71 ± 88.25	8329.52 ± 4403.18	5184.13 ± 1061.43	8242.33 ± 927.47	8063.06 ± 2109.16
Diluent	57.25 ± 6.15	46.72 ± 17.90	693.03 ± 162.88	646.84 ± 118.07	1140.41 ± 61.96	1100.96 ± 130.57	7876.57 ± 4366.63	6435.10 ± 2229.37	8793.52 ± 1746.22	8985.03 ± 1498.45
Ana	47.91 ± 24.01	57.79 ± 35.83	659.05 ± 131.10	658.79 ± 167.32	1144.30 ± 103.19	1066.33 ± 146.63	6579.40 ± 3858.59	6604.09 ± 4414.09	9549.37 ± 2249.90	10015.19 ± 2219.38
AnaAspClop	48.36 ± 28.05	70.05 ± 53.13	552.17 ± 166.49	694.10 ± 137.05	1105.94 ± 122.21	1046.22 ± 65.31	3807.91 ± 2405.18	6070.85 ± 2382.64	9800.83 ± 2260.73	10303.75 ± 2474.04
AspClop	55.64 ± 35.58	53.94 ± 34.29	618.29 ± 126.59	810.60 ± 99.41	1186.61 ± 176.65	1034.51 ± 137.16	3790.23 ± 1525.33	10479.57 ± 5410.47	10969.56 ± 1964.09	9702.40 ± 2477.75

Table 4.6 Detected cytokine levels (ng/ml) in whole blood following exposure to breast cancer cells treated with Anastrozole (Ana), and Atopaxar (AnaAto). The table shows levels of cytokines detected in ascending order. Cytokine secretion in both cell lines followed a similar pattern and while the concentration of these cytokines was generally lower, the drug treatment showed some effect in modulating cytokine secretion. AnaAto-treatment in MCF7 cells reduced Ana-mediated increase in PDGF-AB and increased VEGF-A, TGFβ1-2 and PDGF-BB, in T47D cells it increased PDGF-AB, TGFβ1-2, VEGF-A, and PDGF-BB. Ato-treatment reduced TGFβ1-2 and PDGF-BB in MCF7 cells but increased VEGF-A and PDGF-AB. In T47D cells, Ato-treatment decreased VEGF-A, PDGF-AB, PDGF-BB and TGFβ1-2.

Treatment group	VEGF-A (ng/ml)		TGFβ2 (ng/ml)		PDGF-AB (ng/ml)		TGFβ1 (ng/ml)		PDGF-BB (ng/ml)	
WB	52.41 ± 22.46		665.99 ± 80.82		1071.98 ± 144.38		5094.62 ± 1176.35		8843.15 ± 2082.49	
	MCF7	**T47D**	**MCF7**	**T47D**	**MCF7**	**T47D**	**MCF7**	**T47D**	**MCF7**	**T47D**
Media	46.44 ± 16.91	50.86 ± 23.22	709.71 ± 96.22	647.40 ± 86.41	1178.89 ± 121.40	1201.71 ± 88.25	8329.52 ± 4403.18	5184.13 ± 1061.43	8242.33 ± 927.47	8063.06 ± 2109.16
Diluent	57.25 ± 6.15	46.72 ± 17.90	693.03 ± 162.88	646.84 ± 118.07	1140.41 ± 61.96	1100.96 ± 130.57	7876.57 ± 4366.63	6435.10 ± 2229.37	8793.52 ± 1746.22	8985.03 ± 1498.45
Ana	47.91 ± 24.01	57.79 ± 35.83	659.05 ± 131.10	658.79 ± 167.32	1144.30 ± 103.19	1066.33 ± 146.63	6579.40 ± 3858.59	6604.09 ± 4414.09	9549.37 ± 2249.90	10015.19 ± 2219.38
AnaAto	51.71 ± 27.55	58.78 ± 39.59	794.53 ± 87.60	747.82 ± 102.42	1053.83 ± 124.57	1075.32 ± 100.50	9524.09 ± 4676.22	8666.32 ± 2333.97	10714.08 ± 2359.82	10207.93 ± 1772.20
Ato	55.02 ± 34.13	49.66 ± 30.08	762.21 ± 107.56	746.16 ± 116.18	1231.25 ± 325.43	992.82 ± 94.41	8460.73 ± 4579.92	8282.45 ± 4124.59	10651.62 ± 2390.11	9933.10 ± 2321.53

4.3.3.2 Cytokine secretion in controls

Cytokine levels in whole blood represented baseline secretion, when cytokine levels were compared to whole blood exposed to cells in media the secretion of anti-inflammatory cytokine; IL-4 and some growth factors; TNFα, VEGF-A, and PDGF-BB were reduced in both cell lines (Table 4.3-4.6). In contrast, the levels of certain growth factors; TGFα, TGFβ3, PDGF-AB, and TGFβ1 was increased (Table 4.3-4.6). Differential secretion between the cell lines was observed; the levels of pro-inflammatory cytokine IL-6 were lower in MCF7 cells than in T47D cells; however, the levels of TGFβ2 were higher in MCF7 cells but lower in T47D cells (Table 4.3-4.6).

In general, TGFβ1 and TGFβ3 had the same pattern of expression in both cell lines; whereas TGFβ2 was higher in MCF7 cells. These findings also show that while TGFα levels were generally low compared to other cytokines, its level was still increased by breast cancer cells, suggesting that TGFα plays an important role in mediating survival. These findings also suggest that baseline secretion of cytokines belonging to the platelet-derived growth factor family was higher than most cytokines, even though the PDGF-BB subtype was reduced; its levels were still higher compared to other cytokines.

When compared to baseline and medium control cytokine secretion in whole blood exposed to diluent (DMSO)-treated cells reduced pro-inflammatory marker, IL-6 in T47D cells but increased it in MCF7 cells in relation to medium control; however, it remained lower than baseline (Table 4.3-4.6). In contrast, the levels of the following growth factors were increased in both cell lines compared to baseline and media (with some exceptions); TGFα (reduced levels compared to medium in T47D cells), TGFβ3, PDGF-AB, TGFβ1 and PDGF-BB (Table 4.3-4.6). Differences between cell lines were further observed; anti-inflammatory marker, IL-4 levels remained low in T47D cells but increased in MCF7 cells, suggesting that T47D cells were

more likely to maintain pro-tumour survival environment even when exposed to DMSO and may highlight a stronger stress response or adaptation compared to MCF7 cells (Table 4.3-4.6). Furthermore the following growth factors were differentially secreted in each cell line compared to baseline and media (with some exceptions); TNFα increased in MCF7 cells but remained unaffected in T47D cells, VEGF-A was increased in MCF7 cells but decreased in T47D cells, TGFβ2 levels remained low in T47D cells but were increased in MCF7 cells compared to baseline but lower compared to medium control (Table 4.3-4.6). These findings show that TGF family (especially -β1 and -β3 subtypes were higher in MCF7 cells than T47D cell) and PDGF family (-AB and -BB subtypes) were the main mediators of survival in both cell lines.

4.3.3.3 Anastrozole-mediated cytokine secretion

Anastrozole treatment alone increased the levels of pro-inflammatory marker in both cells lines compared to baseline and media control (with exceptions); IL-6 (lower in T47D cells compared to medium control), and the following growth factors; TGFα (lower in T47D cells compared to medium control), TGFβ3, TGFβ1 (lower in MCF7 cells compared to medium control) and PDGF-BB (Table 4.3-4.6). TGFβ2 secretion was reduced by Ana treatment in both cell lines whereas TNFα was unaffected compared to baseline and media control in both cell lines (Table 4.3-4.6). Differential expression in certain markers was observed; when compared to baseline and medium control anti-inflammatory marker IL-4 remained higher in MCF7 cells than T47D cells (Table 4.3-4.6). Furthermore, growth factors; VEGF-A levels were lower in Ana-treated MCF7 cells compared to baseline but higher compared to medium control, conversely in T47D cells VEGF-A levels were higher compared to baseline and medium control and Ana-treated MCF7 cells (Table 4.3-4.6). PDGF-AB was higher in MCF7 cells compared to baseline and T47D cells at matched treatment but lower than in medium control whereas in T47D cells PDGF-AB levels were reduced compared to baseline and medium control (Table

4.3-4.6). This suggests that while Ana increased the levels of some inflammatory and growth markers, this was often not higher than levels observed in cells in medium control (especially in T47D cells). However, this treatment further increased levels of VEGF-A in both cells, even though they were higher in T47D cells. Thus, suggesting that in addition to the important role played by TGF proteins (especially -β1 and -β3 subtypes) and PDGF-BB, cells increase secretion of VEGF-A in response to Ana and may suggest tumour survival mechanism.

4.3.3.4 Aspirin and Clopidogrel-mediated cytokine secretion with or without Anastrozole

When Aspirin and Clopidogrel were added to Anastrozole (AnaAspClop), IL-6 levels in MCF7 cells were lower than baseline and Ana-treatment alone, but higher than in medium control and T47D cells at matched treatment; however, reduced levels were seen in T47D cells compared to baseline, medium control and Ana-treatment (Table 4.3). AspClop treatment alone reduced the levels of IL-6 in MCF7 cells but increased it in T47D cells (Table 4.3) thus showing that AspClop cocktail induces opposite effects in these cell lines (MCF7 and T47D) when combined with Anastrozole, and increasing inflammation in MCF7 cells when combined with Anastrozole but reduces it when used on its own, the opposite was seen in T47D cells.

TNFα, TGFβ1, TGFβ3 levels were lower in AnaAspClop-treated MCF7 cells compared to whole blood, medium control, Ana-treated cells and T47D cells at matched treatment (Table 4.3 & 4.5). While T47D cells generally induced higher levels of TNFα, TGFβ1, TGFβ3 in comparison to baseline and medium controls and MCF7 cells, TGFβ1 and TGFβ3 levels in T47D cells were lower when compared to Ana-treatment of T47D cells (Table 4.3 & 4.5) thus suggesting that antiplatelet therapy cocktails modulates the effects of Ana-treatment in this cell line. TGFβ2 levels were lower in MCF7 cells compared to baseline, medium control and Ana-treated cells and T47D cells at matched treatments (Table 4.5). AspClop-treatment in MCF7 cells, increased

the levels of TNFα, TGFβ2 and TGFβ3 but reduced TGFβ1 (Table 4.3 & 4.5). In T47D cells, AspClop-treatment decreased TNFα levels but increased TGFβ1, TGFβ2 and TGFβ3 (Table 4.3 & 4.5). This further highlight the differential effects of AspClop in these cell lines and suggests that all TGFβ subtypes play an important role in maintaining pro-inflammatory conditions in T47D cells; and TNFα, TGFβ2 and TGFβ3 mediate this effect in MCF7 cells.

PDGF-AB levels in AnaAspClop-treated MCF7 cells were higher than in whole blood and T47D cells at matched treatments; however, it was lower than in medium control and Ana-treated MCF7 cells suggesting that even though PDGF-AB levels were higher than in whole blood, they may have been reduced minimally by this treatment or bound to platelets (Table 4.5). T47D cells induced lower levels of PDGF-AB than baseline, medium control and Ana-treated T47D cells (Table 4.5). PDGF-BB levels were increased in AnaAspClop-treated cells (MCF7 and T47D cells) than baseline, medium control and Ana-treated cells; however, it was higher in T47D cells than MCF7 cells (Table 4.5). A similar trend was observed with TGFα and VEGF-A (Table 4.3 & 4.5). AspClop treatment alone in MCF7 cells increased the levels of PDGF-AB, PDGF-BB and VEGF-A, but reduced it in T47D cells (Table 4.5). Furthermore AspClop-treatment reduced TGFα levels in both cell lines (Table 4.3). Thus suggesting that this treatment (AspClop) reduced the secretion of growth factors more in T47D cells than MCF7 cells; and thus T47D cells may be more susceptible to its effects than MCF7 cells.

Anti-inflammatory marker IL-4 was reduced in AnaAspClop-treated MCF7 cells compared to whole blood (baseline), Ana-treated MCF7 cells, and T47D cells at matched treatment; conversely in T47D cells, IL-4 levels were increased (Table 4.3). The AspClop cocktail alone induced opposite effects to when it was combined with Ana; it increased the levels of IL-4 in MCF7 cells but reduced it in T47D cells (Table 4.3). Thus suggesting that the AspClop cocktail

may have reduced the inflammatory environment induced by MCF7 cells by increasing IL-4; and this may be attributed to the anti-inflammatory effects of Aspirin (Voelker and Hammer, 2012). However, these effects were not seen in T47D cells and may suggest this cell line is less susceptible to the effects of Aspirin than MCF7 cells.

These findings show that AnaAspClop treatment in MCF7 cells reduces secretion of key growth factors belonging to TGF (all subtypes) and PDGF-BB; however, PDGF-AB levels were higher, suggesting that this cytokine might maintain survival in this cell line. T47D cells further increased TGF proteins and PDGF, in addition in both cell lines TGFα and VEGF-A levels were high, suggesting that these cytokines continue to increase even during stressful conditions and may mediate survival mechanism.

4.3.3.5 Atopaxar-mediated cytokine secretion with or without Anastrozole

When Atopaxar was added to Anastrozole (AnaAto) it reduced the levels of IL-6 in T47D cells compared to baseline, medium control and Ana-treated cells (Table 4.4). In MCF7 cells, this treatment minimally increased IL-6 levels compared to whole blood (baseline) and Ana-treated cells but increased it compared to medium control (Table 4.4). Atopaxar treatment alone increased the levels of IL-6 in both cell lines which suggest that this treatment does not prevent inflammation from occurring, but its effects may be reduced by addition of Anastrozole, especially in T47D cells (Table 4.4).

In both cell lines AnaAto-treatment induced higher levels of TGFα, VEGF-A, TGFβ1, TGFβ2, and PDGF-BB compared to baseline, media control and Ana-treated cells, with the exception that MCF7 cells induced slightly less VEGF-A than baseline (Table 4.4 & 4.6). In contrast Atopaxar treatment alone reduced the secretion of TGFα, TGFβ1, TGFβ2, PDGF-BB and VEFG-A (but increased VEGF-A in MCF7 cells) (Table 4.4 & 4.6) in both cell lines thus suggesting that

used on its own Atopaxar may have reduced the secretion of pro-inflammatory factors, but when combined with Anastrozole it may induce pro-inflammatory effects. Furthermore, the increased levels of VEGF-A induced by MCF7 cells suggests that while this treatment may reduce inflammation, it may adversely affect the risk of angiogenesis.

Differential effects were seen between cell lines; certain growth factors were reduced in AnaAto-treated MCF7 cells but increased in AnaAto-treated T47D cells compared to baseline, media control, Ana-treated cells and T47D cells at matched treatments (with some exceptions); TNFα (higher compared to media control) and PDGF-AB (Table 4.4 & 4.5). Atopaxar treatment alone reduced the level of TNFα in both cell lines whereas PDGF-AB levels were increased in MCF7 cells but reduced in T47D cells (Table 4.5). Conversely TGFβ3 and IL-4 were higher in AnaAto-treated MCF7 cells compared to baseline (whole blood), medium controls and Ana-treated cells and T47D cells at matched treatments (Table 4.4.). Furthermore, in T47D cells TGFβ3 levels were increased compared to baseline and medium control but lower than in Ana-treated T47D cells. Atopaxar treatment alone reduced the levels of TGFβ3 and IL-4 in MCF7 cells but increased the secretion of these markers in T47D cells (Table 4.4), suggesting that Atopaxar had the opposite effect to when it was used combined with Anastrozole. Furthermore, this may show that while Atopaxar alone reduced the secretion of most inflammatory markers and growth factors, it increased the secretion of angiogenesis markers in MCF7 cells and this may be associated with higher risk for the occurrence of angiogenesis. In the T47D cell group Ato-treatment promoted an anti-inflammatory environment thus showing that the T47D cells were more susceptible to its effects.

4.3.3.6 Summary of cytokine secretion findings

These findings show that overall Anastrozole combined with antiplatelet therapy (AspClop/Ato) promotes secretion of pro-inflammatory and angiogenic cytokines in both cell lines when exposed to whole blood. When cells were treated with antiplatelet therapies only (AspClop/ Ato) they reduced the levels of pro-inflammatory cytokines secreted. Furthermore this highlighted the important role of TGFβ subtypes (-1,-2, and -3), TGFα, and PDGF subtypes (-AB and –BB) in mediating differentiation and angiogenesis.

4.4 Discussion

Epithelial to mesenchymal transitions (EMT) are associated with cancer progression and metastasis (Kalluri, 2009; Thiery *et al.*, 2009). In this chapter we investigated whether the reciprocal interactions between breast cancer cells treated with hormone and antiplatelet therapy, followed by exposure to blood components promote EMT. The cells were exposed to blood components in order to investigate cancer-induced coagulation, following the co-incubation thrombin levels (Chapter III), cytokine levels and platelet activation (Chapter III) in whole blood were assessed and gene expression in cells was assessed.

The genes commonly associated with EMT (i.e. *E-cadherin, N-cadherin, TGFβ1* and *vimentin*) were differentially altered by hormone and antiplatelet treatment. It was noted in untreated cells exposed to whole blood that gene expression for *E-cadherin, N-cadherin,* and *vimentin* were increased compared to baseline (albeit not significant), in contrast *TGFβ1* expression levels were comparable to those of baseline. This may highlight the reciprocal interactions between cells and vascular components within the tumour microenvironment which promote tumour survival and progression (Yu *et al.*, 2014; Pang *et al.*, 2015; Elaskalani *et al.*, 2017), as illustrated by the acquisition of mesenchymal features (*N-cadherin,* and *vimentin)* which are associated with EMT (a proxy for tumour survival) (Chekhun *et al.*, 2013; Aleskandarany *et al.*, 2014; Tasdemir *et al.*, 2018).

The cells maintained epithelial features (*E-cadherin*), even when mesenchymal genes were increased (*N-cadherin,* and *vimentin)*; however, while *TGFβ1* gene expression was low, consideration must be given that as the master regulator of EMT, protein expression may be responsible for engaging the downstream effects associated with cadherin and vimentin alteration. Cytokine analysis revealed that tumour cells were able to secrete more TGFβ1 than

that detected in whole blood. While this was not significant, TGFβ1 is implicated in autocrine mechanisms of tumour progression and is thus expected to bind back onto cognate receptors to induce signalling through the Smad signalling pathway which may promote the transcription of proteins involved in cell growth, motility and differentiation (Kubiczkova *et al.*, 2012; Maity *et al.*, 2015).

The tumour microenvironment is rich in growth factors and molecular mediators which promote tumour survival (Guo and Deng, 2018; Waldron *et al.*, 2019) and thus during the co-incubation with whole blood, breast cancer cells were exposed to various cytokines and growth factors which may have activated various signalling pathways involved in their growth and survival. It is worth noting that some cytokines levels were generally lower (i.e. IL-6, TNFα, TGFα, TGFβ3, IL-4) and while this may indicate a low secretion it may have also been attributed the medium of analysis, as it has been shown that cytokine levels were lower in whole blood compared to other medium such as PBMCs, due to some binding to their receptors and being internalised and the presence of more binding targets in whole blood due to various cell populations (van Dooren *et al.,* 2013). However, using PBMCs in this study would have taken into account cytokines stored within these cell types. Furthermore leukocytes might downregulate pro-inflammatory cytokines by enzymatically degrading them (van Dooren *et al.,* 2013).

Cytokine detection in whole blood exposed to untreated MCF7 cells compared to whole blood alone showed an increase in growth factors which promote cell proliferation and migration; TGFα, TGFβ1, TGFβ2, TGFβ3, PDGF-AB (Xian, 2007; Andrae *et al.,* 2008; Raja *et al.,* 2009; Xue *et al.,* 2017) and a decrease in pro-inflammatory; IL-6, TNFα, IL-4 (Marik and Flemmer, 2012), and angiogenesis markers; VEGF-A and PDGF-BB (Bambace and Holmes, 2011; van Dooren,

Duijvis and te Velde, 2013). This implies that the tumour microenvironment was primed by the tumour cells themselves to promote cell growth and survival (Poniatowski *et al.,* 2015; Xue *et al.,* 2017). In T47D cells, a similar pattern in cytokine secretion was observed except IL-6 was increased and PDGF-BB was decreased. While not all the cytokine levels were increased, there were high levels of inflammatory markers released that are implicated in supporting tumour survival (Kubiczkova *et al.*, 2012; Aleskandarany *et al.*, 2014; Nie *et al.*, 2015). This finding supports other studies which show that cancer is a pro-inflammatory condition (Fuentes *et al.,* 2016; Lee *et al.*, 2018). This finding further suggests that cytokines belonging to the transforming growth factor and platelet-derived growth factor families play an important role in mediating tumour survival in breast cancer (Poniatowski *et al.*, 2015;Hachim *et al.*, 2018) and further highlights the differential secretion of certain subtypes belonging to these families in breast cancer cells.

The tumour microenvironment was modulated by various treatment interventions within our experimental model. The effects of the diluent on breast cancer cells exposed to whole blood were assessed; gene expression for *E-cadherin* was comparable to baseline in MCF7 cells, but significantly upregulated in T47D cells. This highlights the differential response of these cell lines (Neve *et al.*, 2006; Dai *et al.*, 2017) and further shows that the diluent did not promote a complete mesenchymal phenotype but maintained epithelial-like features in both cell lines similar to media control (untreated cells). This was further illustrated by gene expression for *N-cadherin, vimentin* and *TGFβ1* which was found to be generally downregulated compared to untreated cells; T47D cells showed higher gene expression levels than MCF7 cells. This shows that the diluent differentially reduced genes associated with mesenchymal phenotype in these cell lines (this feature was more prominent in MCF7 cells than T47D cells), with

minimal adverse effects on cell survival which corroborates with the known toxic effects of DMSO on cells (Deng *et al.*, 2014; Jamalzadeh *et al.*, 2016). The corresponding cytokine secretion in relation to whole blood showed that the diluent-treatment maintained high levels of growth factors and pro-inflammatory markers; TNFα, IL-4, VEGF-A, and PDGF-AB in MCF7 cells but reduced these levels in T47D cells. in MCF7 cells this may reflect the mild toxic effects of the diluent on the cells which would promote inflammation (Junttila, 2018; Deng *et al.,* 2014; Jamalzadeh *et al.,* 2016). Anastrozole treatment maintained the epithelial-like phenotype in both cell lines and further promoted partial-EMT in T47D cells, this suggests that Anastrozole-treatment may promote a more aggressive phenotype in T47D cells as partial-EMT was associated with a more aggressive metastatic profile which is associated with collective cell migration, as observed in this cell line (Saitoh, 2018). Importantly, this occurred following exposure to whole blood highlighting the importance of blood components including platelets in facilitating Anastrozole in promoting breast cancer survival *in vitro*. Clinical trials generally show improved survival with prolonged use of Anastrozole, with few conflicting this finding. The Fulvestrant combined with Anastrozole Clinical trial (FACT) trial and South Western Oncology Group (SWOG) trial showed that Anastrozole alone or combined with another hormone-therapy agent (a selective oestrogen receptor degrader) Fulvestrant, promoted survival, although the combination was more effective (Bergh *et al.*, 2012; Barros-Oliveira *et al.*, 2017). A similar finding was shown when Anastrozole was used in conjunction with exemestane (Johnston *et al.*, 2013). Another study showed a benefit to using Anastrozole to treat early breast cancer, it improved five year disease free survival; however, it showed no benefit to overall survival (Chumsri *et al.,* 2011). The ATAC trial showed better efficacy of Anastrozole on survival and preventing recurrence when used alone than when combined with Tamoxifen (Cuzick, Sestak, *et al.*, 2014).

The tumour microenvironment was further assessed to determine its impact on tumour progression and detected cytokine secretion from Anastrozole-treated MCF7 cells showed that the levels of most pro-inflammatory cytokines and growth factors; IL-6, TGFα, TGFβ3, TGFβ1, PDGF-AB, PDGF-BB were increased. These proinflammatory mediators are known to promote tumour growth and survival (Devarajan *et al.*, 2012; Wei *et al.*, 2015; Okada *et al.,* 2018; Schlesinger, 2018). Interestingly levels of IL-4, an anti-inflammatory marker were also increased in MCF7 cells suggesting that the pro-inflammatory effects of Anastrozole were regulated by anti-inflammatory cytokines (Marik and Flemmer, 2012). In contrast, VEGF-A levels were increased in T47D cells suggesting that Anastrozole-treatment further promoted angiogenesis (Schlesinger, 2018), a process which is essential for tumour metastasis and is associated with poor prognosis (Comşa, Cîmpean and Raica, 2015; Asghar, Parvaiz and Manzoor, 2019). Anastrozole was shown to upregulate the expression of genes involved in inflammation and breast cancer patients taking Anastrozole also had an elevated immune response (Mello-Grand *et al.*, 2010). A similar finding was shown in a rat model of breast cancer whereby Anastrozole use promoted inflammation by increasing the secretion of inflammatory mediators IFNγ and IL-12 and suppressing anti-inflammatory markers IL-4 and IL-10 (Ray and Ficek, 2012). Conversely, another study did not show an increase in inflammation associated with Anastrozole use (Henry *et al.*, 2010). Thus, our findings support other studies which show an elevated inflammatory response with Anastrozole on breast cancer cell exposure to vascular components.

While Anastrozole reduces the amount of oestrogen produced and is effective as a therapy for mitigating growth of hormone-dependant breast tumours (Cuzick, Sestak, *et al.*, 2014; Kemp *et al.*, 2014; Chen *et al.*, 2015), tumour cells are able to undergo evolutionary processes

that allow for adaptation to the environment and encourage a response – in this case cytokine secretion, to facilitate and drive a pro-tumourigenic environment (Smollich *et al.*, 2010; Chen *et al.*, 2015). Anastrozole-mediated anti-cancer properties as shown previously (Harris *et al.,* 2007; Shebl *et al.*, 2012; Qiao *et al.*, 2018), may not provide protection against the formation of pro-tumour survival environment and phenotype. This may partly be facilitated by oestrogen which has been shown to inhibit the transcription of pro-inflammatory genes, therefore suppression of oestrogen by aromatase inhibitors is associated with increased levels of proinflammatory cytokines (Caprioli *et al.*, 2017). These effects may also be mediated by the presence of heterogeneous cell subpopulations which promote resistance to therapy and further facilitates recurrence (Lacroix and Leclercq, 2004; Guo and Deng, 2018; Matthews *et al.*, 2018).

The combined effects of hormone therapy using Anastrozole and antiplatelet therapy using Aspirin and Clopidogrel cocktail were tested to investigate how the addition of antiplatelet therapy modulates cellular response to hormone therapy. When cells were treated with AnaAspClop and exposed to whole blood, epithelial-like phenotype was maintained in MCF7 cells, whereas T47D cells reduced epithelial features by downregulating *E-cadherin*, but it upregulated *N-cadherin* (even though this was not corresponding with an increase in *TGFβ1*). Therefore, this may not reflect a complete EMT but may suggest cell detachment or partial-EMT (Liu *et al.*, 2014; Saitoh, 2018). The effects of Anastrozole combined with Aspirin and Clopidogrel cocktail are not known, however, most studies have shown the beneficial effects of Anastrozole on survival (Mello-Grand *et al.*, 2010; Bergh *et al.*, 2012; Ray and Ficek, 2012; Johnston *et al.*, 2013). The beneficial effect of Aspirin preventing cancer have previously been shown (Harris, Beebe-Donk and Alshafie, 2007; Shebl *et al.*, 2012; Qiao *et al.*, 2018).

Furthermore, Aspirin was shown to reduce metastasis in a mouse model of breast cancer (Lucotti *et al.*, 2019). Clopidogrel effects on cancer are mixed, with some studies showing that it prevents tumours (Coimbra *et al.*, 2015; Kuan *et al.*, 2019) whereas others show it may promote tumour progression (Denslow *et al.*, 2017; Smeda *et al.,* 2018). The findings of this study suggests that the *in vitro* effects of these combined treatments (Anastrozole, Aspirin and Clopidogrel) may have minimal effect or promote tumour progression.

Assessment of tumour microenvironment conditions in promoting tumour survival were also assessed. In MCF7 cells, this finding corresponded with a reduction in most pro-inflammatory cytokines and growth factors; IL-6, TNFα, TGFβ1, TGFβ2, TGFβ3, PDGF-BB, but an increase in angiogenic markers and growth factors; VEGF-A, PDGF-AB and TGFα. Therefore, suggesting that the elevated angiogenic markers and growth factors were the main drivers of survival in this cell line following AnaAspClop treatment (Colciago *et al.*, 2009; Dineen *et al.*, 2009; Chater *et al.*, 2018). In addition, VEGF-A and PDGF-AB are angiogenic markers (Liu *et al.*, 2014; Fuentes, Palomo and Rojas, 2016; Huang *et al.*, 2017; Sun *et al.,* 2018), their increased levels in response to AnaAspClop-treatment in MCF7 cells could indicate higher risk of angiogenesis with this treatment in breast cancer patients.

Studies have shown mixed effects of Aspirin and Clopidogrel on inflammation. Low-dose Aspirin induced anti-inflammatory effects mediated through COX-1 inhibition (Lucotti *et al.*, 2019) whereas the Evaluation of Long-Term Clopidogrel Antiplatelet and Systemic Anti-Inflammatory Effects (ELAPSE) trial showed that in patients with CAD, Clopidogrel treatment was effective in inhibiting platelet aggregation; however, it increased levels of inflammatory mediators (Saw *et al.*, 2008). However, another study showed that when Clopidogrel was combined with Ticagrelor it reduced inflammatory markers (IL-6, TNFα, CCL2) in patients with

Lipopolysaccharides (LPS)-induced inflammation (Thomas and Storey, 2015). In the present study, combined Aspirin and Clopidogrel cocktail was also shown to reduce the levels of pro-inflammatory cytokines including IL-6 and TNFα, thus inhibiting inflammation (Wegiel *et al.*, 2008; Golebiewska and Poole, 2015; Agnoli *et al.*, 2017). However, AnaAspClop-treated T47D cells further increased the levels of growth factors (TNFα, TGFα, TGFβ2), angiogenic/growth factors (VEGF-A and PDGF-BB) and anti-inflammatory marker (IL-4). In contrast to Anastrozole treatment alone, AnaAspClop treatment reduced levels of pro-inflammatory cytokine IL-6 and growth and angiogenic factors (TGFβ1, TGFβ3, and PDGF-AB). The reduction in the expression of *TGFβ1* levels corresponded with reduced translation of this cytokine in both cell lines. Thus the mixed effects of inflammatory markers in both cell lines reflect the clinical outcomes of these treatments on inflammation (Saw *et al.*, 2008; Chen *et al.*, 2018; Lucotti *et al.*, 2019). These findings show that in general pro-inflammatory markers were decreased in both cell lines, reflecting the effects of combined Aspirin and the Aspirin and Clopidogrel cocktail; however, high levels of some inflammatory markers and angiogenic factors may highlight the effects of Clopidogrel on tumour progression.

The effects of Aspirin and Clopidogrel cocktail were also assessed independent of Anastrozole and this treatment was shown to promote EMT in MCF7 cells but restored the epithelial phenotype in T47D cells when compared to AnaAspClop-treatment. This suggests that AspClop treatment may facilitate the establishment of tumour at a secondary site through MET (Moen *et al.*, 2009; Aleskandarany *et al.*, 2014; Jolly *et al.*, 2016) this effect may be higher in T47D cells than MCF7 cells. Studies have shown various outcomes regarding the effects of Aspirin and Clopidogrel on tumours, Clinical studies; the CAPRIE trial and CHARISMA trial have shown that combined Aspirin and Clopidogrel treatment did not promote cancer recurrence

(Bhatt *et al.*, 2006; Mansour *et al.*, 2020), whereas the DAPT trial showed that Aspirin and Clopidogrel cocktail was associated with higher cancer related deaths (Mansour *et al.,* 2020). Furthermore, the effects of the Aspirin in reducing cancer risk have been established (Harris, Beebe-Donk and Alshafie, 2007; Shebl *et al.*, 2012; Qiao *et al.*, 2018), despite the conflicting findings regarding the effects of Clopidogrel (Hicks *et al.,* 2015; Denslow *et al.,* 2017; Ballerini *et al.,* 2018; Smeda *et al.,* 2018). Our finding shows differential effects of Aspirin and Clopidogrel treatment, and shows that this treatment mediated a more pronounced tumour survival phenotype in MCF7 cells than T47D cells. This outcome was complemented with the changes in the tumour microenvironment in order to establish whether the phenotypic changes were supported by the microenvironment.

Corresponding cytokine secretion in the control group (Aspirin and Clopidogrel), when compared to AnaAspClop showed that MCF7 cells exposed to whole blood following treatment, maintained higher levels of most inflammatory, growth and angiogenesis markers, but reduced TGFβ1 secretion even though its gene expression was upregulated. This may have been due to the internalisation of the TGFβ receptor following ligand binding (Valcourt *et al.*, 2005; Moustakas and Heldin, 2016). This facilitates increased transcription through the activation of Smad2 and Smad3 and has been associated with EMT (Valcourt *et al.*, 2005; Moustakas and Heldin, 2016). This concurs with our findings, as EMT was induced in this cell line. In T47D cells most inflammatory cytokines, growth and angiogenic factors were reduced except IL-6, TGFβ1, TGFβ2 and TGFβ3 which may have mediated pro-inflammatory outcome and survival in this cell line (Kubiczkova *et al.*, 2012; Kumari *et al.*, 2016; Hachim *et al.*, 2018). Thus, these findings confirm the pro-survival effects of Aspirin and Clopidogrel on MCF7 cells and show that while this treatment did not induce a more aggressive phenotype in T47D cells,

it still maintained a higher pro-inflammatory microenvironment, which may ultimately promote tumour growth and survival.

The effects of Anastrozole combined with Atopaxar were tested. When cells were treated with AnaAto, then exposed to whole blood, the gene expression profile showed that epithelial-like phenotype was maintained in MCF7 cells and in T47D cells there was a reduction in epithelial and mesenchymal genes. The effects of Atopaxar alone or combined with Anastrozole on breast cancer is unknown. Atopaxar inhibits PAR1 receptors which are over-expressed in breast cancer cells (Diaz *et al.*, 2012; Covic and Kuliopulos, 2018; D'Anselmi *et al.*, 2013; Rizwan *et al.*, 2015) and these receptors have been shown to mediate invasion and metastatic processes which include increasing the binding of cells to the extracellular matrix (Yang *et al.*, 2009; Liu *et al.*, 2017). Atopaxar prevents PAR1 ligands such as thrombin, tissue factor, and MMP1 from binding and thus inhibits their effects (Yang *et al.*, 2009). Furthermore Atopaxar was shown to inhibit JAK-STAT signalling, thus preventing tumour progression (Sun *et al.*, 2019). Given the role of PAR1 in facilitating tumour progression as shown in previously (Yang *et al.*, 2009; Liu *et al.*, 2017b), the direct effects of Atopaxar combined with Anastrozole on breast cancer cells was postulated to inhibit tumour progression.

When the tumour microenvironment was assessed, cytokine secretion showed that levels of pro-inflammatory markers, growth and angiogenic factors; TGFα, TGFβ1, TGFβ2, VEGF-A, PDGF-BB were higher in both cell lines compared to when cells were treated with Anastrozole alone. However, MCF7 cells further increased IL-6, TGFβ3, IL-4 levels whereby these markers were reduced in T47D cells highlighting the heterogeneity between these cell lines (Aka and Lin, 2012; Kochel *et al.*, 2017). Overall these findings indicate that MCF7 cells were less

susceptible to AnaAto effects than T47D cells and may point to a differential expression in PAR-1 receptors in these cells as shown by other studies (D'Anselmi *et al.*, 2013; Rizwan *et al.*, 2015; Covic and Kuliopulos, 2018). As such reduced expression of PAR-1 receptors in MCF7 cells (Meydani *et al.*, 2001), may reduce the efficacy of Ato within the AnaAto cocktail.

The effects of Atopaxar treatment without Anastrozole were shown to promote the acquisition of mesenchymal features while overall maintaining epithelial features; therefore, illustrating a partial-EMT. This is in contrast to the postulated beneficial effects of Atopaxar on tumour survival (Sun *et al.*, 2019). When corresponded with the state of the tumour microenvironment the secretion of proinflammatory cytokines was generally reduced in both cell lines except IL-6. IL-6 mainly mediates a pro-inflammatory tumour microenvironment (Schaper and Rose-john, 2015), thus our findings may be limited by the duration of the culture period. Moreover, levels of angiogenic factors (VEGF-A and PDGF-AB) were higher in MCF7 cells and reduced in T47D cells. These findings show that Atopaxar treatment alone could lead to higher risk of angiogenesis and metastasis (Bambace and Holmes, 2011; Aleskandarany *et al.*, 2014; Tesfamariam, 2016; Asghar *et al.,* 2019). Thrombin was shown to promote the secretion of IL6, VEGF and PDGF (Strande and Phllips, 2009), thus our findings further suggest that Atopaxar may not have been effective in completely blocking PAR1 receptors, resulting in thrombin binding and promoting inflammation through IL-6 and angiogenesis through VEGF.

These findings thus far indicate that combined Anastrozole and antiplatelet therapy (Aspirin and Clopidogrel/Atopaxar) maintains a more differentiated epithelial-like phenotype in MCF7 cells and a reduction of epithelial features in T47D cells, under exposure to whole blood. Whereas Anastrozole alone or antiplatelet therapy alone (Aspirin and Clopidogrel/ Atopaxar)

is associated with EMT or partial EMT (more pronounced in T47D cells), when cancer cells are associated with vascular components. In general the interaction between breast cancer cells and blood components resulted in higher levels of angiogenic mediators and TGFβ1 secretion into the TME and this is typically associated with tumour survival through metastasis (Haddad and Greeno, 2006; Aleskandarany *et al.*, 2014; Pickup *et al.,* 2013; Liu *et al.*, 2014; Formenti *et al.*, 2018). This will thus create favourable conditions within the tumour microenvironment to promote further tumour growth and formation of new blood vessels which will support tumour progression (Du and Tan, 2014; Mosevoll *et al.*, 2018; Schlesinger, 2018). However, the results also indicate that selected pro-tumorigenic effects of anti-platelet therapies may be mitigated by Anastrozole. However, the increased levels of these cytokines suggest that combined hormone and antiplatelet therapy does not prevent the formation of pro-tumorigenic conditions within the tumour microenvironment and may even enhance it by increasing the secretion of growth factors into blood.

4.5 Conclusion

In conclusion, under whole blood exposure, Anastrozole combined with antiplatelet therapy (Aspirin and Clopidogrel cocktail/ Atopaxar) maintains or reduces epithelial phenotypic features but promote inflammation and angiogenesis. Anastrozole alone and Antiplatelet therapies alone (Aspirin and Clopidogrel cocktail/ Atopaxar) promote complete-EMT or partial-EMT, dependant on cancer characteristics and this corresponds with an inflammatory and proangiogenic environment.

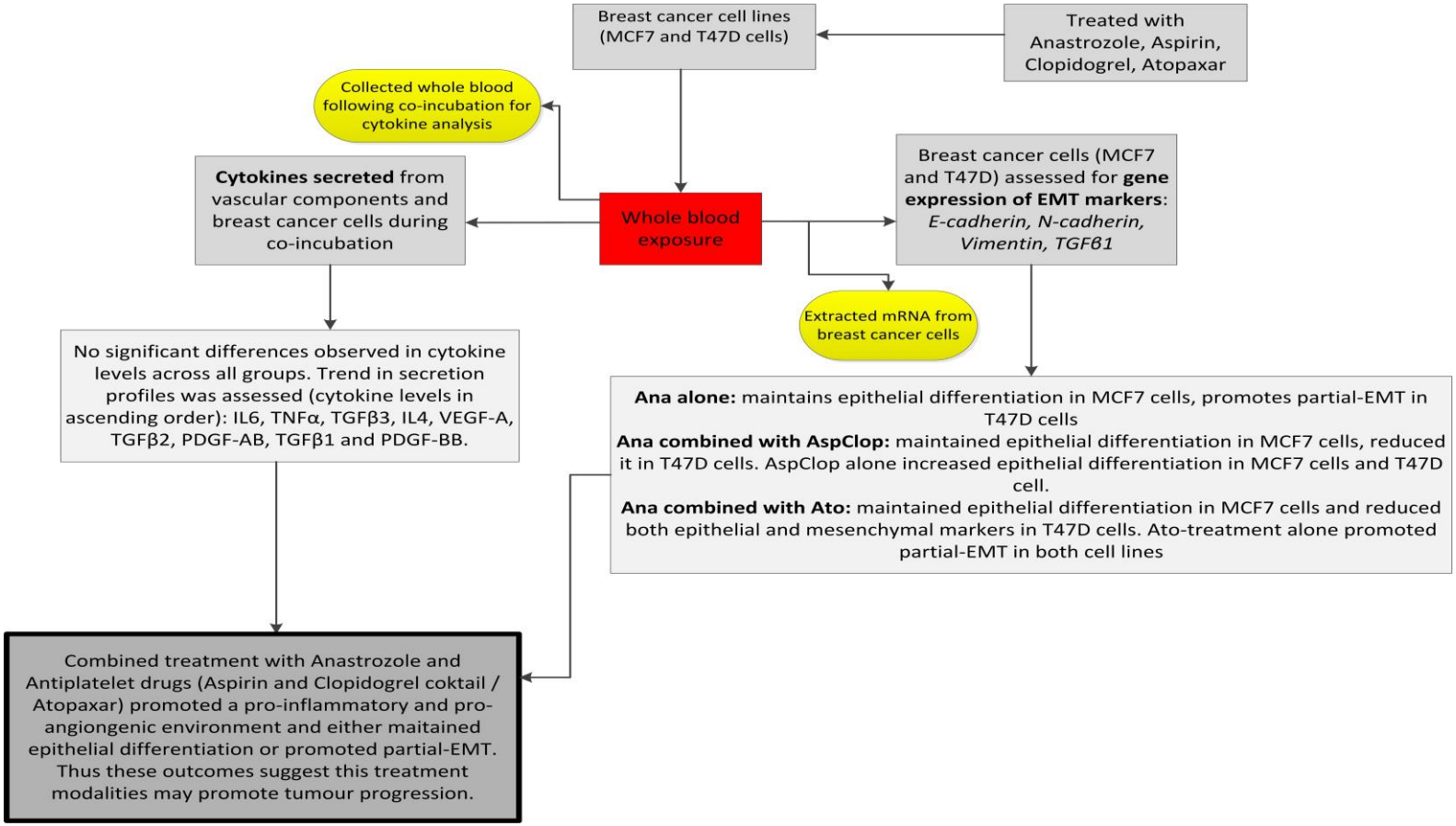


Figure 4.4: An overview of chapter 4 and summary of key findings.

Chapter V: General conclusion

5.1 Introduction and rationale

Thromboembolic disorders are common in breast cancer patients and are associated with high mortality (Lee and Levine, 2003; Walker *et al.*, 2016; Gervaso *et al.*, 2019). The reciprocal interaction between vascular components, specifically platelets, and cancer cells not only promotes thromboembolic disorders but also facilitates tumour progression (Lal, Dittus and Holmes, 2013; Yu *et al.*, 2014; Elaskalani *et al.*, 2017). Hormone dependant breast cancer is the most common subtype of cancer in women and accounts for more than 70% of breast cancers diagnosed (Jia *et al.*, 2016; Hilton, Clarke and Graham, 2018). Hormone therapy is effective in treating hormone-dependant breast cancer but is a risk for the occurrence of thromboembolic disorders (Deitcher and Gomes, 2004; Haddad and Greeno, 2006; Kyriazi, 2012). The use of antiplatelet therapy is effective against thromboembolic disorders associated with the cardiovascular system (Eikelboom *et al.*, 2012; Costopoulos *et al.,* 2013; Olivier *et al.*, 2013); however, its combined used with hormone-therapy in the treatment of breast cancer-associated thromboembolic-disorders is not well established. It is for this reason that this study was undertaken, in order to investigate the potential benefits or risks of combined hormone and antiplatelet therapy in breast cancer.

The experimental model used in this study whereby breast cancer cells where first treated with hormone therapy and/or antiplatelet therapy, then exposed to whole blood aimed to establish the direct effects of treatment on breast cancer cells and how they modulate overall outcome. The reciprocal interaction between platelets and tumour cells is known to mediate a number of processes which promote hypercoagulation and facilitate tumour progression (Bambace and Holmes, 2011; Menter *et al.*, 2014a; Yan and Jurasz, 2016; Heldin, Lennartsson

and Westermark, 2018). Thus, the role of hormone therapy and antiplatelet therapy was investigated in light of these two main processes.

5.2 Findings

5.2.1 Anastrozole-mediated effects

Breast cancer patients inherently are at higher risk for thrombosis due to the hypercoagulable state associated with the tumour (Deitcher and Gomes, 2004; Kyriazi, 2012). Additionally, cancer therapy including chemotherapy and hormone therapy increases this risk (Deitcher and Gomes, 2004; Kyriazi, 2012). The Arimidex, Tamoxifen Alone or in Combination (ATAC) clinical study found that although Anastrozole is associated with less risk for VTE than Tamoxifen, women on Anastrozole still had a higher risk for developing VTE than healthy women (Fabian, 2007; Kahn, 2012; Cuzick, Sestak, *et al.*, 2014; Kemp *et al.*, 2014; Bae *et al.*, 2015). Similarly, the present study found that the reciprocal interactions between whole blood and breast cancer (MCF7 and T47D cells) increased thrombin levels in whole blood with higher levels of thrombin secreted by MCF7 cells than T47D cells, indicating differential responses between the cell lines.

Thrombin, a potent agonist for coagulation, is the main ligand for the PAR1 receptors expressed on tumour cells (Kamath, Meydani and Foss, 2001; Fuentes, Palomo and Rojas, 2016) and platelet membranes (Diaz *et al.*, 2012). Thrombin promotes platelet activation which results in the release of mediators of the coagulation cascade, and factors that can facilitate tumour progression (Holinstat *et al.*, 2009; Tourdot *et al.*, 2018). In this study platelet activation was indicated by the expression of CD62p and CD63 activation markers, quantified as IPA, and was coupled with morphological analysis (Leytin *et al.*, 2000; Augustine *et al.*, 2016). CD62p mediates early events of platelet activation and facilitates platelet

adhesion, hence its expression was lost when cells were bound or fully spread (Xu *et al.*, 2016; Navred *et al.*, 2019). This study found that CD62 expression was generally lower than CD63, and this may be attributed to its role as an adhesion molecule. Additionally, we found that CD63 was more stably expressed during platelet activation, which may be associated with its role in sustaining prolonged platelet activation and mediating fibrinolysis (Muhammad, Moinuddin and Samina, 2013; Vallier *et al.*, 2016). The higher levels of CD63 compared to CD62p may have also been due to detection of secreted microparticles or exosomes (Van Der Zee *et al.*, 2006; Vallier *et al.*, 2016), which were observed in both cell lines following Anastrozole-treatment. CD63 has also been shown to be a signalling protein in cancer whereby it facilitates intracellular trafficking (Pols and Klumperman, 2009) and forms micro-domains which interact with MMPs in order to promote invasion and metastasis (Vences-catalán and Levy, 2018), demonstrating the pleiotropic nature of this marker in facilitating hypercoagulation and promoting tumour progression. When cells were treated with Anastrozole only and not conditioned to whole blood, they displayed a low migration rate, echoing findings from other studies (D'Anselmi *et al.*, 2013; Rizwan *et al.*, 2015; Yu *et al.*, 2017). This highlights that tumour-promoting processes may be dependent on interactions between cells and components of whole blood as it provides a microenvironment rich in chemical mediators which facilitate migration (Menter *et al.*, 2014; Miyashita *et al.*, 2015). Despite this, Anastrozole-treated MCF7 cells showed a higher proliferation rate than T47D cells, and thus suggests that this may be a stress response in MCF7 cells to promote their survival. Conversely T47D cells, may be more resistant to stressors and while proliferation was low, cell survival remained a dominant feature. This highlights the heterogeneity between these cell lines which may result from uneven ER receptor expression (Lazennec *et al.*, 2001; Roger *et al.*, 2001; Sweeney *et al.,* 2012; Miah *et al.*, 2019), or drug metabolizing

enzymes (McDonald *et al.*, 2017) which will ultimately mediate response to Anastrozole. To directly assess the impact on tumour progression, the EMT process was studied as mediated by interactions between cells and blood components within the tumour microenvironment. When Anastrozole-treated cells were conditioned with whole blood, MCF7 cells maintained a more differentiated epithelial-like phenotype and T47D cells underwent partial-EMT as described by gene alterations, contrasting with cell ultrastructural analysis which showed that when cells were not exposed to blood, Anastrozole treatment maintained spread cell monolayers characteristic of epithelial cells. Partial-EMT highlights the plasticity of metastasis in facilitating tumour establishment at distant sites whereby mesenchymal features are lost and tumours differentiate (Jolly *et al.*, 2015; Saitoh, 2018). Partial-EMT indicates a more aggressive tumour (Grosse-Wilde *et al.*, 2015) that facilitates invasion through collective cell migration (Christiansen and Rajasekaran, 2006). T47D cells displayed a more aggressive phenotype following Anastrozole-treatment and exposure to vascular components. The corresponding cytokine secretion from Anastrozole-treated cells and blood components highlighted the role of TGFβ1, TGFβ2, PDGF-BB and VEGF-A in mediating survival effects in these cell lines. Furthermore the secreted cytokines are known to promote angiogenesis (Tian and Schiemann, 2017; Chater *et al.*, 2018; Liu *et al.*, 2018). These findings highlight that Anastrozole treatment was not able to inhibit reciprocal interactions between cancer cells and blood components which not only promote hypercoagulation but promote tumour survival. Clinical studies have shown that the prolonged use of Anastrozole improves patients survival with metastatic breast cancer (Bergh *et al.*, 2012; Mehta *et al.,* 2012). Our study indicates that cells are able to adapt to Anastrozole treatment and this may provide a selective pressure for survival and recurrence (Mello-Grand *et al.*, 2010; Chumsri *et al.,* 2011; Wong and Chen, 2012; Cuzick *et al.*, 2014).

5.2.2 Anastrozole combined with Aspirin and Clopidogrel-cocktail mediated effects

In this study treatment of breast cancer cells (MCF7 and T47D cells) with combined hormone therapy using Anastrozole with Aspirin and Clopidogrel cocktail induced higher thrombin levels detectable in whole blood than Anastrozole-treated cells, with MCF7 cells mediating higher thrombin levels; however, thrombin levels were reduced when cells were treated with Aspirin and Clopidogrel cocktail only. This finding shows that Aspirin and Clopidogrel cocktail combined with Anastrozole is unable to counter Anastrozole-mediated coagulation risk. This study is the first to highlight this effect. The Raloxifene Use for The Heart (RUTH) clinical trial tested the effects of SERM (Raloxifene) combined with Aspirin and found no beneficial effect against VTE (Duvernoy *et al.*, 2010). Thus far, combined hormone and antiplatelet therapy shows no beneficial effects against thromboembolic disorders.

This finding corresponded with more pronounced platelet activation in whole blood exposed to combined Anastrozole with Aspirin and Clopidogrel treated-cells (both MCF7 and T47D) compared to treatment controls, whereby platelets displayed fully spread membrane. Furthermore, differential expression of platelet activation markers was seen; overall lower levels of CD62p IPA were seen compared to CD63, however this apparent loss in CD62p may be related to its role in adhesion and given the fully spread membrane morphology displayed in platelets, it indicates that CD62p was engaged (Augustine *et al.*, 2016; Plantureux *et al.*, 2018b). In both cell lines, combined Anastrozole with Aspirin and Clopidogrel cocktail-treatment did not alter CD63 IPA compared to Anastrozole-treatment, but it remained higher than Aspirin and Clopidogrel cocktail control. While CD63 mediates platelet activation, it is also associated with signalling in cancer (Vences-catalán and Levy, 2018), thus higher levels may suggest a role for combined hormone and antiplatelet therapy in promoting CD63-mediated signalling which involves intracellular trafficking and mediating tumour survival and

metastasis through MMPs (Pols and Klumperman,2009; Vences-catalán and Levy, 2018). Thus far, combined Anastrozole and Aspirin and Clopidogrel cocktail suggest pro-coagulatory effects, contrary to the effects of Aspirin and Clopidogrel in cardiovascular disease alone (Capodanno *et al.,* 2013; Roop *et al.*, 2013; Roe *et al.*, 2016).

Assessment of the combined effect of antiplatelet cocktail: Aspirin and Clopidogrel and Anastrozole in the tumour itself, prior to whole blood exposure in cells, revealed that the migration rate was generally low in both cell lines, despite a slight increase in migration rate in T47D cells, complete wound healing did not occur. This finding corresponds with the classification of these cell lines as low migratory (D'Anselmi *et al.*, 2013; Rizwan *et al.*, 2015; Yu *et al.*, 2017). Furthermore, Aspirin and Clopidogrel cocktail with or without Anastrozole did not significantly increase migration risk in breast cancer, corresponding to the low migration rate in these cell lines (Smollich *et al.*, 2010; Qiao *et al.*, 2018). Interestingly, ultrastructural analysis of breast cancer cells following treatment with Anastrozole combined with Aspirin and Clopidogrel cocktail revealed features which indicate that cell motility in these cells is facilitated by collective migration (Jolly *et al.*, 2015; Pandya *et al.,* 2017). Contradicting evidence for the clinical use of Clopidogrel combined with Aspirin on cancer outcome exists, with studies showing that it promotes cancer (Mauri *et al.*, 2014), reduces it (Bhatt *et al.*, 2006) or is ineffectual (CAPRIE *et al.,* 2001). The CHARISMA clinical trial showed that combined Aspirin and Clopidogrel in cancer reduced mortality (Bhatt *et al.*, 2006). In contrast, the Dual Anti-Platelets Therapy (DAPT) clinical trial showed adverse effects of Aspirin and Clopidogrel/Prasugrel, whereby cancer-related mortality was higher (Mauri *et al.*, 2014). Furthermore an *in vivo* model of metastatic breast cancer in mice showed that

combined Aspirin and Clopidogrel treatment induced vascular mimicry and thus promoted angiogenesis (Smeda *et al.*, 2018).

Anastrozole-mediated increase in MCF7 cell proliferation was attenuated by AnaAspClop-treatment (albeit not significant); however, cell proliferation in MCF7 cells remained significantly higher than in T47D cells at matched treatments, highlighting the difference in response despite both cell lines representing a luminal phenotype (Baxi *et al.*, 2012; Yu *et al.*, 2017). To directly assess the reciprocal interactions between blood components and tumour cells on tumour progression, EMT process in response to combined Anastrozole with Aspirin and Clopidogrel cocktail was studied. Combined Anastrozole with Aspirin and Clopidogrel cocktail maintained an epithelial phenotype in MCF7 but reduced this phenotype in T47D cells, and induced a slight increase in mesenchymal features suggesting it may modulate an EMT in T47D cells when exposed to vascular components. The Aspirin and Clopidogrel cocktail control maintained an epithelial-like phenotype in both cell lines, its effect was more pronounced in MCF7 cells. This highlights that combined Anastrozole with Aspirin and Clopidogrel mediated a more aggressive tumour profile in T47D cells than MCF7 cells; however, these effects were attenuated by Aspirin and Clopidogrel cocktail alone. These findings thus support studies which show that combined hormone and antiplatelet therapy may promote tumour survival (Mauri *et al.*, 2014, 2016; Denslow *et al.*, 2017; Smeda *et al.,* 2018). These effects were mediated by TGFβ1, which acts as the main mediator of EMT through Smad 2/3 signalling (Araki *et al.*, 2011; Plantureux *et al.*, 2018). Cells may undergo complete-EMT, whereby they lose epithelial features and acquire mesenchymal features or they may undergo a partial-EMT which is characterized by a partial loss and/or gain of epithelial and mesenchymal features (Aleskandarany *et al.*, 2014; Jolly *et al.*, 2015; Saitoh,

2018). The partial-EMT is related to collective migration strategy and associated with more aggressive tumour phenotype. In addition, TGFβ1 also acts independent of Smad 2/3 and can promote non-genomic ERα signalling and promote endocrine resistance (Tian and Schiemann, 2017). Analysis of the tumour microenvironment showed that Aspirin and Clopidogrel cocktail with or without Anastrozole induced pro-inflammatory and pro-angiogenic environment, the Aspirin and Clopidogrel controls mediated higher levels in MCF7 cells. Thus, collectively these findings suggest that combined Anastrozole with Aspirin and Clopidogrel maintained tumour survival through non-genomic ERα signalling in MCF7 cells but induced more aggressive tumour effects in T47D cells by promoting induction of partial-EMT. The Aspirin and Clopidogrel cocktail control alone however, maintained survival in both cell lines without promoting a more aggressive tumour profile.

5.2.3 Anastrozole and Atopaxar mediated effects

The role of PAR receptor antagonist on direct tumour outcome has not been well established. It is speculated that PAR receptor agonists may be targeted as part of adjuvant therapy against tumours to prevent PAR receptor-mediated signalling which promotes tumour survival (Egan *et al.*, 2011; Liu *et al.*, 2017; Haemmerle *et al.*, 2018). Furthermore Atopaxar was shown to inhibit the JAK-STAT3 signalling pathway in cell lines representing different tumours (including breast, cervical, and prostate) (Sun *et al.*, 2019). This study thus presents novel findings regarding the role of Atopaxar with or without Anastrozole in breast cancer. In this study, Anastrozole and Atopaxar-treatment of MCF7 cells increased detectable thrombin levels in whole blood compared to individual controls. This showed that Anastrozole combined with Atopaxar may mediate higher risk of hypercoagulation in MCF7 cells by increasing available thrombin in whole blood, as thrombin mediates various processes associated with hypercoagulation and tumour progression (Pan, Boucher and Kaunelis, 2016;

Wojtukiewicz *et al.*, 2016; Gomes *et al.*, 2017). Thrombin binds to PAR receptors expressed on cellular surfaces, thus the reduced circulating thrombin in whole blood exposed to Anastrozole-Atopaxar-treated T47D cells may also reflect thrombin binding to PAR-1 receptors on T47D cells (Kamath *et al.,* 2001; Moschonas, Goudevenos and Tselepis, 2015; Wojtukiewicz *et al.*, 2016) in order to mediate cancer signalling to promote survival. Corresponding platelet activation revealed that CD62p IPA in both cell lines treated with combined Anastrozole and Atopaxar was similar to Anastrozole-treatment but higher than those induced by Atopaxar control. Thus, suggesting that combined Anastrozole and Atopaxar induces higher levels of platelet activation than Atopaxar alone. Platelet morphology showed that most platelets were at early stages of activation, and few platelets were at advanced stages of activation.

CD63 IPA remained higher than CD62p in all treatment groups. Atopaxar exhibits beneficial effects against platelet aggregation in patients suffering with thromboembolic disorders (Kogushi *et al.*, 2011; Chatterjee *et al.,* 2013; Moschonas *et al.,* 2015). The findings of this study suggest that this beneficial effect against thromboembolic disorders may be inhibited in the cancer setting. Furthermore the high levels of CD63 could mediate tumour progression as CD63 levels were found to be elevated in cancer patients and induced EMT by increasing β-catenin (Seubert *et al.*, 2015; Vences-catalán and Levy, 2018). As shown in previous treatments, cell migration was not substantially increased by Anastrozole combined with antiplatelet agents. In contrast, Atopaxar attenuated Anastrozole-induced cell proliferation in MCF7 cells; however, cell proliferation remained higher in this cell line than T47D cells further speaking to differential responses by these cell lines. The reciprocal interactions between blood components and breast cancer cells in promoting EMT were investigated. Anastrozole

combined with Atopaxar maintained epithelial features in MCF7 cells but reduced epithelial and mesenchymal features in T47D cells suggesting that this cell line was more susceptible to its effects. In contrast, Atopaxar alone induced a partial-EMT in both cell lines without loss of epithelial features. Therefore, Atopaxar combined with Anastrozole may promote tumour survival in MCF7 cells but inhibit it in T47D cells. Cytokine analysis showed that Anastrozole and Atopaxar treatment induced inflammation and angiogenesis by elevating levels of TGFα, VEGF-A, TGFβ1, TGFβ2, and PDGF-BB. Whereas Atopaxar alone increased IL-6 levels in both cell lines, VEGF-A and PDGF-AB. These findings highlight the important secretory role of platelets within the tumour microenvironment and how they mediate tumour survival. It is noteworthy that with all the treatments used, the heterogeneous response between MC7 and T47D cells was evident. Even though these cell lines broadly represent luminal A subtype of breast cancer, our result highlight how they modulate different responses to treatments, with MCF7 cells being more susceptible to most treatment modalities than T47D cells (except Atopaxar). This suggests that the drug targets are expressed differentially between these cell lines and thus may contribute to the differenced seen.

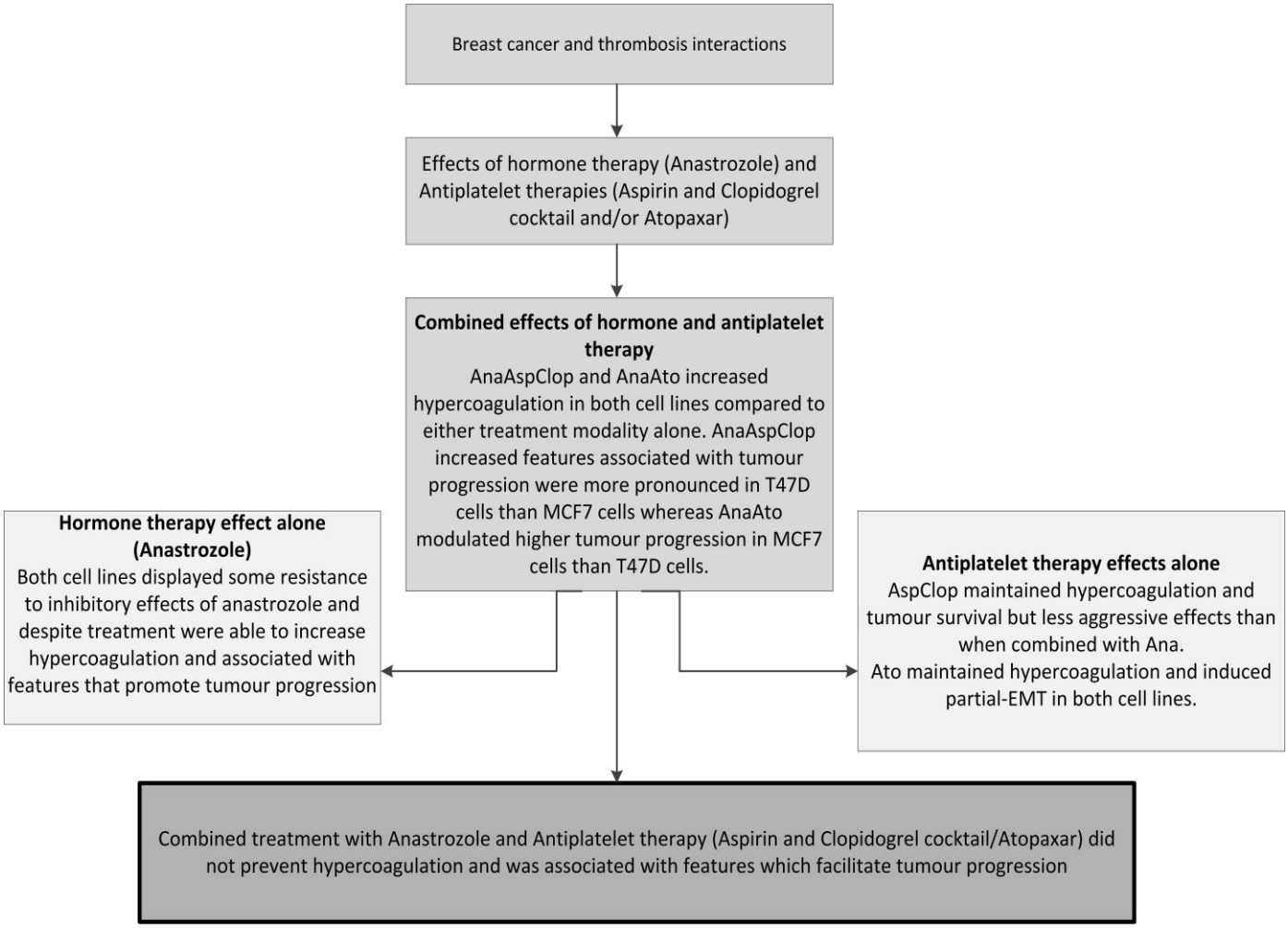


Figure 5.1: An overview of chapter 5 and summary of key findings.

5.3 Limitations of the study and future perspectives

5.3.1 Limitations

The sample size for volunteers was restricted to six because of limited resources thereby reducing the overall sample size. This had an impact in reducing the detection of minor changes. For example, no significant differences were seen between the cytokines with the treatments, meaning that the importance of minor differences in cytokine secretion resulting from treatment may have been lost due to the small sample size.

Due again to resource limitations, the direct effects of Anastrozole and antiplatelet therapy on platelets themselves could not at this time be assessed but would form an additional study and would be beneficial in defining the direct effects of treatment.

Platelet morphology was studied using a confocal microscope instead of the Scanning Electron Microscope because the NOVA 600 Scanning Electron microscope was damaged during the course of experimentation therefore could not be used as initially planned. Unfortunately, platelet morphology was already preserved with a strong fixative (2.5% glutaraldehyde/paraformaldehye) which is ideal for preserving cell architecture for use under a scanning electron microscope. The platelet morphology was instead studied on a Confocal microscope, under phase contrast using a high magnification (63X objective). This enabled viewing the general outline of the platelets and how their morphology was altered by the various treatment interventions. However, finer cell surface details such as presence of microvilli, smoothness of the plasma membrane and clear open canalicular system were not resolved (Fig 5.2). Furthermore, even though the thrombin assay revealed thrombin release, fibrin formation (product of thrombin catalytic activity) which occurs at advanced stages of platelet activation and associates with platelet aggregation, was not detected and since they are better resolved at higher magnification, therefore any fibrin formation was not seen due to magnification.

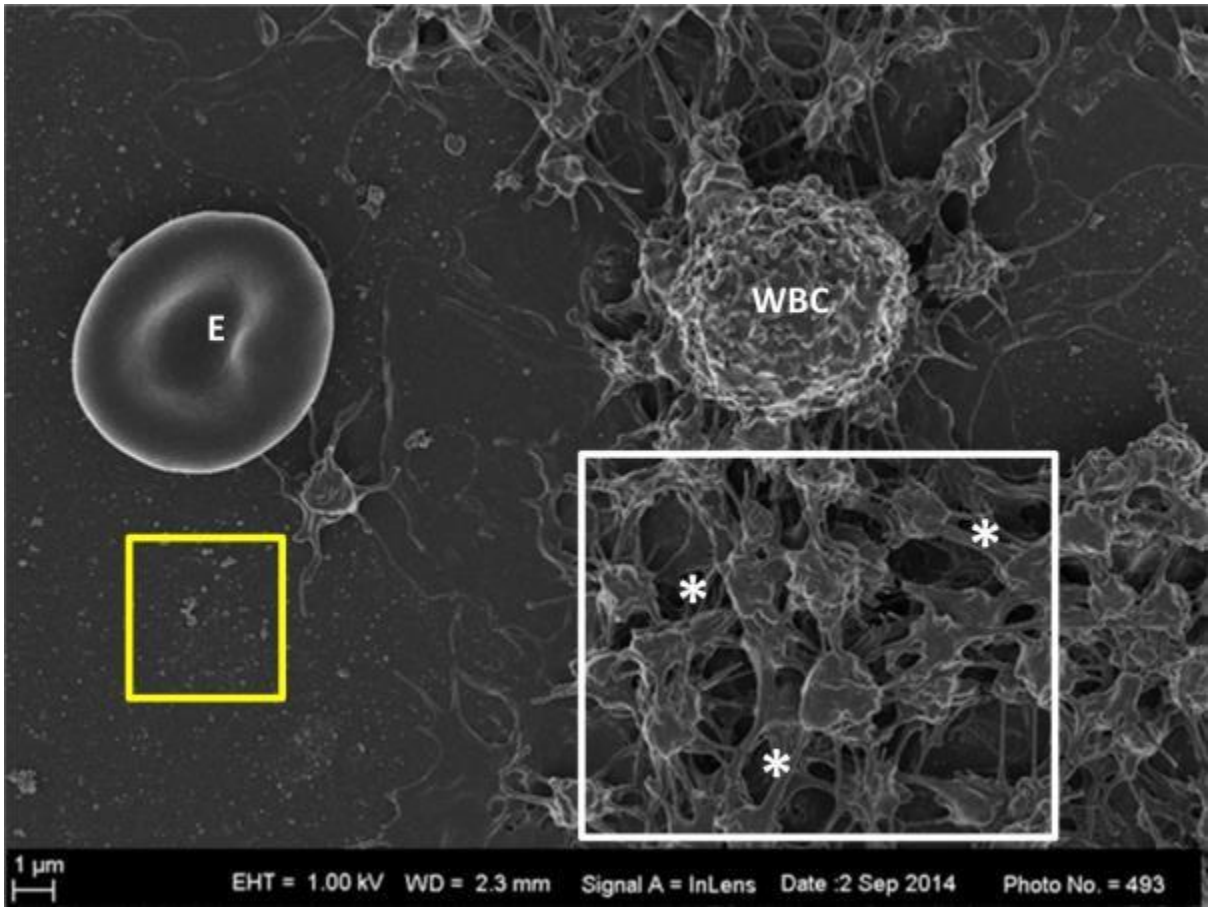


Figure 5.2: A representative electron micrograph displaying a platelet plug which is stabilized by a network of fibrin strands (*) and small microparticles (contained within the yellow square) in the extracellular space. This image further shows the association between platelets and a white blood cell (WBC) and an erythrocyte (E). Photomicrograph imaged by Dr Wendy van der Spuy using a JEOL Scanning Electron Microscope at the University of Pretoria.

5.3.2 Future perspectives

Future studies include investigating the reciprocal interactions of tumour and blood components in preconditioned blood collected from breast cancer patients. This would be done in order to determine the direct effects of hormone and antiplatelet therapies. Liquid biopsies would be collected from cancer patients who are already on hormone therapy or Antiplatelet therapy and molecular markers in blood which indicate thromboembolic disease and tumour progression analysed. In addition, to complement this clinical study, a longer treatment duration *in vitro* may be tested as well in order to determine the long term effects of combined hormone and antiplatelet therapy.

Given the heterogeneity seen in cell line response, it would be worthwhile to characterize molecular markers in these cells and directly examine expression levels of mRNA and translated proteins for ADP receptors and PAR receptors and other regulators of transcription, in order to understand the effects of drug treatment and determine to what extend drug efficacy may be reduced due to breast cancer heterogeneity. The heterogeneity seen between these cell lines is important to note because it may contribute to cancer recurrence in breast cancer patients and thus highlights the need to re-examine treatment strategies even among breast cancers which are molecularly classified as similar but may not respond the same to treatment. Furthermore, it would also be beneficial to identify and characterize subpopulations within each cell line, which may promote resistance and aggressive tumour profile using stem cell markers. Additionally, testing these reciprocal interactions on more aggressive breast tumour subtype like basal-like cell line would be worthwhile.

We also uncovered that CD62p was not always detectable and often lost with the progression of platelet activation due to its role in adhesion, because platelet activation is a quick process, it would be beneficial to add more markers for platelet activation which will be stably expressed and detectable for *in vitro* experimental systems where platelet labelling may not occur rapidly. This might also improve the detection of platelet activation markers at early intervals, and may provide more information regarding the rate of platelet activation induced by various markers. This knowledge would further benefit the clinical application of platelets as diagnostic markers.

5.4 Concluding remarks

In conclusion, we showed that combined Anastrozole and antiplatelet therapy (Aspirin and Clopidogrel cocktail or Atopaxar) promoted hypercoagulation and tumour progression. All treatments induced little cytotoxic effects on breast cancer cells and further highlighted differential response between the cell lines, with T47D cells displaying more resistance to drug treatment by inducing an elevated stress response than MCF7 cells. Low levels of cell migration were induced in both cell lines; with combined Anastrozole with Aspirin and Clopidogrel treatment. In contrast Anastrozole combined with Atopaxar mediated higher migration. Treatment did not promote cell proliferation in T47D cells but induced it in MCF7 cells. Combined Anastrozole with antiplatelet therapy (Aspirin and Clopidogrel/ Atopaxar) mediated a more hypercoagulatory state in MCF7 cells, in contrast, T47D cells may have bound thrombin in order to promote its own survival. In both cell lines, combined therapy induced later stages of platelet activation and this corresponded with high levels of angiogenic factors and growth factors typically released during platelet activation. Tumour survival was not adversely affected with Anastrozole combined with Aspirin and Clopidogrel in both cell lines; however, Anastrozole combined with Atopaxar may modulate inhibitory effects on T47D metastasis and differentiation by reducing epithelial and mesenchymal markers but maintain epithelial phenotype in MCF7 cells.

These findings indicate that the addition of Aspirin and Clopidogrel or Atopaxar to Anastrozole may not yield the desired beneficial effects against thromboembolic disorders but may act as a selective pressure for tumour survival. This effect was not shown to be significantly down regulated by either treatment modality alone (i.e. hormone therapy or antiplatelet therapy). Therefore, it is important to closely monitor disease progression for tumour or thrombosis in breast cancer patients with thromboembolic disease regardless of the treatment modality

because cells display the ability to adapt quickly to various insults and manipulate them to promote their own survival, hence we advise further *in vitro* and *in vivo* studies be done to fully determine these reciprocal effects and caution and close monitoring should this treatment modality be feasible in the future.

References

Adeloye, D. *et al.* (2018) 'Estimating the incidence of breast cancer in Africa: A systematic review and meta-analysis', *Journal of Global Health*, 8(1). doi: 10.7189/jogh.08.010419.

Agnoli, C. *et al.* (2017) 'Biomarkers of inflammation and breast cancer risk: A case-control study nested in the EPIC-Varese cohort', *Scientific Reports*, 7(1), pp. 18–25. doi: 10.1038/s41598-017-12703-x.

Agrawal, A. and Fentiman, I. S. (2008) 'NSAIDs and breast cancer: A possible prevention and treatment strategy', *International Journal of Clinical Practice*, 62(3), pp. 444–449. doi: 10.1111/j.1742-1241.2007.01668.x.

Ahmad, I. and Shagufta (2015) 'Recent developments in steroidal and nonsteroidal aromatase inhibitors for the chemoprevention of estrogen-dependent breast cancer', *European Journal of Medicinal Chemistry*, 102, pp. 375–386. doi: 10.1016/j.ejmech.2015.08.010.

Aka, J. A. and Lin, S. X. (2012) 'Comparison of functional proteomic analyses of human breast cancer cell lines T47D and MCF7', *PLoS ONE*, 7(2), pp. 1–9. doi: 10.1371/journal.pone.0031532.

Akrap, N. *et al.* (2016) 'Identification of Distinct Breast Cancer Stem Cell Populations Based on Single-Cell Analyses of Functionally Enriched Stem and Progenitor Pools', *Stem Cell Reports*, 6(1), pp. 121–136. doi: 10.1016/j.stemcr.2015.12.006.

Aleskandarany, M. A. *et al.* (2014) 'Epithelial mesenchymal transition in early invasive breast cancer: An immunohistochemical and reverse phase protein array study', *Breast Cancer Research and Treatment*, 145(2), pp. 339–348. doi: 10.1007/s10549-014-2927-5.

Algra, A. M. and Rothwell, P. M. (2012) 'Effects of regular aspirin on long-term cancer incidence and metastasis: A systematic comparison of evidence from observational studies versus randomised trials', *The Lancet Oncology*, 13(5), pp. 518–527. doi: 10.1016/S1470-2045(12)70112-2.

Allison, K. H. (2012) 'Molecular pathology of breast cancer: What a pathologist needs to know', *American Journal of Clinical Pathology*, 138(6), pp. 770–780. doi: 10.1309/AJCPIV9IQ1MRQMOO.

Andrae, J., Gallini, R. and Betsholtz, C. (2008) 'Role of platelet-derived growth factors in physiology and medicine', *Genes and Development*, 22(10), pp. 1276–1312. doi: 10.1101/gad.1653708.

Androutsopoulos, V. P., Tsatsakis, A. M. and Spandidos, D. A. (2009) 'Cytochrome P450 CYP1A1: Wider roles in cancer progression and prevention', *BMC Cancer*, 9, pp. 1–17. doi: 10.1186/1471-2407-9-187.

Aonuma, M. *et al.* (1999) 'Vascular endothelial growth factor overproduced by tumour cells acts predominantly as a potent angiogenic factor contributing to malignant progression', *International Journal of Experimental Pathology*, 80(5), pp. 271–281. doi: 10.1046/j.1365-2613.1999.00122.x.

Arab, S. and Hadjati, J. (2019) 'Adenosine blockage in tumor microenvironment and improvement of cancer immunotherapy', *Immune Network*, 19(4), pp. 1–19. doi: 10.4110/in.2019.19.e23.

Araki, K. *et al.* (2011) 'E/N-cadherin switch mediates cancer progression via TGF-β-induced epithelial-to-mesenchymal transition in extrahepatic cholangiocarcinoma', *British Journal of Cancer*, 105(12), pp. 1885–1893. doi: 10.1038/bjc.2011.452.

Aschermann, M. (2013) 'Prevention of arterial and venous thrombosis in cancer patients', *Cor et Vasa*. Elsevier, 55(2), pp. e196–e200. doi: 10.1016/j.crvasa.2013.03.001.

Asghar, S., Parvaiz, F. and Manzoor, S. (2019) 'Multifaceted role of cancer educated platelets in survival of cancer cells', *Thrombosis Research*, 177(February), pp. 42–50. doi:

10.1016/j.thromres.2019.02.026.

Augustine Chen, Henry Beetham, Michael A Black, Rashmi Priya, Bryony J Telford, Joanne Guest, George A R Wiggins, Tanis D Godwin1, A. S. Y. and P. J. G. (2014) 'E-cadherin loss alters cytoskeletal organization and adhesion in non-malignant breast cells but is insufficient to induce an epithelial-mesenchymal transition', *BMC Cancer*, 14, p. 552. doi: 10.1016/j.physbeh.2017.03.040.

Augustine, T. N. *et al.* (2016) 'Thrombin-Mediated Platelet Activation of Lysed Whole Blood and Platelet-Rich Plasma : A Comparison Between Platelet Activation Markers and Ultrastructural Alterations', *Microscopy and Microanalysis* 22(3), pp. 630–639. doi: 10.1017/S1431927616000854.

Awan, A. and Esfahani, K. (2018) 'Endocrine therapy for breast cancer in the primary care setting', *Current Oncology*, 25(4), pp. 285–291. doi: 10.3747/co.25.4139.

Awtry, E. H. and Loscalzo, J. (2014) 'Aspirin', *Circulation*, 101, pp. 1206–1218. doi: 10.1161/01.CIR.101.10.1206.

Azamjah, N., Soltan-Zadeh, Y. and Zayeri, F. (2019) 'Global trend of breast cancer mortality rate: A 25-year study', *Asian Pacific Journal of Cancer Prevention*, 20(7), pp. 2015–2020. doi: 10.31557/APJCP.2019.20.7.2015.

Baaten, C. C. F. M. J. *et al.* (2017) 'Platelet populations and priming in hematological diseases', *Blood Reviews*, 31(6), pp. 389–399. doi: 10.1016/j.blre.2017.07.004.

Baaten, C. C. F. M. J. *et al.* (2018) 'Platelet heterogeneity in activation-induced glycoprotein shedding: Functional effects', *Blood Advances*, 2(18), pp. 2320–2331. doi: 10.1182/bloodadvances.2017011544.

Bae, S. Y. *et al.* (2015) 'Poor prognosis of single hormone receptor- positive breast cancer: Similar outcome as triple-negative breast cancer', *BMC Cancer*, 15(1), pp. 1–9. doi: 10.1186/s12885-015-1121-4.

Bagot, C. N. *et al.* (2010) 'The effect of estrone on thrombin generation may explain the different thrombotic risk between oral and transdermal hormone replacement therapy', *Journal of Thrombosis and Haemostasis*, 8(8), pp. 1736–1744. doi: 10.1111/j.1538-7836.2010.03953.x.

Baguley, B. C. and Leung, E. (1995) 'Heterogeneity of Phenotype in Breast Cancer Cell Lines' *Breast Cancer – Carcinogenesis, Cell Growth and Signalling Pathways*, IntechOpen, pg 245-252.

Ballerini, P. *et al.* (2018) 'P2Y 12 Receptors in Tumorigenesis and Metastasis', *Frontiers in Pharmacology*, 9(February 2018), pp. 1–8. doi: 10.3389/fphar.2018.00066.

Bambace, N. M. and Holmes, C. E. (2011) 'The platelet contribution to cancer progression.', *Journal of thrombosis and haemostasis : JTH*, 9(2), pp. 237–49. doi: 10.1111/j.1538-7836.2010.04131.x.

Barabutis, N. *et al.* (2007) 'Stimulation of proliferation of MCF-7 breast cancer cells by a transfected splice variant of growth hormone-releasing hormone receptor', *Proceedings of the National Academy of Sciences of the United States of America*, 104(13), pp. 5575–5579. doi: 10.1073/pnas.0700407104.

Barros-Oliveira, M. *et al.* (2017) 'Use of anastrozole in the chemoprevention and treatment of breast cancer: A literature review', *Revista da Associacao Medica Brasileira*, 63(4), pp. 371–378. doi: 10.1590/1806-9282.63.04.371.

Barthel, S. R. *et al.* (2007) 'Targeting selectins and selectin ligands in inflammation and cancer', *Expert Opin Ther Targets*, 11(11), pp. 1473–1491. doi: 10.1517/14728222.11.11.1473.

Basheer, L. and Kerem, Z. (2015) 'Interactions between CYP3A4 and Dietary Polyphenols', *Oxidative*

Medicine and Cellular Longevity, 2015. doi: 10.1155/2015/854015.

Baxi, S. M. *et al.* (2012) 'Targeting 3-Phosphoinoside-Dependent Kinase-1 to Inhibit Insulin-Like Growth Factor-I Induced AKT and p70 S6 Kinase Activation in Breast Cancer Cells', *PLoS ONE*, 7(10). doi: 10.1371/journal.pone.0048402.

Bearer, E.L., Prakash, J.M. and Li, Z. (2002) 'Actin Dynamics in Platelets', *Int Rev Cytol*, 217(1), pp. 137–182. doi: 10.1038/jid.2014.371.

Van Den Berg, Y. W. *et al.* (2012) 'The relationship between tissue factor and cancer progression: Insights from bench and bedside', *Blood*, 119(4), pp. 924–932. doi: 10.1182/blood-2011-06-317685.

Bergh, J. *et al.* (2012) 'FACT: An open-label randomized phase III study of fulvestrant and anastrozole in combination compared with anastrozole alone as first-line therapy for patients with receptor-positive postmenopausal breast cancer', *Journal of Clinical Oncology*, 30(16), pp. 1919–1925. doi: 10.1200/JCO.2011.38.1095.

Berndt, M. C., Metharom, P. and Andrews, R. K. (2014) 'Primary haemostasis: Newer insights', *Haemophilia*, 20(S4), pp. 15–22. doi: 10.1111/hae.12427.

Bhatt, D. L. *et al.* (2006) 'Clopidogrel and aspirin versus aspirin alone for the prevention of atherothrombotic events', *New England Journal of Medicine*, 354(16), pp. 1706–1717. doi: 10.1056/NEJMoa060989.

Bhuminder Singh, and R. J. C. (2014) 'From wavy hair to naked proteins: The role of transforming growth factor alpha in health and disease', *Semin Cell Dev Biol*, 28, pp. 12–21. doi: 10.1016/j.semcdb.2014.03.003.

Blair, P. and Flaumenhaft, R. (2009) 'Platelet α-granules: Basic biology and clinical correlates', *Blood Reviews*, 23(4), pp. 177–189. doi: 10.1016/j.blre.2009.04.001.

Blann, A. D. and Dunmore, S. (2011) 'Arterial and venous thrombosis in cancer patients.', *Cardiology research and practice*, 2011, p. 394740. doi: 10.4061/2011/394740.

Blaschuk, O. W. (2015) 'N-cadherin antagonists as oncology therapeutics', *Philosophical Transactions of the Royal Society B: Biological Sciences*, 370(1661), pp. 8–11. doi: 10.1098/rstb.2014.0039.

Boilard, E. *et al.* (2010) 'Platelets Amplify Inflammation in Arthritis via Collagen- Dependent Microparticle Production', *Science,* 327(5965), pp. 580–583. doi: 10.1126/science.1181928.Platelets.

Broos, K. *et al.* (2011) 'Platelets at work in primary hemostasis.', *Blood reviews*, 25(4), pp. 155–67. doi: 10.1016/j.blre.2011.03.002.

Bruno, A. *et al.* (2018) 'Antithrombotic agents and cancer', *Cancers*, 10(8), pp. 1–22. doi: 10.3390/cancers10080253.

Bruno, R. D. and Njar, V. C. O. (2007) 'Targeting cytochrome P450 enzymes: A new approach in anti-cancer drug development', *Bioorganic and Medicinal Chemistry*, 15(15), pp. 5047–5060. doi: 10.1016/j.bmc.2007.05.046.

Brzoska, T. *et al.* (2013) 'Binding of thrombin-activated platelets to a fibrin scaffold through $\alpha(IIb)\beta_3$ evokes phosphatidylserine exposure on their cell surface.', *PloS one*, 8(2), p. e55466. doi: 10.1371/journal.pone.0055466.

Buergy, D. *et al.* (2012) 'Tumor-platelet interaction in solid tumors', *International Journal of Cancer*, 130(12), pp. 2747–2760. doi: 10.1002/ijc.27441.

Burnstock, G. (2017) 'Purinergic Signaling in the Cardiovascular System', *Circulation Research* , pp. 207–228. doi: 10.1161/CIRCRESAHA.116.309726.

Burnstock, G. and Di Virgilio, F. (2013) 'Purinergic signalling and cancer', *Purinergic Signalling*, 9(4), pp. 491–540. doi: 10.1007/s11302-013-9372-5.

Cadavid, A. P. (2017) 'Aspirin: The mechanism of action revisited in the context of pregnancy complications', *Frontiers in Immunology*, 8(MAR). doi: 10.3389/fimmu.2017.00261.

Campagnoli, C. *et al.* (2013) 'Postmenopausal breast cancer, androgens, and aromatase inhibitors', *Breast Cancer Research and Treatment*, 139(1), pp. 1–11. doi: 10.1007/s10549-013-2505-2.

Capodanno, D., Ferreiro, J. L. and Angiolillo, D. J. (2013) 'Antiplatelet therapy: New pharmacological agents and changing paradigms', *Journal of Thrombosis and Haemostasis*, 11(SUPPL.1), pp. 316–329. doi: 10.1111/jth.12219.

CAPRIE et al. (2001) 'Effects of clopidogrel in addition to aspirin in patientswith acute coronary syndromes without ST-segment elevation ', *The new england journal of medicine*, 345(7), pp. 494–502.

Caprioli, M. *et al.* (2017) 'Influence of aromatase inhibitors therapy on the occurrence of rheumatoid arthritis in women with breast cancer: Results from a large population-based study of the Italian Society for Rheumatology', *RMD Open*, 3(2), pp. 1–5. doi: 10.1136/rmdopen-2017-000523.

ten Cate, H. and Hemker, H. C. (2016) 'Thrombin Generation and Atherothrombosis: What Does the Evidence Indicate?', *Journal of the American Heart Association*, 5(8), pp. 1–8. doi: 10.1161/JAHA.116.003553.

Cattaneo, M. *et al.* (2014) 'Adenosine-Mediated Effects of Ticagrelor Evidence and Potential Clinical Relevance', *Journal of the American College of Cardiology*, 63(23), pp. 2503–2509. doi: 10.1016/j.jacc.2014.03.031.

Cedervall, J., Hamidi, A. and Olsson, A. K. (2018) 'Platelets, NETs and cancer', *Thrombosis Research*. Elsevier, 164(December 2017), pp. S148–S152. doi: 10.1016/j.thromres.2018.01.049.

Chadha, A. S. *et al.* (2015) 'Paraneoplastic thrombocytosis independently predicts poor prognosis in patients with locally advanced pancreatic cancer', *Acta Oncologica*, 54(7), pp. 971–978. doi: 10.3109/0284186X.2014.1000466.

Charis Costopoulos a, Maria Niespialowska-Steuden a, Neville Kukreja a, Diana A. Gorog a,b,c (2013) 'Novel oral anticoagulants after an acute coronary syndrome', *International Journal of Cardiology*, 167(4), pp. 2449–2455. doi: 10.1016/j.ijcard.2012.08.014.

Chater, C. *et al.* (2018) 'Intraplatelet Vascular Endothelial Growth Factor and Platelet-Derived Growth Factor: New Biomarkers in Carcinoembryonic Antigen-Negative Colorectal Cancer?', *Gastrointestinal Tumors*, 5(1–2), pp. 32–37. doi: 10.1159/000486894.

Chatterjee, S., Sharma, A. and Mukherjee, D. (2013) 'PAR-1 antagonists: current state of evidence.', *Journal of thrombosis and thrombolysis*, 35(1), pp. 1–9. doi: 10.1007/s11239-012-0752-4.

Chekhun, S. *et al.* (2013) 'Expression of biomarkers related to cell adhesion, metastasis and invasion of breast cancer cell lines of different molecular subtype', *Experimental Oncology*, 35(3), pp. 174–179.

Chen, A. *et al.* (2014) 'E-cadherin loss alters cytoskeletal organization and adhesion in non-malignant breast cells but is insufficient to induce an epithelial-mesenchymal transition', *BMC Cancer*, 14(1), pp.

1–14. doi: 10.1186/1471-2407-14-552.

Chen, R. *et al.* (2015) 'Antiproliferative effects of anastrozole on MCF-7 human breast cancer cells in vitro are significantly enhanced by combined treatment with testosterone undecanoate', *Molecular Medicine Reports*, 12(1), pp. 769–775. doi: 10.3892/mmr.2015.3427.

Chen, X. *et al.* (2018) 'Double-sided effect of tumor microenvironment on platelets targeting nanoparticles', *Biomaterials*, 183, pp. 258–267. doi: 10.1016/j.biomaterials.2018.07.005.

Chirinos, J. a *et al.* (2005) 'Elevation of endothelial microparticles, platelets, and leukocyte activation in patients with venous thromboembolism.', *Journal of the American College of Cardiology*, 45(9), pp. 1467–71. doi: 10.1016/j.jacc.2004.12.075.

Chopra, S. *et al.* (2018) 'Do Different Stemness Markers Identify Different Pools of Cancer Stem Cells in Malignancies: A Study on ER+ and ER-Breast Cancer Cell Lines', *Pathology and Oncology Research*. Pathology & Oncology Research. doi: 10.1007/s12253-018-0503-8.

Choudhury, A. *et al.* (2007) 'Platelet Surface CD62P and CD63 , Mean Platelet Volume , and Soluble / Platelet P-Selectin as Indexes of Platelet Function in Atrial Fibrillation and " Disease Control Subjects " in Sinus Rhythm', 49(19). doi: 10.1016/j.jacc.2007.02.038.

Christiansen, J. J. and Rajasekaran, A. K. (2006) 'Reassessing epithelial to mesenchymal transition as a prerequisite for carcinoma invasion and metastasis', *Cancer Research*, 66(17), pp. 8319–8326. doi: 10.1158/0008-5472.CAN-06-0410.

Chumsri, S., Howes, T., Bao,T., Sabnis, G. and Brodie, A. (2011) 'Aromatase, Aromatase Inhibitors, and Breast Cancer', *J Steroid Biochen Mol Biol*, 125(1), pp. 13–22. doi: 10.1016/j.jsbmb.2011.02.001.

Clemetson, K. J. (2012) 'Platelets and primary haemostasis', *Thrombosis Research*, 129(3), pp. 220–224. doi: 10.1016/j.thromres.2011.11.036.

Coffey, R. J. *et al.* (2007) 'Ménétrier disease and gastrointestinal stromal tumors: Hyperproliferative disorders of the stomach', *Journal of Clinical Investigation*, 117(1), pp. 70–80. doi: 10.1172/JCI30491.

Coimbra, L. S. *et al.* (2015) 'Clopidogrel enhances mesenchymal stem cell proliferation following periodontitis', *Journal of Dental Research*, 94(12), pp. 1691–1697. doi: 10.1177/0022034515598273.

Colás-Algora, N. and Millán, J. (2019) 'How many cadherins do human endothelial cells express?', *Cellular and Molecular Life Sciences*. Springer International Publishing, 76(7), pp. 1299–1317. doi: 10.1007/s00018-018-2991-9.

Colciago, A. *et al.* (2009) 'In vitro effects of PDGF isoforms (AA, BB, AB and CC) on migration and proliferation of SaOS-2 osteoblasts and on migration of human osteoblasts', *International Journal of Biomedical Science*, 5(4), pp. 380–389.

Comşa, Ş., Cîmpean, A. M. and Raica, M. (2015) 'The story of MCF-7 breast cancer cell line: 40 Years of experience in research', *Anticancer Research*, 35(6), pp. 3147–3154.

Connolly, J. *et al.* (2009) 'Effect of Clopidogrel Added to Aspirin in Patients with Atrial Fibrillation'.

Costa, B. *et al.* (2019) 'Intratumoral platelet aggregate formation in a murine preclinical glioma model depends on podoplanin expression on tumor cells', *Blood Advances*, 3(7), pp. 1092–1102. doi: 10.1182/bloodadvances.2018015966.

Coupland, L. A. and Parish, C. R. (2014) 'Platelets, selectins, and the control of tumor metastasis', *Seminars in Oncology*. Elsevier, 41(3), pp. 422–434. doi: 10.1053/j.seminoncol.2014.04.003.

Courtney A G and Domchek, and S. M. (2010) 'Breast cancer in young women', *Breast Cancer Research*, 12, pp. 1–10. doi: 10.5603/GP.2016.0062.

Covic, L. and Kuliopulos, A. (2018) 'Protease-activated receptor 1 as therapeutic target in breast, lung, and ovarian cancer: Pepducin approach', *International Journal of Molecular Sciences*, 19(8), pp. 1–16. doi: 10.3390/ijms19082237.

Cui, J., Shen, Y. and Li, R. (2013) 'Estrogen synthesis and signaling pathways during aging: From periphery to brain', *Trends in Molecular Medicine*, 19(3), pp. 197–209. doi: 10.1016/j.molmed.2012.12.007.

Cuzick, J., Sestak, I., *et al.* (2014) 'Anastrozole for prevention of breast cancer in high-risk postmenopausal women (IBIS-II): An international, double-blind, randomised placebo-controlled trial', *The Lancet*, 383, pp. 1041–1048. doi: 10.1016/S0140-6736(13)62292-8.

Cuzick, J., Thorat, M. A., *et al.* (2014) 'Estimates of benefits and harms of prophylactic use of aspirin in the general population', *Annals of Oncology*, 00, pp. 1–10. doi: 10.1093/annonc/mdu225.

Cuzick, J. *et al.* (2020) 'Use of anastrozole for breast cancer prevention (IBIS-II): long-term results of a randomised controlled trial', *The Lancet*, 395(10218), pp. 117–122. doi: 10.1016/S0140-6736(19)32955-1.

D'Anselmi, F. *et al.* (2013) 'Microenvironment promotes tumor cell reprogramming in human breast cancer cell lines', *PLoS ONE*, 8(12), pp. 1–12. doi: 10.1371/journal.pone.0083770.

Dai, X. *et al.* (2017) 'Breast cancer cell line classification and Its relevance with breast tumor subtyping', *Journal of Cancer*, 8(16), pp. 3131–3141. doi: 10.7150/jca.18457.

Date, K. *et al.* (2013) 'Tumour and microparticle tissue factor expression and cancer thrombosis', *Thrombosis Research*, 131(2), pp. 109–115. doi: 10.1016/j.thromres.2012.11.013.

Deitcher, S. R. and Gomes, M. P. V. (2004) 'The risk of venous thromboembolic disease associated with adjuvant hormone therapy for breast carcinoma: A systematic review', *Cancer*, 101(3), pp. 439–449. doi: 10.1002/cncr.20347.

Deng, R. *et al.* (2014) 'Breast Cancer Dimethyl Sulfoxide Suppresses Mouse 4T1 Breast Cancer Growth by Modulating Tumor-Associated Macrophage Differentiation', 17(1), pp. 25–32.

Denslow, A. *et al.* (2017)'Clopidogrel in a combined therapy with anticancer drugs—effect on tumor growth, metastasis, and treatment toxicity: Studies in animal models', *PLoS ONE*. doi: 10.1371/journal.pone.0188740.

De Placido, S. , Gallo, G., De Laurentiis, M., Bisagni, G., Arpino, G., et al. (2018) 'Adjuvant anastrozole versus exemestrane versus letrozole upfront or after 2 years of tamoxifen in endocrine-sensitive breast cancer (FATA-GIM 3): a randomised phase 3 trial' *Lancet Oncol,* 19, pp.474-85. doi: 10.1016/s1470-2045 (18) 30116-5.

Derycke, L. *et al.* (2006) 'Soluble N-cadherin in human biological fluids', *International Journal of Cancer*, 119(12), pp. 2895–2900. doi: 10.1002/ijc.22219.

Deryugina, E. I. and Quigley, J. P. (2006) 'Matrix metalloproteinases and tumor metastasis', *Cancer and Metastasis Reviews*, 25(1), pp. 9–34. doi: 10.1007/s10555-006-7886-9.

Devarajan, E. *et al.* (2012) 'Epithelial-mesenchymal transition in breast cancer lines is mediated through PDGF-D released by tissue-resident stem cells', *International Journal of Cancer*, 131(5), pp.

1023–1031. doi: 10.1002/ijc.26493.

Diaz, J. *et al.* (2012) 'Progesterone promotes focal adhesion formation and migration in breast cancer cells through induction of protease-activated receptor-1', *Journal of Endocrinology*, 214(2), pp. 165–175. doi: 10.1530/JOE-11-0310.

Dineen, S. P. *et al.* (2009) 'The Acellular Fraction of Stored Platelets Promotes Tumor Cell Invasion', *Journal of Surgical Research*, 153(1), pp. 132–137. doi: 10.1016/j.jss.2008.04.013.

Doane, A. S. *et al.* (2006) 'An estrogen receptor-negative breast cancer subset characterized by a hormonally regulated transcriptional program and response to androgen', *Oncogene*, 25(28), pp. 3994–4008. doi: 10.1038/sj.onc.1209415.

Dolan, A. T. and Diamond, S. L. (2014) 'Systems Modeling of Ca 2 D Homeostasis and Mobilization in Platelets Mediated by IP 3 and Store-Operated Ca 2 D Entry', *Biophysj*, 106(9), pp. 2049–2060. doi: 10.1016/j.bpj.2014.03.028.

Donnellan, E. and Khorana, A. A. (2017) 'Cancer and Venous Thromboembolic Disease: A Review', *The Oncologist*, 22(2), pp. 199–207. doi: 10.1634/theoncologist.2016-0214.

van Dooren, F. H., Duijvis, N. W. and te Velde, A. a (2013) 'Analysis of cytokines and chemokines produced by whole blood, peripheral mononuclear and polymorphonuclear cells.', *Journal of immunological methods*, 396(1–2), pp. 128–33. doi: 10.1016/j.jim.2013.08.006.

Dowset and Early breast cancer trialists collaborative group. (2015) 'Aromatase inhibitors versus tamoxifen in early breast cancer: patient-level meta analysis of the randomised trial', *Lancet*, 386: 1341-42. doi: 10.1016/s60140-6736 (15) 61074-1.

Du, T. and Tan, Z. (2014) 'Relationship between deep venous thrombosis and inflammatory cytokines in postoperative patients with malignant abdominal tumors', 47, pp. 1003–1007.

Dupuis, M. *et al.* (2019) 'Effects of estrogens on platelets and megakaryocytes', *International Journal of Molecular Sciences*, 20(12), pp. 1–10. doi: 10.3390/ijms20123111.

Duvernoy, C. S. *et al.* (2010) 'Antiplatelet therapy use and the risk of venous thromboembolic events in the raloxifene use for the heart (RUTH) trial', *Journal of Women's Health*, 19(8), pp. 1459–1465. doi: 10.1089/jwh.2009.1687.

Eeckhoute, J. *et al.* (2006) 'A cell-type-specific transcriptional network required for estrogen regulation of cyclin D1 and cell cycle progression in breast cancer', *Genes and Development*, 20(18), pp. 2513–2526. doi: 10.1101/gad.1446006.

Egan, K., Crowley, D., Smyth, P., Toole, S. O., *et al.* (2011) 'Platelet Adhesion and Degranulation Induce Pro-Survival and Pro-Angiogenic Signalling in Ovarian Cancer Cells', *PloS one*, 6(10), p. e26125. doi: 10.1371/journal.pone.0026125.

Eikelboom, J. W. *et al.* (2012) 'Antiplatelet drugs - Antithrombotic therapy and prevention of thrombosis, 9th ed: American College of Chest Physicians evidence-based clinical practice guidelines', *Chest*, 141(2 SUPPL.), pp. e89S-e119S. doi: 10.1378/chest.11-2293.

Elaskalani, O. *et al.* (2017) 'Targeting platelets for the treatment of cancer', *Cancers*, 9(7). doi: 10.3390/cancers9070094.

Eliyatkin, N. *et al.* (2015) 'Molecular Classification of Breast Carcinoma: From Traditional, Old-Fashioned Way to A New Age, and A New Way', *Journal of Breast Health*, 11(2), pp. 59–66. doi:

10.5152/tjbh.2015.1669.

Elmariah, S. *et al.* (2018) 'Impact of Clopidogrel Therapy on Mortality and Cancer in Patients with Cardiovascular and Cerebrovascular Disease: A Patient-Level Meta-Analysis', *Circulation: Cardiovascular Interventions*, 11(1). doi: 10.1161/CIRCINTERVENTIONS.117.005795.

Elwood, P. C. *et al.* (2009) 'Aspirin, salicylates, and cancer', *The Lancet*, 373(9671), pp. 1301–1309. doi: 10.1016/S0140-6736(09)60243-9.

Elyamany, G., Alzahrani, A. M. and Bukhary, E. (2014) 'Cancer-associated thrombosis: An overview', *Clinical Medicine Insights: Oncology*, 8, pp. 129–137. doi: 10.4137/CMO.S18991.

Erpenbeck, L. and Schön, M. P. (2010) 'Deadly allies: The fatal interplay between platelets and metastasizing cancer cells', *Blood*, 115(17), pp. 3427–3436. doi: 10.1182/blood-2009-10-247296.

Estevez, B. *et al.* (2016) 'Signaling-mediated cooperativity between glycoprotein Ib-IX and protease-Activated receptors in thrombin-induced platelet activation', *Blood*, 127(5), pp. 626–636. doi: 10.1182/blood-2015-04-638387.

Even-ram, S. C. *et al.* (2001) 'Tumor Cell Invasion Is Promoted by Activation of Protease Activated Receptor-1 in Cooperation with the ⎵v␋5 Integrin', *The Journal of Biological Chemistry*, 276(14), pp. 10952–10962. doi: 10.1074/jbc.M007027200.

Fabian, C. J. (2007) 'The what , why and how of aromatase inhibitors : hormonal agents for treatment and prevention of breast cancer', *Int J Clin Pract*, (December), pp. 2051–2063. doi: 10.1111/j.1742-1241.2007.01587.x.

Fackler, O. T. and Grosse, R. (2008) 'Cell motility through plasma membrane blebbing', *Journal of Cell Biology*, 181(6), pp. 879–884. doi: 10.1083/jcb.200802081.

Falanga, a and Donati, M. B. (2001) 'Pathogenesis of thrombosis in patients with malignancy.', *International journal of hematology*, 73(2), pp. 137–44. Available at: http://www.ncbi.nlm.nih.gov/pubmed/11372723.

Farooqi, A. A. and Siddik, Z. H. (2015) 'Platelet-derived growth factor (PDGF) signalling in cancer: Rapidly emerging signalling landscape', *Cell Biochemistry and Function*, 33(5), pp. 257–265. doi: 10.1002/cbf.3120.

Fennerty, A. (2006) 'Venous thromboembolic disease and cancer', *Postgraduate Medical Journal*, 82(972), pp. 642–648. doi: 10.1136/pgmj.2006.046987.

Ferlay, J. *et al.* (2015) 'Cancer incidence and mortality worldwide: Sources, methods and major patterns in GLOBOCAN 2012', *International Journal of Cancer*, 136(5), pp. E359–E386. doi: 10.1002/ijc.29210.

Fernandez-Cortes, M., Delgado-Bellido, D., Olivier, F.J. (2019) 'Vasculogenic mimicry: become an endothelial cell "But not so much"', *Front Oncol,* 9" 803. doi: 10.3389/fonc.201.

Ferreiro, J. L. and Angiolillo, D. J. (2012) 'New directions in antiplatelet therapy.', *Circulation. Cardiovascular interventions*, 5(3), pp. 433–45. doi: 10.1161/CIRCINTERVENTIONS.111.966176.

Filkova, A. A. *et al.* (2019) 'Quantitative dynamics of reversible platelet aggregation: mathematical modelling and experiments', *Scientific Reports*, 9(1), pp. 1–9. doi: 10.1038/s41598-019-42701-0.

Fillmore, C. M. and Kuperwasser, C. (2008) 'Human breast cancer cell lines contain stem-like cells that

self-renew, give rise to phenotypically diverse progeny and survive chemotherapy', *Breast Cancer Research*, 10(2), pp. 1–13. doi: 10.1186/bcr1982.

Flaumenhaft, R. *et al.* (2017) 'Targeting PAR1: Now what?', *Trends in pharmacological sciences* 38(8), pp. 701–716. doi: 10.1016/j.tips.2017.05.001.

Foley, C. J. *et al.* (2012) 'Matrix metalloprotease-1a promotes tumorigenesis and metastasis', *Journal of Biological Chemistry*, 287(29), pp. 24330–24338. doi: 10.1074/jbc.M112.356303.

Formenti, S. C. *et al.* (2018) 'Focal irradiation and systemic TGFb blockade in metastatic breast cancer', *Clinical Cancer Research*, 24(11), pp. 2493–2504. doi: 10.1158/1078-0432.CCR-17-3322.

Fouad, Y.A., Aanei, C. (2017) 'Revisiting the hallmarks of cancer', *American Journal of Cancer Research*, 7, pp. 1016-1036.

Frangogiannis, N. G. (2008) 'The immune system and cardiac repair', *Pharmacological Research*, 58, pp. 88–111. doi: 10.1016/j.phrs.2008.06.007.

Friedl, P. and Alexander, S. (2011) 'Cancer invasion and the microenvironment: Plasticity and reciprocity', *Cell*, 147(5), pp. 992–1009. doi: 10.1016/j.cell.2011.11.016.

Fuentes, E., Palomo, I. and Rojas, A. (2016) 'Cross-talk between platelet and tumor microenvironment: Role of multiligand/RAGE axis in platelet activation', *Blood Reviews*, 30(3), pp. 213–221. doi: 10.1016/j.blre.2015.11.005.

Gallego-Muñoz, P. *et al.* (2018) 'Human corneal fibroblast migration and extracellular matrix synthesis during stromal repair: Role played by platelet-derived growth factor-BB, basic fibroblast growth factor, and transforming growth factor-β1', *Journal of Tissue Engineering and Regenerative Medicine*, 12(2), pp. e737–e746. doi: 10.1002/term.2360.

Geisler, J. (2011) 'Differences between the non-steroidal aromatase inhibitors anastrozole and letrozole--of clinical importance?', *British journal of cancer*, 104(7), pp. 1059–1066. doi: 10.1038/bjc.2011.58.

Gervaso, L. *et al.* (2019) 'Venous thromboembolism in breast cancer patients receiving cyclin-dependent kinase inhibitors', *Journal of Thrombosis and Haemostasis*, (August), pp. 1–7. doi: 10.1111/jth.14630.

Gest, C. *et al.* (2013) 'Rac3 induces a molecular pathway triggering breast cancer cell aggressiveness: Differences in MDA-MB-231 and MCF-7 breast cancer cell lines', *BMC Cancer*, 13. doi: 10.1186/1471-2407-13-63.

Ghoshal, K. and Bhattacharyya, M. (2014) 'Overview of platelet physiology: Its hemostatic and nonhemostatic role in disease pathogenesis', *The Scientific World Journal*, 2014. doi: 10.1155/2014/781857.

Gierach, G. L. *et al.* (2008) 'Nonsteroidal anti-inflammatory drugs and breast cancer risk in the National Institutes of Health-AARP Diet and Health Study', *Breast Cancer Research*, 10(2), pp. 1–13. doi: 10.1186/bcr2089.

Giordano, S. H. (2005) 'A Review of the Diagnosis and Management of Male Breast Cancer', *The Oncologist*, 10(7), pp. 471–479. doi: 10.1634/theoncologist.10-7-471.

Girgert, R., Emons, G. and Gründker, C. (2019) 'Estrogen signaling in ERα-negative breast cancer: ERβ and GPER', *Frontiers in Endocrinology*, 10(JAN), pp. 1–12. doi: 10.3389/fendo.2018.00781.

Giudice, A. *et al.* (2019) 'Dissecting the prevention of estrogen-dependent breast carcinogenesis through Nrf2-dependent and independent mechanisms', *OncoTargets and Therapy*, 12, pp. 4937–4953. doi: 10.2147/OTT.S183192.

Göbel, K. *et al.* (2018) 'The coagulation factors fibrinogen, thrombin, and factor XII in inflammatory disorders-a systematic review', *Frontiers in Immunology*, 9(JUL). doi: 10.3389/fimmu.2018.01731.

Golebiewska, E. M. and Poole, A. W. (2015) 'Platelet secretion: From haemostasis to wound healing and beyond', *Blood Reviews*, 29(3), pp. 153–162. doi: 10.1016/j.blre.2014.10.003.

Gomes, F. G. *et al.* (2017) 'Breast-cancer extracellular vesicles induce platelet activation and aggregation by tissue factor-independent and -dependent mechanisms', *Thrombosis Research*, 159(September), pp. 24–32. doi: 10.1016/j.thromres.2017.09.019.

Goni, R., García, P. and Foissac, S. (2009) 'The qPCR data statistical analysis', *Integromics SL*, 1, pp. 1–9.

Goto, S. *et al.* (2010) 'Double-blind , placebo-controlled Phase II studies of the protease-activated receptor 1 antagonist E5555 (atopaxar) in Japanese patients with acute coronary syndrome or high-risk coronary artery disease', *European Heart Journal*, 31, pp. 2601–2613. doi: 10.1093/eurheartj/ehq320.

Goubran, H. A. *et al.* (2013) 'European Journal of Internal Medicine The platelet – cancer loop', *European Journal of Internal Medicine*, 24(5), pp. 393–400. doi: 10.1016/j.ejim.2013.01.017.

Grada, A. *et al.* (2018) 'Research Techniques Made Simple : Analysis of Collective Cell Migration Using the Wound Healing Assay', *Journal of Investigative Dermatology*, 137(2), pp. e11–e16. doi: 10.1016/j.jid.2016.11.020.

Grosse-Wilde, A. *et al.* (2015) 'Stemness of the hybrid epithelial/mesenchymal state in breast cancer and its association with poor survival', *PLoS ONE*, 10(5), pp. 1–28. doi: 10.1371/journal.pone.0126522.

Gruba, S. M. *et al.* (2015) 'Platelet membrane variations and their effects on δ-granule secretion kinetics and aggregation spreading among different species', *Biochimica et Biophysica Acta - Biomembranes*, 1848(7), pp. 1609–1618. doi: 10.1016/j.bbamem.2015.04.006.

Guan, X. (2015) 'Cancer metastases: Challenges and opportunities', *Acta Pharmaceutica Sinica B*, 5(5), pp. 402–418. doi: 10.1016/j.apsb.2015.07.005.

Guillem-Llobat, P. *et al.* (2016) 'Aspirin prevents colorectal cancer metastasis in mice by splitting the crosstalk between platelets and tumor cells', *Oncotarget*, 7(22), pp. 32462–32477. doi: 10.18632/oncotarget.8655.

Guo, S. and Deng, C. X. (2018) 'Effect of stromal cells in tumor microenvironment on metastasis initiation', *International Journal of Biological Sciences*, 14(14), pp. 2083–2093. doi: 10.7150/ijbs.25720.

Haase, I., Czarnetzki, B. M. and Rosenbach, T. (1996) 'Thrombin and melittin activate phospholipase C in human HaCaT keratinocytes', *Experimental Dermatology*, 5(2), pp. 84–88. doi: 10.1111/j.1600-0625.1996.tb00099.x.

Hachim, Mahmood Y. *et al.* (2018) 'Differential expression of TGFβ isoforms in breast cancer highlights different roles during breast cancer progression', *Tumor Biology*, 40(2018), pp. 1–12. doi: 10.1177/1010428317748254.

Haddad, T. C. and Greeno, E. W. (2006) 'Chemotherapy-induced thrombosis.', *Thrombosis research*, 118(5), pp. 555–68. doi: 10.1016/j.thromres.2005.10.015.

Haemmerle, M. *et al.* (2018) 'The Platelet Lifeline to Cancer: Challenges and Opportunities', *Cancer Cell*, 33(6), pp. 965–983. doi: 10.1016/j.ccell.2018.03.002.

Halbleib, J. M. and Nelson, W. J. (2006) 'Cadherins in development : cell adhesion , sorting , and tissue morphogenesis', *Genes and Development*, 20, pp. 3199–3214. doi: 10.1101/gad.1486806.ments.

Haldosén, L. A., Zhao, C. and Dahlman-Wright, K. (2014) 'Estrogen receptor beta in breast cancer', *Molecular and Cellular Endocrinology*, 382(1), pp. 665–672. doi: 10.1016/j.mce.2013.08.005.

Han, E. H. *et al.* (2010) 'Prostaglandin E2 induces CYP1B1 expression via ligand-independent activation of the ERα pathway in human breast cancer cells', *Toxicological Sciences*, 114(2), pp. 204–216. doi: 10.1093/toxsci/kfq013.

Han, N. *et al.* (2011) 'Protease-activated receptors in cancer: A systematic review', *Oncology Letters*, 2(4), pp. 599–608. doi: 10.3892/ol.2011.291.

Harris, R. E., Beebe-Donk, J. and Alshafie, G. A. (2007) 'Reduction in the risk of human breast cancer by selective cyclooxygenase-2 (COX-2) inhibitors: Final results of a case control study', *International Journal of Cancer Prevention*, 3(1–2), pp. 1–7.

He, P. *et al.* (2019) 'Timely and large dose of clotting factor IX provides better joint wound healing after hemarthrosis in hemophilia B mice', *International Journal of Hematology*, 110(1), pp. 59–68. doi: 10.1007/s12185-019-02639-5.

Hechler, B. and Gachet, C. (2015) 'Purinergic Receptors in Thrombosis and Inflammation', *Arteriosclerosis, thrombosis, and vascular biology*, 35, pp. 2307–2315. doi: 10.1161/ATVBAHA.115.303395.

Heijnen, H. and van der Sluijs, P. (2015) 'Platelet secretory behaviour: As diverse as the granules... or not?', *Journal of Thrombosis and Haemostasis*, 13(12), pp. 2141–2151. doi: 10.1111/jth.13147.

Heldin, C. (2013) 'Targeting the PDGF signaling pathway in tumor treatment', *Cell communication and signalling*, 11, pp. 1–18.

Heldin, C. H., Lennartsson, J. and Westermark, B. (2018) 'Involvement of platelet-derived growth factor ligands and receptors in tumorigenesis', *Journal of Internal Medicine*, 283(1), pp. 16–44. doi: 10.1111/joim.12690.

Hellemans, J. *et al.* (2007) 'qBase relative quantification framework and software for management and automated analysis of real-time quantitative PCR data', *Genome Biology*, 8(2). doi: 10.1186/gb-2007-8-2-r19.

Henry, N. L. *et al.* (2010) 'Inflammatory cytokines and aromatase inhibitor-associated musculoskeletal syndrome: A case-control study', *British Journal of Cancer*, 103(3), pp. 291–296. doi: 10.1038/sj.bjc.6605768.

Heuberger, D. M. and Schuepbach, R. A. (2019) 'Protease-activated receptors (PARs): mechanisms of action and potential therapeutic modulators in PAR-driven inflammatory diseases'. *Thrombosis Journal*, 8, pp. 1–24.

Hikita, T. *et al.* (2018) 'Sensitive and rapid quantification of exosomes by fusing luciferase to exosome marker proteins', *Scientific Reports*, 8(1), pp. 1–14. doi: 10.1038/s41598-018-32535-7.

Hilberg, T. *et al.* (2003) 'Platelet activity and sensitivity to agonists after exhaustive treadmill exercise', *Journal of Sports Science and Medicine*, 2(1), pp. 15–22.

Hilton, H. N., Clarke, C. L. and Graham, J. D. (2018) 'Estrogen and progesterone signalling in the normal breast and its implications for cancer development', *Molecular and Cellular Endocrinology*, 466, pp. 2–14. doi: 10.1016/j.mce.2017.08.011.

Hoellen, F. *et al.* (2011) 'Impact of cyclooxygenase-2 in breast cancer', *Anticancer Research*, 31(12), pp. 4359–4367.

Holinstat, J. Y. and M. (2012) 'Newer agents in antiplatelet therapy : a review', *Journal of Blood Medicine*, 3, pp. 33–42.

Holinstat, M. *et al.* (2009) 'Irreversible platelet activation requires protease-activated receptor 1-mediated signaling to phosphatidylinositol phosphates', *Molecular Pharmacology*, 76(2), pp. 301–313. doi: 10.1124/mol.109.056622.

Hollestelle, A. *et al.* (2013) 'Loss of E-cadherin is not a necessity for epithelial to mesenchymal transition in human breast cancer', *Breast Cancer Research and Treatment*, 138(1), pp. 47–57. doi: 10.1007/s10549-013-2415-3.

Holliday, D. L. and Speirs, V. (2011) 'Choosing the right cell line for breast cancer research '*Breast Cancer Research*, 13, 215.

Holmes, M. D. *et al.* (2010) 'Aspirin intake and survival after breast cancer', *Journal of Clinical Oncology*, 28(9), pp. 1467–1472. doi: 10.1200/JCO.2009.22.7918.

Horváth, I. *et al.* (2008) 'Membrane-associated stress proteins: More than simply chaperones', *Biochimica et Biophysica Acta - Biomembranes*, 1778, pp. 1653–1664. doi: 10.1016/j.bbamem.2008.02.012.

Hu, Q. P. *et al.* (2016) 'Beyond a tumor suppressor: Soluble E-cadherin promotes the progression of cancer', *International Journal of Cancer*, 138(12), pp. 2804–2812. doi: 10.1002/ijc.29982.

Hua, H. *et al.* (2018) 'Mechanisms for estrogen receptor expression in human cancer', *Experimental Hematology & Oncology*, 7(1), pp. 1–11. doi: 10.1186/s40164-018-0116-7.

Huang, F. *et al.* (2017) 'PDGF signaling in cancer progression', *International Journal of Clinical and Experimental Medicine*, 10(7), pp. 9918–9929.

Hulit, J. *et al.* (2007) 'N-cadherin signaling potentiates mammary tumor metastasis via enhanced extracellular signal-regulated kinase activation', *Cancer Research*, 67(7), pp. 3106–3116. doi: 10.1158/0008-5472.CAN-06-3401.

Hussein A. A. *et al.* (2013) 'Epidemiology and prognosis of breast cancer in young women', *J Thorac Dis*, 5(1), pp. 2–8. doi: 10.3978/j.issn.2072-1439.2013.05.24.

Inkielewicz-Stepniak, I. *et al.* (2010) 'The effect of new aspirin prodrugs on blood platelet and tumor cells in an "in vitro" study', *Toxicology Letters*, 196(2010), pp. S258–S259. doi: 10.1016/j.toxlet.2010.03.862.

Jacobo-Herrera, N. J. *et al.* (2014) 'Clinical evidence of the relationship between aspirin and breast cancer risk (review)', *Oncology Reports*, 32(2), pp. 451–461. doi: 10.3892/or.2014.3270.

Jacobs, E. J. *et al.* (2007) 'A large cohort study of long-term daily use of adult-strength aspirin and cancer incidence', *Journal of the National Cancer Institute*, 99(8), pp. 608–615. doi:

10.1093/jnci/djk132.

Jamalzadeh, L. *et al.* (2016) 'Cytotoxic Effects of Some Common Organic Solvents on MCF-7 , RAW-264 . 7 and Human Umbilical Vein Endothelial Cells', *Avicenna J Med Biochem*, 4(1), pp. 1–6. doi: 10.17795/ajmb-33453.

Jedy-Agba, E. *et al.* (2016) 'Stage at diagnosis of breast cancer in sub-Saharan Africa: a systematic review and meta-analysis', *The Lancet Global Health*, 4(12), pp. e923–e935. doi: 10.1016/S2214-109X(16)30259-5.

Jennings, L. K. (2009) 'Mechanisms of platelet activation: need for new strategies to protect against platelet-mediated atherothrombosis.', *Thrombosis and haemostasis*, 102(2), pp. 248–57. doi: 10.1160/TH09-03-0192.

Jia, M. *et al.* (2016) 'Estrogen receptor a promotes breast cancer by reprogramming choline metabolism', *Cancer Research*, 76(19), pp. 5634–5646. doi: 10.1158/0008-5472.CAN-15-2910.

Xu, J., Lamouille, S., and Derynck. R. (2009) 'TGF-β-induced epithelial to mesenchymal transition', *Cell Res*, 19(2), pp. 156–172. doi: 10.1016/j.physbeh.2017.03.040.

Jin, M. *et al.* (2018) 'Effects of aspirin on proliferation, invasion and apoptosis of hep-2 cells via the PTEN/AKT/NF-κB/survivin signaling pathway', *Oncology Letters*, 15(6), pp. 8454–8460. doi: 10.3892/ol.2018.8377.

Joffe, M. *et al.* (2018) 'Barriers to early presentation of breast cancer among women in Soweto, South Africa', *PLoS ONE*, 13(2), pp. 1–16. doi: 10.1371/journal.pone.0192071.

Johnson, B., Fletcher, S. J. and Morgan, N. V. (2016) 'Inherited thrombocytopenia: novel insights into megakaryocyte maturation, proplatelet formation and platelet lifespan', *Platelets*, 27(6), pp. 519–525. doi: 10.3109/09537104.2016.1148806.

Johnston, S. R. D. *et al.* (2013) 'Fulvestrant plus anastrozole or placebo versus exemestane alone after progression on non-steroidal aromatase inhibitors in postmenopausal patients with hormone-receptor-positive locally advanced or metastatic breast cancer (SoFEA): A composite, multicentr', *The Lancet Oncology*, 14(10), pp. 989–998. doi: 10.1016/S1470-2045(13)70322-X.

Jolly, M. K. *et al.* (2015) 'Implications of the hybrid epithelial/mesenchymal phenotype in metastasis', *Frontiers in Oncology*, 5, p. 155. doi: 10.3389/fonc.2015.00155.

Jolly, M. K. *et al.* (2016) 'Stability of the hybrid epithelial/mesenchymal phenotype', *Oncotarget*, 7(19), pp. 27067–27084. doi: 10.18632/oncotarget.8166.

Jolly, M. K. *et al.* (2017) 'Epithelial/mesenchymal plasticity: how have quantitative mathematical models helped improve our understanding?', *Molecular Oncology*, 11(2017), pp. 739–754. doi: 10.1002/1878-0261.12084.

Juncker-jensen, A. *et al.* (2014) 'Tumor MMP-1 Activates Endothelial PAR1 to Facilitate Vascular Intravasation and Metastatic Dissemination', *Cancer Research*, 73(14), pp. 4196–4211. doi: 10.1158/0008-5472.CAN-12-4495.

Junttila, I. S. (2018) 'Tuning the Cytokine Responses : An Update on interleukin (iL) -4 and iL-13 Receptor Complexes', *Frontiers in Immunology*, 9(June). doi: 10.3389/fimmu.2018.00888.

Kahn, S. R. (2012) 'Prevention of VTE in Nonsurgical Patients Antithrombotic Therapy and Prevention of Thrombosis , *Chest*, 141 (2, e195S-e226S. doi: 10.1378/chest.11-2296.

Kalwa, H. *et al.* (2014) 'Central role for hydrogen peroxide in P2Y1 ADP receptor-mediated cellular responses in vascular endothelium', *Proceedings of the National Academy of Sciences of the United States of America*, 111(9), pp. 3383–3388. doi: 10.1073/pnas.1320854111.

Kamath, L., Meydani, A. and Foss, F. (2001) 'Signaling from Protease-activated Receptor-1 Inhibits Migration and Invasion of Breast Cancer Cells', *Cancer Research*, 61(3), pp. 5933–5940.

Kamel, M. M. *et al.* (2014) 'P selectin and T cell profiles provide verification to understand the pathogenesis of liver cirrhosis in HCV and Schistosoma mansoni infections.', *Microbial pathogenesis*, 73, pp. 19–24. doi: 10.1016/j.micpath.2014.05.006.

Kamel, M. M., Fouad, S. A. and Basyoni, M. M. A. (2014) 'P Selectins and immunological profiles in HCV and Schistosoma mansoni induced chronic liver disease', *BMC Gastroenterology*, 14(1), pp. 1–9. doi: 10.1186/1471-230X-14-132.

Katrin Sangkuhla, Teri E. Kleina, and R. B. A. (2010) 'Clopidogrel pathway', *Pharmacogenet Genomics*, 20(7), pp. 463–465. doi: 10.1097/FPC.0b013e3283385420.

Kaur, S. *et al.* (2018) 'CD63, MHC class 1, and CD47 identify subsets of extracellular vesicles containing distinct populations of noncoding RNAs', *Scientific Reports*, 8(1), pp. 1–17. doi: 10.1038/s41598-018-20936-7.

Kemp, A. *et al.* (2014) 'Women commencing anastrozole, letrozole or tamoxifen for early breast cancer: The impact of comorbidity and demographics on initial choice', *PLoS ONE*, 9(1). doi: 10.1371/journal.pone.0084835.

Kempton, C. L. *et al.* (2005) 'Variation in Coagulation Complexes on Platelet Subpopulations', *Arterioscler Thromb Vasc Biol*, 25, pp. 861–866. doi: 10.1161/01.ATV.0000155987.26583.9b.

Key, N. S. *et al.* (2016) 'Thrombosis in cancer: Research priorities identified by a national cancer institute/national heart, lung, and blood institute strategic working group', *Cancer Research*, 76(13), pp. 3671–3675. doi: 10.1158/0008-5472.CAN-15-3100.

Klopp, A. H. *et al.* (2010) 'Mesenchymal stem cells promote mammosphere formation and decrease E-Cadherin in normal and malignant breast cells', *PLoS ONE*, 5(8), pp. 1–9. doi: 10.1371/journal.pone.0012180.

Ko, K. I. *et al.* (2015) 'Diabetes reduces mesenchymal stem cells in fracture healing through a TNFα-mediated mechanism', *Diabetologia*, 58(3), pp. 633–642. doi: 10.1007/s00125-014-3470-y.

Kochel, T. J. *et al.* (2017) 'Multiple drug resistance-associated protein (MRP4) exports prostaglandin E2 (PGE2) and contributes to metastasis in basal/ triple negative breast cancer', *Oncotarget*, 8(4), pp. 6540–6554. doi: 10.18632/oncotarget.14145.

Kochel, T. J., Goloubeva, O. G. and Fulton, A. M. (2016) 'Upregulation of cyclooxygenase-2/prostaglandin E2 (COX-2/PGE2) pathway member multiple drug resistance-associated protein 4 (MRP4) and downregulation of prostaglandin transporter (PGT) and 15-prostaglandin dehydrogenase (15-PGDH) in triple-negative breast', *Breast Cancer: Basic and Clinical Research*, 10, pp. 61–70. doi: 10.4137/BCBCr.s38529.

Kogushi, M. *et al.* (2011) 'The novel and orally active thrombin receptor antagonist E5555 (Atopaxar) inhibits arterial thrombosis without affecting bleeding time in guinea pigs', *European Journal of Pharmacology*, 657, pp. 131–137. doi: 10.1016/j.ejphar.2011.01.058.

Kopp, H. G., Placke, T. and Salih, H. R. (2009) 'Platelet-derived transforming growth factor-β down-

regulates NKG2D thereby inhibiting natural killer cell antitumor reactivity', *Cancer Research*, 69(19), pp. 7775–7783. doi: 10.1158/0008-5472.CAN-09-2123.

Kotha Subbaramaiah1, Patrick G. Morris2, Xi Kathy Zhou3, Monica Morrow4, Baoheng Du1, Dilip Giri5, Levy Kopelovich6, Clifford A. Hudis1,2, and A. J. D. (2012) 'Obese Women', *Cancer Discov*, 2(4), pp. 356–365. doi: 10.1158/2159-8290.CD-11-0241.

Koupenova, M. *et al.* (2017) 'Thrombosis and platelets: An update', *European Heart Journal*, 38(11), pp. 785–791. doi: 10.1093/eurheartj/ehw550.

Koupenova, M. and Ravid, K. (2018) 'Biology of platelet purinergic receptors and implications for platelet heterogeneity', *Frontiers in Pharmacology*, 9(JAN), pp. 1–9. doi: 10.3389/fphar.2018.00037.

Kruger, WM and Apffelstaedt, J. (2009) 'Young breast cancer patients in the developing world : incidence , choice of', *SA Journal of Gynaecological Oncology*, 1(1), pp. 29–31.

Kuan, Y. C. *et al.* (2019) 'Effects of aspirin or clopidogrel on colorectal cancer chemoprevention in patients with type 2 diabetes mellitus', *Cancers*, 11(10), 1468. doi: 10.3390/cancers11101468.

Kubiczkova, L. *et al.* (2012) 'TGF-β - an excellent servant but a bad master', *Journal of Translational Medicine*, 10(1), pp. 1–24. doi: 10.1186/1479-5876-10-183.

Kumari, N. *et al.* (2016) 'Role of interleukin-6 in cancer progression and therapeutic resistance', *Tumor Biology*, pp. 11553–11572. doi: 10.1007/s13277-016-5098-7.

Kyriazi, V. (2012) 'Breast Cancer Breast Cancer as an Acquired Thrombophilic State', *Journal of Breast Cancer* , 15(2), pp. 148–156.

Labelle, M., Begum, S. and Hynes, R. O. (2011) 'Direct Signaling between Platelets and Cancer Cells Induces an Epithelial-Mesenchymal-Like Transition and Promotes Metastasis', *Cancer Cell*, 20(5), pp. 576–590. doi: 10.1016/j.ccr.2011.09.009.

Lacroix, M. and Leclercq, G. (2004) 'Relevance of breast cancer cell lines as models for breast tumours: An update', *Breast Cancer Research and Treatment*, 83(3), pp. 249–289. doi: 10.1023/B:BREA.0000014042.54925.cc.

Lal, I., Dittus, K. and Holmes, C. E. (2013) 'Platelets , coagulation and fi brinolysis in breast cancer progression'*Breast Cancer Research*, 15, 207.

Langley, R. E. *et al.* (2011) 'Aspirin and cancer: Has aspirin been overlooked as an adjuvant therapy', *British Journal of Cancer*, 105(8), pp. 1107–1113. doi: 10.1038/bjc.2011.289.

Langley, R. E. (2013) 'Clinical evidence for the use of aspirin in the treatment of cancer', *Ecancermedicalscience*, 7(1), pp. 1–11. doi: 10.3332/ecancer.2013.297.

Larco, J. E. D. E. and Todaro, G. J. (1978) 'Growth factors from murine sarcoma virus-transformed cells', *Proc Natl Acad Sci USA*, 75(8), pp. 4001–4005.

Laurent, P. A. *et al.* (2014) 'Class I PI 3-kinases signaling in platelet activation and thrombosis: PDK1/Akt/GSK3 axis and impact of PTEN and SHIP1', *Advances in Biological Regulation*, 54(1), pp. 162–174. doi: 10.1016/j.jbior.2013.09.006.

Lazennec, G. *et al.* (2001) 'ERβ inhibits proliferation and invasion of breast cancer cells', *Endocrinology*, 142(9), pp. 4120–4130. doi: 10.1210/endo.142.9.8395.

Leader, A. *et al.* (2017) 'The Effect of Combined Aspirin and Clopidogrel Treatment on Cancer

Incidence', *American Journal of Medicine*, 130(7), pp. 826–832. doi: 10.1016/j.amjmed.2017.01.022.

Leblanc, R. and Peyruchaud, O. (2016) 'Metastasis: New functional implications of platelets and megakaryocytes', *Blood*, 128(1), pp. 24–31. doi: 10.1182/blood-2016-01-636399.

Lee, A. Y. Y. and Levine, M. N. (2003) 'Venous thromboembolism and cancer: Risks and outcomes', *Circulation*, 107(SUPPL. 23). doi: 10.1161/01.CIR.0000078466.72504.AC.

Lee, H. S. *et al.* (2009) 'RIAM activates integrins by linking talin to Ras GTPase membrane-targeting sequences', *Journal of Biological Chemistry*, 284(8), pp. 5119–5122. doi: 10.1074/jbc.M807117200.

Lee, S. Y. *et al.* (2018) 'Regulation of Tumor Progression by Programmed Necrosis', *Oxidative Medicine and Cellular Longevity*, 2018. doi: 10.1155/2018/3537471.

Lee, Y.H and Schiemann, W.P. (2014). 'Chemotherapeutic targeting of the transforming growth factor-β pathway in breast cancer', *Breast Cancer Manag*, 3(1), pp. 73-85. doi: 10.2217/bmt.13.74.

Lehtinen, L. *et al.* (2013) 'High-throughput RNAi screening for novel modulators of vimentin expression identifies MTHFD2 as a regulator of breast cancer cell migration and invasion', *Oncotarget*, 4(1), pp. 48–63. doi: 10.18632/oncotarget.756.

Leite, A. de M. *et al.* (2018) 'Antiplatelet therapy in breast cancer patients using hormonal therapy: Myths, evidence and potentialities – Systematic review', *Arquivos Brasileiros de Cardiologia*, 111(2), pp. 205–212. doi: 10.5935/abc.20180138.

Leonardi, S., Tricoci, P. and Mahaffey, K. W. (2012) 'Promises of PAR-1 inhibition in acute coronary syndrome', *Current Cardiology Reports*, 14(1), pp. 32–39. doi: 10.1007/s11886-011-0232-z.

Leung, T. *et al.* (2013) 'Cytochrome P450 2E1 (CYP2E1) regulates the response to oxidative stress and migration of breast cancer cells', *Breast Cancer Research*, 15(6), pp. 1–12. doi: 10.1186/bcr3574.

Leytin, Valery *et al.* (2000) 'Flow Cytometric Parameters for Characterizing Platelet Activation by Measuring P-Selectin (CD62) Expression: Theoretical Consideration and Evaluation in Thrombin-Treated Platelet Populations', *Biochemical and Biophysical Research Communications*, 269(1), pp. 85–90. doi: 10.1006/bbrc.2000.2255.

Leytin, V *et al.* (2000b) 'Quantification of platelet activation status by analyzing P-selectin expression.', *Biochemical and biophysical research communications*, 273(2), pp. 565–570. doi: 10.1006/bbrc.2000.2977.

Li, N. (2016) 'Platelets in cancer metastasis: To help the "villain" to do evil', *International Journal of Cancer*, 138(9), pp. 2078–2087. doi: 10.1002/ijc.29847.

Li, R. *et al.* (2014) 'Presence of intratumoral platelets is associated with tumor vessel structure and metastasis', *BMC Cancer*. 14(1), pp. 1–10. doi: 10.1186/1471-2407-14-167.

Li, Y. *et al.* (2017) 'Tumoral expression of drug and xenobiotic metabolizing enzymes in breast cancer patients of different ethnicities with implications to personalized medicine', *Scientific Reports*, 7(1), pp. 1–11. doi: 10.1038/s41598-017-04250-2.

Li, Z. *et al.* (2017) 'LncRNA ANCR down-regulation promotes TGF-β-induced EMT and metastasis in breast cancer', *Oncotarget*, 8(40), pp. 67329–67343. doi: 10.18632/oncotarget.18622.

Lian, L. *et al.* (2013) 'Inhibition of MCF-7 breast cancer cell-induced platelet aggregation using a combination of antiplatelet drugs', *Oncology Letters*, 5(2), pp. 675–680. doi: 10.3892/ol.2012.1074.

Liang, C. C., Park, A. Y. and Guan, J. L. (2007) 'In vitro scratch assay: A convenient and inexpensive method for analysis of cell migration in vitro', *Nature Protocols*, 2(2), pp. 329–333. doi: 10.1038/nprot.2007.30.

Lima, L. G. and Monteiro, R. Q. (2013) 'Activation of blood coagulation in cancer : implications for tumour progression', *BioSci Rep* , 33, pp. 701–710. doi: 10.1042/BSR20130057.

Lipets, E. N. and Ataullakhanov, F. I. (2015) 'Global assays of hemostasis in the diagnostics of hypercoagulation and evaluation of thrombosis risk', *Thrombosis Journal*, 13(1). doi: 10.1186/s12959-015-0038-0.

Liu, B., Qu, L. and Yan, S. (2015) 'Cyclooxygenase-2 promotes tumor growth and suppresses tumor immunity', *Cancer Cell International*, 15(1), pp. 2–7. doi: 10.1186/s12935-015-0260-7.

Liu, C. Y. *et al.* (2015) 'Vimentin contributes to epithelial-mesenchymal transition ancer cell mechanics by mediating cytoskeletal organization and focal adhesion maturation', *Oncotarget*, 6(18), pp. 15966–15983. doi: 10.18632/oncotarget.3862.

Liu, J. *et al.* (2014) 'Overexpression of both platelet-derived growth factor-BB and vascular endothelial growth factor-C and its association with lymphangiogenesis in primary human non-small cell lung cancer', *Diagnostic Pathology*, 9, p. 128. doi: 10.1186/1746-1596-9-128.

Liu, T. *et al.* (2018) 'PDGF-mediated mesenchymal transformation renders endothelial resistance to anti-VEGF treatment in glioblastoma', *Nature Communications*, 9(1). doi: 10.1038/s41467-018-05982-z.

Liu, X. *et al.* (2017) 'Protease-activated receptor-1 (PAR-1): a promising molecular target for cancer.', *Oncotarget*, 8(63), pp. 107334–107345. doi: 10.18632/oncotarget.21015.

Loh *et al.* (2019) 'The E-Cadherin and N-Cadherin Switch in Epithelial-to-Mesenchymal Transition: Signaling, Therapeutic Implications, and Challenges', *Cells,* 8, 1118. doi: 10.3390/cells8101118.

Lopez, E. *et al.* (2015) 'Relationship between calcium mobilization and platelet α- And δ-granule secretion. A role for TRPC6 in thrombin-evoked δ-granule exocytosis', *Archives of Biochemistry and Biophysics*, 585, pp. 75–81. doi: 10.1016/j.abb.2015.09.012.

Louise Brinton, Jonine Figueroa, Ernest Adjei, Daniel Ansong, Richard Biritwum, Lawrence Edusei5, Kofi M. Nyarko, Seth Wiafe, Joel Yarney, Beatrice Wiafe Addai, Baffour Awuah, and J. N. C.-L. (2017) 'Factors Contributing to Delays in Diagnosis of Breast Cancers in Ghana, West Africa', *Breast Cancer Research and Treatment*, 162(1), pp. 105–114. doi: 10.1007/s10549-016-4088-1.

Lu, Q. and Malinauskas, R. A. (2010) 'Comparison of Two Platelet Activation Markers Using Flow Cytometry After In Vitro Shear Stress Exposure of Whole Human Blood', *Artificial Organs*, 35(2), pp. 137–144. doi: 10.1111/j.1525-1594.2010.01051.x.

Lucotti, S. *et al.* (2019) 'Aspirin blocks formation of metastatic intravascular niches by inhibiting platelet-derived COX-1/ thromboxane A2', *Journal of Clinical Investigation*, 129(5), pp. 1845–1862. doi: 10.1172/JCI121985.

Lumachi, F. *et al.* (2013) 'Treatment of Estrogen Receptor-Positive Breast Cancer', *Current Medicinal Chemistry*, 20(5), pp. 596–604. doi: 10.2174/092986713804999303.

Lymperatou, D. *et al.* (2013) 'The exposure of breast cancer cells to fulvestrant and tamoxifen modulates cell migration differently', *BioMed Research International*, 2013. doi: 10.1155/2013/147514.

Machlus, K. R. and Italiano, J. E. (2013) 'The incredible journey: From megakaryocyte development to platelet formation', *Journal of Cell Biology*, 201(6), pp. 785–796. doi: 10.1083/jcb.201304054.

Maguire, A. *et al.* (2007) 'Determinants of cholesterol and triglycerides recording in patients treated with lipid lowering therapy in UK primary care', *Pharmacoepidemiology and drug safety*, 16(May), pp. 228–228. doi: 10.1002/pds.

Maity, G. *et al.* (2015) 'Aspirin blocks growth of breast tumor cells and tumor-initiating cells and induces reprogramming factors of mesenchymal to epithelial transition', *Laboratory Investigation*, 95(7), pp. 702–717. doi: 10.1038/labinvest.2015.49.

Mammadova-Bach, E. *et al.* (2015) 'Platelet glycoprotein VI binds to polymerized fibrin and promotes thrombin generation', *Blood*, 126(5), pp. 683–691. doi: 10.1182/blood-2015-02-629717.

Mansour, A. *et al.* (2020) 'P2Y 12 Inhibition beyond Thrombosis : E ff ects on Inflammation', *International Journal of Molecular Sciences*, 21, pp. 1–25. doi: 10.3390/ijms21041391.

Marat, A. L. and Haucke, V. (2016) 'Phosphatidylinositol 3-phosphates—at the interface between cell signalling and membrane traffic', *The EMBO Journal*, 35(6), pp. 561–579. doi: 10.15252/embj.201593564.

Marik, P. E. and Flemmer, M. (2012) 'The immune response to surgery and trauma : Implications for treatment', *J Trauma Acute Care Surg* , 73(4), pp. 801–808. doi: 10.1097/TA.0b013e318265cf87.

Marquardt, L. *et al.* (2002) 'Course of platelet activation markers after ischemic stroke', *Stroke*, 33(11), pp. 2570–2574. doi: 10.1161/01.STR.0000034398.34938.20.

Martelotto, Luciano G. *et al.* (2014) 'Breast cancer intra-tumor heterogeneity', *Breast Cancer Research*, 16(3), pp. 1–11. doi: 10.1186/bcr3658.

Matthews, A. *et al.* (2018) 'Long term adjuvant endocrine therapy and risk of cardiovascular disease in female breast cancer survivors: Systematic review', *BMJ (Online)*, 363, pp. 10–13. doi: 10.1136/bmj.k3845.

Mauri, L. *et al.* (2014) 'Twelve or 30 Months of Dual Antiplatelet Therapy After Drug- eluting Stents', *N Engl J Med*, 371(23), pp. 2155–2166. doi: 10.1056/NEJMoa1409312.

Mauri, L. *et al.* (2016) 'Causes of late mortality with dual antiplatelet therapy after coronary stents', *European Heart Journal*, 37, pp. 378–385. doi: 10.1093/eurheartj/ehv614.

Mccormack, J. J. *et al.* (2017) 'Weibel − Palade bodies at a glance', *Journal of cell science*, 1962, pp. 3611–3617. doi: 10.1242/jcs.208033.

McDonald, M. G. *et al.* (2017) 'Expression and functional characterization of breast cancer-associated cytochrome P450 4Z1 in saccharomyces cerevisiae', *Drug Metabolism and Disposition*, 45(12), pp. 1364–1371. doi: 10.1124/dmd.117.078188.

Meikle, C. K. S. *et al.* (2017) 'Cancer and Thrombosis: The Platelet Perspective', *Frontiers in Cell and Developmental Biology*, 4(January), pp. 1–10. doi: 10.3389/fcell.2016.00147.

Mekaj, Y. H. (2016) 'The roles of platelets in inflammation, immunity, wound healing and malignancy', *International Journal of Clinical and Experimental Medicine*, 9(3), pp. 5347–5358.

Mello-Grand, M. *et al.* (2010) 'Gene expression profiling and prediction of response to hormonal neoadjuvant treatment with anastrozole in surgically resectable breast cancer', *Breast Cancer Research and Treatment*, 121(2), pp. 399–411. doi: 10.1007/s10549-010-0887-y.

Mello, P. de A., Coutinho-Silva, R. and Savio, L. E. B. (2017) 'Multifaceted effects of extracellular adenosine triphosphate and adenosine in the tumor-host interaction and therapeutic perspectives', *Frontiers in Immunology*, 8(NOV), pp. 1–17. doi: 10.3389/fimmu.2017.01526.

Mendes, R. T., Stanczyk, C. P. and Sordi, R. (2012) 'Selective inhibition of cyclooxygenase-2 : risks and benefi ts', *Rev Bras Reumatol*, 52(5).

Menter, D. G. *et al.* (2014) 'Platelets and cancer: A casual or causal relationship: Revisited', *Cancer and Metastasis Reviews*, 33(1), pp. 231–269. doi: 10.1007/s10555-014-9498-0.

Meydani, A. *et al.* (2001) 'Signaling from protease-activated receptor-1 inhibits migration and invasion of breast cancer cells', *Cancer Research*, 61(15), pp. 5933–5940.

Mezouar, S. *et al.* (2015) 'Inhibition of platelet activation prevents the P-selectin and integrin-dependent accumulation of cancer cell microparticles and reduces tumor growth and metastasis in vivo', *International Journal of Cancer*, 136(2), pp. 462–475. doi: 10.1002/ijc.28997.

Miah, S. *et al.* (2019) 'Estrogen receptor signaling regulates the expression of the breast tumor kinase in breast cancer cells', *BMC Cancer*, 19(1), pp. 1–12. doi: 10.1186/s12885-018-5186-8.

Michael, M. and Doherty, M. M. (2005) 'Tumoral drug metabolism: Overview and its implications for cancer therapy', *Journal of Clinical Oncology*, 23(1), pp. 205–229. doi: 10.1200/JCO.2005.02.120.

O'Donoghue, M. *et al.* (2011) 'Safety and Tolerability of Atopaxar in the Treatment of The Lessons From Antagonizing the Cellular Effects of Thrombin – Acute Coronary Syndromes Trial', *Circulation*, pp. 1843–1853. doi: 10.1161/CIRCULATIONAHA.110.000786.

Miller, L. A. *et al.* (1994) 'New T47D Breast Cancer Cell Lines for the Independent Study of Progesterone B- and A-Receptors: Only Antiprogestin-occupied B-Receptors Are Switched to Transcriptional Agonists by cAMP', *Cancer Research*, 54(14), pp. 3868–3877.

Mitjavila-garcia, M. T. *et al.* (2002) 'Expression of CD41 on hematopoietic progenitors derived from embryonic hematopoietic cells', *Development* , 2013(2002), pp. 2003–2013.

Miyashita, T. *et al.* (2015) 'Metastasis-promoting role of extravasated platelet activation in tumor', *Journal of Surgical Research*, 193(1), pp. 289–294. doi: 10.1016/j.jss.2014.07.037.

Moen, I. *et al.* (2009) 'Hyperoxic treatment induces mesenchymal-to-epithelial transition in a rat adenocarcinoma model', *PLoS One*, 4(7). doi: 10.1371/journal.pone.0006381.

Montt-Guevara, M. M. *et al.* (2016) 'Androgens regulate T47D cells motility and invasion through actin cytoskeleton remodeling', *Frontiers in Endocrinology*, 7, p. 136. doi: 10.3389/fendo.2016.00136.

Moodley, J. *et al.* (2016) 'Understanding pathways to breast cancer diagnosis among women in the Western Cape Province, South Africa: A qualitative study', *BMJ Open*, 6(1). doi: 10.1136/bmjopen-2015-009905.

Moschonas, I. C., Goudevenos, J. A. and Tselepis, A. D. (2015) 'Protease-activated receptor-1 antagonists in long-term antiplatelet therapy. Current state of evidence and future perspectives', *International Journal of Cardiology*, 185, pp. 9–18. doi: 10.1016/j.ijcard.2015.03.049.

Mosevoll, K. A. *et al.* (2018) 'Cytokines , Adhesion Molecules , and Matrix Metalloproteases as Predisposing , Diagnostic , and Prognostic Factors in Venous Thrombosis', *Frontiers in Medicine*, 5(May), pp. 1–11. doi: 10.3389/fmed.2018.00147.

Mosoyan, G. *et al.* (2013) 'Multiple Breast Cancer Cell-Lines Derived from a Single Tumor Differ in Their

Molecular Characteristics and Tumorigenic Potential', *PLoS One*, 8(1), pp. 1–14. doi: 10.1371/journal.pone.0055145.

Mota, A. de L. *et al.* (2017) 'Molecular characterization of breast cancer cell lines by clinical immunohistochemical markers', *Oncology Letters*, 13(6), pp. 4708–4712. doi: 10.3892/ol.2017.6093.

Moustakas, A. and Heldin, C. (2016) 'Mechanisms of TGF β -Induced Epithelial – Mesenchymal Transition', *Journal of Clinical Medicine*, 5, 63. doi: 10.3390/jcm5070063.

Moustakas, A. and Heldin, C. H. (2007) 'Signaling networks guiding epithelial-mesenchymal transitions during embryogenesis and cancer progression', *Cancer Science*, 98(10), pp. 1512–1520. doi: 10.1111/j.1349-7006.2007.00550.x.

Mrozik, K. M. *et al.* (2018) 'N-cadherin in cancer metastasis, its emerging role in haematological malignancies and potential as a therapeutic target in cancer 11 Medical and Health Sciences 1112 Oncology and Carcinogenesis 06 Biological Sciences 0601 Biochemistry and Cell Biology', *BMC Cancer*. , 18(1), pp. 1–16. doi: 10.1186/s12885-018-4845-0.

Muhammad, S., Moinuddin, M. and Samina, I. (2013) 'Brief Communication New Horizons in Platelets Flow Cytometry', *Malays J Med Sci*, 20(2), pp. 62–66.

Munnix, I. C. A. *et al.* (2009) 'Platelet response heterogeneity in thrombus formation', *Thrombosis and Haemostasis*, 102(6), pp. 1149–1156. doi: 10.1160/TH09-05-0289.

Nagasaki, T. *et al.* (2014) 'Interleukin-6 released by colon cancer-associated fibroblasts is critical for tumour angiogenesis: Anti-interleukin-6 receptor antibody suppressed angiogenesis and inhibited tumour-stroma interaction', *British Journal of Cancer*, 110(2), pp. 469–478. doi: 10.1038/bjc.2013.748.

Nakshatri, H., Srour, E. and Badve, S. (2009) 'Breast Cancer Stem Cells and Intrinsic Subtypes: Controversies Rage On', *Current Stem Cell Research & Therapy*, 4(1), pp. 50–60. doi: 10.2174/157488809787169110.

Navred, K. *et al.* (2019) 'A simplified flow cytometric method for detection of inherited platelet disorders—A comparison to the gold standard light transmission aggregometry', *PLoS One*, 14(1), pp. 1–12. doi: 10.1371/journal.pone.0211130.

Neumüller, J. *et al.* (2013) 'Monitoring of platelet activation in platelet concentrates using transmission electron microscopy', *Transfusion Medicine and Hemotherapy*, 40(2), pp. 101–107. doi: 10.1159/000350034.

Neve, Richard M *et al.* (2006) 'A collection of breast cancer cell lines for the study of functionally', *Cancer Cell*, 10(6), pp. 515–527. doi: 10.1016/j.ccr.2006.10.008.A.

New, S. E. P. and Aikawa, E. (2011) 'Cardiovascular Calcification', *Circulation Journal*, 75(June), 1305-1313. doi: 10.1253/circj.CJ-11-0395.

Newman Osafo, Christian Agyare, D. D. O. and A. O. A. et al (2016) 'Mechanism of Action of Nonsteroidal Anti- Inflammatory Drugs´, *Nonsteroidal Anti-Inflammatory Drugs*. doi: http://dx.doi.org/10.5772/68090.

Nie, Z. *et al.* (2015) 'Transforming growth factor-beta increases breast cancer stem cell population partially through upregulating PMEPA1 expression', *Acta Biochimica et Biophysica Sinica*, 48(2), pp. 194–201. doi: 10.1093/abbs/gmv130.

Nieto, M. A. (2011) 'The Ins and Outs of the Epithelial to Mesenchymal Transition in Health and

Disease', *Annual Review of Cell and Developmental Biology*, 27(1), pp. 347–376. doi: 10.1146/annurev-cellbio-092910-154036.

Nilsson, G. M. A. *et al.* (2014) 'Loss of E-cadherin expression is not a prerequisite for c-erbB2-induced epithelial-mesenchymal transition', *International Journal of Oncology*, 45(1), pp. 82–94. doi: 10.3892/ijo.2014.2424.

Nilsson, R. J. A. *et al.* (2011) 'Blood platelets contain tumor-derived RNA biomarkers', *Blood*, 118(13), pp. 3680–3683. doi: 10.1182/blood-2011-03-344408.

Minaeva, O. V. *et al.* (2017) 'Comparative study of cytotoxicity of ferromagnetic nanoparticles and magnetitecontaining polyelectrolyte microcapsules', *Journal of Physics: Conference Series*, 784, pp. 1–11. doi: 10.1088/1742-6596/755/1/011001.

Olivier, C. *et al.* (2013) 'Thrombin Receptor Antagonism in Antiplatelet Therapy', *Cardiology and Therapy*, 2(1), pp. 57–68. doi: 10.1007/s40119-013-0013-4.

Onder, T. T. *et al.* (2008) 'Loss of E-cadherin promotes metastasis via multiple downstream transcriptional pathways', *Cancer Research*, 68(10), pp. 3645–3654. doi: 10.1158/0008-5472.CAN-07-2938.

Orellana, R. *et al.* (2015) 'Platelets enhance tissue factor protein and metastasis initiating cell markers, and act as chemoattractants increasing the migration of ovarian cancer cells', *BMC Cancer*, 15(1). doi: 10.1186/s12885-015-1304-z.

Oueslati, M. *et al.* (2017) 'ERα and ERβ co-expression: An indicator of aggressive tumors and hormonal sensitivity', *Oncology Letters*, 14(2), pp. 1675–1682. doi: 10.3892/ol.2017.6314.

Owens, A. P. and MacKman, N. (2011) 'Microparticles in hemostasis and thrombosis', *Circulation Research*, 108(10), pp. 1284–1297. doi: 10.1161/CIRCRESAHA.110.233056.

Padua, D. and Massagué, J. (2009) 'Roles of TGFβ in metastasis', *Cell Research*, 19(1), pp. 89–102. doi: 10.1038/cr.2008.316.

Paik, J. *et al.* (2004) 'A multigene assay to predict recurrence of tamoxifen-treated, node-negative breast cancer', *The New England Journal of Medicine*, 351(27), pp 2817-2826. doi: 10.1101/gad.1227804.uncontrolled.

Palumbo, J. S. (2008) 'Mechanisms linking tumor cell-associated procoagulant function to tumor dissemination', *Seminars in Thrombosis and Hemostasis*, 34(2), pp. 154–160. doi: 10.1055/s-2008-1079255.

Pan, H., Boucher, M. and Kaunelis, D. (2016) 'PAR-1 Antagonists: An Emerging Antiplatelet Drug Class', *CADTH Issues in Emerging Health Technologies*, pp. 1–17.

Pandya, P., Orgaz, J. L. and Sanz-Moreno, V. (2017) 'Modes of invasion during tumour dissemination', *Molecular oncology*, 11(1), pp. 5–27. doi: 10.1002/1878-0261.12019.

Pang, J. H. *et al.* (2015) 'Activation of tumour cell ECM degradation by thrombin-activated platelet membranes: potentially a P-selectin and GPIIb/IIIa-dependent process', *Clinical and Experimental Metastasis*. Springer Netherlands, 32(5), pp. 495–505. doi: 10.1007/s10585-015-9722-5.

Pang, M. F. *et al.* (2016) 'TGF-β1-induced EMT promotes targeted migration of breast cancer cells through the lymphatic system by the activation of CCR7/CCL21-mediated chemotaxis', *Oncogene*. Nature Publishing Group, 35(6), pp. 748–760. doi: 10.1038/onc.2015.133.

Panis, C. *et al.* (2013) 'Screening of circulating tgf-β levels and its clinicopathological significance in human breast cancer', *Anticancer Research*, 33(2), pp. 737–742.

Papaxoinis, G. *et al.* (2018) 'Predictive factors of thromboembolic complications in patients with esophagogatric adenocarcinoma undergoing preoperative chemotherapy', *Acta Oncologica*. Informa UK Limited, trading as Taylor & Francis Group, 57(6), pp. 790–798. doi: 10.1080/0284186X.2017.1423375.

Paskauskas, S., Pundzius, J. and Barauskas, G. (2008) 'Venous thromboembolism and prophylaxis in cancer patients.', *Medicina (Kaunas, Lithuania)*, 44(3), pp. 175–181. doi: 10.3390/medicina44030022.

Passacquale, G. and Ferro, A. (2011) 'Current concepts of platelet activation: Possibilities for therapeutic modulation of heterotypic vs. homotypic aggregation', *British Journal of Clinical Pharmacology*, 72(4), pp. 604–618. doi: 10.1111/j.1365-2125.2011.03906.x.

Pather, K. *et al.* (2019) 'Breast cancer cell-induced platelet activation is compounded by tamoxifen and anastrozole in vitro', *Thrombosis Research*, 177(February), pp. 51–58. doi: 10.1016/j.thromres.2019.02.027.

Phillips, K. G. *et al.* (2015) 'The thrombotic potential of circulating tumor microemboli: Computational modeling of circulating tumor cell-induced coagulation', *American Journal of Physiology - Cell Physiology*, 308(3), pp. C229–C236. doi: 10.1152/ajpcell.00315.2014.

Piccin, A., Murphy, W. G. and Smith, O. P. (2007) 'Circulating microparticles: pathophysiology and clinical implications', *Blood Reviews*, 21(3), pp. 157–171. doi: 10.1016/j.blre.2006.09.001.

Pilatova, K., Zdrazilova-Dubska, L., and L. K. G. (2012) 'The Role of Platelets in Tumour Growth', *Klin Onkol*, 25(Suppl 2), pp. 2S50-2S57.

Pinto, B. I. *et al.* (2018) 'Estrogen Mitigates the Negative Effects of Arsenic Contamination in an in Vitro Wound Model', *Applied In Vitro Toxicology*, 4(1), pp. 24–29. doi: 10.1089/aivt.2017.0020.

Pinto, M. P. *et al.* (2014) 'Malignant stroma increases luminal breast cancer cell proliferation and angiogenesis through platelet-derived growth factor signaling', *BMC Cancer*, 14(1), pp. 1–12. doi: 10.1186/1471-2407-14-735.

Pircher, J. *et al.* (2012) 'Prothrombotic effects of tumor necrosis factor alpha in vivo are amplified by the absence of TNF-alpha receptor subtype 1 and require TNF-alpha receptor subtype 2', *Arthritis Research & Therapy*, 14(5), p. R225. doi: 10.1186/ar4064.

Placke, T. *et al.* (2012) 'Platelet-derived MHC class I confers a pseudonormal phenotype to cancer cells that subverts the antitumor reactivity of natural killer immune cells', *Cancer Research*, 72(2), pp. 440–448. doi: 10.1158/0008-5472.CAN-11-1872.

Plantureux, L. *et al.* (2018) 'Effects of platelets on cancer progression', *Thrombosis Research*, 164(January), pp. S40–S47. doi: 10.1016/j.thromres.2018.01.035.

Pokrovskaya, I. D. *et al.* (2018) 'SNARE-dependent membrane fusion initiates α-granule matrix decondensation in mouse platelets', *Blood Advances*, 2(21), pp. 2947–2958. doi: 10.1182/bloodadvances.2018019158.

Polanowska-Grabowska, R. *et al.* (2010) 'P-selectin-mediated platelet-neutrophil aggregate formation activates neutrophils in mouse and human sickle cell disease.', *Arteriosclerosis, thrombosis, and vascular biology*, 30(12), pp. 2392–2399. doi: 10.1161/ATVBAHA.110.211615.

Pols, M. S. and Klumperman, J. (2009) 'Trafficking and function of the tetraspanin CD63', *Experimental Cell Research*, 315(9), pp. 1584–1592. doi: 10.1016/j.yexcr.2008.09.020.

Polyak, K. (2011) 'Review series introduction Heterogeneity in breast cancer', *J.Clin.Invest.*, 121(10), pp. 2011–2013. doi: 10.1172/JCI60534.3786.

Poniatowski, L. A. *et al.* (2015) 'Transforming growth factor beta family: Insight into the role of growth factors in regulation of fracture healing biology and potential clinical applications', *Mediators of Inflammation*, 2015. doi: 10.1155/2015/137823.

Prandoni, P., Falanga, A. and Piccioli, A. (2005) 'Cancer and venous thromboembolism', *The Lancet*, 6(June), 401-410.

Pretorius, E., Engelbrecht, M. J. and Duim, W. (2012) 'Thromboembolic ischemic stroke and the presence of necrotic platelets: A scanning electron microscopy investigation', *Ultrastructural Pathology*, 36(1), pp. 19–22. doi: 10.3109/01913123.2011.620219.

Projahn, D. and Koenen, R. R. (2012) 'Platelets: key players in vascular inflammation.', *Journal of leukocyte biology*, 92(6), pp. 1167–75. doi: 10.1189/jlb.0312151.

Puhalla, S., Bhattacharya, S. and Davidson, N. E. (2012) 'Hormonal therapy in breast cancer: A model disease for the personalization of cancer care', *Molecular Oncology*, 6(2), pp. 222–236. doi: 10.1016/j.molonc.2012.02.003.

Qiao, Y. *et al.* (2018) 'Associations between aspirin use and the risk of cancers: A meta-analysis of observational studies', *BMC Cancer*, 18(1). doi: 10.1186/s12885-018-4156-5.

Radde, B. N. *et al.* (2015) 'Bioenergetic differences between MCF-7 and T47D breast cancer cells and their regulation by oestradiol and tamoxifen', *Biochemical Journal*, 465, pp. 49–61. doi: 10.1042/BJ20131608.

Raghu Kalluri, and R. A. W. (2009) 'Particle-in-cell simulations of a beam driven plasma', *The Journal of clinical investigation*, 119, pp. 1420–1428. doi: 10.1172/JCI39104.

Rao, P. P. N. and Knaus, E. E. (2008) 'Evolution of nonsteroidal anti-inflammatory drugs (NSAIDs): Cyclooxygenase (COX) inhibition and beyond', *Journal of Pharmacy and Pharmaceutical Sciences*, 11(2), pp. 81–110. doi: 10.18433/j3t886.

Ray, A. and Ficek, M. (2012) 'Immunomodulatory effects of anti-estrogenic drugs', *Acta Pharmaceutica*, 62(2), pp. 141–155. doi: 10.2478/v10007-012-0012-3.

Razak, N. B. A. *et al.* (2018) 'Cancer-associated thrombosis: An overview of mechanisms, risk factors, and treatment', *Cancers*, 10(10), pp. 1–21. doi: 10.3390/cancers10100380.

Remšík, J. *et al.* (2018) 'Plasticity and intratumoural heterogeneity of cell surface antigen expression in breast cancer', *British Journal of Cancer*, 118(6), pp. 813–819. doi: 10.1038/bjc.2017.497.

Rendic, S. P. and Peter Guengerich, F. (2018) 'Human cytochrome P450 enzymes 5–51 as targets of drugs and natural and environmental compounds: mechanisms, induction, and inhibition–toxic effects and benefits', *Drug Metabolism Reviews*, 50(3), pp. 256–342. doi: 10.1080/03602532.2018.1483401.

Renni, M. J. P. *et al.* (2017) 'Mechanisms of venous thromboembolism in cancer: A literature review', *Jornal Vascular Brasileiro*, 16(4), pp. 308–313. doi: 10.1590/1677-5449.007817.

Repsold, L., Pretorius, E. and Joubert, A. M. (2015) 'Ex vivo Determination of an Estradiol Analogue-Induced Changes on Platelet Morphology and Angiogenic Biomarkers', *Microscopy and Microanalysis*,

21(6), pp. 1491–1503. doi: 10.1017/S1431927615015214.

Mehta, R. S. *et al.* (2012) 'Combination Anastrozole and Fulvestrant in Metastatic Breast Cancer', *N Engl J Med*, 367(1), pp. 435–444. doi: 10.1056/NEJMoa1201622.

Rizwan, A. *et al.* (2015) 'Breast cancer cell adhesome and degradome interact to drive metastasis', *npj Breast Cancer*, 1(September), pp. 1–11. doi: 10.1038/npjbcancer.2015.17.

Roden, D. M. and Stein, C. M. (2009) 'Clopidogrel and the concept of high-risk pharmacokinetics', *Circulation*, 119(16), pp. 2127–2130. doi: 10.1161/CIRCULATIONAHA.109.865907.

Roe, M. T. *et al.* (2016) 'Ascertainment, classification, and impact of neoplasm detection during prolonged treatment with dual antiplatelet therapy with prasugrel vs. clopidogrel following acute coronary syndrome', *European Heart Journal*, 37(4), pp. 412–422. doi: 10.1093/eurheartj/ehv611.

Roger, P. *et al.* (2001) 'Decreased expression of estrogen receptor β protein in proliferative preinvasive mammary tumors', *Cancer Research*, 61(6), pp. 2537–2541.

Roop, Ryan P *et al.* (2013) 'A randomized phase II trial investigating the effect of platelet function inhibition on circulating tumor cells in patients with metastatic breast cancer.', *Clinical breast cancer*, 13(6), pp. 409–15. doi: 10.1016/j.clbc.2013.08.006.

Rosso, M. *et al.* (2017) 'E-cadherin: A determinant molecule associated with ovarian cancer progression, dissemination and aggressiveness', *PLoS One*, 12(9), pp. 1–25. doi: 10.1371/journal.pone.0184439.

Rudolph, V. and Freeman, B. A. (2009) 'Cardiovascular Consequences When Nitric Oxide and Lipid Signaling Converge'. *Circulation Research*, (2009), pp511-522. doi: 10.1161/CIRCRESAHA.109.202077.

Ruiz, F. A. *et al.* (2004) 'Human Platelet Dense Granules Contain Polyphosphate and Are Similar to Acidocalcisomes of Bacteria and Unicellular Eukaryotes ', *The Journal of biological chemistry* 279(43), pp. 44250–44257. doi: 10.1074/jbc.M406261200.

Saboor, M. (2013) 'Comparison of Platelet CD Markers between Normal Individuals and Untreated Patients with Type 2 Diabetes Mellitus', *Journal of Hematology & Thromboembolic Diseases*, 02(01), pp. 2–5. doi: 10.4172/2329-8790.1000123.

Saboor, M. *et al.* (2013) 'Platelet receptors: An instrumental of platelet physiology', *Pakistan Journal of Medical Sciences*, 29(3). doi: 10.12669/pjms.293.3497.

Sabrkhany, S. *et al.* (2017) 'A combination of platelet features allows detection of early-stage cancer', *European Journal of Cancer*, 80, pp. 5–13. doi: 10.1016/j.ejca.2017.04.010.

Saitoh, M. (2018) 'JB special review-cellular plasticity in epithelial homeostasis and diseases: Involvement of partial EMT in cancer progression', *Journal of Biochemistry*, 164(4), pp. 257–264. doi: 10.1093/jb/mvy047.

Shattil, S.J., Kim, C and Ginsberg, M.H. (2010) 'The final steps of integrin activation: the end game', *Nature reviews Molecular cell biology*, 11(4), pp. 288–300. doi: 10.1038/nrm2871.

Sastre-Serra, J. *et al.* (2012) 'The effects of 17β-estradiol on mitochondrial biogenesis and function in breast cancer cell lines are dependent on the ERα/ERβ Ratio', *Cellular Physiology and Biochemistry*, 29(1–2), pp. 261–268. doi: 10.1159/000337607.

Satelli, A. and Li, S. (2011) 'Vimentin as a potential molecular target in cancer therapy Or Vimentin, an overview and its potential as a molecular target for cancer therapy', *Cell Mol Life Sci.*, 68(18), pp. 3033–

3046. doi: 10.1007/s00018-011-0735-1.

Saw, J. *et al.* (2008) 'The ELAPSE (Evaluation of Long-Term Clopidogrel Antiplatelet and Systemic Anti-Inflammatory Effects) Study', *Journal of the American College of Cardiology*. American College of Cardiology Foundation, 52(23), pp. 1826–1833. doi: 10.1016/j.jacc.2008.08.047.

Schaper, F. and Rose-john, S. (2015) 'Cytokine & Growth Factor Reviews Interleukin-6 : Biology , signaling and strategies of blockade IL-6', *Cytokine & growth factor reviews*, 26, pp. 475–487.

Schlesinger, M. (2018) 'Role of platelets and platelet receptors in cancer metastasis'. *Journal of Hematology & Oncology*, pp. 1–15.

Seddiki, R. *et al.* (2018) 'Force-dependent binding of vinculin to α-catenin regulates cell-cell contact stability and collective cell behavior', *Molecular Biology of the Cell*, 29(4), pp. 380–388. doi: 10.1091/mbc.E17-04-0231.

Sehgal, S. and Storrie, B. (2007) 'Evidence that differential packaging of the major platelet granule proteins von Willebrand factor and fibrinogen can support their differential release', *Journal of Thrombosis and Haemostasis*, 5(10), pp. 2009–2016. doi: 10.1111/j.1538-7836.2007.02698.x.

Sek, K. *et al.* (2018) 'Targeting adenosine receptor signaling in cancer immunotherapy', *International Journal of Molecular Sciences*, 19(12). doi: 10.3390/ijms19123837.

Seliger, B. (2014) 'The link between MHC class I abnormalities of tumors, oncogenes, tumor suppressor genes, and transcription factors', *Journal of Immunotoxicology*, 11(4), pp. 308–310. doi: 10.3109/1547691X.2013.875084.

Serhan, K., Gartung, A. and Panigrahy, D. (2018) 'Drawing a link between the thromboxane A2 pathway and the role of platelets and tumor cells in ovarian cancer', *Prostaglandins and Other Lipid Mediators*, 137(March), pp. 40–45. doi: 10.1016/j.prostaglandins.2018.06.001.

Seubert, B. *et al.* (2015) 'Tetraspanin CD63 acts as a pro-metastatic factor via β-catenin stabilization', *International Journal of Cancer*, 136(10), pp. 2304–2315. doi: 10.1002/ijc.29296.

Sharma, G. and Berger, J. S. (2011) 'Platelet activity and cardiovascular risk in apparently healthy individuals: A review of the data', *Journal of Thrombosis and Thrombolysis*, 32(2), pp. 201–208. doi: 10.1007/s11239-011-0590-9.

Shebl, F. M. *et al.* (2012) 'Aspirin but not ibuprofen use is associated with reduced risk of prostate cancer: A PLCO Study', *British Journal of Cancer*, 107(1), pp. 207–214. doi: 10.1038/bjc.2012.227.

Singh, E. *et al.* (2017) 'Breast cancer trends differ by ethnicity: a report from the South African National Cancer Registry (1994-2009)', *European journal of public health*, 27(1), pp. 173–178. doi: 10.1093/eurpub/ckw191.

Slupsky, J. R. *et al.* (1997) 'The platelet antigens CD9 , CD42 and integrin aII ,, ~ IIIa can be topographically associated and transduce functionally similar signals', *Eur J Biochem*, 244, pp. 168–175.

Smeda, M., Kieronska, A., Proniewski, B. *et al.* (2018) 'Dual antiplatelet therapy with clopidogrel and aspirin increases mortality in 4T1 metastatic breast cancer-bearing mice by inducing vascular mimicry in primary tumour', *Oncotarget*, 9(25), pp. 17810–17824. doi: 10.18632/oncotarget.24891.

Smith, S. M. *et al.* (2011) 'A Simple Protocol for Using a LDH-Based Cytotoxicity Assay to Assess the Effects of Death and Growth Inhibition at the Same Time', *PLoS One*, 6(11).

doi:10.1371/journal.pone.0026908.

Smollich, M. *et al.* (2010) 'ETAR antagonist ZD4054 exhibits additive effects with aromatase inhibitors and fulvestrant in breast cancer therapy, and improves in vivo efficacy of anastrozole', *Breast Cancer Research and Treatment*, 123(2), pp. 345–357. doi: 10.1007/s10549-009-0644-2.

Soule, H. D. *et al.* (1973) 'A human cell line from a pleural effusion derived from a breast carcinoma1,2', *Journal of the National Cancer Institute*, 51(5), pp. 1409–1416. doi: 10.1093/jnci/51.5.1409.

Stalker, T.J., Newman, D.K., Ma, P., Wannemacher, K.M and Bras, L. F. (2012) 'Platelet Signaling', *Handbook of Experimental Pharmacology*, 210, pp. 59–85. doi: 10.1007/978-3-642-29423-5.

Stavropoulou, E., Pircalabioru, G. G. and Bezirtzoglou, E. (2018) 'The role of cytochromes P450 in infection', *Frontiers in Immunology*, 9(JAN), pp. 1–7. doi: 10.3389/fimmu.2018.00089.

Stemmler, M. P. (2008) 'Cadherins in development and cancer', *Molecular BioSystems*, 4(8), pp. 835–850. doi: 10.1039/b719215k.

Strande, J. L. and Phillips, S. A. (2009) 'Thrombin increases inflammatory cytokine and angiogenic growth factor secretion in human adipose cells in vitro', *Journal of Inflammation*, 6, pp. 1–10. doi: 10.1186/1476-9255-6-4.

Strauss, R. *et al.* (2011) 'Analysis of epithelial and mesenchymal markers in ovarian cancer reveals phenotypic heterogeneity and plasticity', *PLoS One*, 6(1), pp. 1–20. doi: 10.1371/journal.pone.0016186.

Su, Y. *et al.* (2016) 'N-cadherin functions as a growth suppressor in a model of K-ras-induced PanIN', *Oncogene*, 35(25), pp. 3335–3341. doi: 10.1038/onc.2015.382.

Sun, J. *et al.* (2019) 'Discovery and evaluation of Atopaxar hydrobromide, a novel JAK1 and JAK2 inhibitor, selectively induces apoptosis of cancer cells with constitutively activated STAT3', *Investigational New Drugs*. Investigational New Drugs. doi: 10.1007/s10637-019-00853-w.

Sweeney, E.E., McDaniel, R.E., Maximov, P.Y., Fan, P., and Jordan, V. C. (2012) 'Models and Mechanisms of Acquired Antihormone Resistance in Breast Cancer: Significant Clinical Progress Despite Limitations', *Horm Mol Biol Clin Investig*, 9(2), pp. 143–163. doi: 10.1515/hmbci-2011-0004.

Swieringa, F. *et al.* (2018) 'Integrating platelet and coagulation activation in fibrin clot formation', *Research and Practice in Thrombosis and Haemostasis*, 2(3), pp. 450–460. doi: 10.1002/rth2.12107.

Synowiec, E. *et al.* (2015) 'Doxorubicin Differentially Induces Apoptosis, Expression of Mitochondrial Apoptosis-Related Genes, and Mitochondrial Potential in BCR-ABL1-Expressing Cells Sensitive and Resistant to Imatinib', *BioMed Research International*, 2015, pp. 1–10. doi: 10.1155/2015/673512.

Tang, P. and Tse, G. M. (2016) 'Immunohistochemical surrogates for molecular classification of breast carcinoma: A 2015 update', *Archives of Pathology and Laboratory Medicine*, 140(8), pp. 806–814. doi: 10.5858/arpa.2015-0133-RA.

Tao, S. C., Guo, S. C. and Zhang, C. Q. (2017) 'Platelet-derived extracellular vesicles: An emerging therapeutic approach', *International Journal of Biological Sciences*, 13(7), pp. 828–834. doi: 10.7150/ijbs.19776.

Tasdemir, N. *et al.* (2018) 'Comprehensive phenotypic characterization human invasive lobular carcinoma cell lines in 2D and 3D cultures', *Cancer Research*, 78(21), pp. 6209–6222. doi: 10.1158/0008-5472.CAN-18-1416.

Taylor, M. A, Parvani, T. G. and Schiemann, W. P. (2010) 'The pathophysiology of epithelial-mesenchymal transition induced by transforming growth factor-β in normal and malignant mammary epithelial cells', *J Mammary Gland Biol Neoplasia,* 15(2), pp.169-190. doi: 10.1007/s 10911-010-9181-1.

Taylor, S. C. *et al.* (2019) 'The Ultimate qPCR Experiment: Producing Publication Quality, Reproducible Data the First Time', *Trends in Biotechnology*, 37(7), pp. 761–774. doi: 10.1016/j.tibtech.2018.12.002.

Tello-Montoliu, A. *et al.* (2011) 'Antiplatelet therapy: thrombin receptor antagonists.', *British journal of clinical pharmacology*, 72(4), pp. 658–71. doi: 10.1111/j.1365-2125.2010.03884.x.

Tesfamariam, B. (2016) 'Involvement of platelets in tumor cell metastasis', *Pharmacology and Therapeutics*, 157, pp. 112–119. doi: 10.1016/j.pharmthera.2015.11.005.

Thiery, J. P. *et al.* (2009) 'Epithelial-Mesenchymal Transitions in Development and Disease', *Cell*, 139(5), pp. 871–890. doi: 10.1016/j.cell.2009.11.007.

Thomas, M. R. and Storey, R. F. (2015) 'Effect of P2Y12 inhibitors on inflammation and immunity', *Thrombosis and Haemostasis*, 114(3), pp. 490–497. doi: 10.1160/TH14-12-1068.

Thompson, E. W. and Newgreen, D. F. (2005) 'Carcinoma invasion and metastasis: A role for epithelial-mesenchymal transition?', *Cancer Research*, 65(14), pp. 5991–5995. doi: 10.1158/0008-5472.CAN-05-0616.

Thon, J. N. and Italiano, J. E. (2012) 'Platelets: Past, present and future', *Handbook of Experimental Pharmacology*, pp. 4–20. doi: 10.1007/978-3-642-29423-5.

Tian, M. and Schiemann, W. P. (2017) 'TGF-β stimulation of EMT programs elicits non-genomic ER-α activity and anti-estrogen resistance in breast cancer cells', *Journal of Cancer Metastasis and Treatment*, 3(8), p. 150. doi: 10.20517/2394-4722.2017.38.

Tomaiuolo, M., Brass, L. F. and Stalker, T. J. (2017) 'Regulation of Platelet Activation and Coagulation and Its Role in Vascular Injury and Arterial Thrombosis', *Interventional Cardiology Clinics*, 6(1), pp. 1–12. doi: 10.1016/j.iccl.2016.08.001.

Tourdot, B. E. *et al.* (2018) 'Genetic variant in human PAR (Protease-Activated Receptor) 4 enhances thrombus formation resulting in resistance to antiplatelet therapeutics', *Arteriosclerosis, Thrombosis, and Vascular Biology*, 38(7), pp. 1632–1643. doi: 10.1161/ATVBAHA.118.311112.

Tripodi, A. (2016) 'Thrombin generation assay and its application in the clinical laboratory', *Clinical Chemistry*, 62(5), pp. 699–707. doi: 10.1373/clinchem.2015.248625.

Valcourt, U. *et al.* (2005) 'TGF-b and the Smad Signaling Pathway Support Transcriptomic Reprogramming during Epithelial- Mesenchymal Cell Transition', *Molecular Biology of the Cell*, 16(April), pp. 1987–2002. doi: 10.1091/mbc.E04.

Valentijn, K. M. *et al.* (2010) 'Multigranular exocytosis of Weibel-Palade bodies in vascular endothelial cells', 116(10), pp. 1807–1816. doi: 10.1182/blood-2010-03-274209.

Vallier, L. *et al.* (2016) ' Microparticles and Fibrinolysis', *Seminars in Thrombosis and Hemostasis*, 43, pp 129-134.

Varga-Szabo, D., Braun, A. and Nieswandt, B. (2011) 'STIM and Orai in platelet function', *Cell Calcium*, 50(3), pp. 270–278. doi: 10.1016/j.ceca.2011.04.002.

Vélez, P. and García, Á. (2015) 'Platelet proteomics in cardiovascular diseases', *Translational*

Proteomics, 7, pp. 15–29. doi: 10.1016/j.trprot.2014.09.002.

Vences-catalán, F. and Levy, S. (2018) 'Immune Targeting of Tetraspanins Involved in Cell Invasion and Metastasis', *Frontiers in Immunology*, 9(June), pp. 1–7. doi: 10.3389/fimmu.2018.01277.

Versteeg, H. H. *et al.* (2013) 'New Fundamentals in hemostasis', *Physiological Reviews*, 93(1), pp. 327–358. doi: 10.1152/physrev.00016.2011.

Vestweber, D. (2015) 'Cadherins in tissue architecture and disease', *Journal of Molecular Medicine*, 93(1), pp. 5–11. doi: 10.1007/s00109-014-1231-5.

Viale, P. H. (2005) 'Abnormal clotting in cancer: an overview of pathophysiology and etiology.', *Seminars in oncology nursing*, 21(4 Suppl 1), pp. 12–20. doi: 10.1016/j.soncn.2005.10.013.

Vinholt, P. J. *et al.* (2016) 'Platelet count is associated with cardiovascular disease, cancer and mortality: A population-based cohort study', *Thrombosis Research*, 148, pp. 136–142. doi: 10.1016/j.thromres.2016.08.012.

Voelker, M. and Hammer, M. (2012) 'Dissolution and pharmacokinetics of a novel micronized aspirin formulation', *Inflammopharmacology*, 20(4), pp. 225–231. doi: 10.1007/s10787-011-0099-z.

Vorobiof, D. A., Sitas, F. and Vorobiof, G. (2001) 'Breast Cancer Incidents South Africa', *J Clin Oncol*, 19(18), pp. 125–127.

Voutsadakis, I. A. (2014) 'Thrombocytosis as a prognostic marker in gastrointestinal cancers', *World Journal of Gastrointestinal Oncology*, 6(2), p. 34. doi: 10.4251/wjgo.v6.i2.34.

Waldron, B. *et al.* (2019) 'The clinical role of the TME in solid cancer', *British Journal of Cancer*. Springer US, 120(1), pp. 45–53. doi: 10.1038/s41416-018-0327-z.

Walker, A. J. *et al.* (2016) 'When are breast cancer patients at highest risk of venous thromboembolism? a cohort study using english health care data', *Blood*, 127(7), pp. 849–857. doi: 10.1182/blood-2015-01-625582.

Wang, D. and Dubois, R. N. (2006) 'Prostaglandins and cancer', *Gut*, 55(1), pp. 115–122. doi: 10.1136/gut.2004.047100.

Wang, H. *et al.* (2016) 'Global, regional, and national life expectancy, all-cause mortality, and cause-specific mortality for 249 causes of death, 1980–2015: a systematic analysis for the Global Burden of Disease Study 2015', *The Lancet*, 388(10053), pp. 1459–1544. doi: 10.1016/S0140-6736(16)31012-1.

Wang, M. *et al.* (2016) 'N-cadherin promotes epithelial-mesenchymal transition and cancer stem cell-like traits via ErbB signaling in prostate cancer cells', *International Journal of Oncology*, 48(2), pp. 595–606. doi: 10.3892/ijo.2015.3270.

Wang, R. *et al.* (2015) 'Electron cryotomography reveals ultrastructure alterations in platelets from patients with ovarian cancer', *Proceedings of the National Academy of Sciences of the United States of America*, 112(46), pp. 14266–14271. doi: 10.1073/pnas.1518628112.

Wang, S., Li, Z. and Xu, R. (2018) 'Human Cancer and Platelet Interaction, a Potential Therapeutic Target.', *International journal of molecular sciences*, 19(4), pp. 1246; doi:10.3390/ijms19041246. doi: 10.3390/ijms19041246.

Wang, Y. *et al.* (2016) 'Twist-mediated Epithelial-mesenchymal Transition Promotes Breast Tumor Cell Invasion via Inhibition of Hippo Pathway', *Scientific Reports*. Nature Publishing Group, 6(April), pp. 1–10. doi: 10.1038/srep24606.

Wang, Y. *et al.* (2018) 'TGF-β1 mediates the effects of aspirin on colonic tumor cell proliferation and apoptosis', *Oncology Letters*, 15(4), pp. 5903–5909. doi: 10.3892/ol.2018.8047.

Weber, M. R. *et al.* (2016) 'Activated tumor cell integrin αvβ3 cooperates with platelets to promote extravasation and metastasis from the blood stream', *Thrombosis Research*, 140, pp. S27–S36. doi: 10.1016/S0049-3848(16)30095-0.

Wegiel, B. *et al.* (2008) 'Interleukin-6 activates PI3K/Akt pathway and regulates cyclin A1 to promote prostate cancer cell survival', *International Journal of Cancer*, 122(7), pp. 1521–1529. doi: 10.1002/ijc.23261.

Wei, C. K. *et al.* (2015) 'Inhibition of the interactions between metastatic human breast cancer cells and platelets by β-nitrostyrene derivatives', *Life Sciences*, 143, pp. 147–155. doi: 10.1016/j.lfs.2015.11.003.

Welsh, A. W. *et al.* (2012) 'Cytoplasmic estrogen receptor in breast cancer', *Clinical Cancer Research*, 18(1), pp. 118–126. doi: 10.1158/1078-0432.CCR-11-1236.

Wiviott, S. D. *et al.* (2007) 'Prasugrel versus Clopidogrel in Patients with Acute Coronary Syndromes', *The new england journal of medicine*, 357, pp. 2001–2015.

Wiviott, S. D., Flather, M. D., O'Donoghue, M. L., *et al.* (2011) 'Randomized trial of atopaxar in the treatment of patients with coronary artery disease: the lessons from antagonizing the cellular effect of Thrombin–Coronary Artery Disease Trial.', *Circulation*, 123(17), pp. 1854–63. doi: 10.1161/CIRCULATIONAHA.110.001404.

Wojtukiewicz, M. Z. *et al.* (2016) 'Thrombin—Unique coagulation system protein with multifaceted impacts on cancer and metastasis', *Cancer and Metastasis Reviews*, 35(2), pp. 213–233. doi: 10.1007/s10555-016-9626-0.

Wojtukiewicz, M. Z. *et al.* (2017) 'Antiplatelet agents for cancer treatment: a real perspective or just an echo from the past?', *Cancer and Metastasis Reviews*, 36(2), pp. 305–329. doi: 10.1007/s10555-017-9683-z.

Wong, C and Chen, S. (2012) 'The development, application and limitations of breast cancer cell lines to study tamoxifen and aromatase inhibitor resistance', *J Steroid Biochen Mol Biol*, 131(3–5), pp. 83–92. doi: 10.1016/j.jsbmb.2011.12.005.

Xian, C. J. (2007) 'Roles of epidermal growth factor family in the regulation of postnatal somatic growth', *Endocrine Reviews*, 28(3), pp. 284–296. doi: 10.1210/er.2006-0049.

Xu, X. R. *et al.* (2016) 'Platelets and platelet adhesion molecules : novel mechanisms of thrombosis and anti-thrombotic therapies', *Thrombosis Journal*, 14(Suppl 1). doi: 10.1186/s12959-016-0100-6.

Xu, Y. *et al.* (2019) 'Clinical and prognostic significance of hypercoagulability in patients with metastatic colorectal cancer', *Int J Clin Exp Med*, 12(7), pp. 9175–9181. Available at: http://www.ijcem.com/files/ijcem0090059.pdf.

Yadav, P. and Shankar, B. S. (2019) 'Radio resistance in breast cancer cells is mediated through TGF-β signalling, hybrid epithelial-mesenchymal phenotype and cancer stem cells', *Biomedicine and Pharmacotherapy*, 111(July 2018), pp. 119–130. doi: 10.1016/j.biopha.2018.12.055.

Yalaza, M. and , Aydın İnan, M. B. (2016) 'Male breast cancer', *J Breast Health*, (12), pp. 1–8. doi: 110.5152/tjbh.2015.2711.

Yan, M. J. and Jurasz, P. (2016) 'The role of platelets in the tumor microenvironment: From solid tumors to leukemia', *Biochimica et Biophysica Acta - Molecular Cell Research*, 1863(3), pp. 392–400. doi: 10.1016/j.bbamcr.2015.07.008.

Yang, E. *et al.* (2009) 'Blockade of PAR1 Signaling with Cell-Penetrating Pepducins Inhibits Akt Survival Pathways in Breast Cancer Cells and Suppresses Tumor Survival and Metastasis', *Cancer Research* , 69(15), pp. 6223–6232. doi: 10.1158/0008-5472.CAN-09-0187.

Yersal, O. and Barutca, S. (2014) 'Biological subtypes of breast cancer: Prognostic and therapeutic implications', *World Journal of Clinical Oncology*, 5(3), pp. 412–424. doi: 10.5306/wjco.v5.i3.412.

Yi, X. *et al.* (2016) 'Association of Cytochrome P450 Genetic Variants with Clopidogrel Resistance and Outcomes in Acute Ischemic Stroke', *Journal of Atherosclerosis and Thrombosis*, 23(10), pp. 1188–1200. doi: 10.5551/jat.33290.

Yip, C. *et al.* (2013) 'First report of elevated monocyte-platelet aggregates in healthy children.', *PloS one*, 8(6), p. e67416. doi: 10.1371/journal.pone.0067416.

Youlden, D. R. *et al.* (2012) 'The descriptive epidemiology of female breast cancer: an international comparison of screening, incidence, survival and mortality.', *Cancer epidemiology* , 36(3), pp. 237–48. doi: 10.1016/j.canep.2012.02.007.

Yu, L. *et al.* (2014) 'Platelets promote tumour metastasis via interaction between TLR4 and tumour cell-released high-mobility group box1 protein', *Nature Communications*, 5, 5256. doi: 10.1038/ncomms6256.

Yu, Q. *et al.* (2011) 'Expression of androgen receptor in breast cancer and its significance as a prognostic factor', *Annals of Oncology*, 22(6), pp. 1288–1294. doi: 10.1093/annonc/mdq586.

Yu, S. *et al.* (2017) 'The T47D cell line is an ideal experimental model to elucidate the progesterone-specific effects of a luminal A subtype of breast cancer', *Biochemical and Biophysical Research Communications*, 486(3), pp. 752–758. doi: 10.1016/j.bbrc.2017.03.114.

Klymenko,Y. *et al.* (2017) 'Cadherin Composition and Multicellular Aggregate Invasion In Organotypic Models of Epithelial Ovarian Cancer Intraperitoneal Metastasis', *Oncogene*, 36(42), pp. 5840–5851. doi: 10.1016/j.physbeh.2017.03.040.

Yun, S. H. *et al.* (2016) 'Platelet activation: The mechanisms and potential biomarkers', *BioMed Research International*, 2016, pp. 10–14. doi: 10.1155/2016/9060143.

Zarà, M. *et al.* (2018) 'Molecular mechanisms of platelet activation and aggregation induced by breast cancer cells', *Cellular Signalling*, 48, pp. 45–53. doi: 10.1016/j.cellsig.2018.04.008.

Zarzynska, J. M. (2014) 'Two faces of TGF-beta1 in breast cancer', *Mediators of Inflammation*, 2014. doi: 10.1155/2014/141747.

Van Der Zee, P. M. *et al.* (2006) 'P-selectin- and CD63-exposing platelet microparticles reflect platelet activation in peripheral arterial disease and myocardial infarction', *Clinical Chemistry*, 52(4), pp. 657–664. doi: 10.1373/clinchem.2005.057414.

Zeisberg, M. and Neilson, E. G. (2009) 'Review series personal perspective Biomarkers for epithelial-mesenchymal transitions', *The Journal of clinical investigation*, 119(6), pp. 1429–1437. doi: 10.1172/JCI36183.

Zhang, H. *et al.* (2013) 'Microenvironmental regulation of metastasis by exosomes', *Trends in Cell Biol*,

24(3), pp. 153–160. doi: 10.1016/j.tcb.2013.09.007.

Zhang, Q. *et al.* (2017) 'Patterns and functional implications of platelets upon tumor "education"', *International Journal of Biochemistry and Cell Biology*, 90(April), pp. 68–80. doi: 10.1016/j.biocel.2017.07.018.

Zhang, X. *et al.* (2018) 'Aspirin promotes apoptosis and inhibits proliferation by blocking G 0 /G 1 into S phase in rheumatoid arthritis fibroblast-like synoviocytes via downregulation of JAK/STAT3 and NF-κB signaling pathway', *International Journal of Molecular Medicine*, 42(6), pp. 3135–3148. doi: 10.3892/ijmm.2018.3883.

Zhang, Y.E. (2017) 'Non-Smad signaling pathways of the TGFβ family', *Cold Spring Harb Perspect Biol*, 9: pp.1-18. doi: 10.1101/cshperpect.a022129.

Zhong, S. *et al.* (2015) 'Aspirin use and risk of breast cancer: Systematic review and meta-analysis of observational studies', *Cancer Epidemiology Biomarkers and Prevention*, 24(11), pp. 1645–1655. doi: 10.1158/1055-9965.EPI-15-0452.

Zhou, X. Y. *et al.* (2019) 'Enzymatic activities of CYP3A4 allelic variants on quinine 3-hydroxylation in vitro', *Frontiers in Pharmacology*, 10(MAY). doi: 10.3389/fphar.2019.00591.

Zou, J. J. *et al.* (2012) 'Bioequivalence study of clopidogrel 75 Mg tablets in healthy male volunteers', *Journal of Bioequivalence and Bioavailability*, 4(1), pp. 006–009. doi: 10.4172/jbb.1000102.

APPENDICES

APPENDIX A: Chapter II supplementary information

A1: Drug preparation

The drugs were weighted as indicated in Table 1 and dissolved in 100µl of DMSO and 900µl of distilled water in order to obtain a primary stock solution that was highly concentrated. The primary stock solution was further diluted in media to obtain a secondary stock solution. Working solutions were prepared by diluting the secondary stock solutions in media in order to obtain concentrations which correspond to the 1X Cmax, 2X Cmax, 4X Cmax, 8X Cmax and 10X Cmax. The drug cocktails were combined at a ratio of 1:1 (Table 1).

Table 1: The Cmax concentrations of the drugs used in the study and the amount weighed out in preparation of the primary stock solutions.

	Concentration	**Reference**
Anastrozole	Cmax= 16.16 ng/ml	Product monograph, 2013
Aspirin	Cmax= 4.4 µg/ml	Voelker and Hammer, 2012
Clopidogrel	Cmax= 1.86ng/ml	Zou *et al.,* 2012
Atopaxar	Inhibitory []= 0.064 µM	Kogushi *et al.,* 2011

STEP 1: CONVERT ALL CONCENTRATIONS TO BE THE SAME UNIT (mg/ml)

- **Anastrozole**; 16.16 ng/ml divide by 10^6 = 1.6 x 10^{-5}mg/ml
- **Aspirin;** 4.4 µg/ml divide by 10^3 = 4.4 x 10^{-3}mg/ml
- **Clopidogrel;** 1.86ng/ml divide by 10^6 = 1.86 x10^{-6}mg/ml
- **Atopaxar;** convert µM to M; 0.064 µM divide by 10^6 = 6.4 x 10^{-8} M

Convert molarity (M) to mg/ml; molarity (M) x molar mass (Mr)

= (6.4 x 10^{-8}moles/litre) (608.54 g/moles)

= (3.895x10^{-5} g/L)(10^3)

= 0.039 mg/ml

STEP 2: CONCENTRATION RANGE OF INTEREST

Table 2.1: A range of concentrations to be tested in a dose-dependent study using LDH cytotoxicity assay

	1X (mg/ml)	**2X** (mg/ml)	**4X** (mg/ml)	**8X** (mg/ml)	**10X** (mg/ml)
Anastrozole	1.6 x 10^{-5}	3.2 x 10^{-5}	6.4 x 10^{-5}	1.28 x 10^{-4}	1.6 x10^{-4}
Aspirin	4.4 x10^{-3}	8.8 x 10^{-3}	0.018	0.035	0.044
Clopidogrel	1.86 x 10^{-6}	3.72 x 10^{-6}	7.44 x 10^{-6}	1.488 x 10^{-5}	1.86 x 10^{-5}
Atopaxar	0.039	0.078	0.156	0.312	0.39

STEP 3: PREPARING STOCK SOLUTIONS

Resource limitation: The scale measures grams (g) and milligrams (mg) only (up to four decimal places) therefore have to calculate the lowest concentration of the drug that can be measured in mg and will give the concentrations of interest when diluted with media.

Table 3.1: Drug concentrations to be used to prepare stock solutions

	1X [mg/ml]	Multiply by	[mg/ml]	**[g]**
Anastrozole	1.6×10^{-5}	10^6	16	**0.016**
Aspirin	4.4×10^{-3}	10^4	44	**0.044**
Clopidogrel	1.86×10^{-6}	10^7	18.6	**0.0186**
Atopaxar	0.039	10^3	39	**0.039**

- The drugs will be measured in grams as indicated in the table **[g]** and dissolved in 1ml of 10% DMSO solution in order to make the stock solution
- To make 10% DMSO solution; mix 100µl DMSO and 900 µl distilled water to make 1ml highly concentrated solution

STEP 4: PREPARING WORKING SOLUTIONS

- Calculate the volume needed from stock solution (V1) to make 10ml of working solution using the C1V1=C2V2 formula
- Table 4.1: Concentration (mg) of the drug found in different volumes (µl) of the stock solution

	Stock 1	**Stock 2**	**Stock 3**	**10X stock**
Anastrozole	16mg/ml in 1ml solution (**0.1µl**)	Take 1ml (V1) from stock 1 to make 10ml of 1.6mg/ml solution (**1µl**)	Take 1ml (V1) from stock 2 to make 10ml of 0.16mg/ml solution (**10µl**)	Take 10µl (V1) from stock 3 to make 10ml of 1.6×10^{-4} mg/ml working solution
Aspirin	44mg/ml in 1ml solution	-	-	Take 10µl from stock 1 to make 10ml 0.044mg/ml solution
Clopidogrel	18.6mg/ml in 1ml solution (**0.01 µl**)	Take 1ml from stock 1 to make 10ml of 1.86mg/ml solution (**0.1µl**)	Take 1ml from stock 2 to make 10ml of 0.186mg/ml solution (**1µl**)	Take 1µl from stock 3 to make 10ml of 1.86×10^5mg/ml solution
Atopaxar	39mg/ml in 1ml solution	-	-	Take 10µl from stock 1 to make 10ml solution with [] of 0.39mg/ml

- 10 µl of the stock solution will be used to prepare the working solutions because it will give a final percentage of maximum 0.1% DMSO and it has a concentration which is 10X of the highest concentration (10X) for all the drugs.
- c1v1=c2v2 formula was used to calculate the total volume needed which contains the required concentration table 4.2 a-d.

Table 4.2 (a): Preparing working solutions for Anastrozole

Concentration of interest (mg)	**Stock (µl)**	**Media (µl)**	**Total (µl)**
1x (1.6×10^{-5})	10	990	**1000**
2x (3.2×10^{-5})	10	490	**500**
4x (6.4×10^{-5})	10	240	**250**
8x (1.28×10^{-4})	10	115	**125**
10x (1.6×10^{-4})	10	90	**100**

Table 4.2 (b): Preparing working solutions for Aspirin

Concentration of interest (mg)	**Stock (µl)**	**Media (µl)**	**Total (µl)**
1x (4.4×10^{-3})	10	990	**1000**
2x (8.8×10^{-3})	10	490	**500**
4x (0.018)	10	240	**250**
8x (0.035)	10	115	**125**
10x (0.044)	10	90	**100**

Table 4.2 (c): Preparing working solutions for Clopidogrel

Concentration of interest (mg)	**Stock (µl)**	**Media (µl)**	**Total (ml)**
1x (1.86×10^{-6})	10	9990	**10**
2x (3.72×10^{-6})	10	4990	**5**
4x (7.44×10^{-6})	10	2490	**2.5**
8x (1.488×10^{-5})	10	1240	**1.25**
10x (1.86×10^{-5})	10	990	**1**

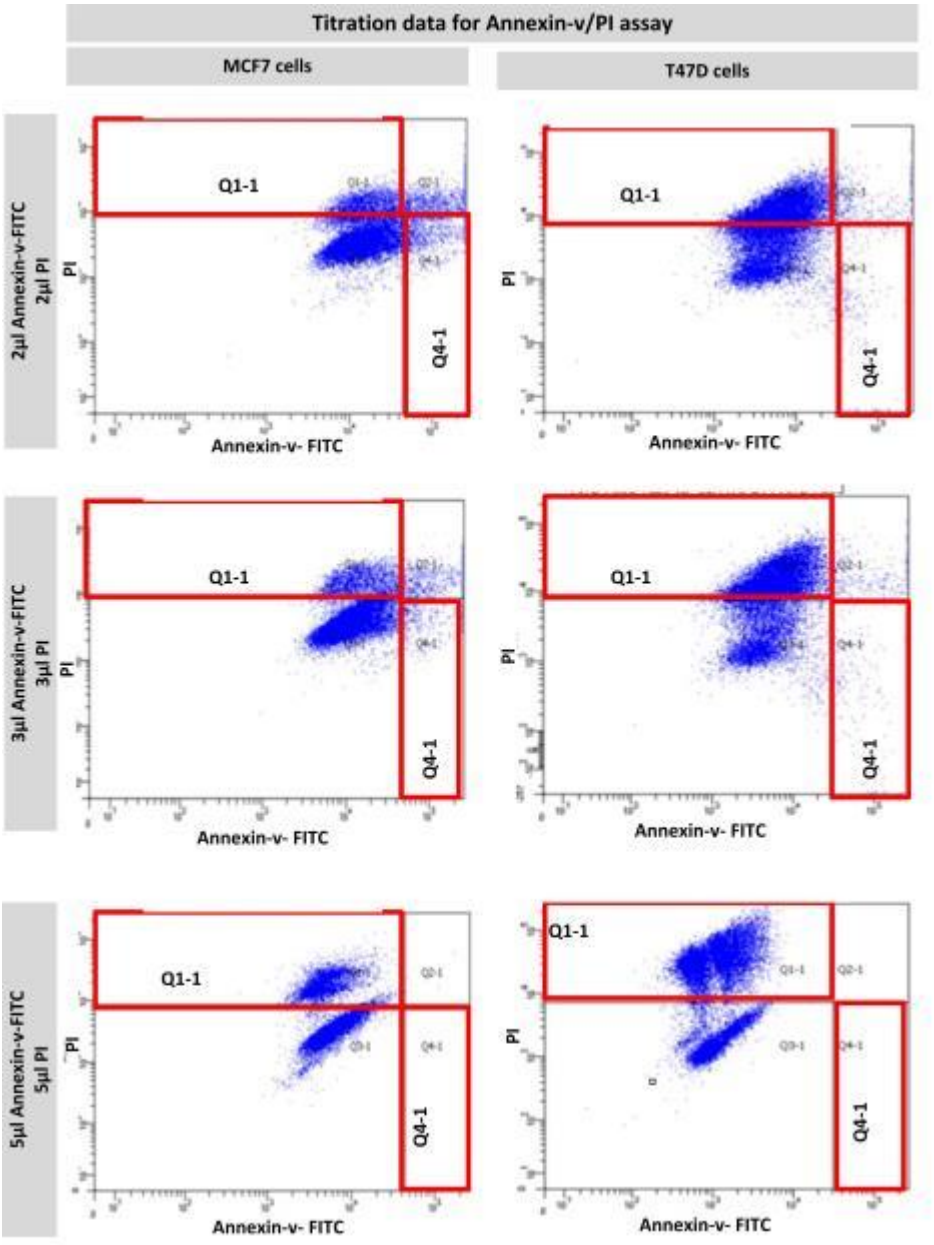
Table 4.2 (d): Preparing working solutions for Atopaxar

Concentration of interest (mg)	**Stock (µl)**	**Media (µl)**	**Total (µl)**
1x (0.039)	10	990	**1000**
2x (0.078)	10	490	**500**
4x (0.156)	10	240	**250**
8x (0.312)	10	115	**125**
10x (0.39)	10	90	**100**

A2: Cytotoxicity parameters statistical output (Neutral Red assay, Lactate Dehydrogenase assay, Annexin-V/PI assay)

A2.1 Titration for Annexin-V and PI

Fig A2.1: Different volumes of the annexin-v and PI antibodies were tested (2µl, 3µl and 5µl). 2µl was chosen to be the optimal concentration because it resolved both annexin-v-FITC (Q4-1) and PI (Q1-1) optimally. PI was generally detected in all volumes; however, annexin-v-FITC was lower when 3µl of antibody was used and undetected when 5µl of antibody was used.



A2.2: Statistica outcome for MCF7 cells

Statistica Friedman output for cytotoxicity parameters in MCF7 cells

Friedman ANOVA and Kendall Coeff. of Concordance (Log layouts (1 and 2) for stats)
ANOVA Chi Sqr. (N = 81, df = 5) = 389.9594 p =0.00000
Coeff. of Concordance = .96286 Aver. rank r = .96240

Variable	Average Rank	Sum of Ranks	Mean	Std.Dev.
LOG Q1-1 (Necrosis)	4.000000	324.0000	1.301507	0.114240
LOG Q2-1 (L.Apo)	1.604938	130.0000	0.513306	0.175867
LOG Q3-1 (Live)	5.049383	409.0000	1.859847	0.034830
LOG Q4-1 (E.Apo)	1.419753	115.0000	0.424694	0.235475
LOG Cyto (LDH)	2.975309	241.0000	0.999511	0.018333
LOG Viab (NR)	5.950617	482.0000	1.993059	0.103737

Part A: Statistica Friedman post hoc output for cytotoxicity parameters in MCF7 cells

Ana

Absolute Differences between Average RankApprox. significant if > 1.69463820347543 at .05 significance level

	1 LOG Q1-1 (Necrosis)	2 LOG Q2-1 (L.Apo)	3 LOG Q3-1 (Live)	4 LOG Q4-1 (E.Apo)	5 LOG Cyto (LDH)	6 LOG Viab (NR)
LOG Q1-1 (Necrosis)	---	2.57142857	1	2.33333333	1.0952381	2
LOG Q2-1 (L.Apo)	2.57142857	---	3.57142857	0.238095238	1.47619048	4.57142857
LOG Q3-1 (Live)	1	3.57142857	---	3.33333333	2.0952381	1
LOG Q4-1 (E.Apo)	2.33333333	0.238095238	3.33333333	---	1.23809524	4.33333333
LOG Cyto (LDH)	1.0952381	1.47619048	2.0952381	1.23809524	---	3.0952381
LOG Viab (NR)	2	4.57142857	1	4.33333333	3.0952381	---

AnaAspClop

Absolute Differences between Average RankApprox. significant if > 1.69463820347543 at .05 significance level

	1 LOG Q1-1 (Necrosis)	2 LOG Q2-1 (L.Apo)	3 LOG Q3-1 (Live)	4 LOG Q4-1 (E.Apo)	5 LOG Cyto (LDH)	6 LOG Viab (NR)
LOG Q1-1 (Necrosis)	---	2.38095238	1.14285714	2.52380952	1.0952381	1.85714286
LOG Q2-1 (L.Apo)	2.38095238	---	3.52380952	0.142857143	1.28571429	4.23809524
LOG Q3-1 (Live)	1.14285714	3.52380952	---	3.66666667	2.23809524	0.714285714
LOG Q4-1 (E.Apo)	2.52380952	0.142857143	3.66666667	---	1.42857143	4.38095238
LOG Cyto (LDH)	1.0952381	1.28571429	2.23809524	1.42857143	---	2.95238095
LOG Viab (NR)	1.85714286	4.23809524	0.714285714	4.38095238	2.95238095	---

Part B: Statistica Friedman post hoc output for cytotoxicity parameters in MCF7 cells

AspClop

Absolute Differences between Average RankApprox. significant if > 1.69463820347543 at .05 significance level

	1 LOG Q1-1 (Necrosis)	2 LOG Q2-1 (L.Apo)	3 LOG Q3-1 (Live)	4 LOG Q4-1 (E.Apo)	5 LOG Cyto (LDH)	6 LOG Viab (NR)
LOG Q1-1 (Necrosis)	---	2.61904762	1	2.28571429	1.0952381	2
LOG Q2-1 (L.Apo)	2.61904762	---	3.61904762	0.333333333	1.52380952	4.61904762
LOG Q3-1 (Live)	1	3.61904762	---	3.28571429	2.0952381	1
LOG Q4-1 (E.Apo)	2.28571429	0.333333333	3.28571429	---	1.19047619	4.28571429
LOG Cyto (LDH)	1.0952381	1.52380952	2.0952381	1.19047619	---	3.0952381
LOG Viab (NR)	2	4.61904762	1	4.28571429	3.0952381	---

AnaAto

Absolute Differences between Average RankApprox. significant if > 1.69463820347543 at .05 significance level

	1 LOG Q1-1 (Necrosis)	2 LOG Q2-1 (L.Apo)	3 LOG Q3-1 (Live)	4 LOG Q4-1 (E.Apo)	5 LOG Cyto (LDH)	6 LOG Viab (NR)
LOG Q1-1 (Necrosis)	---	2.19047619	1	2.71428571	1.0952381	2
LOG Q2-1 (L.Apo)	2.19047619	---	3.19047619	0.523809524	1.0952381	4.19047619
LOG Q3-1 (Live)	1	3.19047619	---	3.71428571	2.0952381	1
LOG Q4-1 (E.Apo)	2.71428571	0.523809524	3.71428571	---	1.61904762	4.71428571
LOG Cyto (LDH)	1.0952381	1.0952381	2.0952381	1.61904762	---	3.0952381
LOG Viab (NR)	2	4.19047619	1	4.71428571	3.0952381	---

Ato

Absolute Differences between Average RankApprox. significant if > 1.69463820347543 at .05 significance level

	1 LOG Q1-1 (Necrosis)	2 LOG Q2-1 (L.Apo)	3 LOG Q3-1 (Live)	4 LOG Q4-1 (E.Apo)	5 LOG Cyto (LDH)	6 LOG Viab (NR)
LOG Q1-1 (Necrosis)	---	2.33333333	1.04761905	2.57142857	1.0952381	1.95238095
LOG Q2-1 (L.Apo)	2.33333333	---	3.38095238	0.238095238	1.23809524	4.28571429
LOG Q3-1 (Live)	1.04761905	3.38095238	---	3.61904762	2.14285714	0.904761905
LOG Q4-1 (E.Apo)	2.57142857	0.238095238	3.61904762	---	1.47619048	4.52380952
LOG Cyto (LDH)	1.0952381	1.23809524	2.14285714	1.47619048	---	3.04761905
LOG Viab (NR)	1.95238095	4.28571429	0.904761905	4.52380952	3.04761905	---

A2.3: Statistica outcome for T47D cells

Statistica Friedman output for cytotoxicity parameters in T47D cells

Friedman ANOVA and Kendall Coeff. of Concordance (Log layouts (1 and 2) for stats)
ANOVA Chi Sqr. (N = 80, df = 5) = 382.3214 p =0.00000
Coeff. of Concordance = .95580 Aver. rank r = .95524

Variable	Average Rank	Sum of Ranks	Mean	Std.Dev.
LOG Q1-1 (Necrosis)	4.225000	338.0000	1.526711	0.138642
LOG Q2-1 (L.Apo)	1.112500	89.0000	0.384142	0.242480
LOG Q3-1 (Live)	4.775000	382.0000	1.738595	0.118475
LOG Q4-1 (E.Apo)	2.000000	160.0000	0.650830	0.234887
LOG Cyto (LDH)	2.887500	231.0000	0.998594	0.005060
LOG Viab (NR)	6.000000	480.0000	1.993676	0.083163

Statistica Friedman post hoc output for cytotoxicity parameters in T47D cells

Ana

Absolute Differences between Average RankApprox. significant if > 1.69463820347543 at .05 significance level

	1 LOG Q1-1 (Necrosis)	2 LOG Q2-1 (L.Apo)	3 LOG Q3-1 (Live)	4 LOG Q4-1 (E.Apo)	5 LOG Cyto (LDH)	6 LOG Viab (NR)
LOG Q1-1 (Necrosis)	---	2.9047619	0.904761905	2.04761905	1.19047619	1.95238095
LOG Q2-1 (L.Apo)	2.9047619	---	3.80952381	0.857142857	1.71428571	4.85714286
LOG Q3-1 (Live)	0.904761905	3.80952381	---	2.95238095	2.0952381	1.04761905
LOG Q4-1 (E.Apo)	2.04761905	0.857142857	2.95238095	---	0.857142857	4
LOG Cyto (LDH)	1.19047619	1.71428571	2.0952381	0.857142857	---	3.14285714
LOG Viab (NR)	1.95238095	4.85714286	1.04761905	4	3.14285714	---

AnaAspClop

Absolute Differences between Average RankApprox. significant if > 1.69463820347543 at .05 significance level

	1 LOG Q1-1 (Necrosis)	2 LOG Q2-1 (L.Apo)	3 LOG Q3-1 (Live)	4 LOG Q4-1 (E.Apo)	5 LOG Cyto (LDH)	6 LOG Viab (NR)
LOG Q1-1 (Necrosis)	---	3.14285714	0.523809524	2.19047619	1.38095238	1.76190476
LOG Q2-1 (L.Apo)	3.14285714	---	3.66666667	0.952380952	1.76190476	4.9047619
LOG Q3-1 (Live)	0.523809524	3.66666667	---	2.71428571	1.9047619	1.23809524
LOG Q4-1 (E.Apo)	2.19047619	0.952380952	2.71428571	---	0.80952381	3.95238095
LOG Cyto (LDH)	1.38095238	1.76190476	1.9047619	0.80952381	---	3.14285714
LOG Viab (NR)	1.76190476	4.9047619	1.23809524	3.95238095	3.14285714	---

Statistica Friedman post hoc output for cytotoxicity parameters in T47D cells

AspClop

Absolute Differences between Average RankApprox. significant if > 1.7364874237127 at .05 significance level

	1 LOG Q1-1 (Necrosis)	2 LOG Q2-1 (L.Apo)	3 LOG Q3-1 (Live)	4 LOG Q4-1 (E.Apo)	5 LOG Cyto (LDH)	6 LOG Viab (NR)
LOG Q1-1 (Necrosis)	---	3.5	0.3	2.35	2.1	1.35
LOG Q2-1 (L.Apo)	3.5	---	3.2	1.15	1.4	4.85
LOG Q3-1 (Live)	0.3	3.2	---	2.05	1.8	1.65
LOG Q4-1 (E.Apo)	2.35	1.15	2.05	---	0.25	3.7
LOG Cyto (LDH)	2.1	1.4	1.8	0.25	---	3.45
LOG Viab (NR)	1.35	4.85	1.65	3.7	3.45	---

AnaAto

Absolute Differences between Average RankApprox. significant if > 1.69463820347543 at .05 significance level

	1 LOG Q1-1 (Necrosis)	2 LOG Q2-1 (L.Apo)	3 LOG Q3-1 (Live)	4 LOG Q4-1 (E.Apo)	5 LOG Cyto (LDH)	6 LOG Viab (NR)
LOG Q1-1 (Necrosis)	---	2.85714286	0.80952381	2.19047619	1.23809524	1.9047619
LOG Q2-1 (L.Apo)	2.85714286	---	3.66666667	0.666666667	1.61904762	4.76190476
LOG Q3-1 (Live)	0.80952381	3.66666667	---	3	2.04761905	1.0952381
LOG Q4-1 (E.Apo)	2.19047619	0.666666667	3	---	0.952380952	4.0952381
LOG Cyto (LDH)	1.23809524	1.61904762	2.04761905	0.952380952	---	3.14285714
LOG Viab (NR)	1.9047619	4.76190476	1.0952381	4.0952381	3.14285714	---

Ato

Absolute Differences between Average RankApprox. significant if > 1.69463820347543 at .05 significance level

	1 LOG Q1-1 (Necrosis)	2 LOG Q2-1 (L.Apo)	3 LOG Q3-1 (Live)	4 LOG Q4-1 (E.Apo)	5 LOG Cyto (LDH)	6 LOG Viab (NR)
LOG Q1-1 (Necrosis)	---	2.85714286	0.904761905	2.0952381	1.19047619	1.95238095
LOG Q2-1 (L.Apo)	2.85714286	---	3.76190476	0.761904762	1.66666667	4.80952381
LOG Q3-1 (Live)	0.904761905	3.76190476	---	3	2.0952381	1.04761905
LOG Q4-1 (E.Apo)	2.0952381	0.761904762	3	---	0.904761905	4.04761905
LOG Cyto (LDH)	1.19047619	1.66666667	2.0952381	0.904761905	---	3.14285714
LOG Viab (NR)	1.95238095	4.80952381	1.04761905	4.04761905	3.14285714	---

A2.4: Statistica outcome between cell lines

Statistica Kruskal-Wallis output for cytotoxicity parameters between cell lines

Live

Kruskal-Wallis ANOVA by Ranks; LOG Q3-1 (Live) (Log layouts (1 and 2) for stats)
Independent (grouping) variable: Cell line
Kruskal-Wallis test: H (1, N= 162) =69.85130 p =.0000

Depend.: LOG Q3-1 (Live)	Code	Valid N	Sum of Ranks	Mean Rank
MCF7	1	81	9096.500	112.3025
T47D	2	81	4106.500	50.6975

Early Apoptosis

Kruskal-Wallis ANOVA by Ranks; LOG Q4-1 (E.Apo) (Log layouts (1 and 2) for stats)
Independent (grouping) variable: Cell line
Kruskal-Wallis test: H (1, N= 161) =32.36594 p =.0000

Depend.: LOG Q4-1 (E.Apo)	Code	Valid N	Sum of Ranks	**Mean Rank**
MCF7	1	81	4878.500	60.2284
T47D	2	80	8162.500	102.0313

Late Apoptosis

Kruskal-Wallis ANOVA by Ranks; LOG Q2-1 (L.Apo) (Log layouts (1 and 2) for stats)
Independent (grouping) variable: Cell line
Kruskal-Wallis test: H (1, N= 161) =17.34073 p =.0000

Depend.: LOG Q2-1 (L.Apo)	Code	Valid N	Sum of Ranks	Mean Rank
MCF7	1	81	7792.500	96.20370
T47D	2	80	5248.500	65.60625

Necrosis

Kruskal-Wallis ANOVA by Ranks; LOG Q1-1 (Necrosis) (Log layouts (1 and 2) for stats)
Independent (grouping) variable: Cell line
Kruskal-Wallis test: H (1, N= 162) =75.70891 p =.0000

Depend.: LOG Q1-1 (Necrosis)	Code	Valid N	Sum of Ranks	Mean Rank
MCF7	1	81	4004.000	49.4321
T47D	2	81	9199.000	113.5679

NR assay

Kruskal-Wallis ANOVA by Ranks; LOG Viab (NR) (Log layouts (1 and 2) for stats)
Independent (grouping) variable: Cell line
Kruskal-Wallis test: H (1, N= 162) =.1122E-4 p =.9973

Depend.: LOG Viab (NR)	Code	Valid N	Sum of Ranks	**Mean Rank**
MCF7	1	81	6600.500	81.48765
T47D	2	81	6602.500	81.51235

LDH assay

Kruskal-Wallis ANOVA by Ranks; LOG Cyto (LDH) (Log layouts (1 and 2) for stats)
Independent (grouping) variable: Cell line
Kruskal-Wallis test: H (1, N= 162) =.0370988 p =.8473

Depend.: LOG Cyto (LDH)	Code	Valid N	Sum of Ranks	Mean Rank
MCF7	1	81	6659.000	82.20988
T47D	2	81	6544.000	80.79012

A3: Scanning Electron Microscopy statistical output

Part A: Statistica Kruskal-Wallis output for changes in cell morphology

MCF7 cells

Filopodia

Kruskal-Wallis ANOVA by Ranks; Filopodia (friedman layout T47D)
Independent (grouping) variable: Cell line and treatment
Kruskal-Wallis test: H (6, N= 243) =6.400601 p =.3798

Depend.: Filopodia	Code	Valid N	Sum of Ranks	Mean Rank
M UT	1	9	1053.000	117.0000
M DC	2	9	1053.000	117.0000
M Ana	3	45	4842.000	107.6000
M Anaaspclop	4	45	5782.500	128.5000
M Aspclop	5	45	5530.500	122.9000
M Anaato	6	45	6246.000	138.8000
M Ato	7	45	5139.000	114.2000

Pseudopodia

Kruskal-Wallis ANOVA by Ranks; Pseudopodia (friedman layout T47D)
Independent (grouping) variable: Cell line and treatment
Kruskal-Wallis test: H (6, N= 243) =12.39457 p =.0537

Depend.: Pseudopodia	Code	Valid N	Sum of Ranks	Mean Rank
M UT	1	9	957.000	106.3333
M DC	2	9	1026.500	114.0556
M Ana	3	45	5052.500	112.2778
M Anaaspclop	4	45	6106.500	135.7000
M Aspclop	5	45	5352.500	118.9444
M Anaato	6	45	6455.000	143.4444
M Ato	7	45	4696.000	104.3556

Bleb density

Kruskal-Wallis ANOVA by Ranks; Bleb density (friedman layout T47D)
Independent (grouping) variable: Cell line and treatment
Kruskal-Wallis test: H (6, N= 242) =28.49987 p =.0001

Depend.: Bleb density	Code	Valid N	Sum of Ranks	Mean Rank
M UT	1	9	926.500	102.9444
M DC	2	9	1043.000	115.8889
M Ana	3	45	5215.000	115.8889
M Anaaspclop	4	44	5678.000	129.0455
M Aspclop	5	45	5349.000	118.8667
M Anaato	6	45	6879.500	152.8778
M Ato	7	45	4312.000	95.8222

T47D cells

Filopodia

Kruskal-Wallis ANOVA by Ranks; Filopodia (friedman layout T47D)
Independent (grouping) variable: Cell line and treatment
Kruskal-Wallis test: H (6, N= 241) =33.66052 p =.0000

Depend.: Filopodia	Code	Valid N	Sum of Ranks	Mean Rank
T UT	1	9	844.500	93.8333
T DC	2	9	1588.500	176.5000
T Ana	3	43	4141.000	96.3023
T Anaaspclop	4	45	5023.000	111.6222
T Aspclop	5	45	5210.500	115.7889
T Anaato	6	45	7199.000	159.9778
T Ato	7	45	5154.500	114.5444

Pseudopodia

Kruskal-Wallis ANOVA by Ranks; Pseudopodia (friedman layout T47D)
Independent (grouping) variable: Cell line and treatment
Kruskal-Wallis test: H (6, N= 241) =30.04365 p =.0000

Depend.: Pseudopodia	Code	Valid N	Sum of Ranks	Mean Rank
T UT	1	9	1014.000	112.6667
T DC	2	9	1647.000	183.0000
T Ana	3	43	4270.500	99.3140
T Anaaspclop	4	45	4955.500	110.1222
T Aspclop	5	45	4993.000	110.9556
T Anaato	6	45	7056.000	156.8000
T Ato	7	45	5225.000	116.1111

Bleb density

Kruskal-Wallis ANOVA by Ranks; Bleb density (friedman layout T47D)
Independent (grouping) variable: Cell line and treatment
Kruskal-Wallis test: H (6, N= 242) =28.91573 p =.0001

Depend.: Bleb density	Code	Valid N	Sum of Ranks	Mean Rank
T UT	1	9	1153.500	128.1667
T DC	2	9	1153.500	128.1667
T Ana	3	45	5297.500	117.7222
T Anaaspclop	4	45	5577.500	123.9444
T Aspclop	5	45	4742.500	105.3889
T Anaato	6	44	6886.000	156.5000
T Ato	7	45	4592.500	102.0556

Part B: Statistica Kruskal-Wallis output for changes in cell morphology

MCF7 cells

Bleb size

Kruskal-Wallis ANOVA by Ranks; Bleb size (friedman layout T47D)
Independent (grouping) variable: Cell line and treatment
Kruskal-Wallis test: H (6, N= 243) =12.11123 p =.0595

Depend.: Bleb size	Code	Valid N	Sum of Ranks	Mean Rank
M UT	1	9	994.000	110.4444
M DC	2	9	1119.500	124.3889
M Ana	3	45	5514.000	122.5333
M Anaaspclop	4	45	6092.000	135.3778
M Aspclop	5	45	5543.500	123.1889
M Anaato	6	45	5808.500	129.0778
M Ato	7	45	4574.500	101.6556

Microvilli density

Kruskal-Wallis ANOVA by Ranks; Microvilli density (friedman layout T47D)
Independent (grouping) variable: Cell line and treatment
Kruskal-Wallis test: H (6, N= 243) =8.237906 p =.2212

Depend.: Microvilli density	Code	Valid N	Sum of Ranks	Mean Rank
M UT	1	9	1067.000	118.5556
M DC	2	9	981.000	109.0000
M Ana	3	45	5832.000	129.6000
M Anaaspclop	4	45	5349.500	118.8778
M Aspclop	5	45	4948.000	109.9556
M Anaato	6	45	6356.000	141.2444
M Ato	7	45	5112.500	113.6111

T47D cells

Kruskal-Wallis ANOVA by Ranks; Bleb size (friedman layout T47D)
Independent (grouping) variable: Cell line and treatment
Kruskal-Wallis test: H (6, N= 243) =7.522869 p =.2752

Depend.: Bleb size	Code	Valid N	Sum of Ranks	Mean Rank
T UT	1	9	1224.000	136.0000
T DC	2	9	1188.000	132.0000
T Ana	3	45	5590.500	124.2333
T Anaaspclop	4	45	5781.500	128.4778
T Aspclop	5	45	5043.000	112.0667
T Anaato	6	45	5873.500	130.5222
T Ato	7	45	4945.500	109.9000

Kruskal-Wallis ANOVA by Ranks; Microvilli density (friedman layout T47D)
Independent (grouping) variable: Cell line and treatment
Kruskal-Wallis test: H (6, N= 243) =9.889001 p =.1294

Depend.: Microvilli density	Code	Valid N	Sum of Ranks	Mean Rank
T UT	1	9	1153.500	128.1667
T DC	2	9	969.000	107.6667
T Ana	3	45	5130.500	114.0111
T Anaaspclop	4	45	4780.500	106.2333
T Aspclop	5	45	5634.000	125.2000
T Anaato	6	45	6457.000	143.4889
T Ato	7	45	5521.500	122.7000

Part C: Statistica Kruskal-Wallis output for changes in cell morphology

MCF7 cells

Microvilli shape

Kruskal-Wallis ANOVA by Ranks; Microvilli shape (friedman layout T47D)
Independent (grouping) variable: Cell line and treatment
Kruskal-Wallis test: H (6, N= 243) =5.608883 p =.4684

Depend.: Microvilli shape	Code	Valid N	Sum of Ranks	Mean Rank
M UT	1	9	996.000	110.6667
M DC	2	9	1164.000	129.3333
M Ana	3	45	5691.000	126.4667
M Anaaspclop	4	45	5411.000	120.2444
M Aspclop	5	45	4980.000	110.6667
M Anaato	6	45	6185.000	137.4444
M Ato	7	45	5219.000	115.9778

ECM secretions

Kruskal-Wallis ANOVA by Ranks; secretions (scoring data v3 (latest))
Independent (grouping) variable: Cell line and treatment
Kruskal-Wallis test: H (6, N= 81) =40.27566 p =.0000

Depend.: secretions	Code	Valid N	Sum of Ranks	Mean Rank
M UT	1	3	147.0000	49.00000
M DC	2	3	147.0000	49.00000
M Ana	3	15	241.0000	16.06667
M Anaaspclop	4	15	545.0000	36.33333
M Aspclop	5	15	651.0000	43.40000
M Anaato	6	15	735.0000	49.00000
M Ato	7	15	855.0000	57.00000

T47D cells

Kruskal-Wallis ANOVA by Ranks; Microvilli shape (friedman layout T47D)
Independent (grouping) variable: Cell line and treatment
Kruskal-Wallis test: H (6, N= 242) =9.270185 p =.1589

Depend.: Microvilli shape	Code	Valid N	Sum of Ranks	Mean Rank
T UT	1	9	1136.000	126.2222
T DC	2	9	981.000	109.0000
T Ana	3	45	5707.000	126.8222
T Anaaspclop	4	45	4665.000	103.6667
T Aspclop	5	45	5121.000	113.8000
T Anaato	6	44	6123.000	139.1591
T Ato	7	45	5670.000	126.0000

Kruskal-Wallis ANOVA by Ranks; secretions (scoring data v3 (latest))
Independent (grouping) variable: Cell line and treatment
Kruskal-Wallis test: H (6, N= 81) =39.09774 p =.0000

Depend.: secretions	Code	Valid N	Sum of Ranks	Mean Rank
T UT	1	3	139.5000	46.50000
T DC	2	3	139.5000	46.50000
T Ana	3	15	235.5000	15.70000
T Anaaspclop	4	15	714.0000	47.60000
T Aspclop	5	15	697.5000	46.50000
T Anaato	6	15	697.5000	46.50000
T Ato	7	15	697.5000	46.50000

A4.1: Scratch assay supplementary images

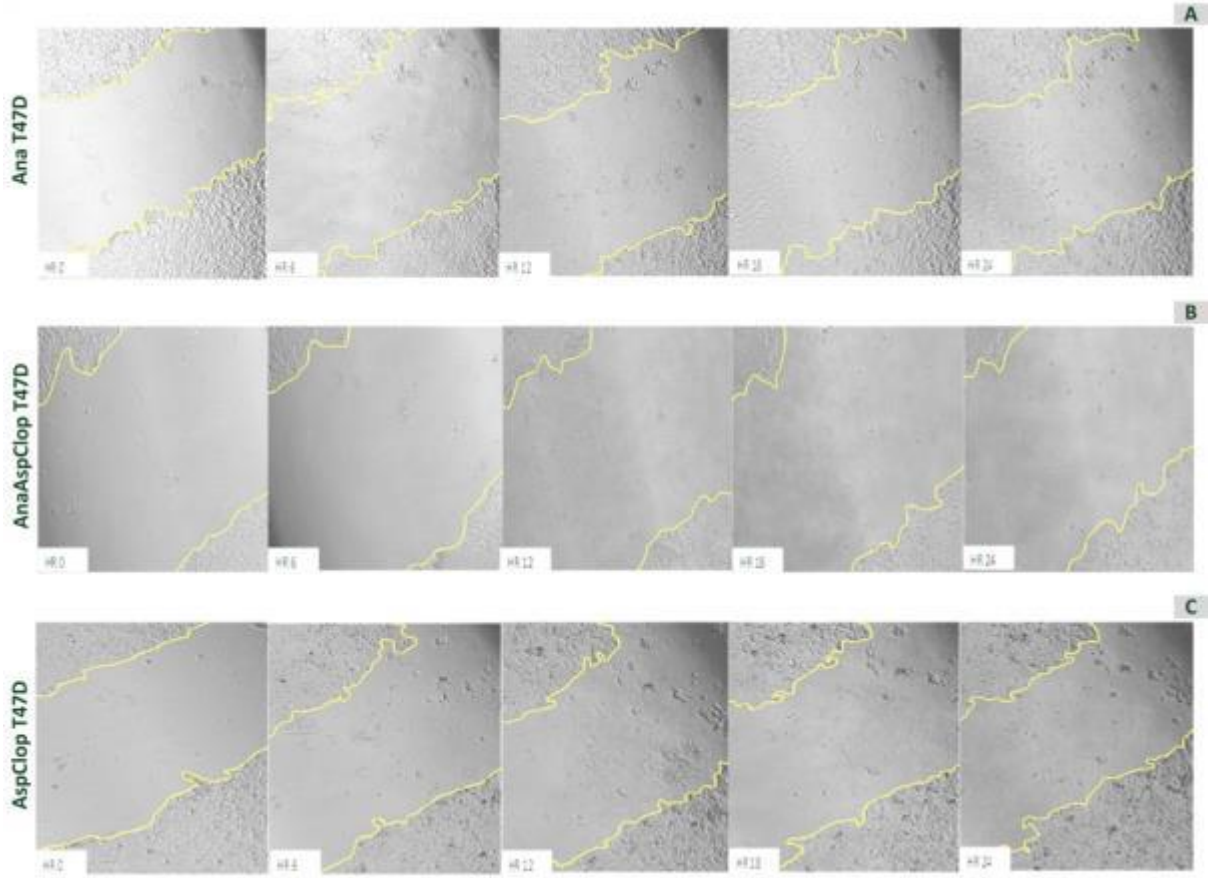


Figure A4.1: Representative micrographs of the migration of T47D cells exposed to A) Ana, B) AnaAspClop and C) AspClop imaged at 0 hrs, 6 hrs, 12 hrs, 18 hrs and 24 hrs. Few cells were observed at the exposed area reflecting a low migratory rate in these cell lines. Images taken at 10X magnification.

A4.2: Scratch assay supplementary images

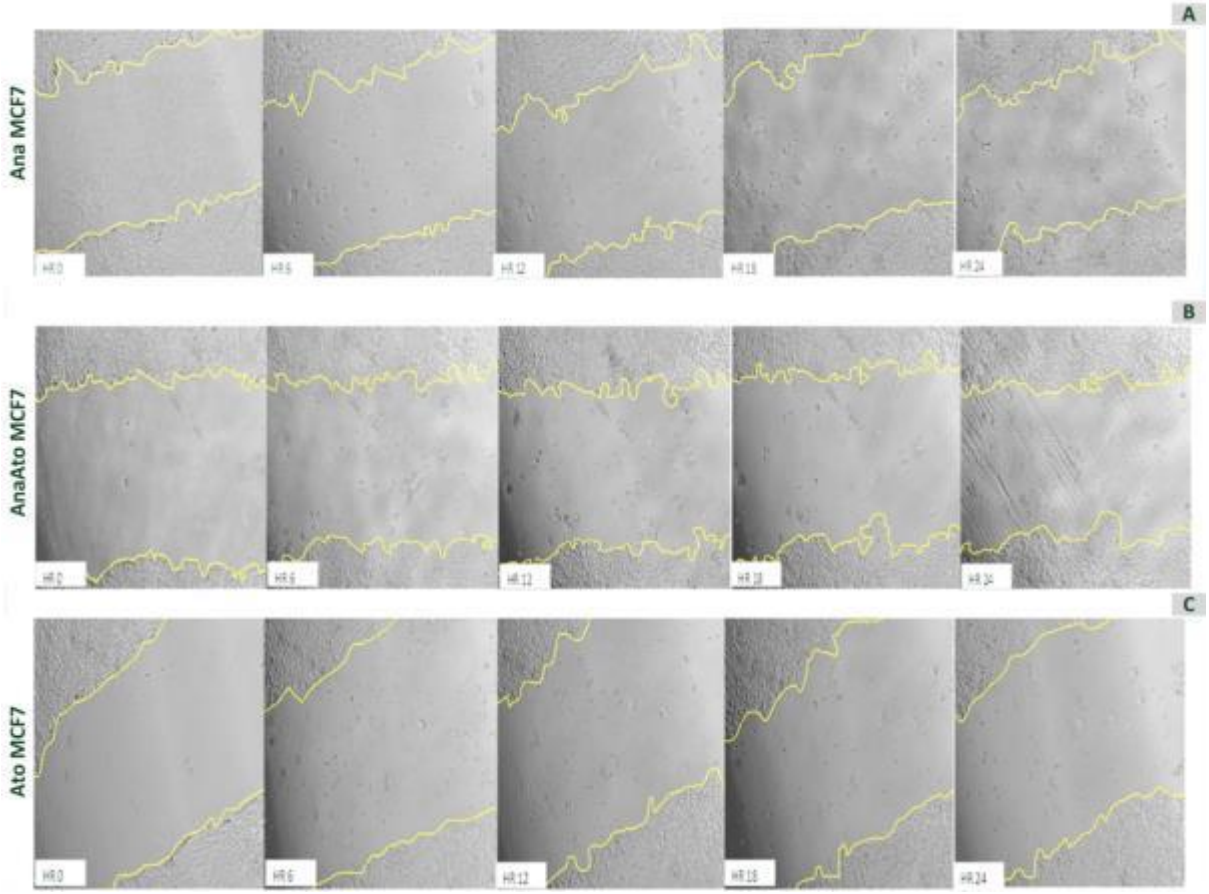


Figure A 4.2: Representative micrographs of the migration of MCF7 cells exposed to **A)** Ana, **B)** AnaAto and **C)** Ato imaged at 0 hrs, 6 hrs, 12 hrs, 18 hrs and 24 hrs. Few cells were observed at the exposed area reflecting a low migratory rate in these cell lines. Images taken at 10X magnification.

A4.3: PAST Friedman output for migration assay within cell lines

PAST output for migration statistics

Treatments within MCF7 cells

Friedman MCF7 (Migration over 24hrs) — A

Test for equal medians

chi2:	132.53	Degrees of freedom:	6
chi2, tie corrected:	132.53		
chi2, continuity correctec	132.51		
p (same), asymptotic:	3.80E-26		

Post hoc Wilcoxon

	M Untreated	M Diluent	M Anas	M AnasAsp Clop	M AspClop	M AnasAto	M Ato
M Untreated		1.73E-06	1.73E-06	0.008217	0.7971	1.73E-06	1.73E-06
M Diluent	1.73E-06		0.102	1.73E-06	2.13E-06	1.73E-06	0.221
M Anas	1.73E-06	0.102		1.73E-06	3.18E-06	1.73E-06	0.000115
M AnasAspClop	0.008217	1.73E-06	1.73E-06		0.001593	0.000894	1.73E-06
M AspClop	0.7971	2.13E-06	3.18E-06	0.001593		0.003162	0.002255
M AnasAto	1.73E-06	1.73E-06	1.73E-06	0.000894	0.003162		1.73E-06
M Ato	1.73E-06	0.221	0.000115	1.73E-06	0.002255	1.73E-06	

Treatments within T47D cells

Friedman T47D (migration over 24hrs) — B

Test for equal medians

chi2:	162.31	Degrees of freedom:	6
chi2, tie corrected:	162.31		
chi2, continuity corrected:	162.29		
p (same), asymptotic:	1.93E-32		

Post hoc Wilcoxon

	T Untreate	T Diluent	T Anas	T AnasAsp	T AspClop	T AnasAto	T Ato
T Untreated		1.73E-06	1.73E-06	0.3086	1.73E-06	1.73E-06	1.73E-06
T Diluent	1.73E-06		3.11E-05	1.73E-06	1.73E-06	1.13E-05	0.004682
T Anas	1.73E-06	3.11E-05		1.73E-06	1.73E-06	0.007731	1.73E-06
T AnasAspClop	0.3086	1.73E-06	1.73E-06		1.73E-06	1.73E-06	1.73E-06
T AspClop	1.73E-06	1.73E-06	1.73E-06	1.73E-06		1.73E-06	1.73E-06
T AnasAto	1.73E-06	1.13E-05	0.007731	1.73E-06	1.73E-06		2.60E-06
T Ato	1.73E-06	0.004682	1.73E-06	1.73E-06	1.73E-06	2.60E-06	

A4.4: PAST Friedman output within each treatment group at different time points

Part A: PAST output for migration statistics: differences in time points within the group

M UT	Friedman					A1
	Test for equal medians					
			Degrees of			
	chi2:	17.333	freedom:	4		
	chi2, tie corrected:	17.333				
	chi2, continuity corrected:	17.171				
	p (same), asymptotic:	0.00179				
	Post hoc wilcoxon					
		M UT Hr 0	M UT Hr 6	M UT Hr 12	M UT Hr 18	M UT Hr 24
	M UT Hr 0		0.1692	0.04615	0.04615	0.3231
	M UT Hr 6	0.1692		0.6923	0.04615	0.1077
	M UT Hr 12	0.04615	0.6923		0.04615	0.04615
	M UT Hr 18	0.04615	0.04615	0.04615		0.1077
	M UT Hr 24	0.3231	0.1077	0.04615	0.1077	

T UT	Friedman					A2
	Test for equal medians					
			Degrees of			
	chi2:	12.267	freedom:	4		
	chi2, tie corrected:	12.267				
	chi2, continuity corrected:	12.133				
	p (same), asymptotic:	0.016392				
	Post hoc wilcoxon					
		T UT Hr 0	T UT Hr 6	T UT Hr 12	T UT Hr 18	T UT Hr 24
	T UT Hr 0		0.04615	0.04615	0.8462	0.4462
	T UT Hr 6	0.04615		0.1077	0.04615	0.07692
	T UT Hr 12	0.04615	0.1077		0.07692	0.1692
	T UT Hr 18	0.8462	0.04615	0.07692		0.3231
	T UT Hr 24	0.4462	0.07692	0.1692	0.3231	

M DC	Friedman					B1
	Test for equal medians					
			Degrees of			
	chi2:	1.7333	freedom:	4		
	chi2, tie corrected:	1.7333				
	chi2, continuity corrected:	1.6575				
	p (same), asymptotic:	0.79843				
	Post hoc wilcoxon					
		M DC Hr 0	M DC Hr 6	M DC Hr 12	M DC Hr 18	M DC Hr 24
	M DC Hr 0		0.5692	0.8462	0.2308	0.6923
	M DC Hr 6	0.5692		0.5692	0.2308	1
	M DC Hr 12	0.8462	0.5692		0.07692	0.6923
	M DC Hr 18	0.2308	0.2308	0.07692		0.4462
	M DC Hr 24	0.6923	1	0.6923	0.4462	

Part B: PAST output for migration statistics: differences in time points within the group

T DC	Friedman						B2
	Test for equal medians						
	chi2:	22.133	Degrees of freedom:	4			
	chi2, tie corrected:	22.133					
	chi2, continuity corrected:	21.945					
	p (same), asymptotic:	0.000206					
	Post hoc wilcoxon						
		T DC Hr 0	T DC Hr 6	T DC Hr 12	T DC Hr 18	T DC Hr 24	
	T DC Hr 0		0.04615	0.04615	0.04615	0.04615	
	T DC Hr 6	0.04615		0.04615	0.04615	0.4462	
	T DC Hr 12	0.04615	0.04615		0.1077	0.04615	
	T DC Hr 18	0.04615	0.04615	0.1077		0.04615	
	T DC Hr 24	0.04615	0.4462	0.04615	0.04615		

M Ana	Friedman						C1
	Test for equal medians						
	chi2:	21.867	Degrees of freedom:	4			
	chi2, tie corrected:	21.867					
	chi2, continuity corrected:	21.68					
	p (same), asymptotic:	0.000232					
	Post hoc wilcoxon						
		M Ana Hr 0	M Ana Hr 6	M Ana Hr 12	M Ana Hr 18	M Ana Hr 24	
	M Ana Hr 0		0.04615	0.3231	0.04615	0.04615	
	M Ana Hr 6	0.04615		0.04615	0.04615	0.04615	
	M Ana Hr 12	0.3231	0.04615		0.04615	0.04615	
	M Ana Hr 18	0.04615	0.04615	0.04615		0.4462	
	M Ana Hr 24	0.04615	0.04615	0.04615	0.4462		

T Ana	Friedman						C2
	Test for equal medians						
	chi2:	19.333	Degrees of freedom:	4			
	chi2, tie corrected:	19.333					
	chi2, continuity corrected:	19.16					
	p (same), asymptotic:	0.000731					
	Post hoc wilcoxon						
		T Ana Hr 0	T Ana Hr 6	T Ana Hr 12	T Ana Hr 18	T Ana Hr 24	
	T Ana Hr 0		0.04615	0.04615	0.4462	0.04615	
	T Ana Hr 6	0.04615		0.3231	0.04615	0.04615	
	T Ana Hr 12	0.04615	0.3231		0.04615	0.04615	
	T Ana Hr 18	0.4462	0.04615	0.04615		0.4462	
	T Ana Hr 24	0.04615	0.04615	0.04615	0.4462		

4.5 PAST Friedman output for within each treatment group at different time points

Part A: PAST output for migration statistics: differences in time points within the group

A1

M AnaAspClop	Friedman					
	Test for equal medians					
	chi2:	2.5333	Degrees of freedom:	4		
	chi2, tie corrected:	2.5333				
	chi2, continuity corrected:	2.453				
	p (same), asymptotic:	0.65306				
	Post hoc wilcoxon					
		M AnaAspClop Hr 0	M AnaAspClop Hr 6	M AnaAspClop Hr 12	M AnaAspClop Hr 18	M AnaAspClop Hr 24
	M AnaAspClop Hr 0		0.04615	0.4462	0.4462	0.6923
	M AnaAspClop Hr 6	0.04615		0.4462	0.1692	0.4462
	M AnaAspClop Hr 12	0.4462	0.4462		0.4462	0.4462
	M AnaAspClop Hr 18	0.4462	0.1692	0.4462		0.3231
	M AnaAspClop Hr 24	0.6923	0.4462	0.4462	0.3231	

A2

T AnaAspClop	Friedman					
	Test for equal medians					
	chi2:	22	Degrees of freedom:	4		
	chi2, tie corrected:	22				
	chi2, continuity corrected:	21.812				
	p (same), asymptotic:	0.000218				
	Post hoc wilcoxon					
		T AnaAspClop Hr 0	T AnaAspClop Hr 6	T AnaAspClop Hr 12	T AnaAspClop Hr 18	T AnaAspClop Hr 24
	T AnaAspClop Hr 0		0.04615	0.07692	0.04615	0.04615
	T AnaAspClop Hr 6	0.04615		0.04615	0.04615	0.04615
	T AnaAspClop Hr 12	0.07692	0.04615		0.4462	0.04615
	T AnaAspClop Hr 18	0.04615	0.04615	0.4462		0.04615
	T AnaAspClop Hr 24	0.04615	0.04615	0.04615	0.04615	

B1

M AspClop	Friedman					
	Test for equal medians					
	chi2:	10.533	Degrees of freedom:	4		
	chi2, tie corrected:	10.533				
	chi2, continuity corrected:	10.409				
	p (same), asymptotic:	0.034076				
	Post hoc wilcoxon					
		M AspClop Hr 0	M AspClop Hr 6	M AspClop Hr 12	M AspClop Hr 18	M AspClop Hr 24
	M AspClop Hr 0		0.4462	0.4462	0.4462	0.04615
	M AspClop Hr 6	0.4462		1	0.07692	0.04615
	M AspClop Hr 12	0.4462	1		0.07692	0.04615
	M AspClop Hr 18	0.4462	0.07692	0.07692		0.4462
	M AspClop Hr 24	0.04615	0.04615	0.04615	0.4462	

B2

T AspClop	Friedman					
	Test for equal medians					
	chi2:	22.8	Degrees of freedom:	4		
	chi2, tie corrected:	22.8				
	chi2, continuity corrected:	22.608				
	p (same), asymptotic:	0.000152				
	Post hoc wilcoxon					
		T AspClop Hr 0	T AspClop Hr 6	T AspClop Hr 12	T AspClop Hr 18	T AspClop Hr 24
	T AspClop Hr 0		0.04615	0.04615	0.04615	0.04615
	T AspClop Hr 6	0.04615		0.04615	0.04615	0.04615
	T AspClop Hr 12	0.04615	0.04615		0.04615	0.04615
	T AspClop Hr 18	0.04615	0.04615	0.04615		0.4462
	T AspClop Hr 24	0.04615	0.04615	0.04615	0.4462	

Part B: PAST output for migration statistics: differences in time points within the group

C1

M AnaAto	Friedman					
	Test for equal medians					
			Degrees of			
	chi2:	19.2	freedom:	4		
	chi2, tie corrected:	19.2				
	chi2, continuity corrected:	19.028				
	p (same), asymptotic:	0.000776				
	Post hoc wilcoxon					
		M AnaAto Hr 0	M AnaAto Hr 6	M AnaAto Hr 12	M AnaAto Hr 18	M AnaAto Hr 24
	M AnaAto Hr 0		0.04615	0.04615	0.5692	0.4462
	M AnaAto Hr 6	0.04615		0.4462	0.04615	0.04615
	M AnaAto Hr 12	0.04615	0.4462		0.04615	0.04615
	M AnaAto Hr 18	0.5692	0.04615	0.04615		0.04615
	M AnaAto Hr 24	0.4462	0.04615	0.04615	0.04615	

C2

T AnaAto	Friedman					
	Test for equal medians					
			Degrees of			
	chi2:	12.533	freedom:	4		
	chi2, tie corrected:	12.533				
	chi2, continuity corrected:	12.398				
	p (same), asymptotic:	0.014626				
	Post hoc wilcoxon					
		T AnaAto Hr 0	T AnaAto Hr 6	T AnaAto Hr 12	T AnaAto Hr 18	T AnaAto Hr 24
	T AnaAto Hr 0		0.04615	0.04615	0.04615	0.04615
	T AnaAto Hr 6	0.04615		0.07692	0.8462	0.4462
	T AnaAto Hr 12	0.04615	0.07692		0.4462	0.8462
	T AnaAto Hr 18	0.04615	0.8462	0.4462		0.4462
	T AnaAto Hr 24	0.04615	0.4462	0.8462	0.4462	

D1

M Ato	Friedman					
	Test for equal medians					
			Degrees of			
	chi2:	14.8	freedom:	4		
	chi2, tie corrected:	14.8				
	chi2, continuity corrected:	14.652				
	p (same), asymptotic:	0.00548				
	Post hoc wilcoxon					
		M Ato Hr 0	M Ato Hr 6	M Ato Hr 12	M Ato Hr 18	M Ato Hr 24
	M Ato Hr 0		0.04615	0.04615	0.04615	0.07692
	M Ato Hr 6	0.04615		0.07692	0.07692	0.07692
	M Ato Hr 12	0.04615	0.07692		0.1692	0.1077
	M Ato Hr 18	0.04615	0.07692	0.1692		0.4462
	M Ato Hr 24	0.07692	0.07692	0.1077	0.4462	

D2

T Ato	Friedman					
	Test for equal medians					
			Degrees of			
	chi2:	16.4	freedom:	4		
	chi2, tie corrected:	16.4				
	chi2, continuity corrected:	16.243				
	p (same), asymptotic:	0.00271				
	Post hoc wilcoxon					
		T Ato Hr 0	T Ato Hr 6	T Ato Hr 12	T Ato Hr 18	T Ato Hr 24
	T Ato Hr 0		0.04615	0.04615	0.04615	0.04615
	T Ato Hr 6	0.04615		0.4462	0.1692	0.04615
	T Ato Hr 12	0.04615	0.4462		0.3231	0.4462
	T Ato Hr 18	0.04615	0.1692	0.3231		0.04615
	T Ato Hr 24	0.04615	0.04615	0.4462	0.04615	

A4.6: PAST output for migration assay at matched treatments between cell lines

Part A: PAST output for migration statistics: differences in time points at matched treatments

A

Friedman 0hrs cells at matched treatments			
Test for equal medians			
chi2:	66.267	Degrees of freedom:	13
chi2, tie corrected:	66.267		
chi2, continuity corrected:	66.241		
p (same), asymptotic:	3.92E-09		

Post hoc (Wilcoxon) 0hrs

	T Untreated	T Diluent	T Anas	T AnasAspClop	T AspClop	T AnasAto	T Ato
M Untreated	0.04615	0.4462	0.4462	0.04615	0.04615	0.04615	0.04615
M Diluent	0.04615	0.04615	0.04615	0.04615	0.04615	0.04615	0.1077
M Anas	0.04615	0.04615	0.04615	0.04615	0.04615	0.04615	0.04615
M AnasAspClop	0.04615	0.4462	0.4462	0.04615	0.04615	0.04615	0.04615
M AspClop	0.04615	0.4462	0.4462	0.04615	0.04615	0.04615	0.4462
M AnasAto	0.04615	0.04615	0.04615	0.04615	0.04615	0.1077	0.04615
M Ato	0.04615	0.4462	0.04615	0.04615	0.04615	0.04615	0.8462

B

Friedman 6hrs cells at matched treatments			
Test for equal medians			
chi2:	67.238	Degrees of freedom:	13
chi2, tie corrected:	67.238		
chi2, continuity corrected:	67.212		
p (same), asymptotic:	2.61E-09		

Post hoc (Wilcoxon) 6hrs

	T Untreated	T Diluent	T Anas	T AnasAspClop	T AspClop	T AnasAto	T Ato
M Untreated	0.04615	0.4462	0.4462	0.04615	0.04615	0.4462	0.04615
M Diluent	0.04615	0.4462	0.04615	0.04615	0.04615	0.04615	0.04615
M Anas	0.04615	0.4462	0.04615	0.04615	0.04615	0.04615	0.4462
M AnasAspClop	0.04615	0.04615	0.04615	0.04615	0.04615	0.04615	0.04615
M AspClop	0.04615	0.04615	0.04615	0.04615	0.04615	0.5692	0.04615
M AnasAto	0.04615	0.04615	0.04615	0.04615	0.04615	0.04615	0.04615
M Ato	0.04615	0.4462	0.4462	0.04615	0.04615	0.04615	0.4462

C

Friedman 12hrs cells at matched treatments			
Test for equal medians			
chi2:	67.79	Degrees of freedom:	13
chi2, tie corrected:	67.79		
chi2, continuity corrected:	67.764		
p (same), asymptotic:	2.07E-09		

Post hoc (Wilcoxon) 12hrs

	T Untreated	T Diluent	T Anas	T AnasAspClop	T AspClop	T AnasAto	T Ato
M Untreated	0.04615	0.4462	0.4462	0.04615	0.04615	0.4462	0.04615
M Diluent	0.04615	0.8462	0.04615	0.04615	0.04615	0.04615	0.1692
M Anas	0.04615	0.4462	0.07692	0.04615	0.04615	0.04615	0.04615
M AnasAspClop	0.04615	0.04615	0.04615	0.04615	0.4462	0.04615	0.04615
M AspClop	0.04615	0.04615	0.04615	0.04615	0.04615	0.4462	0.04615
M AnasAto	0.04615	0.04615	0.04615	0.04615	0.04615	0.04615	0.04615
M Ato	0.04615	0.4462	0.4462	0.04615	0.04615	0.04615	0.04615

Part B: PAST output for migration statistics: differences in time points at matched treatments

D

Friedman 18hrs cells at matched treatments			
Test for equal medians			
chi2:	68.99	Degrees of freedom:	13
chi2, tie corrected:	68.99		
chi2, continuity corrected:	68.964		
p (same), asymptotic:	1.24E-09		

Post hoc (Wilcoxon) 18hrs

	T Untreated	T Diluent	T Anas	T AnasAspClop	T AspClop	T AnasAto	T Ato
M Untreated	0.04615	0.04615	0.4462	0.04615	0.04615	0.3231	0.04615
M Diluent	0.04615	0.4462	0.4462	0.04615	0.04615	0.1077	0.04615
M Anas	0.04615	0.4462	0.4462	0.04615	0.04615	0.04615	0.04615
M AnasAspClop	0.04615	0.04615	0.4462	0.04615	0.04615	0.04615	0.04615
M AspClop	0.04615	0.04615	0.04615	0.04615	0.04615	0.04615	0.04615
M AnasAto	0.04615	0.04615	0.04615	0.04615	0.04615	0.04615	0.04615
M Ato	0.04615	0.4462	0.4462	0.04615	0.04615	0.4462	0.04615

E

Friedman 24hrs cells at matched treatments			
Test for equal medians			
chi2:	66.019	Degrees of freedom:	13
chi2, tie corrected:	66.019		
chi2, continuity corrected:	65.993		
p (same), asymptotic:	4.35E-09		

Post hoc (Wilcoxon) 24hrs

	T Untreated	T Diluent	T Anas	T AnasAspClop	T AspClop	T AnasAto	T Ato
M Untreated	0.04615	0.2308	0.4462	0.04615	0.04615	0.4462	0.04615
M Diluent	0.04615	0.1692	0.04615	0.04615	0.04615	0.04615	0.4462
M Anas	0.04615	1	0.4462	0.04615	0.04615	0.4462	0.04615
M AnasAspClop	0.04615	0.04615	0.04615	0.04615	0.04615	0.4462	0.04615
M AspClop	0.04615	0.04615	0.04615	0.04615	0.07692	0.04615	0.04615
M AnasAto	0.04615	0.04615	0.04615	0.04615	0.5692	0.04615	0.04615
M Ato	0.04615	0.5692	0.4462	0.04615	0.04615	0.4462	0.04615

A5: PAST output for cell proliferation data

PAST output for cell proliferation statistics

Treatments within MCF7 cells

Friedman test MCF7 — A

Test for equal medians

chi2:	20	Degrees of freedom:	7
chi2, tie corrected:	20		
chi2, continuity corrected:	19.946		
p (same), asymptotic:	0.005688		

Post Hoc Wilcoxon

	M Untreated	M Diluent	M Media Control	M Anas	M AnasAspClop	M AspClop	M AnasAto	M Ato
M Untreated		0.8462	0.04615	0.8462	1	0.2308	0.4462	0.04615
M Diluent	0.8462		0.04615	0.5692	1	0.1692	0.2308	0.1692
M Media Control	0.04615	0.04615		0.04615	0.04615	0.04615	0.04615	0.04615
M Anas	0.8462	0.5692	0.04615		0.6923	0.5692	0.4462	0.1692
M AnasAspClop	1	1	0.04615	0.6923		0.1077	0.3231	0.1077
M AspClop	0.2308	0.1692	0.04615	0.5692	0.1077		0.4462	1
M AnasAto	0.4462	0.2308	0.04615	0.4462	0.3231	0.4462		0.4462
M Ato	0.04615	0.1692	0.04615	0.1692	0.1077	1	0.4462	

Treatments within T47D cells

Friedman test T47D — B

Test for equal medians

chi2:	23.111	Degrees of freedom:	7
chi2, tie corrected:	23.111		
chi2, continuity corrected:	23.053		
p (same), asymptotic:	0.001669		

Post Hoc Wilcoxon

	T Untreated	T Diluent	T Media Control	T Anas	T AnasAspClop	T AspClop	T AnasAto	T Ato
T Untreated		0.07692	0.04615	0.2308	0.3231	1	0.07692	0.8462
T Diluent	0.07692		0.04615	0.1692	0.1692	0.04615	0.1077	0.04615
T Media Control	0.04615	0.04615		0.04615	0.04615	0.04615	0.04615	0.04615
T Anas	0.2308	0.1692	0.04615		1	0.1692	0.8462	0.4462
T AnasAspClop	0.3231	0.1692	0.04615	1		0.1692	0.8462	0.1077
T AspClop	1	0.04615	0.04615	0.1692	0.1692		0.4462	0.6923
T AnasAto	0.07692	0.1077	0.04615	0.8462	0.8462	0.4462		0.4462
T Ato	0.8462	0.04615	0.04615	0.4462	0.1077	0.6923	0.4462	

Treatments between cell lines

Kruskal-Wallis test for equal medians — C

H (chi2):	83.07
Hc (tie corrected):	83.07
p (same):	1.91E-11

There is a significant difference between sample medians

Dunn's post hoc

	T Untreated	T Diluent	T Media Control	T Anas	T AnasAspClop	T AspClop	T AnasAto	T Ato
M Untreated	0.007274	0.1454	4.07E-05	0.03632	0.03112	0.005481	0.03153	0.008228
M Diluent	0.006836	0.1397	3.72E-05	0.03451	0.02954	0.005142	0.02993	0.007738
M Media Control	0.2587	0.01839	0.7717	0.08539	0.0973	0.3001	0.09626	0.2416
M Anas	0.002478	0.07218	8.76E-06	0.01488	0.01251	0.001813	0.01269	0.00284
M AnasAspClop	0.007274	0.1454	4.07E-05	0.03632	0.03112	0.005481	0.03153	0.008228
M AspClop	0.000394	0.02055	6.91E-07	0.003142	0.002564	0.000275	0.002609	0.000461
M AnasAto	0.002197	0.06662	7.40E-06	0.01345	0.01128	0.001602	0.01145	0.002521
M Ato	0.000664	0.02954	1.41E-06	0.0049	0.004031	0.00047	0.004098	0.000772

APPENDIX B: Chapter III supplementary information

B1: Ethics document

R14/49 Ms Kutlwano Thabethe et al

HUMAN RESEARCH ETHICS COMMITTEE (MEDICAL)

CLEARANCE CERTIFICATE NO. M150263

NAME: (Principal Investigator)	Ms Kutlwano Thabethe et al
DEPARTMENT:	Internal Medicine School of Anatomical Sciences
PROJECT TITLE:	The Effects of Antiplatelet Drugs on Plate Following Exposure to Breast Cancer Cell Lines Treated with Hormone Therapy
DATE CONSIDERED:	27/02/2015
DECISION:	Approved unconditionally
CONDITIONS:	
SUPERVISOR:	Dr Raquel Duarte
APPROVED BY:	Professor P Cleaton-Jones, Chairperson, HREC (Medical)
DATE OF APPROVAL:	08/04/2015

This clearance certificate is valid for 5 years from date of approval. Extension may be applied for.

DECLARATION OF INVESTIGATORS

To be completed in duplicate and **ONE COPY** returned to the Secretary in Room 10004, 10th floor, Senate House, University.

I/we fully understand the conditions under which I am/we are authorized to carry out the above-mentioned research and I/we undertake to ensure compliance with these conditions. Should any departure be contemplated, from the research protocol as approved, I/we undertake to resubmit the application to the Committee. **I agree to submit a yearly progress report.**

Principal Investigator Signature

Date April 2015

PLEASE QUOTE THE PROTOCOL NUMBER IN ALL ENQUIRIES

B2: Solutions

0.1M Phosphate buffered saline (PBS) pH 7.4

- 8 g NaCl
- 1.15 g Na_2HPO_4
- 0.2 g KCl
- 0.2 g KH_2PO_4
- 1l distilled water

Ammonium chloride erythrocyte lysis buffer (10X)

- 8.02 g NH_4Cl
- 0.84 g $NaHCO_3$
- 0.37 g EDTA disodium
- 1l distilled water

Tyrode's buffer pH 7.4

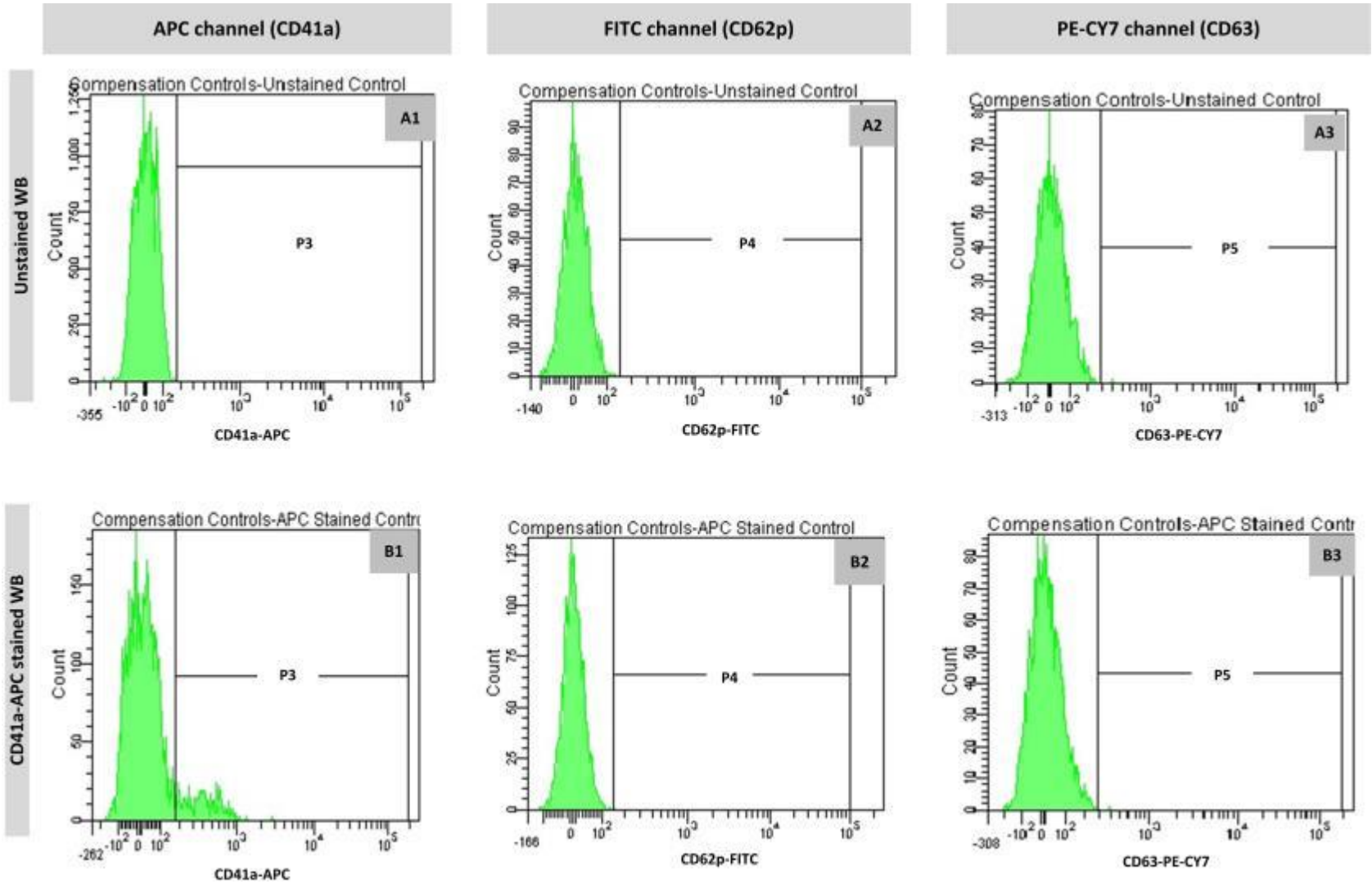
- 7.83g NaCl
- 0.1g $NaHCO_3$
- 0.22 g KCl
- 0.05 g Na_2HPO_4
- 0.1 g $MgCl_2$
- 2.38 g HEPES
- 1l distilled water

B3: Thrombin activity output PAST Friedman test and Wilcoxon post hoc

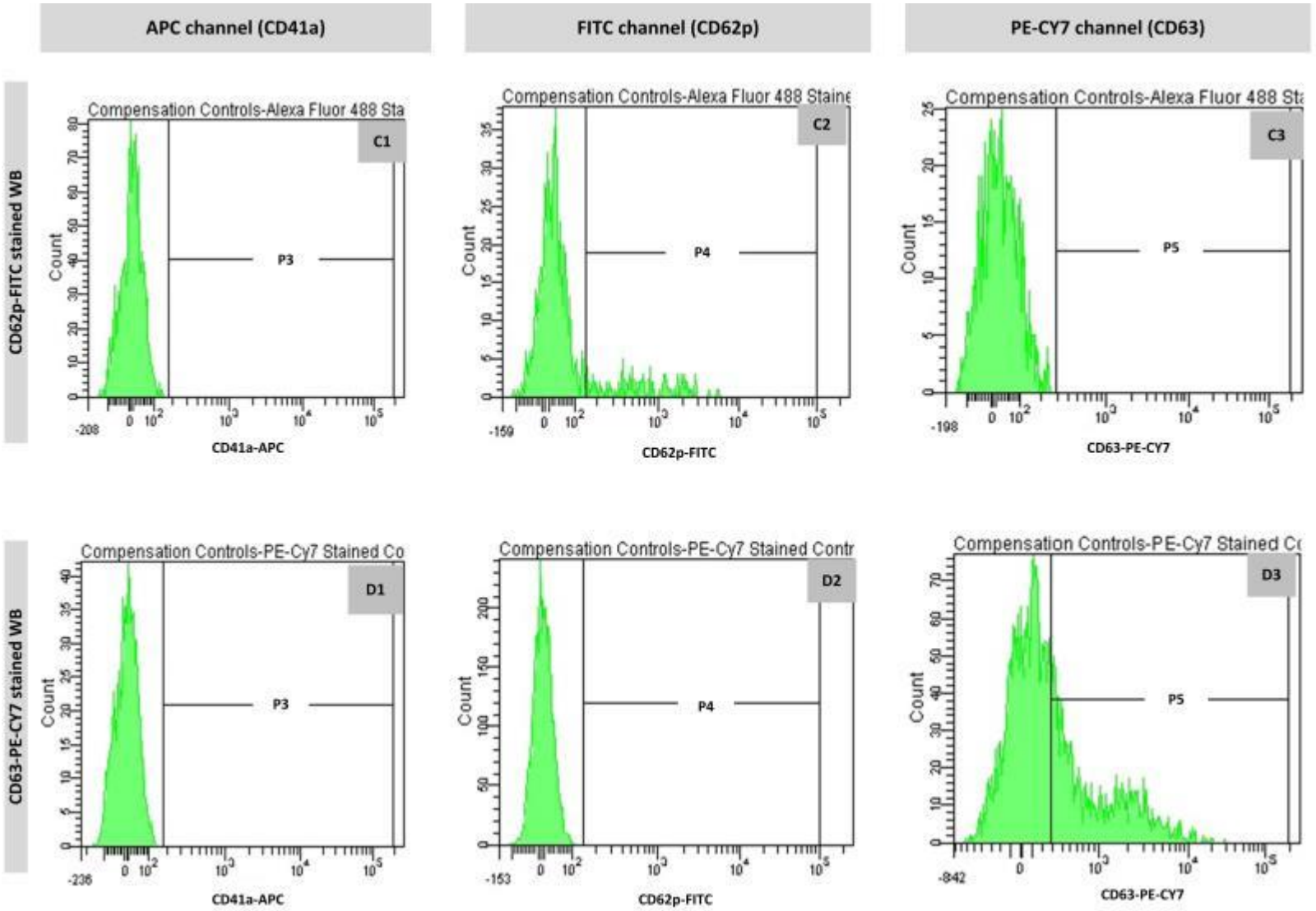
Thrombin Activity			
Test for equal medians			
chi2:	1988.3	Degrees of freedom:	13
chi2, tie corrected:	1990		
chi2, continuity corrected:	1990		
p (same), asymptotic:	0		

	MCF7 DC+ WB	T47D DC+ WB	MCF7 UT+WB	T47D UT+ WB	Ana MCF7+ WB	AnaAspClop MCF7+WB	AnaAto MCF7+WB	AspClop MCF7+WB	Ato MCF7+WB	Ana T47D+ WB	AnaAspClop T47D+WB	AnaAto T47D+WB	AspClop T47D+WB	Ato T47D+WB
MCF7 DC+ WB		5.25E-43	3.66E-27	1.80E-37	3.03E-46	4.79E-61	2.11E-23	5.02E-19	3.70E-24	4.84E-59	4.43E-40	1.56E-47	3.69E-48	8.30E-23
T47D DC+ WB	5.25E-43		7.54E-53	0.09368	1.81E-53	1.39E-60	4.16E-52	1.95E-45	2.53E-49	0.3653	1.48E-05	0.1926	0.02409	1.97E-18
MCF7 UT+WB	3.66E-27	7.54E-53		3.24E-45	1.20E-25	1.02E-54	0.1514	2.37E-07	0.2884	7.08E-69	2.44E-51	1.88E-58	6.55E-57	1.23E-34
T47D UT+ WB	1.80E-37	0.09368	3.24E-45		3.06E-54	2.38E-63	2.62E-47	2.69E-44	6.94E-50	2.49E-05	0.4507	0.01433	2.51E-11	6.69E-05
Ana MCF7+ WB	3.03E-46	1.81E-53	1.20E-25	3.06E-54		2.57E-11	1.02E-20	1.43E-12	1.54E-29	7.13E-64	1.99E-51	1.75E-58	9.32E-58	2.86E-36
AnaAspClop MCF7+WB	4.79E-61	1.39E-60	1.02E-54	2.38E-63	2.57E-11		6.85E-45	1.03E-12	7.06E-36	1.38E-70	3.19E-60	1.34E-65	6.65E-66	3.80E-51
AnaAto MCF7+WB	2.11E-23	4.16E-52	0.1514	2.62E-47	1.02E-20	6.85E-45		0.001061	0.8656	3.63E-65	7.16E-46	1.98E-55	1.65E-55	6.98E-31
AspClop MCF7+WB	5.02E-19	1.95E-45	2.37E-07	2.69E-44	1.43E-12	1.03E-12	0.001061		0.001569	2.32E-57	1.87E-43	9.32E-47	2.24E-52	5.94E-27
Ato MCF7+WB	3.70E-24	2.53E-49	0.2884	6.94E-50	1.54E-29	7.06E-36	0.8656	0.001569		5.03E-64	6.52E-46	1.19E-51	2.77E-56	6.09E-30
Ana T47D+ WB	4.84E-59	0.3653	7.08E-69	2.49E-05	7.13E-64	1.38E-70	3.63E-65	2.32E-57	5.03E-64		2.38E-09	2.12E-08	0.03154	1.23E-24
AnaAspClop T47D+WB	4.43E-40	1.48E-05	2.44E-51	0.4507	1.99E-51	3.19E-60	7.16E-46	1.87E-43	6.52E-46	2.38E-09		0.004426	8.43E-09	2.04E-08
AnaAto T47D+WB	1.56E-47	0.1926	1.88E-58	0.01433	1.75E-58	1.34E-65	1.98E-55	9.32E-47	1.19E-51	2.12E-08	0.004426		0.003707	4.72E-10
AspClop T47D+WB	3.69E-48	0.02409	6.55E-57	2.51E-11	9.32E-58	6.65E-66	1.65E-55	2.24E-52	2.77E-56	0.03154	8.43E-09	0.003707		3.74E-22
Ato T47D+WB	8.30E-23	1.97E-18	1.23E-34	6.69E-05	2.86E-36	3.80E-51	6.98E-31	5.94E-27	6.09E-30	1.23E-24	2.04E-08	4.72E-10	3.74E-22	

B4.1: Compensation control (Part A)

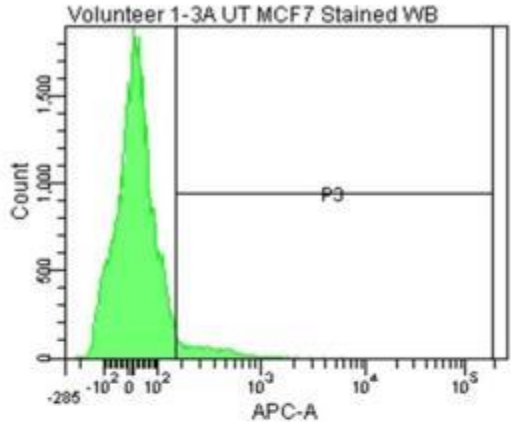
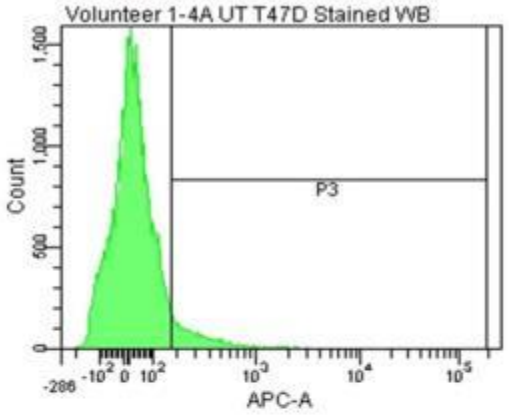
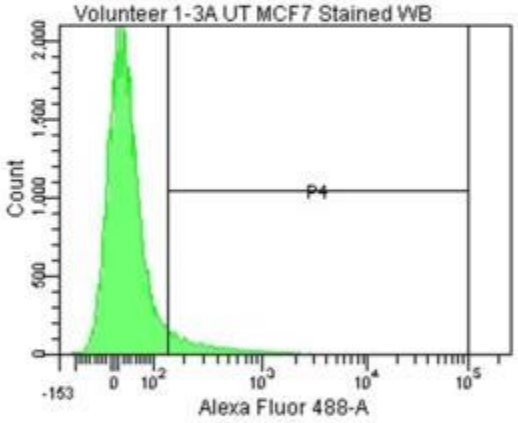
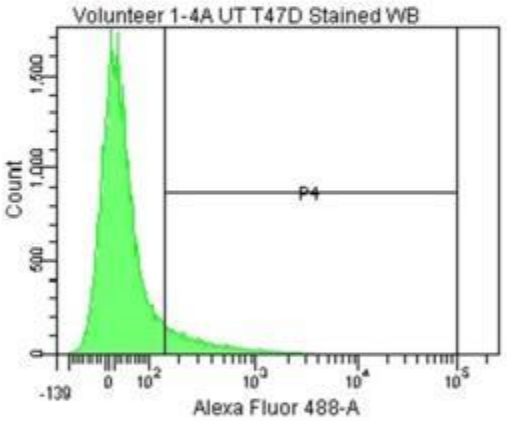
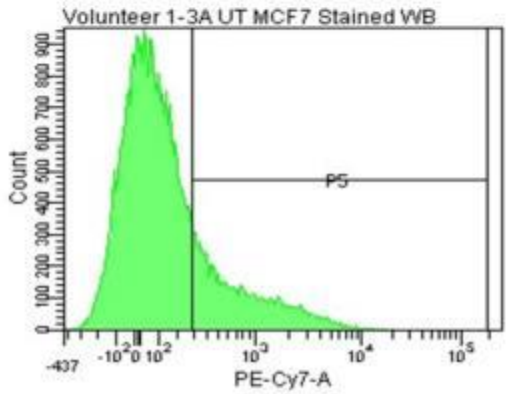
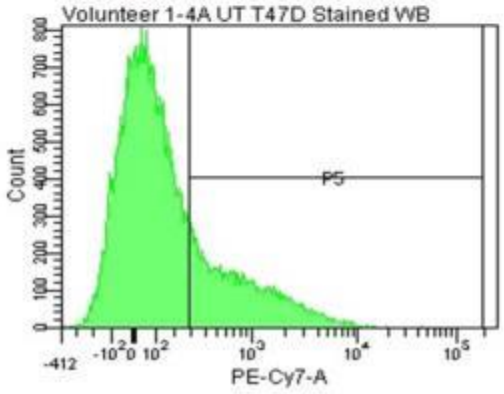


B4.1: Compensation control (Part B)

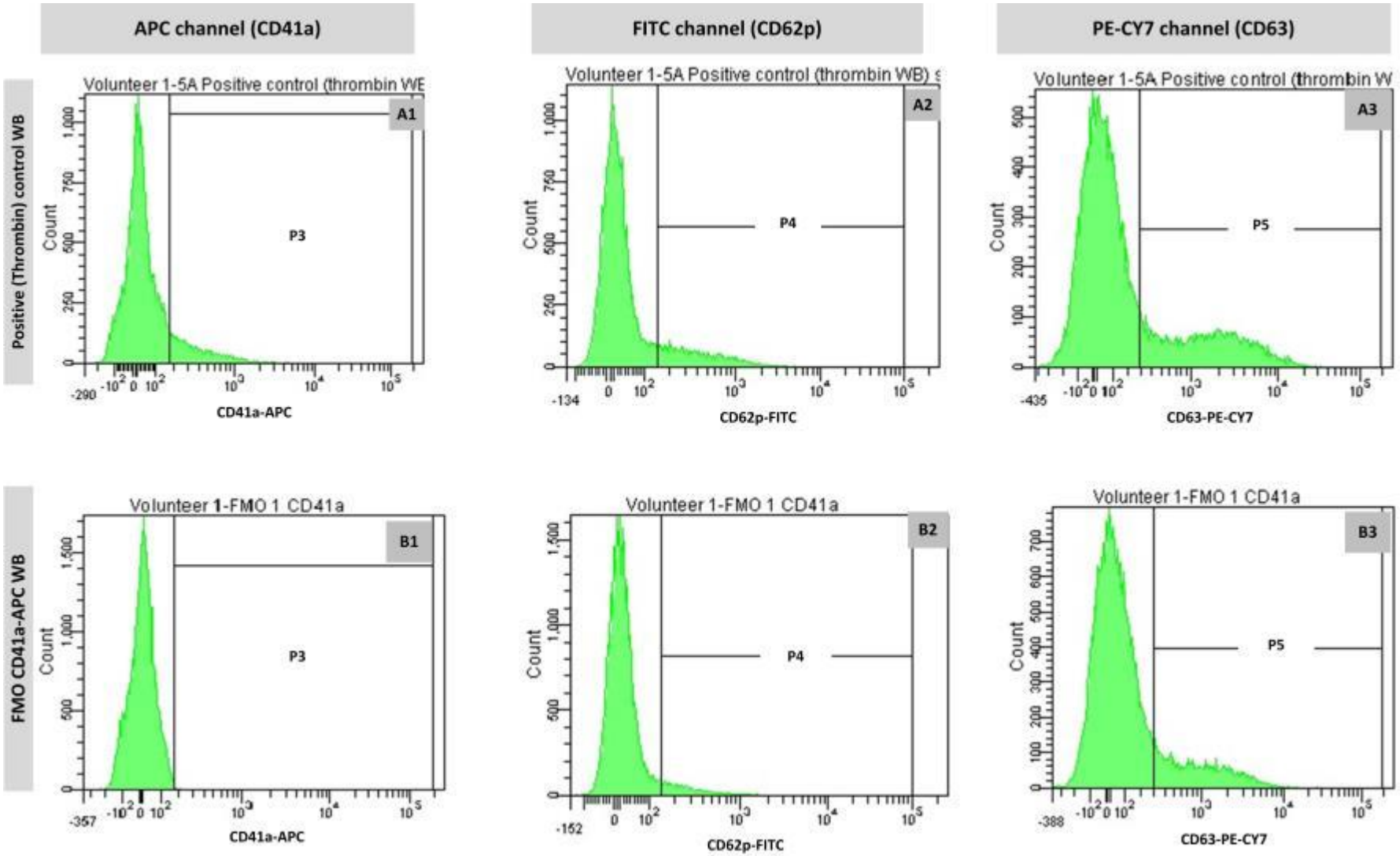


B4.2: Titration controls

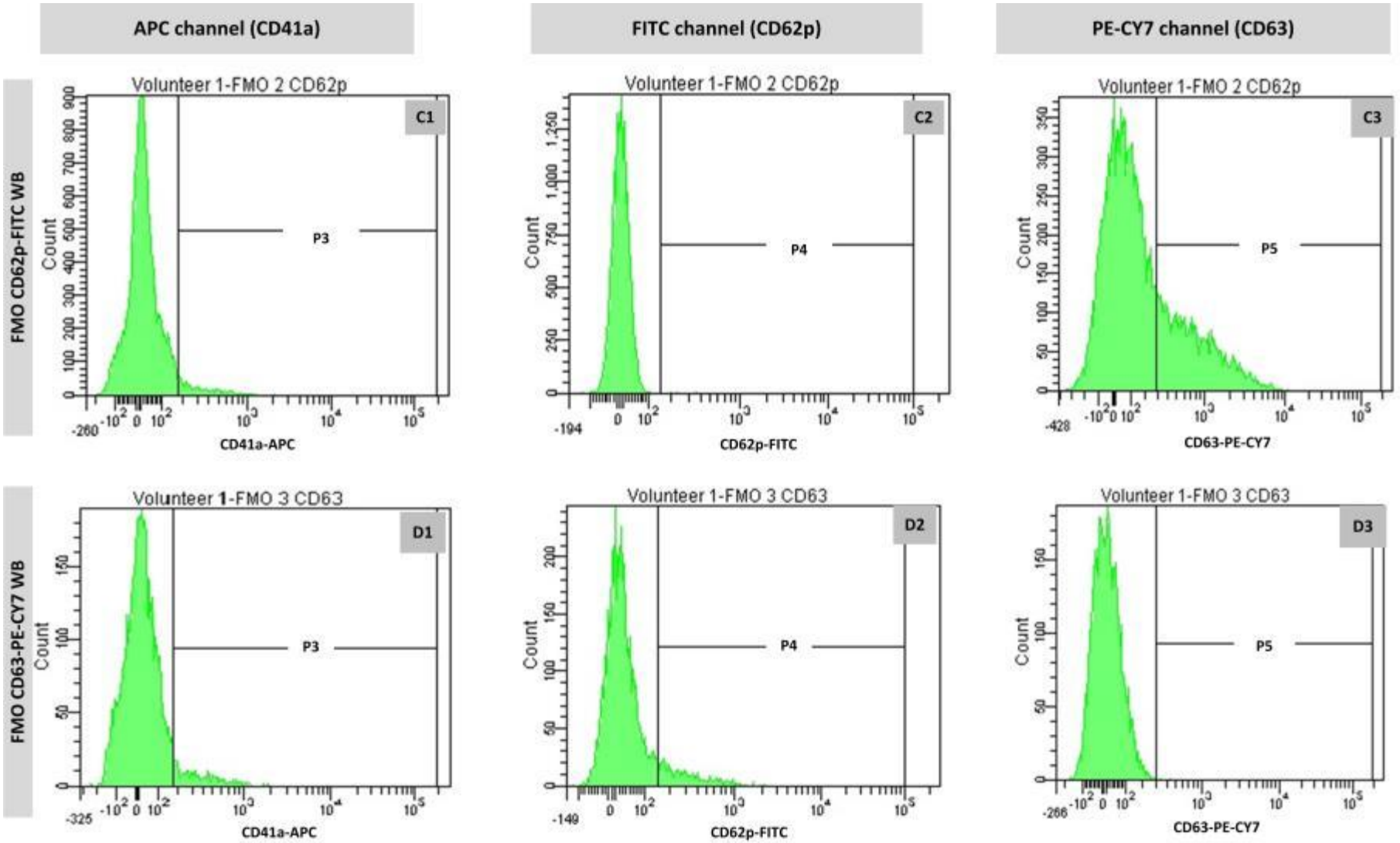
Optimal volumes for platelet activation markers antibodies for flow cytometry

	MCF7 cells	T47D cells
CD41a-APC (10 µl)		
CD62p-FITC (10 µl)		
CD63-PE-CY7 (2.5 µl)		

B4.3: FMO controls (Part A)



B4.3: FMO controls (Part B)



B4.4: Total IPA

PAST output for Total CD62p-IPA and CD63-IPA (Quadrant 3)

MCF7

A

Friedman Q3 CD62p-FITC MCF7

Test for equal medians

chi2:	8.9444	Degrees of freedom:	7
chi2, tie corrected:	8.9444		
chi2, continuity corrected:	8.9049		
p (same), asymptotic:	0.25956		

Post hoc (Wilcoxon)

	UT WB	UT MCF7+WB	DMSO MCF7+WB	Ana MCF7+ WB	AnaAspClop MCF7+WB	AnaAto MCF7+WB	AspClop MCF7+WB	Ato MCF7+WB
UT WB		0.5692	0.5692	0.07692	0.2308	0.5692	0.6923	0.4462
UT MCF7+WB	0.5692		0.8462	1	1	0.4462	0.4462	0.3231
DMSO MCF7+WB	0.5692	0.8462		0.4462	1	0.4462	0.4462	0.5692
Ana MCF7+ WB	0.07692	1	0.4462		0.8462	0.8462	0.07692	0.1692
AnaAspClop MCF7+WB	0.2308	1	1	0.8462		0.5692	0.1692	0.3231
AnaAto MCF7+WB	0.5692	0.4462	0.4462	0.8462	0.5692		0.6923	0.2308
AspClop MCF7+WB	0.6923	0.4462	0.4462	0.07692	0.1692	0.6923		0.4462
Ato MCF7+WB	0.4462	0.3231	0.5692	0.1692	0.3231	0.2308	0.4462	

T47D

B

Friedman Q3 CD62p-FITC T47D

Test for equal medians

chi2:	7.5556	Degrees of freedom:	7
chi2, tie corrected:	7.5556		
chi2, continuity corrected:	7.5178		
p (same), asymptotic:	0.37702		

Post hoc (Wilcoxon)

	UT WB	UT T47D+WB	DMSO T47D+WB	Ana T47D+ WB	AnaAspClop T47D+WB	AnaAto T47D+WB	AspClop T47D+WB	Ato T47D+WB
UT WB		0.5692	0.4462	0.4462	0.6923	0.8462	0.5692	1
UT T47D+WB	0.5692		0.2308	0.8462	0.5692	0.6923	0.3231	0.4462
DMSO T47D+WB	0.4462	0.2308		0.07692	0.4462	0.2308	0.4462	0.1692
Ana T47D+ WB	0.4462	0.8462	0.07692		0.1692	0.4462	0.07692	0.3231
AnaAspClop T47D+WB	0.6923	0.5692	0.4462	0.1692		0.3231	1	0.8462
AnaAto T47D+WB	0.8462	0.6923	0.2308	0.4462	0.3231		0.3231	0.6923
AspClop T47D+WB	0.5692	0.3231	0.4462	0.07692	1	0.3231		0.1692
Ato T47D+WB	1	0.4462	0.1692	0.3231	0.8462	0.6923	0.1692	

B4.5: CD62p Intervals (1-2)

Part A: PAST output for CD62p-IPA within Intervals

Interval 1

A

Friedman P1 CD62p-FITC MCF7

Test for equal medians

chi2:	18.722	Degrees of freedom:	7
chi2, tie corrected:	18.722		
chi2, continuity corrected:	18.67		
p (same), asymptotic:	0.009287		

Post hoc (Wilcoxon)

	UT WB	UT MCF7+WB	DMSO MCF7+WB	Ana MCF7+ WB	AnaAspClop MCF7+WB	AnaAto MCF7+WB	AspClop MCF7+WB	Ato MCF7+WB
UT WB		0.07692	0.04615	0.1077	0.4462	0.6923	0.4462	0.6923
UT MCF7+WB	0.07692		1	0.5692	0.3231	0.1077	0.04615	0.07692
DMSO MCF7+WB	0.04615	1		0.8462	0.1692	0.04615	0.04615	0.1692
Ana MCF7+ WB	0.1077	0.5692	0.8462		0.4462	0.07692	0.04615	0.1077
AnaAspClop MCF7+WB	0.4462	0.3231	0.1692	0.4462		0.4462	0.1077	0.4462
AnaAto MCF7+WB	0.6923	0.1077	0.04615	0.07692	0.4462		0.2308	0.6923
AspClop MCF7+WB	0.4462	0.04615	0.04615	0.04615	0.1077	0.2308		0.8462
Ato MCF7+WB	0.6923	0.07692	0.1692	0.1077	0.4462	0.6923	0.8462	

B

Friedman P1 CD62p-FITC T47D

Test for equal medians

chi2:	10	Degrees of freedom:	7
chi2, tie corrected:	10		
chi2, continuity corrected:	9.959		
p (same), asymptotic:	0.19091		

Post hoc (Wilcoxon)

	UT WB	UT T47D+WB	DMSO T47D+WB	Ana T47D+ WB	AnaAspClop T47D+WB	AnaAto T47D+WB	AspClop T47D+WB	Ato T47D+WB
UT WB		0.1077	0.4462	0.04615	0.8462	0.1692	0.8462	0.4462
UT T47D+WB	0.1077		0.3231	0.6923	0.2308	0.2308	0.1692	0.1692
DMSO T47D+WB	0.4462	0.3231		0.2308	0.3231	0.5692	0.1692	1
Ana T47D+ WB	0.04615	0.6923	0.2308		0.1692	0.2308	0.07692	0.1077
AnaAspClop T47D+WB	0.8462	0.2308	0.3231	0.1692		0.5692	0.6923	0.6923
AnaAto T47D+WB	0.1692	0.2308	0.5692	0.2308	0.5692		0.1692	0.3231
AspClop T47D+WB	0.8462	0.1692	0.1692	0.07692	0.6923	0.1692		0.2308
Ato T47D+WB	0.4462	0.1692	1	0.1077	0.6923	0.3231	0.2308	

Part B: PAST output for CD62p-IPA within Intervals

Interval 2

C

Friedman P2 CD62p-FITC MCF7									
Test for equal medians									
chi2:	17.778	Degrees of freedom:	7						
chi2, tie corrected:	17.778								
chi2, continuity corrected:	17.727								
p (same), asymptotic:	0.013267								
Post hoc (Wilcoxon)									
	UT WB	UT MCF7+WB	DMSO MCF7+WB	Ana MCF7+ WB	AnaAspClop MCF7+WB	AnaAto MCF7+WB	AspClop MCF7+WB	Ato MCF7+WB	
UT WB		0.04615	0.5692	0.1692	1	0.1692	1	0.4462	
UT MCF7+WB	0.04615		0.07692	0.04615	0.04615	0.1077	0.04615	0.04615	
DMSO MCF7+WB	0.5692	0.07692		1	0.3231	1	0.2308	0.3231	
Ana MCF7+ WB	0.1692	0.04615	1		0.5692	1	0.2308	0.1077	
AnaAspClop MCF7+WB	1	0.04615	0.3231	0.5692		0.8462	0.5692	0.4462	
AnaAto MCF7+WB	0.1692	0.1077	1	1	0.8462		0.5692	0.2308	
AspClop MCF7+WB	1	0.04615	0.2308	0.2308	0.5692	0.5692		0.8462	
Ato MCF7+WB	0.4462	0.04615	0.3231	0.1077	0.4462	0.2308	0.8462		

D

Friedman P2 CD62p-FITC T47D									
Test for equal medians									
chi2:	10.444	Degrees of freedom:	7						
chi2, tie corrected:	10.444								
chi2, continuity corrected:	10.403								
p (same), asymptotic:	0.16687								
Post hoc (Wilcoxon)									
	UT WB	UT T47D+WB	DMSO T47D+WB	Ana T47D+ WB	AnaAspClop T47D+WB	AnaAto T47D+WB	AspClop T47D+WB	Ato T47D+WB	
UT WB		0.5692	0.5692	0.5692	0.8462	0.6923	0.8462	0.07692	
UT T47D+WB	0.5692		0.3231	0.5692	0.3231	0.1692	0.5692	0.1077	
DMSO T47D+WB	0.5692	0.3231		1	0.8462	0.6923	0.6923	0.4462	
Ana T47D+ WB	0.5692	0.5692	1		0.3231	1	0.3231	0.04615	
AnaAspClop T47D+WB	0.8462	0.3231	0.8462	0.3231		0.5692	0.5692	0.1077	
AnaAto T47D+WB	0.6923	0.1692	0.6923	1	0.5692		0.6923	0.1692	
AspClop T47D+WB	0.8462	0.5692	0.6923	0.3231	0.5692	0.6923		0.07692	
Ato T47D+WB	0.07692	0.1077	0.4462	0.04615	0.1077	0.1692	0.07692		

B4.6: CD62p Intervals (3-4)

Part A: PAST output for CD62p-IPA within Intervals

Interval 3

A

Friedman P3 CD62p-FITC MCF7									
Test for equal medians									
chi2:	24.333	Degrees of freedom:	7						
chi2, tie corrected:	24.333								
chi2, continuity corrected:	24.273								
p (same), asymptotic:	0.00102								
Post hoc (Wilcoxon)									
	UT WB	UT MCF7+WB		DMSO MCF7+WB	Ana MCF7+ WB	AnaAspClop MCF7+WB	AnaAto MCF7+WB	AspClop MCF7+WB	Ato MCF7+WB
UT WB			0.8462	0.07692	0.1692	0.07692	0.1077	0.1692	0.8462
UT MCF7+WB	0.8462			0.04615	0.07692	0.04615	0.04615	0.04615	0.8462
DMSO MCF7+WB	0.07692	0.04615			0.1692	0.1077	0.8462	0.4462	0.04615
Ana MCF7+ WB	0.1692	0.07692	0.1692			0.07692	0.1692	0.8462	0.07692
AnaAspClop MCF7+WB	0.07692	0.04615	0.1077	0.07692			0.1077	0.04615	0.04615
AnaAto MCF7+WB	0.1077	0.04615	0.8462	0.1692	0.1077			0.3231	0.04615
AspClop MCF7+WB	0.1692	0.04615	0.4462	0.8462	0.04615	0.3231			0.1077
Ato MCF7+WB	0.8462	0.8462	0.04615	0.07692	0.04615	0.04615	0.1077		

B

Friedman P3 CD62p-FITC T47D									
Test for equal medians									
chi2:	26.556	Degrees of freedom:	7						
chi2, tie corrected:	26.556								
chi2, continuity corrected:	26.493								
p (same), asymptotic:	0.000411								
Post hoc (Wilcoxon)									
	UT WB	UT T47D+WB		DMSO T47D+WB	Ana T47D+ WB	AnaAspClop T47D+WB	AnaAto T47D+WB	AspClop T47D+WB	Ato T47D+WB
UT WB			0.04615	0.04615	0.1692	0.1692	0.1077	0.04615	0.5692
UT T47D+WB	0.04615			0.4462	0.1692	0.07692	0.04615	0.3231	0.04615
DMSO T47D+WB	0.04615	0.4462			0.1692	0.07692	0.1692	1	0.04615
Ana T47D+ WB	0.1692	0.1692	0.1692			0.3231	0.5692	0.3231	0.04615
AnaAspClop T47D+WB	0.1692	0.07692	0.07692	0.3231			0.2308	0.1692	0.04615
AnaAto T47D+WB	0.1077	0.04615	0.1692	0.5692	0.2308			0.1692	0.04615
AspClop T47D+WB	0.04615	0.3231	1	0.3231	0.1692	0.1692			0.04615
Ato T47D+WB	0.5692	0.04615	0.04615	0.04615	0.04615	0.04615	0.04615		

Part B: PAST output for CD62p-IPA within Intervals

Interval 4

C

Friedman P4 CD62p-FITC MCF7								
Test for equal medians								
chi2:	34.278	Degrees of freedom:	7					
chi2, tie corrected:	34.278							
chi2, continuity corrected:	34.205							
p (same), asymptotic:	1.58E-05							
Post hoc (Wilcoxon)								
	UT WB	UT MCF7+WB	DMSO MCF7+WB	Ana MCF7+ WB	AnaAspClop MCF7+WB	AnaAto MCF7+WB	AspClop MCF7+WB	Ato MCF7+WB
UT WB		0.04615	0.5692	0.04615	0.04615	0.3231	0.5692	0.04615
UT MCF7+WB	0.04615		0.04615	0.04615	0.1692	0.04615	0.04615	0.04615
DMSO MCF7+WB	0.5692	0.04615		0.04615	0.04615	0.4462	0.6923	0.07692
Ana MCF7+ WB	0.04615	0.04615	0.04615		0.04615	0.07692	0.07692	0.1077
AnaAspClop MCF7+WB	0.04615	0.1692	0.04615	0.04615		0.04615	0.04615	0.04615
AnaAto MCF7+WB	0.3231	0.04615	0.4462	0.07692	0.04615		0.04615	0.04615
AspClop MCF7+WB	0.5692	0.04615	0.6923	0.07692	0.04615	0.04615		0.04615
Ato MCF7+WB	0.04615	0.04615	0.07692	0.1077	0.04615	0.04615	0.04615	

D

Friedman P4 CD62p-FITC T47D								
Test for equal medians								
chi2:	20.597	Degrees of freedom:	7					
chi2, tie corrected:	20.638							
chi2, continuity corrected:	20.583							
p (same), asymptotic:	0.004439							
Post hoc (Wilcoxon)								
	UT WB	UT T47D+WB	DMSO T47D+WB	Ana T47D+ WB	AnaAspClop T47D+WB	AnaAto T47D+WB	AspClop T47D+WB	Ato T47D+WB
UT WB		0.6923	0.07692	0.04615	0.4462	0.3231	1	1
UT T47D+WB	0.6923		0.09091	0.04615	1	0.2308	0.8462	1
DMSO T47D+WB	0.07692	0.09091		0.1077	0.07692	0.07692	0.07692	0.07692
Ana T47D+ WB	0.04615	0.04615	0.1077		0.04615	0.04615	0.04615	0.04615
AnaAspClop T47D+WB	0.4462	1	0.07692	0.04615		0.4462	0.5692	0.6923
AnaAto T47D+WB	0.3231	0.2308	0.07692	0.04615	0.4462		0.07692	0.1077
AspClop T47D+WB	1	0.8462	0.07692	0.04615	0.5692	0.07692		0.1077
Ato T47D+WB	1	1	0.07692	0.04615	0.6923	0.1077	0.1077	

B4.7: CD63 Intervals (1-2)

Part A: PAST output for CD63-IPA within Intervals

Interval 1

A

Friedman P1 CD63-PECY7 MCF7

Test for equal medians			
chi2:	24.833	Degrees of freedom:	7
chi2, tie corrected:	24.833		
chi2, continuity corrected:	24.773		
p (same), asymptotic:	0.000832		

Post hoc (Wilcoxon)

	UT WB	UT MCF7+WB	DMSO MCF7+WB	Ana MCF7+ WB	AnaAspClop MCF7+WB	AnaAto MCF7+WB	AspClop MCF7+WB	Ato MCF7+WB
UT WB		0.04615	0.1077	0.4462	0.1077	0.2308	0.1077	0.8462
UT MCF7+WB	0.04615		0.04615	0.04615	0.4462	0.04615	0.04615	0.04615
DMSO MCF7+WB	0.1077	0.04615		0.8462	0.2308	0.1077	0.04615	0.1692
Ana MCF7+ WB	0.4462	0.04615	0.8462		0.1692	0.07692	0.04615	0.2308
AnaAspClop MCF7+WB	0.1077	0.4462	0.2308	0.1692		0.07692	0.07692	0.1692
AnaAto MCF7+WB	0.2308	0.04615	0.1077	0.07692	0.07692		0.3231	1
AspClop MCF7+WB	0.1077	0.04615	0.04615	0.04615	0.07692	0.3231		0.2308
Ato MCF7+WB	0.8462	0.04615	0.1692	0.2308	0.1692	1	0.2308	

B

Friedman P1 CD63-PECY7 T47D

Test for equal medians			
chi2:	7.2778	Degrees of freedom:	7
chi2, tie corrected:	7.2778		
chi2, continuity corrected:	7.2404		
p (same), asymptotic:	0.40428		

Post hoc (Wilcoxon)

	UT WB	UT T47D+WB	DMSO T47D+WB	Ana T47D+ WB	AnaAspClop T47D+WB	AnaAto T47D+WB	AspClop T47D+WB	Ato T47D+WB
UT WB		0.8462	0.6923	0.8462	0.8462	1	0.3231	0.4462
UT T47D+WB	0.8462		0.6923	0.6923	0.8462	0.6923	0.3231	0.8462
DMSO T47D+WB	0.6923	0.6923		0.8462	0.6923	1	0.3231	0.07692
Ana T47D+ WB	0.8462	0.6923	0.8462		0.8462	0.6923	0.2308	0.3231
AnaAspClop T47D+WB	0.8462	0.8462	0.6923	0.8462		1	0.4462	0.2308
AnaAto T47D+WB	1	0.6923	1	0.6923	1		0.2308	0.2308
AspClop T47D+WB	0.3231	0.3231	0.3231	0.2308	0.4462	0.2308		0.5692
Ato T47D+WB	0.4462	0.8462	0.07692	0.3231	0.2308	0.2308	0.5692	

Part B: PAST output for CD63-IPA within Intervals

Interval 2

C

Friedman P2 CD63-PECY7 MCF7								
Test for equal medians								
chi2:	10.389	Degrees of freedom:	7					
chi2, tie corrected:	10.389							
chi2, continuity corrected:	10.347							
p (same), asymptotic:	0.16973							
Post hoc (Wilcoxon)								
	UT WB	UT MCF7+WB	DMSO MCF7+WB	Ana MCF7+ WB	AnaAspClop MCF7+WB	AnaAto MCF7+WB	AspClop MCF7+WB	Ato MCF7+WB
UT WB		0.2308	0.1077	0.07692	0.6923	0.1692	1	1
UT MCF7+WB	0.2308		0.5692	1	0.3231	0.6923	0.1692	0.3231
DMSO MCF7+WB	0.1077	0.5692		0.6923	0.04615	0.3231	0.07692	0.1692
Ana MCF7+ WB	0.07692	1	0.6923		0.1077	0.4462	0.07692	0.04615
AnaAspClop MCF7+WB	0.6923	0.3231	0.04615	0.1077		0.4462	0.6923	0.8462
AnaAto MCF7+WB	0.1692	0.6923	0.3231	0.4462	0.4462		0.6923	0.4462
AspClop MCF7+WB	1	0.1692	0.07692	0.07692	0.6923	0.6923		1
Ato MCF7+WB	1	0.3231	0.1692	0.04615	0.8462	0.4462	1	

D

Friedman P2 CD63-PECY7 T47D								
Test for equal medians								
chi2:	11.5	Degrees of freedom:	7					
chi2, tie corrected:	11.5							
chi2, continuity corrected:	11.457							
p (same), asymptotic:	0.11989							
Post hoc (Wilcoxon)								
	UT WB	UT T47D+WB	DMSO T47D+WB	Ana T47D+ WB	AnaAspClop T47D+WB	AnaAto T47D+WB	AspClop T47D+WB	Ato T47D+WB
UT WB		0.1692	1	0.8462	0.4462	0.2308	0.4462	0.1692
UT T47D+WB	0.1692		0.4462	0.1077	0.07692	0.07692	0.07692	0.1077
DMSO T47D+WB	1	0.4462		0.5692	0.6923	0.4462	0.6923	0.1077
Ana T47D+ WB	0.8462	0.1077	0.5692		1	0.6923	0.8462	0.07692
AnaAspClop T47D+WB	0.4462	0.07692	0.6923	1		0.4462	0.6923	0.5692
AnaAto T47D+WB	0.2308	0.07692	0.4462	0.6923	0.4462		0.2308	0.6923
AspClop T47D+WB	0.4462	0.07692	0.6923	0.8462	0.6923	0.2308		0.3231
Ato T47D+WB	0.1692	0.1077	0.1077	0.07692	0.5692	0.6923	0.3231	

B4.8: CD63 Intervals (3-4)

Part A: PAST output for CD63-IPA within Intervals

Interval 3

A

Friedman P3 CD63-PECY7 MCF7

Test for equal medians

chi2:	12.056	Degrees of freedom:	7
chi2, tie corrected:	12.056		
chi2, continuity corrected:	12.012		
p (same), asymptotic:	0.10017		

Post hoc (Wilcoxon)

	UT WB	UT MCF7+WB	DMSO MCF7+WB	Ana MCF7+ WB	AnaAspClop MCF7+WB	AnaAto MCF7+WB	AspClop MCF7+WB	Ato MCF7+WB
UT WB		0.5692	0.1077	0.04615	0.1077	0.3231	0.4462	0.07692
UT MCF7+WB	0.5692		0.07692	0.07692	0.07692	0.1692	0.1077	0.1077
DMSO MCF7+WB	0.1077	0.07692		0.3231	0.2308	1	0.4462	0.6923
Ana MCF7+ WB	0.04615	0.07692	0.3231		0.6923	0.4462	0.8462	0.8462
AnaAspClop MCF7+WB	0.1077	0.07692	0.2308	0.6923		0.3231	0.8462	0.8462
AnaAto MCF7+WB	0.3231	0.1692	1	0.4462	0.3231		1	0.8462
AspClop MCF7+WB	0.4462	0.1077	0.4462	0.8462	0.8462	1		0.8462
Ato MCF7+WB	0.07692	0.1077	0.6923	0.8462	0.8462	0.8462	0.8462	

B

Friedman P3 CD63-PECY7 T47D

Test for equal medians

chi2:	18.556	Degrees of freedom:	7
chi2, tie corrected:	18.556		
chi2, continuity corrected:	18.503		
p (same), asymptotic:	0.009894		

Post hoc (Wilcoxon)

	UT WB	UT T47D+WB	DMSO T47D+WB	Ana T47D+ WB	AnaAspClop T47D+WB	AnaAto T47D+WB	AspClop T47D+WB	Ato T47D+WB
UT WB		0.5692	0.5692	0.2308	0.3231	0.07692	0.4462	0.1077
UT T47D+WB	0.5692		0.04615	0.04615	0.1077	0.04615	0.04615	0.04615
DMSO T47D+WB	0.5692	0.04615		0.4462	0.8462	0.3231	0.2308	0.07692
Ana T47D+ WB	0.2308	0.04615	0.4462		1	0.04615	0.4462	0.1077
AnaAspClop T47D+WB	0.3231	0.1077	0.8462	1		0.4462	0.8462	0.2308
AnaAto T47D+WB	0.07692	0.04615	0.3231	0.04615	0.4462		1	0.4462
AspClop T47D+WB	0.4462	0.04615	0.2308	0.4462	0.8462	1		0.3231
Ato T47D+WB	0.1077	0.04615	0.07692	0.1077	0.2308	0.4462	0.3231	

Part B: PAST output for CD63-IPA within Intervals

Interval 4

C

Friedman P4 CD63-PECY7 MCF7

Test for equal medians

Test for equal medians

chi2:	12.833	Degrees of freedom:	7
chi2, tie corrected:	12.833		
chi2, continuity corrected:	12.789		
p (same), asymptotic:	0.077429		

Post hoc (Wilcoxon)

	UT WB	UT MCF7+WB	DMSO MCF7+WB	Ana MCF7+ WB	AnaAspClop MCF7+WB	AnaAto MCF7+WB	AspClop MCF7+WB	Ato MCF7+WB
UT WB		0.2308	0.8462	1	0.5692	0.07692	1	1
UT MCF7+WB	0.2308		0.3231	0.2308	0.1077	0.04615	0.5692	0.1077
DMSO MCF7+WB	0.8462	0.3231		0.4462	0.07692	0.1077	0.8462	0.8462
Ana MCF7+ WB	1	0.2308	0.4462		0.8462	0.1692	0.5692	0.6923
AnaAspClop MCF7+WB	0.5692	0.1077	0.07692	0.8462		0.3231	0.6923	0.3231
AnaAto MCF7+WB	0.07692	0.04615	0.1077	0.1692	0.3231		0.3231	0.07692
AspClop MCF7+WB	1	0.5692	0.8462	0.5692	0.6923	0.3231		1
Ato MCF7+WB	1	0.1077	0.8462	0.6923	0.3231	0.07692	1	

D

Friedman P4 CD63-PECY7 T47D

Test for equal medians

chi2:	15.556	Degrees of freedom:	7
chi2, tie corrected:	15.556		
chi2, continuity corrected:	15.507		
p (same), asymptotic:	0.03002		

Post hoc (Wilcoxon)

	UT WB	UT T47D+WB	DMSO T47D+WB	Ana T47D+ WB	AnaAspClop T47D+WB	AnaAto T47D+WB	AspClop T47D+WB	Ato T47D+WB
UT WB		0.2308	0.6923	1	0.3231	0.5692	0.8462	0.4462
UT T47D+WB	0.2308		0.2308	0.04615	0.04615	0.1692	0.04615	0.04615
DMSO T47D+WB	0.6923	0.2308		0.1077	0.1077	0.4462	0.3231	0.1077
Ana T47D+ WB	1	0.04615	0.1077		0.4462	0.5692	0.2308	0.5692
AnaAspClop T47D+WB	0.3231	0.04615	0.1077	0.4462		0.3231	0.1692	0.8462
AnaAto T47D+WB	0.5692	0.1692	0.4462	0.5692	0.3231		0.6923	0.2308
AspClop T47D+WB	0.8462	0.04615	0.3231	0.2308	0.1692	0.6923		0.07692
Ato T47D+WB	0.4462	0.04615	0.1077	0.5692	0.8462	0.2308	0.07692	

APPENDIX C: Chapter IV supplementary information

C1: RNA concentration and purity

1µl of RNA was pipetted onto the nanodrop in order to measure RNA concentration. The A260/280 ratio gives an indication of the purity of the nucleic acid and acceptable values are in the following range; [1.8-2.1].

Table C1.1: Control samples for MCF7 and T47D cells

		UT cells + media only		UT cells+ WB		DMSO treated cells+ WB	
		[RNA] ng/ul	A260/280	[RNA] ng/ul	A260/280	[RNA] ng/ul	A260/280
MCF7 cells	Volunteer 1	37.4	2.09	13.4	2.43	13.2	2.01
	Volunteer 2	4.3	2.56	3.3	2.43	2.4	2.31
	Volunteer 3	133.2	2.09	30	1.56	76.8	2.04
	Volunteer 4	257.9	2.09	159	2.11	129.4	2.09
	Volunteer 5	72.6	1.98	22.1	2.21	46.2	2.09
	Volunteer 6	31.3	2.11	4.8	3.37	2.7	2.08
T47D cells	Volunteer 1	198.8	2.1	232.1	2.09	159.5	2.12
	Volunteer 2	58.8	2.08	38.4	2.04	12.8	2.09
	Volunteer 3	5.3	2.48	10.9	2.03	*missing sample*	
	Volunteer 4	403.6	2.08	222.9	2.1	49.2	1.95
	Volunteer 5	111.1	2.09	53.3	2.09	72.6	2.07
	Volunteer 6	34.2	2.17	18.4	2.15	11.2	2.01

Table C1.2: Treated samples for MCF7 and T47D cells

		Ana treated cells+ WB		AnaAspClop treated cells+ WB		AnaAto treated cells+ WB		AspClop treated cells+ WB		Ato treated cells+ WB	
		[RNA] ng/ul	A260/280	[RNA] ng/ul	A260/280	[RNA] ng/ul	A260/280	[RNA] ng/ul	A260/280	[RNA] ng/ul	A260/280
MCF7 cells	Volunteer 1	23.7	2.03	14.4	2.04	11.1	2.48	34	2.07	41.1	2.09
	Volunteer 2	3.6	2.01	5.7	2.42	5.3	6.35	1.9	2.54	5.9	2.28
	Volunteer 3	114.5	2.07	64.3	2.07	7.8	2.83	3.2	2.38	64.6	2.06
	Volunteer 4	185.7	2.08	125.3	2.14	8.5	2.57	145.4	2.12	183.6	2.12
	Volunteer 5	93.7	2.08	28.6	2.15	8.8	2.35	21.2	1.96	31.3	1.99
	Volunteer 6	5.5	1.81	5	3.19	3.4	3.29	7.6	2.17	9.7	2.22
T47D cells	Volunteer 1	327.5	2.09	231.8	2.11	83.7	2.12	224.5	2.09	262.2	2.1
	Volunteer 2	17.4	2.12	42.7	2.09	29.5	2.18	79.5	2.1	51.9	2.11
	Volunteer 3	17.5	2.01	11.6	2.64	10.1	2.36	6.2	2.14	11.8	2.12
	Volunteer 4	270.6	2.09	55.9	2.11	143.2	2.1	37.9	2.13	92.4	2.09
	Volunteer 5	82.1	2.1	58.8	2.1	44.9	2.1	50.6	2.05	58.6	2.09
	Volunteer 6	26.6	1.99	5.5	2.33	4.8	2.79	10.2	2.27	11.4	2.18

Table C1.3: Thermal cycler conditions for cDNA synthesis.

	Step 1	Step 2	Step 3	Step 4
Temperature	25°C	37°C	85°C	4°C
Time	10mins	120mins	5sec	∞

Table C1.4: thermal cycler conditions for qPCR reaction

	Hold stage	Denature stage	Annealing stage
Temperature	95°C	95°C	60°C
Time	10mins	30sec	1min

C2.1: Gene expression statistics

Part A: PAST output for gene expression between treatments per cell line

MCF7

E-Cadherin — A1

Friedman test *E-Cadherin*
Test for equal medians

chi2:	7.1111	Degrees of freedom:	7
chi2, tie corrected:	7.1111		
chi2, continuity corrected:	7.074		
p (same), asymptotic:	0.42122		

Post hoc (Wilcoxon)

	Media+MCF7	UT MCF7+WB	DMSO MCF7+WB	Ana MCF7+ WB	AnaAspClop MCF7+WB	AnaAto MCF7+WB	AspClop MCF7+WB	Ato MCF7+WB
Media+MCF7		0.5692	0.6923	0.5692	0.8462	0.3231	0.5692	0.04615
UT MCF7+WB	0.5692		0.5692	0.6923	0.4462	0.4462	0.6923	0.3231
DMSO MCF7+WB	0.6923	0.5692		1	0.8462	0.4462	0.5692	0.04615
Ana MCF7+ WB	0.5692	0.6923	1		0.8462	0.4462	0.5692	0.04615
AnaAspClop MCF7+WB	0.8462	0.4462	0.8462	0.8462		0.6923	1	0.6923
AnaAto MCF7+WB	0.3231	0.4462	0.4462	0.4462	0.6923		0.8462	0.6923
AspClop MCF7+WB	0.5692	0.6923	0.5692	0.5692	1	0.8462		0.4462
Ato MCF7+WB	0.04615	0.3231	0.04615	0.04615	0.6923	0.6923	0.4462	

N-Cadherin — B1

Friedman test *N-Cadherin*
Test for equal medians

chi2:	18.389	Degrees of freedom:	7
chi2, tie corrected:	18.389		
chi2, continuity corrected:	18.337		
p (same), asymptotic:	0.010539		

Post hoc (Wilcoxon)

	Media+MCF7	UT MCF7+WB	DMSO MCF7+WB	Ana MCF7+ WB	AnaAspClop MCF7+WB	AnaAto MCF7+WB	AspClop MCF7+WB	Ato MCF7+WB
Media+MCF7		0.04615	0.4462	0.6923	0.1077	1	0.3231	0.1077
UT MCF7+WB	0.04615		0.07692	0.1692	0.6923	0.07692	0.5692	1
DMSO MCF7+WB	0.4462	0.07692		0.04615	0.04615	0.4462	0.07692	0.04615
Ana MCF7+ WB	0.6923	0.1692	0.04615		0.1692	1	0.5692	0.07692
AnaAspClop MCF7+WB	0.1077	0.6923	0.04615	0.1692		0.3231	0.6923	0.8462
AnaAto MCF7+WB	1	0.07692	0.4462	1	0.3231		0.4462	0.07692
AspClop MCF7+WB	0.3231	0.5692	0.07692	0.5692	0.6923	0.4462		0.5692
Ato MCF7+WB	0.1077	1	0.04615	0.07692	0.8462	0.07692	0.5692	

T47D

E-Cadherin — A2

Friedman test *E-Cadherin*
Test for equal medians

chi2:	26.444	Degrees of freedom:	7
chi2, tie corrected:	26.444		
chi2, continuity corrected:	26.382		
p (same), asymptotic:	0.00043		

Post hoc (Wilcoxon)

	Media+T47D	UT T47D+WB	DMSO T47D+WB	Ana T47D+ WB	AnaAspClop T47D+WB	AnaAto T47D+WB	AspClop T47D+WB	Ato T47D+WB
Media+T47D		0.8462	0.04615	0.3231	0.07692	0.04615	0.1692	0.2308
UT T47D+WB	0.8462		0.04615	1	0.1692	0.07692	0.1692	0.3231
DMSO T47D+WB	0.04615	0.04615		0.04615	0.04615	0.04615	0.04615	0.04615
Ana T47D+ WB	0.3231	1	0.04615		0.07692	0.04615	0.07692	0.04615
AnaAspClop T47D+WB	0.07692	0.1692	0.04615	0.07692		0.07692	0.1692	0.4462
AnaAto T47D+WB	0.04615	0.07692	0.04615	0.04615	0.07692		0.07692	0.07692
AspClop T47D+WB	0.1692	0.1692	0.04615	0.07692	0.1692	0.07692		0.8462
Ato T47D+WB	0.2308	0.3231	0.04615	0.04615	0.4462	0.07692	0.8462	

N-Cadherin — B2

Friedman test *N-Cadherin*
Test for equal medians

chi2:	21.444	Degrees of freedom:	7
chi2, tie corrected:	21.444		
chi2, continuity corrected:	21.388		
p (same), asymptotic:	0.0032359		

Post hoc (Wilcoxon)

	Media+T47D	UT T47D+WB	DMSO T47D+WB	Ana T47D+ WB	AnaAspClop T47D+WB	AnaAto T47D+WB	AspClop T47D+WB	Ato T47D+WB
Media+T47D		0.2308	0.3231	0.1692	0.8462	0.04615	0.07692	0.07692
UT T47D+WB	0.2308		0.04615	0.6923	0.1692	0.07692	0.04615	0.04615
DMSO T47D+WB	0.3231	0.04615		0.04615	0.4462	1	0.5692	0.5692
Ana T47D+ WB	0.1692	0.6923	0.04615		0.1692	0.1077	0.04615	0.07692
AnaAspClop T47D+WB	0.8462	0.1692	0.4462	0.1692		0.1077	0.04615	0.07692
AnaAto T47D+WB	0.04615	0.07692	1	0.1077	0.1077		0.6923	0.6923
AspClop T47D+WB	0.07692	0.04615	0.5692	0.04615	0.04615	0.6923		0.8462
Ato T47D+WB	0.07692	0.04615	0.5692	0.07692	0.07692	0.6923	0.8462	

Part B: PAST output for gene expression between treatments per cell line

MCF7

Vimentin

C1

Friedman test *Vimentin*
Test for equal medians

chi2:	8.4444	Degrees of freedom:	7
chi2, tie corrected:	8.4444		
chi2, continuity corrected:	8.4055		
p (same), asymptotic:	0.29819		

Post hoc (Wilcoxon)

	Media+MCF7	UT MCF7+WB	DMSO MCF7+WB	Ana MCF7+ WB	AnaAspClop MCF7+WB	AnaAto MCF7+WB	AspClop MCF7+WB	Ato MCF7+WB
Media+MCF7		1	0.5692	0.8462	1	0.4462	0.1077	0.3231
UT MCF7+WB	1		0.2308	1	0.3231	0.6923	0.2308	0.4462
DMSO MCF7+WB	0.5692	0.2308		0.2308	0.1692	0.1692	1	0.07692
Ana MCF7+ WB	0.8462	1	0.2308		0.4462	1	0.3231	0.8462
AnaAspClop MCF7+WB	1	0.3231	0.1692	0.4462		0.6923	0.1077	1
AnaAto MCF7+WB	0.4462	0.6923	0.1692	1	0.6923		0.1692	0.8462
AspClop MCF7+WB	0.1077	0.2308	1	0.3231	0.1077	0.1692		0.1077
Ato MCF7+WB	0.3231	0.4462	0.07692	0.8462	1	0.8462	0.1077	

TGFβ1

D1

Friedman test *TGF ß1*
Test for equal medians

chi2:	17	Degrees of freedom:	7
chi2, tie corrected:	17		
chi2, continuity corrected:	16.95		
p (same), asymptotic:	0.017723		

Post hoc (Wilcoxon)

	Media+MCF7	UT MCF7+WB	DMSO MCF7+WB	Ana MCF7+ WB	AnaAspClop MCF7+WB	AnaAto MCF7+WB	AspClop MCF7+WB	Ato MCF7+WB
Media+MCF7		0.8462	0.04615	0.04615	0.3231	0.1077	0.6923	0.6923
UT MCF7+WB	0.8462		0.07692	0.6923	0.2308	0.3231	0.5692	0.8462
DMSO MCF7+WB	0.04615	0.07692		0.1077	0.3231	0.1692	0.04615	0.04615
Ana MCF7+ WB	0.04615	0.6923	0.1077		0.4462	0.8462	0.1077	0.2308
AnaAspClop MCF7+WB	0.3231	0.2308	0.3231	0.4462		1	0.1692	0.3231
AnaAto MCF7+WB	0.1077	0.3231	0.1692	0.8462	1		0.1692	0.1692
AspClop MCF7+WB	0.6923	0.5692	0.04615	0.1077	0.1692	0.1692		1
Ato MCF7+WB	0.6923	0.8462	0.04615	0.2308	0.3231	0.1692	1	

T47D

C2

Friedman test *Vimentin*
Test for equal medians

chi2:	21.889	Degrees of freedom:	7
chi2, tie corrected:	21.889		
chi2, continuity corrected:	21.832		
p (same), asymptotic:	0.002715		

Post hoc (Wilcoxon)

	Media+T47D	UT T47D+WB	DMSO T47D+WB	Ana T47D+ WB	AnaAspClop T47D+WB	AnaAto T47D+WB	AspClop T47D+WB	Ato T47D+WB
Media+T47D		0.2308	0.1077	0.1077	0.4462	0.04615	0.2308	0.8462
UT T47D+WB	0.2308		0.5692	0.8462	0.3231	0.07692	0.07692	0.07692
DMSO T47D+WB	0.1077	0.5692		1	0.1692	0.04615	0.04615	0.04615
Ana T47D+ WB	0.1077	0.8462	1		0.1692	0.04615	0.04615	0.04615
AnaAspClop T47D+WB	0.4462	0.3231	0.1692	0.1692		0.04615	0.04615	0.3231
AnaAto T47D+WB	0.04615	0.07692	0.04615	0.04615	0.04615		0.1692	0.4462
AspClop T47D+WB	0.2308	0.07692	0.04615	0.04615	0.04615	0.1692		0.6923
Ato T47D+WB	0.8462	0.07692	0.04615	0.04615	0.3231	0.4462	0.6923	

D2

Friedman test *Vimentin*
Test for equal medians

chi2:	21.889	Degrees of freedom:	7
chi2, tie corrected:	21.889		
chi2, continuity corrected:	21.832		
p (same), asymptotic:	0.002715		

Post hoc (Wilcoxon)

	Media+T47D	UT T47D+WB	DMSO T47D+WB	Ana T47D+ WB	AnaAspClop T47D+WB	AnaAto T47D+WB	AspClop T47D+WB	Ato T47D+WB
Media+T47D		0.2308	0.1077	0.1077	0.4462	0.04615	0.2308	0.8462
UT T47D+WB	0.2308		0.5692	0.8462	0.3231	0.07692	0.07692	0.07692
DMSO T47D+WB	0.1077	0.5692		1	0.1692	0.04615	0.04615	0.04615
Ana T47D+ WB	0.1077	0.8462	1		0.1692	0.04615	0.04615	0.04615
AnaAspClop T47D+WB	0.4462	0.3231	0.1692	0.1692		0.04615	0.04615	0.3231
AnaAto T47D+WB	0.04615	0.07692	0.04615	0.04615	0.04615		0.1692	0.4462
AspClop T47D+WB	0.2308	0.07692	0.04615	0.04615	0.04615	0.1692		0.6923
Ato T47D+WB	0.8462	0.07692	0.04615	0.04615	0.3231	0.4462	0.6923	

C2.2: Statistics output *TGFβ1* expression

Part A: PAST output for gene expression between cell lines

UT cells	Test for equal medians *TGFβ1*			A
	chi2:	0.66667	Degrees of freedom:	1
	chi2, tie corrected:	0.66667		
	chi2, continuity corrected:	0.3		
	p (same), asymptotic:	0.58388		
		UT MCF7+WB	UT T47D+WB	
	UT MCF7+WB		0.8462	
	UT T47D+WB	0.8462		

DMSO	Test for equal medians *TGFβ1*			B
	chi2:	6	Degrees of freedom:	1
	chi2, tie corrected:	6		
	chi2, continuity corrected:	5.1		
	p (same), asymptotic:	0.023926		
		DMSO MCF7+WB	DMSO T47D+WB	
	DMSO MCF7+WB		0.04615	
	DMSO T47D+WB	0.04615		

Ana	Test for equal medians *TGFβ1*			C
	chi2:	2.6667	Degrees of freedom:	1
	chi2, tie corrected:	2.6667		
	chi2, continuity corrected:	2.1		
	p (same), asymptotic:	0.1473		
		Ana MCF7+ WB	Ana T47D+ WB	
	Ana MCF7+ WB		0.1692	
	Ana T47D+ WB	0.1692		

AnaAspClop	Test for equal medians *TGFβ1*			D
	chi2:	0.66667	Degrees of freedom:	1
	chi2, tie corrected:	0.66667		
	chi2, continuity corrected:	0.3		
	p (same), asymptotic:	0.58388		
		AnaAspClop MCF7+WB	AnaAspClop T47D+WB	
	AnaAspClop MCF7+WB		0.8462	
	AnaAspClop T47D+WB	0.8462		

Part B: PAST output for gene expression between cell lines

AspClop	Test for equal medians *TGFβ1*			E
	chi2:	2.6667	Degrees of freedom:	1
	chi2, tie corrected:	2.6667		
	chi2, continuity corrected:	2.1		
	p (same), asymptotic:	0.1473		

	AspClop MCF7+WB	AspClop T47D+WB
AspClop MCF7+WB		0.2308
AspClop T47D+WB	0.2308	

AnaAto	Test for equal medians *TGFβ1*			F
	chi2:	0	Degrees of freedom:	1
	chi2, tie corrected:	0		
	chi2, continuity corrected:	0		
	p (same), asymptotic:	1		

	AnaAto MCF7+WB	AnaAto T47D+WB
AnaAto MCF7+WB		1
AnaAto T47D+WB	1	

Ato	Test for equal medians *TGFβ1*			G
	chi2:	0.66667	Degrees of freedom:	1
	chi2, tie corrected:	0.66667		
	chi2, continuity corrected:	0.3		
	p (same), asymptotic:	0.58388		

	Ato MCF7+WB	Ato T47D+WB
Ato MCF7+WB		0.3231
Ato T47D+WB	0.3231	

C2.3: Statistics output *Vimentin* expression

Part A: PAST output for gene expression between cell lines

UT cells	Test for equal medians *Vimentin*			A
	chi2:	0	Degrees of freedom:	1
	chi2, tie corrected:	0		
	chi2, continuity corrected:	0		
	p (same), asymptotic:	1		
		UT MCF7+WB	UT T47D+WB	
	UT MCF7+WB		0.8462	
	UT T47D+WB	0.8462		

DMSO	Test for equal medians *Vimentin*			B
	chi2:	6	Degrees of freedom:	1
	chi2, tie corrected:	6		
	chi2, continuity corrected:	5.1		
	p (same), asymptotic:	0.023926		
		DMSO MCF7+WB	DMSO T47D+WB	
	DMSO MCF7+WB		0.04615	
	DMSO T47D+WB	0.04615		

Ana	Test for equal medians *Vimentin*			C
	chi2:	0.66667	Degrees of freedom:	1
	chi2, tie corrected:	0.66667		
	chi2, continuity corrected:	0.3		
	p (same), asymptotic:	0.58388		
		Ana MCF7+ WB	Ana T47D+ WB	
	Ana MCF7+ WB		0.4462	
	Ana T47D+ WB	0.4462		

AnaAspClop	Test for equal medians *Vimentin*			D
	chi2:	0.66667	Degrees of freedom:	1
	chi2, tie corrected:	0.66667		
	chi2, continuity corrected:	0.3		
	p (same), asymptotic:	0.58388		
		AnaAspClop MCF7+WB	AnaAspClop T47D+WB	
	AnaAspClop MCF7+WB		1	
	AnaAspClop T47D+WB	1		

Part B: PAST output for gene expression between cell lines

AspClop	Test for equal medians ***Vimentin***				E
	chi2:	0	Degrees of freedom:	1	
	chi2, tie corrected:	0			
	chi2, continuity corrected:	0			
	p (same), asymptotic:	1			
		AspClop MCF7+WB	AspClop T47D+WB		
	AspClop MCF7+WB		0.6923		
	AspClop T47D+WB	0.6923			

AnaAto	Test for equal medians ***Vimentin***				F
	chi2:	2.6667	Degrees of freedom:	1	
	chi2, tie corrected:	2.6667			
	chi2, continuity corrected:	2.1			
	p (same), asymptotic:	0.1473			
		AnaAto MCF7+WB	AnaAto T47D+WB		
	AnaAto MCF7+WB		0.1692		
	AnaAto T47D+WB	0.1692			

Ato	Test for equal medians ***Vimentin***				G
	chi2:	0	Degrees of freedom:	1	
	chi2, tie corrected:	0			
	chi2, continuity corrected:	0			
	p (same), asymptotic:	1			
		Ato MCF7+WB	Ato T47D+WB		
	Ato MCF7+WB		0.4462		
	Ato T47D+WB	0.4462			

C2.4: Statistics output *N-cadherin* expression

Part A: PAST output for gene expression between cell lines

UT cells	Test for equal medians *N-Cadherin*			A
	chi2:	0.66667	Degrees of freedom:	1
	chi2, tie corrected:	0.66667		
	chi2, continuity corrected:	0.3		
	p (same), asymptotic:	0.58388		
		UT MCF7+WB	UT T47D+WB	
	UT MCF7+WB		0.5692	
	UT T47D+WB	0.5692		

DMSO	Test for equal medians *N-Cadherin*			B
	chi2:	0.66667	Degrees of freedom:	1
	chi2, tie corrected:	0.66667		
	chi2, continuity corrected:	0.3		
	p (same), asymptotic:	0.58388		
		DMSO MCF7+WB	DMSO T47D+WB	
	DMSO MCF7+WB		0.6923	
	DMSO T47D+WB	0.6923		

Ana	Test for equal medians *N-Cadherin*			C
	chi2:	2.6667	Degrees of freedom:	1
	chi2, tie corrected:	2.6667		
	chi2, continuity corrected:	2.1		
	p (same), asymptotic:	0.1473		
		Ana MCF7+ WB	Ana T47D+ WB	
	Ana MCF7+ WB		0.1692	
	Ana T47D+ WB	0.1692		

AnaAspClop	Test for equal medians *N-Cadherin*			D
	chi2:	0.66667	Degrees of freedom:	1
	chi2, tie corrected:	0.66667		
	chi2, continuity corrected:	0.3		
	p (same), asymptotic:	0.58388		
		AnaAspClop MCF7+WB	AnaAspClop T47D+WB	
	AnaAspClop MCF7+WB		0.3231	
	AnaAspClop T47D+WB	0.3231		

Part B: PAST output for gene expression between cell lines

AspClop	Test for equal medians *N-Cadherin*				E
	chi2:	2.6667	Degrees of freedom:	1	
	chi2, tie corrected:	2.6667			
	chi2, continuity corrected:	2.1			
	p (same), asymptotic:	0.1473			
		AspClop MCF7+WB	AspClop T47D+WB		
	AspClop MCF7+WB		0.1692		
	AspClop T47D+WB	0.1692			

AnaAto	Test for equal medians *N-Cadherin*				F
	chi2:	6	Degrees of freedom:	1	
	chi2, tie corrected:	6			
	chi2, continuity corrected:	5.1			
	p (same), asymptotic:	0.023926			
		AnaAto MCF7+WB	AnaAto T47D+WB		
	AnaAto MCF7+WB		0.04615		
	AnaAto T47D+WB	0.04615			

Ato	Test for equal medians *N-Cadherin*				G
	chi2:	6	Degrees of freedom:	1	
	chi2, tie corrected:	6			
	chi2, continuity corrected:	5.1			
	p (same), asymptotic:	0.023926			
		Ato MCF7+WB	Ato T47D+WB		
	Ato MCF7+WB		0.04615		
	Ato T47D+WB	0.04615			

C2.5: Statistics output *E-cadherin* expression

Part A: PAST output for gene expression between cell lines

UT cells	Test for equal medians *E-Cadherin*			A
	chi2:	0	Degrees of freedom:	1
	chi2, tie corrected:	0		
	chi2, continuity corrected:	0		
	p (same), asymptotic:	1		
		UT MCF7+WB	UT T47D+WB	
	UT MCF7+WB		1	
	UT T47D+WB	1		

DMSO	Test for equal medians *E-Cadherin*			B
	chi2:	6	Degrees of freedom:	1
	chi2, tie corrected:	6		
	chi2, continuity corrected:	5.1		
	p (same), asymptotic:	0.023926		
		DMSO MCF7+WB	DMSO T47D+WB	
	DMSO MCF7+WB		0.04615	
	DMSO T47D+WB	0.04615		

Ana	Test for equal medians *E-Cadherin*			C
	chi2:	0.66667	Degrees of freedom:	1
	chi2, tie corrected:	0.66667		
	chi2, continuity corrected:	0.3		
	p (same), asymptotic:	0.58388		
		Ana MCF7+ WB	Ana T47D+ WB	
	Ana MCF7+ WB		0.5692	
	Ana T47D+ WB	0.5692		

AnaAspClop	Test for equal medians *E-Cadherin*			D
	chi2:	2.6667	Degrees of freedom:	1
	chi2, tie corrected:	2.6667		
	chi2, continuity corrected:	2.1		
	p (same), asymptotic:	0.1473		
		AnaAspClop MCF7+WB	AnaAspClop T47D+WB	
	AnaAspClop MCF7+WB		0.07692	
	AnaAspClop T47D+WB	0.07692		

Part B: PAST output for gene expression between cell lines

AspClop	Test for equal medians *E-Cadherin*			E
	chi2:	0.66667	Degrees of freedom:	1
	chi2, tie corrected:	0.66667		
	chi2, continuity corrected:	0.3		
	p (same), asymptotic:	0.58388		
		AspClop MCF7+WB	AspClop T47D+WB	
	AspClop MCF7+WB		0.3231	
	AspClop T47D+WB	0.3231		

AnaAto	Test for equal medians *E-Cadherin*			F
	chi2:	6	Degrees of freedom:	1
	chi2, tie corrected:	6		
	chi2, continuity corrected:	5.1		
	p (same), asymptotic:	0.023926		
		AnaAto MCF7+WB	AnaAto T47D+WB	
	AnaAto MCF7+WB		0.04615	
	AnaAto T47D+WB	0.04615		

Ato	Test for equal medians *E-Cadherin*			G
	chi2:	6	Degrees of freedom:	1
	chi2, tie corrected:	6		
	chi2, continuity corrected:	5.1		
	p (same), asymptotic:	0.023926		
		Ato MCF7+WB	Ato T47D+WB	
	Ato MCF7+WB		0.04615	
	Ato T47D+WB	0.04615		

C3.1: Cytokine standards preparation

Reconstitute 1 each of the unique standard cocktails provided with the Calibrator diluent RD6-52, as indicated in the certificate of analysis for reconstitution volumes. As follows;

Plate: 1

Standard	Lot #	Reconstitute in RD652 (ml)
A	1517071	0.225
V	1527996	0.225

Plate: 2

Standard	Lot #	Reconstitute in RD652 (ml)
R	1490945	0.3
B	1511314	0.25
A	1517071	0.225
H	1499230	0.25
L	1505485	0.225

- Allowed the standard cocktails to sit for 15 mins with gentle agitation (prior to making dilutions).
- Upon reconstitution, each standard cocktail was 10X concentrated
- **Make up Standard 1:**
  (combined 100ul of each standard cocktail with RD6-52 into standard 1 tube to a final volume of 1000ul.
  Plate 1: 100ul (std A) +100ul (std V) + 800ul RD6-52
  Plate 2: 100ul (std R) + 100ul (std B) + 100ul (std A) + 100ul (std H) + 100ul (std L) + 500ul RD6- 52

Dilution series prep (PLATE 1): 1 in 3 dilution series (100 µl Standard: 200 ul RD6-52)

Standard	Vol Std	Vol RD6-52	IL-1β (BR28) pg/ml	TNF-α (BR12) pg/ml	PDGF-AB (BR35) pg/ml
S1	See above		3950	2050	5380
S2	100 µl S1	200 µl	1317	683	1793
S3	100 µl S2	200 µl	439	228	598
S4	100 µl S3	200 µl	146	76	199
S5	100 µl S4	200 µl	49	25	66
S6	100 µl S5	200 µl	16	8.4	22
S7	100 µl S6	200 µl	5.4	2.8	7.4
S8	100 µl S6	200 µl	1.8	0.9	2.5
Blank	-	200 µl			

Dilution series prep (PLATE 2): 1 in 3 dilution series (100 µl Standard: 200 ul RD6-52)

Standard	Vol Std	Vol RD6-52	IFN-β (BR21) pg/ml	IL-6 (BR13) pg/ml	IL-4 (BR39) pg/ml	IL10 (BR22) pg/ml	TGFα (BR63) pg/ml	VEGF-A (BR26) pg/ml	PDGF-BB (BR18) pg/ml
S1	See above		2800	730	3380	900	1640	1790	3140
S2	100 µl S1	200 µl	933	243	1127	300	547	597	1046
S3	100 µl S2	200 µl	311	81	376	100	182	199	349
S4	100 µl S3	200 µl	104	27	125	33	61	66	116
S5	100 µl S4	200 µl	35	9	42	11	20	22	39
S6	100 µl S5	200 µl	12	3	14	3.7	6.7	7.4	13
S7	100 µl S6	200 µl	3.8	1	4.6	1.2	2.2	2.5	4.3
S8	100 µl S6	200 µl	1.3	.3	1.5	0.4	0.7	0.8	1.4
Blank	-	200 µl							

TGFB cytokines

Reconstitute standard vial:

1. Gently tapped the vial containing lypholised standard.
2. Added 500 µl diluent Standard/Sample diluent (1:3)
3. Gently vortexed reconstituted standard for 5 sec
4. Incubated on ice for 30 min

1 in 4 dilution series [50 µl Standard: 150 ul Diluent(1:3)]

Standard	Vol Std	Vol Diluent (1:3)	TGFβ1 (BR13) (pg/ml)	TGFβ2 (BR72) (pg/ml)	TGFβ3 (BR66) (pg/ml)
S1	128 µl reconstituted standard	72 µl	26 688	18 925	17 128
S2	50 µl S1	150 µl	6 672	4 731.2	4 282
S3	50 µl S2	150 µl	1 668	1 182.8	1 070.5
S4	50 µl S3	150 µl	417	295.7	267.6
S5	50 µl S4	150 µl	104.25	73.9	66.9
S6	50 µl S5	150 µl	26.06	18.5	16.7
S7	50 µl S6	150 µl	6.5	4.62	4.18
S8	50 µl S7	150 µl	1.6	1.16	1.05
Blank	-				

C3.2: Cytokine statistics output 1

PAST output for cytokine secretion

MCF7

IL-4

A1

Friedman IL-4

Test for equal medians

chi2:	12.517	Degrees of freedom:	7
chi2, tie corrected:	12.916		
chi2, continuity corrected:	12.858		
p (same), asymptotic:	0.075656		

Post hoc Wilcoxon

	WB	Media MCF7	Diluent MCF7	Ana MCF7	AnaAspClop MCF7	AspClop MCF7	AnaAto MCF7	Ato MCF7
WB		0.2121	0.3333	0.6364	0.2941	0.4118	0.8788	0.09091
Media MCF7	0.2121		0.1515	0.1515	1	0.1515	0.3333	0.8182
Diluent MCF7	0.3333	0.1515		1	0.1515	0.6471	0.8182	0.09091
Ana MCF7	0.6364	0.1515	1		0.2941	0.6364	1	0.2121
AnaAspClop MCF7	0.2941	1	0.1515	0.2941		0.09091	0.1765	1
AspClop MCF7	0.4118	0.1515	0.6471	0.6364	0.09091		0.5758	0.1765
AnaAto MCF7	0.8788	0.3333	0.8182	1	0.1765	0.5758		0.4118
Ato MCF7	0.09091	0.8182	0.09091	0.2121	1	0.1765	0.4118	

IL-6

B1

Friedman IL-6

Test for equal medians

chi2:	8.9	Degrees of freedom:	7
chi2, tie corrected:	10.68		
chi2, continuity corrected:	10.62		
p (same), asymptotic:	0.15609		

Post hoc Wilcoxon

	WB	Media MCF7	Diluent MCF7	Ana MCF7	AnaAspClop MCF7	AspClop MCF7	AnaAto MCF7	Ato MCF7
WB		0.3333	0.7778	0.7778	1	0.6471	1	0.8824
Media MCF7	0.3333		0.3333	0.1765	0.1765	1	0.6471	0.09091
Diluent MCF7	0.7778	0.3333		1	1	0.6471	0.8824	0.7576
Ana MCF7	0.7778	0.1765	1		0.6471	0.1765	1	1
AnaAspClop MCF7	1	0.1765	1	0.6471		0.2941	1	0.6
AspClop MCF7	0.6471	1	0.6471	0.1765	0.2941		0.5294	0.1765
AnaAto MCF7	1	0.6471	0.8824	1	1	0.5294		0.5556
Ato MCF7	0.8824	0.09091	0.7576	1	0.6	0.1765	0.5556	

T47D

A2

Friedman IL-4

Test for equal medians

chi2:	7.4	Degrees of freedom:	7
chi2, tie corrected:	7.6364		
chi2, continuity corrected:	7.5875		
p (same), asymptotic:	0.37037		

Post hoc Wilcoxon

	WB	Media T47D	Diluent T47D	Ana T47D	AnaAspClop T47D	AspClop T47D	AnaAto T47D	Ato T47D
WB		0.3333	0.4545	1	0.6471	0.5556	0.2941	0.2121
Media T47D	0.3333		0.3939	0.6471	0.09091	0.3939	0.8824	0.8182
Diluent T47D	0.4545	0.3939		0.7576	0.4545	1	1	0.6364
Ana T47D	1	0.6471	0.7576		0.6471	1	0.3333	0.6364
AnaAspClop T47D	0.6471	0.09091	0.4545	0.6471		0.2941	0.2121	0.09091
AspClop T47D	0.5556	0.3939	1	1	0.2941		0.4118	0.8182
AnaAto T47D	0.2941	0.8824	1	0.3333	0.2121	0.4118		0.8824
Ato T47D	0.2121	0.8182	0.6364	0.6364	0.09091	0.8182	0.8824	

B2

Friedman IL-6

Test for equal medians

chi2:	3.4333	Degrees of freedom:	7
chi2, tie corrected:	3.866		
chi2, continuity corrected:	3.8211		
p (same), asymptotic:	0.80013		

Post hoc Wilcoxon

	WB	Media T47D	Diluent T47D	Ana T47D	AnaAspClop T47D	AspClop T47D	AnaAto T47D	Ato T47D
WB		0.5294	0.8788	0.8182	0.7778	1	0.8824	0.8824
Media T47D	0.5294		0.3333	1	0.5758	0.6364	0.7778	0.6364
Diluent T47D	0.8788	0.3333		1	0.5758	0.7576	1	0.6364
Ana T47D	0.8182	1	1		0.6	0.5556	0.7778	0.8824
AnaAspClop T47D	0.7778	0.5758	0.5758	0.6		1	1	0.7778
AspClop T47D	1	0.6364	0.7576	0.5556	1		1	0.6471
AnaAto T47D	0.8824	0.7778	1	0.7778	1	1		1
Ato T47D	0.8824	0.6364	0.6364	0.8824	0.7778	0.6471	1	

PAST output for cytokine secretion

MCF7

TNFα

Friedman TNFα — C1

Test for equal medians

chi2:	11.933	Degrees of freedom:	7
chi2, tie corrected:	13.62		
chi2, continuity corrected:	13.556		
p (same), asymptotic:	0.059672		

Post hoc Wilcoxon

	WB	Media MCF7	Diluent MCF7	Ana MCF7	AnaAspClop MCF7	AspClop MCF7	AnaAto MCF7	Ato MCF7
WB		0.4118	0.3333	1	0.3333	0.8824	1	0.3333
Media MCF7	0.4118		0.1765	0.4118	0.7647	0.5152	0.697	0.6
Diluent MCF7	0.3333	0.1765		0.3333	0.1765	0.8824	0.3939	0.1765
Ana MCF7	1	0.4118	0.3333		0.3333	0.7647	1	0.3333
AnaAspClop MCF7	0.3333	0.7647	0.1765	0.3333		0.2727	0.6471	1
AspClop MCF7	0.8824	0.5152	0.8824	0.7647	0.2727		0.3333	0.4545
AnaAto MCF7	1	0.697	0.3939	1	0.6471	0.3333		0.7576
Ato MCF7	0.3333	0.6	0.1765	0.3333	1	0.4545	0.7576	

TGFα

Friedman TGFα — D1

Test for equal medians

chi2:	4.05	Degrees of freedom:	7
chi2, tie corrected:	4.3504		
chi2, continuity corrected:	4.3064		
p (same), asymptotic:	0.74389		

Post hoc Wilcoxon

	WB	Media MCF7	Diluent MCF7	Ana MCF7	AnaAspClop MCF7	AspClop MCF7	AnaAto MCF7	Ato MCF7
WB		0.4118	0.09091	0.6364	0.5152	0.6364	0.4545	0.4545
Media MCF7	0.4118		0.1765	1	1	1	1	1
Diluent MCF7	0.09091	0.1765		0.7647	0.8182	0.6364	0.7576	0.6364
Ana MCF7	0.6364	1	0.7647		1	0.5556	0.5294	1
AnaAspClop MCF7	0.5152	1	0.8182	1		1	0.7778	1
AspClop MCF7	0.6364	1	0.6364	0.5556	1		0.3333	0.7778
AnaAto MCF7	0.4545	1	0.7576	0.5294	0.7778	0.3333		0.7778
Ato MCF7	0.4545	1	0.6364	1	1	0.7778	0.7778	

T47D

TNFα

Friedman TNFα — C2

Test for equal medians

chi2:	1.95	Degrees of freedom:	7
chi2, tie corrected:	2.2135		
chi2, continuity corrected:	2.1715		
p (same), asymptotic:	0.94974		

Post hoc Wilcoxon

	WB	Media T47D	Diluent T47D	Ana T47D	AnaAspClop T47D	AspClop T47D	AnaAto T47D	Ato T47D
WB		0.7778	0.8788	0.7778	0.3333	0.6471	0.7778	0.8824
Media T47D	0.7778		1	0.8824	0.3333	0.7576	0.7778	0.8824
Diluent T47D	0.8788	1		0.8788	0.4545	1	0.7778	1
Ana T47D	0.7778	0.8824	0.8788		0.2941	1	1	0.8824
AnaAspClop T47D	0.3333	0.3333	0.4545	0.2941		0.2941	0.8182	0.3333
AspClop T47D	0.6471	0.7576	1	1	0.2941		0.7647	1
AnaAto T47D	0.7778	0.7778	0.7778	1	0.8182	0.7647		0.5556
Ato T47D	0.8824	0.8824	1	0.8824	0.3333	1	0.5556	

TGFα

Friedman TGFα — D2

Test for equal medians

chi2:	14.283	Degrees of freedom:	7
chi2, tie corrected:	14.703		
chi2, continuity corrected:	14.641		
p (same), asymptotic:	0.040883		

Post hoc Wilcoxon

	WB	Media T47D	Diluent T47D	Ana T47D	AnaAspClop T47D	AspClop T47D	AnaAto T47D	Ato T47D
WB		0.09091	0.09091	0.3333	0.2121	1	0.09091	0.6364
Media T47D	0.09091		0.3333	0.8182	1	0.1765	0.7576	0.4118
Diluent T47D	0.09091	0.3333		1	1	0.1765	0.7576	0.6471
Ana T47D	0.3333	0.8182	1		0.6471	0.3333	0.6364	0.5294
AnaAspClop T47D	0.2121	1	1	0.6471		0.09091	1	0.1515
AspClop T47D	1	0.1765	0.1765	0.3333	0.09091		0.1765	0.6471
AnaAto T47D	0.09091	0.7576	0.7576	0.6364	1	0.1765		0.2121
Ato T47D	0.6364	0.4118	0.6471	0.5294	0.1515	0.6471	0.2121	

C3.3 Cytokine statistics output 2

Part A: PAST output for cytokine secretion

MCF7

PDGF-AB

A1

Friedman PDGF-AB

Test for equal medians

chi2:	9.4	Degrees of freedom:	7
chi2, tie corrected:	9.4		
chi2, continuity corrected:	9.3489		
p (same), asymptotic:	0.22857		

Post hoc Wilcoxon

	WB	Media MCF7	Diluent MCF7	Ana MCF7	AnaAspCl op MCF7	AspClop MCF7	AnaAto MCF7	Ato MCF7
WB		0.2121	0.3333	0.6364	0.8182	0.8182	0.8182	0.4545
Media MCF7	0.2121		0.2121	0.6364	0.3333	1	0.2121	1
Diluent MCF7	0.3333	0.2121		1	0.8182	0.6364	0.2121	1
Ana MCF7	0.6364	0.6364	1		0.3333	0.4545	0.09091	0.8182
AnaAspClop MCF7	0.8182	0.3333	0.8182	0.3333		0.09091	0.09091	0.4545
AspClop MCF7	0.8182	1	0.6364	0.4545	0.09091		0.09091	0.6364
AnaAto MCF7	0.8182	0.2121	0.2121	0.09091	0.09091	0.09091		0.3333
Ato MCF7	0.4545	1	1	0.8182	0.4545	0.6364	0.3333	

PDGF-BB

B1

Friedman PDGF-BB

Test for equal medians

chi2:	11.333	Degrees of freedom:	7
chi2, tie corrected:	11.333		
chi2, continuity corrected:	11.279		
p (same), asymptotic:	0.12692		

Post hoc Wilcoxon pairwise

	WB	Media MCF7	Diluent MCF7	Ana MCF7	AnaAspCl op MCF7	AspClop MCF7	AnaAto MCF7	Ato MCF7
WB		1	1	0.6364	0.6364	0.3333	0.3333	0.4545
Media MCF7	1		0.2121	0.4545	0.2121	0.1515	0.1515	0.1515
Diluent MCF7	1	0.2121		0.6364	0.3333	0.2121	0.2121	0.2121
Ana MCF7	0.6364	0.4545	0.6364		0.6364	0.09091	0.09091	0.2121
AnaAspClop MCF7	0.6364	0.2121	0.3333	0.6364		0.09091	0.1515	0.1515
AspClop MCF7	0.3333	0.1515	0.2121	0.09091	0.09091		0.6364	0.3333
AnaAto MCF7	0.3333	0.1515	0.2121	0.09091	0.1515	0.6364		1
Ato MCF7	0.4545	0.1515	0.2121	0.2121	0.1515	0.3333	1	

T47D

A2

Friedman PDGF-AB

Test for equal medians

chi2:	15.8	Degrees of freedom:	7
chi2, tie corrected:	15.8		
chi2, continuity corrected:	15.737		
p (same), asymptotic:	0.027634		

Post hoc Wilcoxon

	WB	Media T47D	Diluent T47D	Ana T47D	AnaAspCl op T47D	AspClop T47D	AnaAto T47D	Ato T47D
WB		0.2121	0.1515	0.8182	0.6364	0.8182	0.8182	0.4545
Media T47D	0.2121		0.3939	0.1515	0.09091	0.09091	0.1515	0.09091
Diluent T47D	0.1515	0.3939		0.8182	0.6364	0.6364	0.8182	0.3333
Ana T47D	0.8182	0.1515	0.8182		0.8182	0.1515	0.8182	0.09091
AnaAspClop T47D	0.6364	0.09091	0.6364	0.8182		0.8788	0.3333	0.09091
AspClop T47D	0.8182	0.09091	0.6364	0.1515	0.8788		0.6364	0.2121
AnaAto T47D	0.8182	0.1515	0.8182	0.8182	0.3333	0.6364		0.09091
Ato T47D	0.4545	0.09091	0.3333	0.09091	0.09091	0.2121	0.09091	

B2

Friedman PDGF-BB

Test for equal medians

chi2:	6.4	Degrees of freedom:	7
chi2, tie corrected:	6.4		
chi2, continuity corrected:	6.3546		
p (same), asymptotic:	0.49901		

Post hoc Wilcoxon pairwise

	WB	Media T47D	Diluent T47D	Ana T47D	AnaAspCl op T47D	AspClop T47D	AnaAto T47D	Ato T47D
WB		1	0.6364	0.3333	0.3333	0.6364	0.4545	0.4545
Media T47D	1		0.1515	0.1515	0.1515	0.2121	0.3333	0.2121
Diluent T47D	0.6364	0.1515		0.3333	0.2121	0.8182	0.3333	0.4545
Ana T47D	0.3333	0.1515	0.3333		0.8182	0.6364	0.8182	1
AnaAspClop T47D	0.3333	0.1515	0.2121	0.8182		0.3333	1	0.4545
AspClop T47D	0.6364	0.2121	0.8182	0.6364	0.3333		0.4545	0.8182
AnaAto T47D	0.4545	0.3333	0.3333	0.8182	1	0.4545		0.6364
Ato T47D	0.4545	0.2121	0.4545	1	0.4545	0.8182	0.6364	

Part B: PAST output for cytokine secretion

VEGF-A

MCF7

Friedman VEGF-A — C1

Test for equal medians

chi2:	5.1667	Degrees of freedom:	7
chi2, tie corrected:	5.2415		
chi2, continuity corrected:	5.1978		
p (same), asymptotic:	0.63584		

Post hoc Wilcoxon pairwise

	WB	Media MCF7	Diluent MCF7	Ana MCF7	AnaAspClop MCF7	AspClop MCF7	AnaAto MCF7	Ato MCF7
WB		0.4545	0.6364	1	1	1	0.8182	1
Media MCF7	0.4545		0.1515	1	0.8824	0.4545	0.6364	0.6364
Diluent MCF7	0.6364	0.1515		0.3333	0.4545	1	0.8824	1
Ana MCF7	1	1	0.3333		0.8182	0.3333	0.3333	0.3333
AnaAspClop MCF7	1	0.8824	0.4545	0.8182		0.2121	0.3333	0.1515
AspClop MCF7	1	0.4545	1	0.3333	0.2121		0.6471	0.8182
AnaAto MCF7	0.8182	0.6364	0.8824	0.3333	0.3333	0.6471		0.6364
Ato MCF7	1	0.6364	1	0.3333	0.1515	0.8182	0.6364	

T47D

Friedman VEGF-A — C2

Test for equal medians

chi2:	7	Degrees of freedom:	7
chi2, tie corrected:	7.0843		
chi2, continuity corrected:	7.0372		
p (same), asymptotic:	0.42502		

Post hoc Wilcoxon pairwise

	WB	Media T47D	Diluent T47D	Ana T47D	AnaAspClop T47D	AspClop T47D	AnaAto T47D	Ato T47D
WB		1	0.6471	0.8182	0.6364	1	1	1
Media T47D	1		0.2121	0.4545	0.4545	1	0.8182	0.8824
Diluent T47D	0.6471	0.2121		0.4545	0.3333	0.6364	0.4545	1
Ana T47D	0.8182	0.4545	0.4545		0.3333	0.4545	1	0.1765
AnaAspClop T47D	0.6364	0.4545	0.3333	0.3333		0.4545	0.1515	0.09091
AspClop T47D	1	1	0.6364	0.4545	0.4545		0.8182	0.4545
AnaAto T47D	1	0.8182	0.4545	1	0.1515	0.8182		0.1765
Ato T47D	1	0.8824	1	0.1765	0.09091	0.4545	0.1765	

C3.4: Cytokine statistics output 3

Part A: PAST output for cytokine secretion

MCF7

TGFβ1

A1

Friedman TGFβ1

Test for equal medians

chi2:	17.133	Degrees of freedom:	7
chi2, tie corrected:	17.133		
chi2, continuity corrected:	17.067		
p (same), asymptotic:	0.016966		

Post hoc Wilcoxon

	WB	Media MCF7	Diluent MCF7	Ana MCF7	AnaAspCl op MCF7	AspClop MCF7	AnaAto MCF7	Ato MCF7
WB		0.1515	0.1515	0.6364	0.4545	0.2121	0.1515	0.2121
Media MCF7	0.1515		0.1515	0.6364	0.2121	0.1515	0.8182	1
Diluent MCF7	0.1515	0.1515		0.6364	0.2121	0.2121	0.8182	1
Ana MCF7	0.6364	0.6364	0.6364		0.09091	0.09091	0.1515	0.2121
AnaAspClop MCF7	0.4545	0.2121	0.2121	0.09091		0.6364	0.09091	0.09091
AspClop MCF7	0.2121	0.1515	0.2121	0.09091	0.6364		0.09091	0.09091
AnaAto MCF7	0.1515	0.8182	0.8182	0.1515	0.09091	0.09091		1
Ato MCF7	0.2121	1	1	0.2121	0.09091	0.09091	1	

TGFβ2

B1

Friedman TGFβ2

Test for equal medians

chi2:	14.4	Degrees of freedom:	7
chi2, tie corrected:	14.4		
chi2, continuity corrected:	14.339		
p (same), asymptotic:	0.045464		

Post hoc Wilcoxon

	WB	Media MCF7	Diluent MCF7	Ana MCF7	AnaAspCl op MCF7	AspClop MCF7	AnaAto MCF7	Ato MCF7
WB		0.3333	0.6364	1	0.3333	0.4545	0.1515	0.2121
Media MCF7	0.3333		1	0.6364	0.2121	0.3333	0.4545	0.6364
Diluent MCF7	0.6364	1		0.6364	0.4545	0.6364	0.4545	1
Ana MCF7	1	0.6364	0.6364		0.1515	0.6364	0.1515	0.3333
AnaAspClop MCF7	0.3333	0.2121	0.4545	0.1515		0.1515	0.09091	0.09091
AspClop MCF7	0.4545	0.3333	0.6364	0.6364	0.1515		0.1515	0.09091
AnaAto MCF7	0.1515	0.4545	0.4545	0.1515	0.09091	0.1515		1
Ato MCF7	0.2121	0.6364	1	0.3333	0.09091	0.09091	1	

T47D

A2

Friedman TGFβ1

Test for equal medians

chi2:	14.783	Degrees of freedom:	7
chi2, tie corrected:	14.819		
chi2, continuity corrected:	14.757		
p (same), asymptotic:	0.039242		

Post hoc Wilcoxon

	WB	Media T47D	Diluent T47D	Ana T47D	AnaAspCl op T47D	AspClop T47D	AnaAto T47D	Ato T47D
WB		0.6471	0.09091	1	0.6364	0.09091	0.09091	0.1515
Media T47D	0.6471		0.09091	1	0.6364	0.09091	0.09091	0.2121
Diluent T47D	0.09091	0.09091		0.8182	0.8182	0.3333	0.2121	0.4545
Ana T47D	1	1	0.8182		1	0.09091	0.4545	0.4545
AnaAspClop T47D	0.6364	0.6364	0.8182	1		0.1515	0.2121	0.3333
AspClop T47D	0.09091	0.09091	0.3333	0.09091	0.1515		0.8182	0.4545
AnaAto T47D	0.09091	0.09091	0.2121	0.4545	0.2121	0.8182		1
Ato T47D	0.1515	0.2121	0.4545	0.4545	0.3333	0.4545	1	

B2

Friedman TGFβ2

Test for equal medians

chi2:	11.8	Degrees o	7
chi2, tie corrected:	11.8		
chi2, continuity corrected:	11.744		
p (same), asymptotic:	0.10929		

Post hoc Wilcoxon

	WB	Media T47D	Diluent T47D	Ana T47D	AnaAspCl op T47D	AspClop T47D	AnaAto T47D	Ato T47D
WB		0.3333	0.4545	1	1	0.09091	0.09091	0.2121
Media T47D	0.3333		0.5758	1	0.8182	0.09091	0.09091	0.1515
Diluent T47D	0.4545	0.5758		0.8182	0.8182	0.1515	0.1515	0.1515
Ana T47D	1	1	0.8182		0.8182	0.09091	0.3333	0.2121
AnaAspClop T47D	1	0.8182	0.8182	0.8182		0.3333	0.8182	0.6364
AspClop T47D	0.09091	0.09091	0.1515	0.09091	0.3333		0.6364	0.3333
AnaAto T47D	0.09091	0.09091	0.1515	0.3333	0.8182	0.6364		1
Ato T47D	0.2121	0.1515	0.1515	0.2121	0.6364	0.3333	1	

Part B: PAST output for cytokine secretion

TGFβ3

MCF7

Friedman TGFβ3 — C1

Test for equal medians

chi2:	10.983	Degrees of freedom:	7
chi2, tie corrected:	11.197		
chi2, continuity corrected:	11.141		
p (same), asymptotic:	0.13257		

Post hoc Wilcoxon

	WB	Media MCF7	Diluent MCF7	Ana MCF7	AnaAspClop MCF7	AspClop MCF7	AnaAto MCF7	Ato MCF7
WB		0.8182	0.1515	1	0.4118	0.6471	0.2727	0.4545
Media MCF7	0.8182		0.09091	1	0.4545	0.6364	0.4545	0.6364
Diluent MCF7	0.1515	0.09091		0.6364	0.2121	0.3333	1	0.8824
Ana MCF7	1	1	0.6364		0.1765	0.2121	0.2941	0.4545
AnaAspClop MCF7	0.4118	0.4545	0.2121	0.1765		0.2941	0.09091	0.1515
AspClop MCF7	0.6471	0.6364	0.3333	0.2121	0.2941		0.1765	0.1765
AnaAto MCF7	0.2727	0.4545	1	0.2941	0.09091	0.1765		0.6364
Ato MCF7	0.4545	0.6364	0.8824	0.4545	0.1515	0.1765	0.6364	

T47D

Friedman TGFβ3 — C2

Test for equal medians

chi2:	8.1833	Degrees of freedom:	7
chi2, tie corrected:	8.424		
chi2, continuity corrected:	8.3738		
p (same), asymptotic:	0.30079		

Post hoc Wilcoxon

	WB	Media T47D	Diluent T47D	Ana T47D	AnaAspClop T47D	AspClop T47D	AnaAto T47D	Ato T47D
WB		0.6364	0.09091	0.3333	0.4545	0.1515	0.8182	0.4118
Media T47D	0.6364		0.2121	0.4545	0.6364	0.3333	1	0.7576
Diluent T47D	0.09091	0.2121		1	1	0.4545	0.6364	0.8182
Ana T47D	0.3333	0.4545	1		0.8182	0.3333	0.4545	0.8182
AnaAspClop T47D	0.4545	0.6364	1	0.8182		0.2941	0.6471	1
AspClop T47D	0.1515	0.3333	0.4545	0.3333	0.2941		0.3333	0.1765
AnaAto T47D	0.8182	1	0.6364	0.4545	0.6471	0.3333		1
Ato T47D	0.4118	0.7576	0.8182	0.8182	1	0.1765	1	

C3.5: Cytokine statistics 4

PAST output for cytokine secretion

Friedman			
Test for equal medians			
chi2:	731.69	Degrees of freedom:	19
chi2, tie corrected:	732.82		
chi2, continuity corrected:	732.82		
p (same), asymptotic:	3.97E-143		

Wilcoxon pairwise	T47D IL6	T47D TNFa	T47D IL4	T47D TGFa	T47D VGEF	T47D PDGF-AB	T47D PDGF-BB	T47D TGFβ1	T47D TGFβ2	T47D TGFβ3
MCF7 IL6	0.3578	5.66E-07	3.53E-08	3.51E-08	3.56E-08	3.57E-08	3.57E-08	3.57E-08	3.57E-08	3.53E-08
MCF7 TNFa	2.97E-07	0.4244	3.52E-08	0.001373	3.56E-08	3.57E-08	3.57E-08	3.57E-08	3.57E-08	3.55E-08
MCF7 IL4	3.53E-08	3.55E-08	0.1578	3.55E-08	5.52E-05	3.57E-08	3.57E-08	3.57E-08	3.57E-08	3.09E-06
MCF7 TGFa	3.47E-08	0.1661	3.55E-08	0.04868	3.56E-08	3.57E-08	3.57E-08	3.57E-08	3.57E-08	3.55E-08
MCF7 VEGF	3.57E-08	3.57E-08	1.31E-06	3.57E-08	0.5961	3.57E-08	3.57E-08	3.57E-08	3.57E-08	1.82E-06
MCF7 PDGF-AB	3.57E-08	3.57E-08	3.57E-08	3.57E-08	3.57E-08	0.001516	3.57E-08	3.57E-08	3.57E-08	3.57E-08
MCF7 PDGF-BB	3.57E-08	3.57E-08	3.57E-08	3.57E-08	3.57E-08	3.57E-08	0.6702	4.65E-05	3.57E-08	3.57E-08
MCF7 TGFβ1	3.57E-08	3.57E-08	3.57E-08	3.57E-08	3.57E-08	3.57E-08	0.000135	0.6465	3.57E-08	3.57E-08
MCF7 TGFβ2	3.57E-08	3.57E-08	3.57E-08	3.57E-08	3.57E-08	3.57E-08	3.57E-08	3.57E-08	0.3257	3.57E-08
MCF7 TGFβ3	3.56E-08	9.48E-08	7.33E-05	8.80E-08	1.49E-06	3.57E-08	3.57E-08	3.57E-08	3.57E-08	0.7388

APPENDIX D: General documents

D1.1: Plagiarism declaration



PLAGIARISM DECLARATION TO BE SIGNED BY ALL HIGHER DEGREE STUDENTS

SENATE PLAGIARISM POLICY: APPENDIX ONE

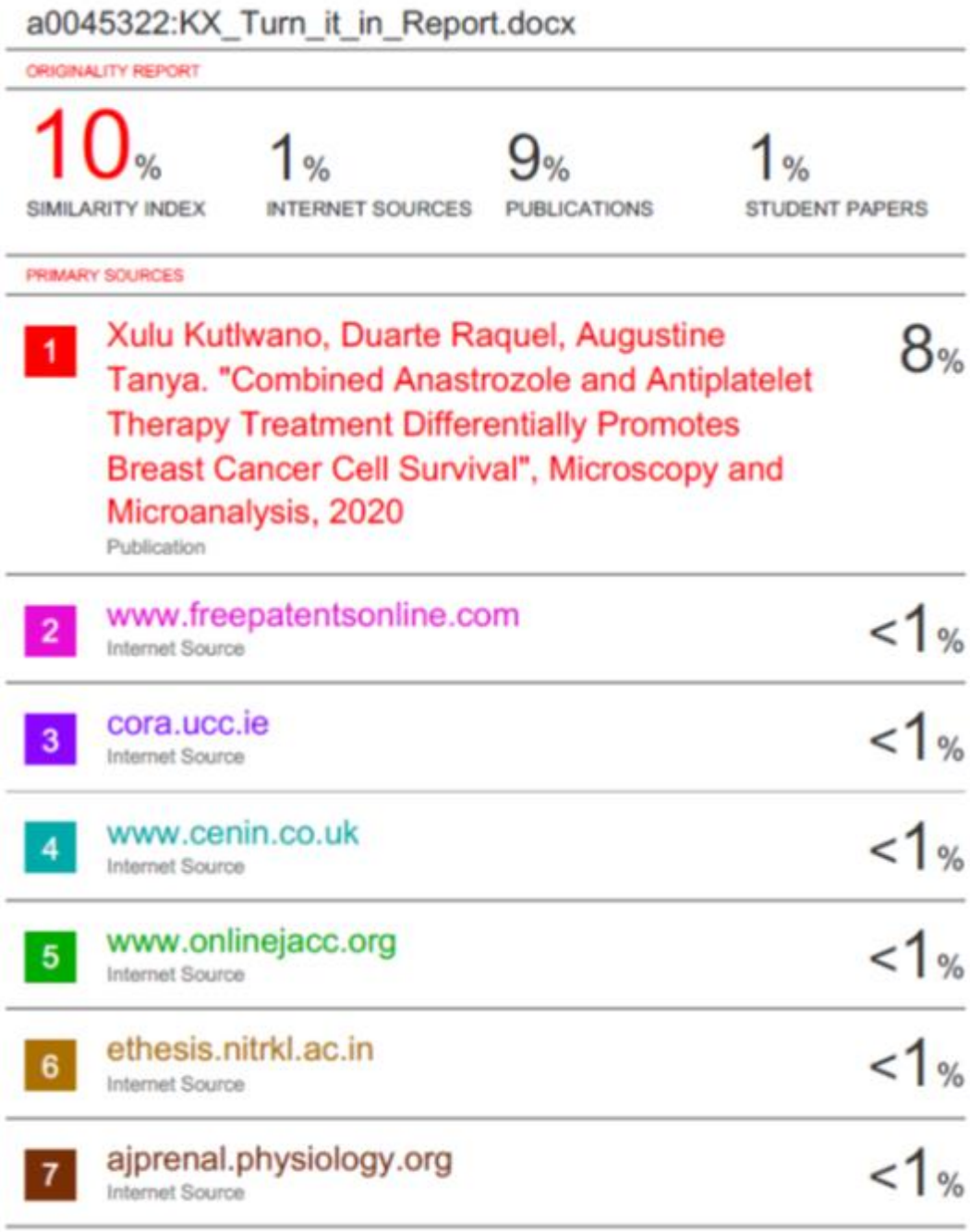
I Kutlwano Xulu (Student number: 303233) am a student registered for the degree of Doctor of Philosophy in the academic year 2020.

I hereby declare the following:

- I am aware that plagiarism (the use of someone else's work without their permission and/or without acknowledging the original source) is wrong.
- I confirm that the work submitted for assessment for the above degree is my own unaided work except where I have explicitly indicated otherwise.
- I have followed the required conventions in referencing the thoughts and ideas of others.
- I understand that the University of the Witwatersrand may take disciplinary action against me if there is a belief that this is not my own unaided work or that I have failed to acknowledge the source of the ideas or words in my writing.
- I have included as an appendix a report from "Turnitin" (or other approved plagiarism detection) software indicating the level of plagiarism in my research document.

Signature: K.Xulu Date: 19 October 2020

D1.2: Turn it in report summary



a0045322:KX_Turn_it_in_Report.docx

ORIGINALITY REPORT

10%	1%	9%	1%
SIMILARITY INDEX	INTERNET SOURCES	PUBLICATIONS	STUDENT PAPERS

PRIMARY SOURCES

1	Xulu Kutlwano, Duarte Raquel, Augustine Tanya. "Combined Anastrozole and Antiplatelet Therapy Treatment Differentially Promotes Breast Cancer Cell Survival", Microscopy and Microanalysis, 2020 Publication	8%
2	www.freepatentsonline.com Internet Source	<1%
3	cora.ucc.ie Internet Source	<1%
4	www.cenin.co.uk Internet Source	<1%
5	www.onlinejacc.org Internet Source	<1%
6	ethesis.nitrkl.ac.in Internet Source	<1%
7	ajprenal.physiology.org Internet Source	<1%

D1.3: Proof of manuscript acceptance

Microscopy and Microanalysis - Decision on Manuscript ID MAM-18-N/A-185.R2

From: Microscopy and Microanalysis (onbehalfof@manuscriptcentral.com)

To: kutlwano.xulu@wits.ac.za; kutlwanothabethe@ymail.com

Date: Thursday, March 19, 2020, 09:37 PM GMT+2

19-Mar-2020

Dear Ms. Xulu:

Apologies for all the delays!

It is a pleasure to accept your manuscript entitled "Combined Anastrozole and Antiplatelet therapy treatment differentially promotes breast cancer cell survival" for publication in Microscopy and Microanalysis.

Your manuscript has been forwarded to our production editors, who will be contacting you soon about the page proofs of your article. Please pay attention to the proofs, as this will be your last chance to correct any typos or errors and to make sure that any of our editorial changes have not affected the sense of the manuscript. Note that after proofing, the manuscript will appear on-line prior to actual print publication.

If you haven't yet completed the transfer of copyright form, please complete the form attached to this email and return it to me. If you have already, please disregard this attachment.

PLEASE NOTE: Microscopy and Microanalysis offers authors the option to publish their article through an Open Access model (see https://www.cambridge.org/core/services/open-access-policies/introduction-to-open-access), on payment of an Article Processing Charge. For the Article Processing Charge for Microscopy and Microanalysis, please visit:
https://www.cambridge.org/core/services/open-access-policies/open-access-journals/gold-open-access-journals
If you wish to publish your paper under the Open Access model, please send an e-mail stating this choice to johnshields59@gmail.com and complete the appropriate form accordingly. Once you have returned the form, you will be contacted by CCC-Rightslink who are acting on our behalf to collect the Article Processing Charges (APCs). Please follow their instructions in order to avoid any delay in the publication of your article.

Thank you for your fine contribution. On behalf of the Editors of Microscopy and Microanalysis, we look forward to your continued contributions to the Journal.

Sincerely,
Dr. John Mansfield
Editor-in-Chief, Microscopy and Microanalysis
thejfmjfm@me.com

* MAM-CTF1.docx
26.7kB